Natural Product Reports

ROYAL SOCIETY OF CHEMISTRY

REVIEW

View Article Online
View Journal | View Issue

Cite this: *Nat. Prod. Rep.*, 2024, **41**, 1652

Isolation, biological activity, and synthesis of isoquinoline alkaloids†

Xiaorong Yang,[ab] Xiaolou Miao,[ab] Lixia Dai,[ac] Xiao Guo,[d] Janar Jenis,[e] Jiyu Zhang[ab] and Xiaofei Shang *[abcd]

Received 21st May 2024

DOI: 10.1039/d4np00023d

rsc.li/npr

Covering: 2019 to 2023

Isoquinoline alkaloids, an important class of *N*-based heterocyclic compounds, have attracted considerable attention from researchers worldwide. To follow up on our prior review (covering 2014–2018) and present the progress of this class of compounds, this review summarizes and provides updated literature on novel isoquinoline alkaloids isolated during the period of 2019–2023, together with their biological activity and underlying mechanisms of action. Moreover, with the rapid development of synthetic modification strategies, the synthesis strategies of isoquinoline alkaloids have been continuously optimized, and the total synthesis of these classes of natural products is reviewed critically herein. Over 250 molecules with a broad range of bioactivities, including antitumor, antibacterial, cardioprotective, anti-inflammatory, neuroprotective and other activities, are isolated and discussed. The total synthesis of more than nine classes of isoquinoline alkaloids is presented, and thirteen compounds constitute the first total synthesis. This survey provides new indications or possibilities for the discovery of new drugs from the original naturally occurring isoquinoline alkaloids.

[a]*Key Laboratory of Veterinary Pharmaceutical Development of Ministry of Agriculture, Key Laboratory of New Animal Drug Project, Lanzhou Institute of Husbandry and Pharmaceutical Sciences, Chinese Academy of Agricultural Sciences, Lanzhou 730050, Gansu Province, PR China. E-mail: shangxiaofei@caas.cn; Tel: (+86) 931-2115262*

[b]*China-Kazakh Joint Research Center for Natural Veterinary Drug, Lanzhou 730050, P. R. China*

[c]*College of Veterinary Medicine, Gansu Agricultural University, Lanzhou 730070, China*

[d]*Tibetan Medicine Research Center of Qinghai University, Qinghai University Tibetan Medical College, Qinghai University, Xining 810016, P. R. China*

[e]*The Research Center for Medicinal Plants, Al-Farabi Kazakh National University, Almaty 050040, Kazakhstan*

† Electronic supplementary information (ESI) available. See DOI: https://doi.org/10.1039/d4np00023d

1. Introduction

Isoquinoline alkaloids, an important class of *N*-heterocyclic bioactive natural products, are common throughout living organisms, predominantly in the plant kingdom.[1] Derived from tyrosine or phenylalanine building blocks, isoquinoline alkaloids are thought to be highly conserved metabolites in ancient vascular plants at the chemotaxonomic level.[2,3] Since the first bioactive isoquinoline alkaloid and nitrogen-containing natural product, morphine, was isolated from the opium plant *Papaver somniferum* in the early 19th century,[4] increasing numbers of isoquinoline alkaloids, such as benzylisoquinolines, aporphines, berberines, protopines, *etc.*, have been identified from natural sources over the past 200 years, resulting in a wide range of structural diversity (Fig. 1).[5–8] Most of these compounds and their derivatives exhibit significant bioactivities, such as antitumor, antidiabetic, metabolic, anti-inflammatory, antibacterial, antiparasitic, cardioprotective, neuroprotective and other effects (Fig. 1).[9–11]

Although there is a long history and large gap between pharmacological research and the clinical use of natural products, isoquinoline alkaloids have high probabilities of success in the drug discovery and development process.[12] Many of them and their derivatives are used as pharmaceutical drugs to treat various diseases,[13–16] such as the analgesic morphine, the antitussive codeine,[13] the antibacterial berberine, the antihuntingtonian tetrabenazine,[14] the antirheumatic sinomenine,[15] the muscle relaxant agent cisatracurium,[14] and the antiparkinsonian apomorphine.[14] In the past five years, duvelisib, a PI3K inhibitor approved by the FDA, has been used to treat adult patients with relapsed or refractory CLL/SLL;[17] roxadustat, which is approved in China, has been used to treat anaemia;[18] and tenapanor, which was approved by the FDA in 2019, has been used to treat

Xiaorong Yang

Xiaorong Yang received his BS in Applied Chemistry from Tiangong University in 2012 and PhD in Organic Chemistry from Lanzhou University in 2020. He is currently a assistant professor of Lanzhou Institute of Husbandry and Pharmaceutical Sciences, CAAS. His research interests include the methodological study of visible light catalysis, structural modification of bioactive compounds from natural products. He has published about 13 articles, applied for more than 10 patents and received several projects.

Xiaolou Miao

Xiaolou Miao received his BS in Pharmacy of Shenyang Pharmaceutical University in 1996. He is currently a associate professor at the Key Laboratory of Veterinary Pharmaceutical Development of Ministry of Agriculture, Lanzhou Institute of Husbandry and Pharmaceutical Sciences, CAAS. His research interests include the design and synthesis of bioactive compounds and natural products, as well as the discovery of antiparasitic lead compounds. He has published about 30 articles, applied for more than 10 patents and received several projects.

Lixia Dai

Lixia Dai received her BS degree in Animal science from Gansu Agricultural University in 2013 and her MS degree in Animal nutrition and feed science from Northwest Agriculture and Forestry University in 2016, and she is currently a PhD student in College of Veterinary Medicine of Gansu Agricultural University. Her research interests include the discovery and mechanism of action of anti parasitic lead compounds, and the comprehensive utilization of non medicinal parts of medicinal materials.

Xiao Guo

Xiao Guo received her BS degree in Bioscience from Northwest Normal University in 2010 and her MS degree in Plant sciences from Northwest Normal University in 2013, and her PhD degree in Veterinary Science from Chinese Academy of Agricultural Science in 2017. Now she is currently an associate professor of Tibetan Medicine College in Qinghai University. Her research interests include the isolation, structural elucidation, and bioactivity of natural products.

constipated irritable bowel syndrome (IBS-C). Recently, lurbinectedin and ensifentrine have also been approved to treat adult patients with metastatic small cell lung cancer (SCLC) disease progression after platinum-based chemotherapy and chronic obstructive pulmonary disease (COPD), respectively. SJ733 and JNJ-74856665 have advanced into the phase 1a/b trials, showing antimalarial efficacy and anti-acute myeloid leukemia (AML) activity, respectively (Fig. 2).[19] Moreover, isoquinoline alkaloids from *Macleaya cordata* exhibit growth-promoting effect, and are widely applied in agricultural fields.[20] Therefore, the search for novel isoquinolines as promising drug leads remains an active area in natural product chemistry.

In view of the importance and significant biological activities of isoquinoline alkaloids, thousands of publications have been released over the past 200 years. We previously reviewed the developments in this field from the perspective of biological activities (covering 2014–2018).[6] Over the past five years, along with novel technology applications, many new studies have been widely performed, and more new alkaloids have been isolated from plants and microorganisms as new leads in the discovery of useful chemotherapeutic agents. Owing to their wide structural diversity and biological activity, isoquinoline alkaloids have always been an important synthetic target for organic synthesis, and chemical synthesis has made considerable progress in the past five years.[14] Moreover, their novel pharmacological activities and comprehensive mechanisms of action have been explored. In 2020, 242 publications were released in the Scopus database, and 105 articles were published in the areas of pharmacology, toxicology, and pharmaceutics.[9] The increasing number of publications reflects the research intensity of this class of compounds, as well as their importance for drug development. A more comprehensive and up-to-date review is merited.

To show the progress of this class of compounds from 2019 to 2023, this review covers for two aspects, (i) the chemical structures and biological activities of newly isolated isoquinoline alkaloids; and (ii) the updated total synthesis and biosynthesis of this class of natural products and the application of new synthesis methodologies and strategies. We hope that this review provides new clues for the discovery of new drugs from naturally occurring isoquinoline alkaloids.

Xiaofei Shang

Xiaofei Shang received his BS degree in Bioscience from Londong University in 2007, his MS degree in Biochemistry from Lanzhou University in 2010, and his PhD degree in Medicinal Chemistry Biology from Lanzhou University in 2019. He worked as a postdoctoral scholar in Beijing Youan Hospital of Capital Medical University in 2020–2023. He is currently a professor of Lanzhou Institute of Husbandry and Pharmaceutical Sciences, CAAS. His research interests include the isolation, structural elucidation, and structural modification of bioactive compounds from natural products. He has published about 50 articles, applied for more than 10 patents and received several projects, including the National Youth Talent Support Program, National Key Research and Development Program of China.

2. Structures and bioactivities of isolated isoquinoline alkaloids

In the past five years, in addition to classical phytochemical methods, modern chromatographic technologies have been widely used to identify isoquinoline alkaloids. A total of 253 new compounds with varied chemical spaces and structural diversities have been isolated and identified from microorganisms and plants, which are present mainly in primitive angiosperms of the families Ranunculaceae, Berberidaceae, Papaveraceae, and Fumariaceae (Table S1†).

2.1. Simple isoquinoline alkaloids

Simple isoquinoline alkaloids are distributed mainly in the genera *Papaver*, *Corydalis*, *Thalictrum* and others, and thirty of

Janar Jenis

Janar Jenis received her BS in applied chemistry from Xinjiang University in 1999 and her PhD in organo-metalic chemistry, catalyze and plant chemistry from Al-Farabi Kazakh National University in 2009. She is currently a Professor at Al-Farabi Kazakh National University. Her research interests include the isolation and identify of bioactive compounds from natural source. She has published more than 80 research articles, applied for more than 10 patents, and directed several projects.

Jiyu Zhang

Jiyu Zhang received his BS in veterinary science from Beijing Agricultural University in 1991 and his PhD in basic veterinary medicine from Jilin University in 2002. He is currently a Professor at Lanzhou Institute of Husbandry and Pharmaceutical Sciences, CAAS. His research interests include the design and synthesis of bioactive compounds as veterinary medicines, as well as drug resistance and safety evaluation. He has published more than 100 research articles, applied for more than 30 patents, and directed several projects.

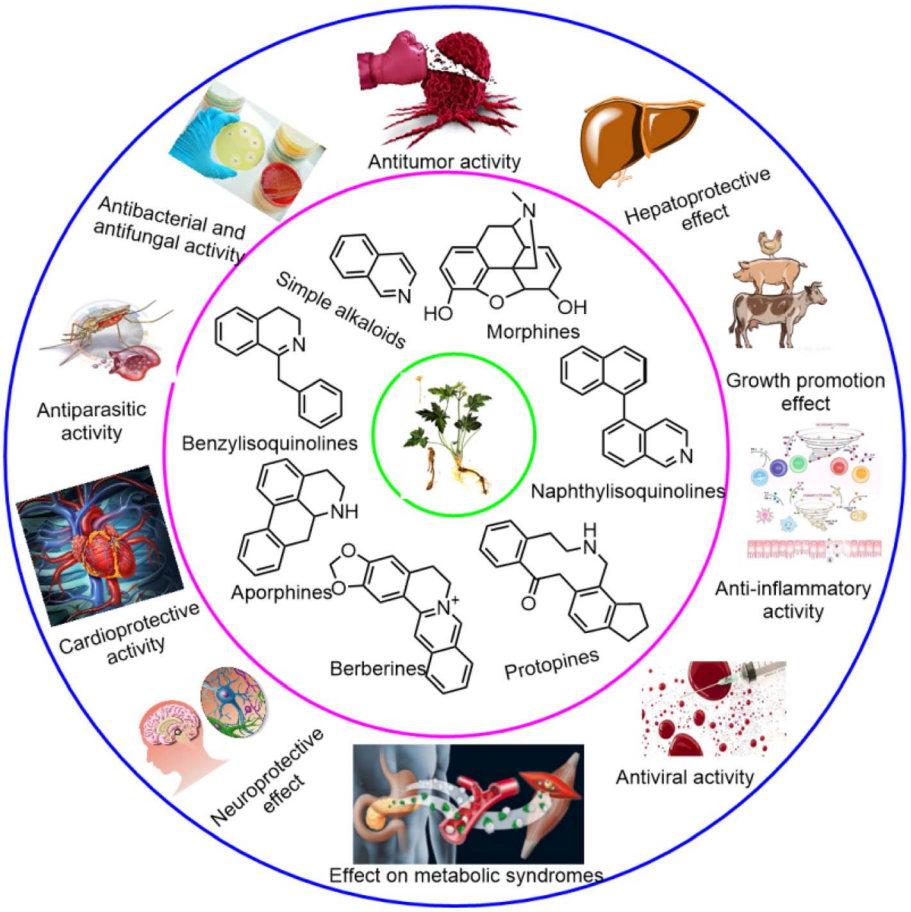

Fig. 1 The structural diversity and bioactivities of isoquinoline alkaloids in nature source.

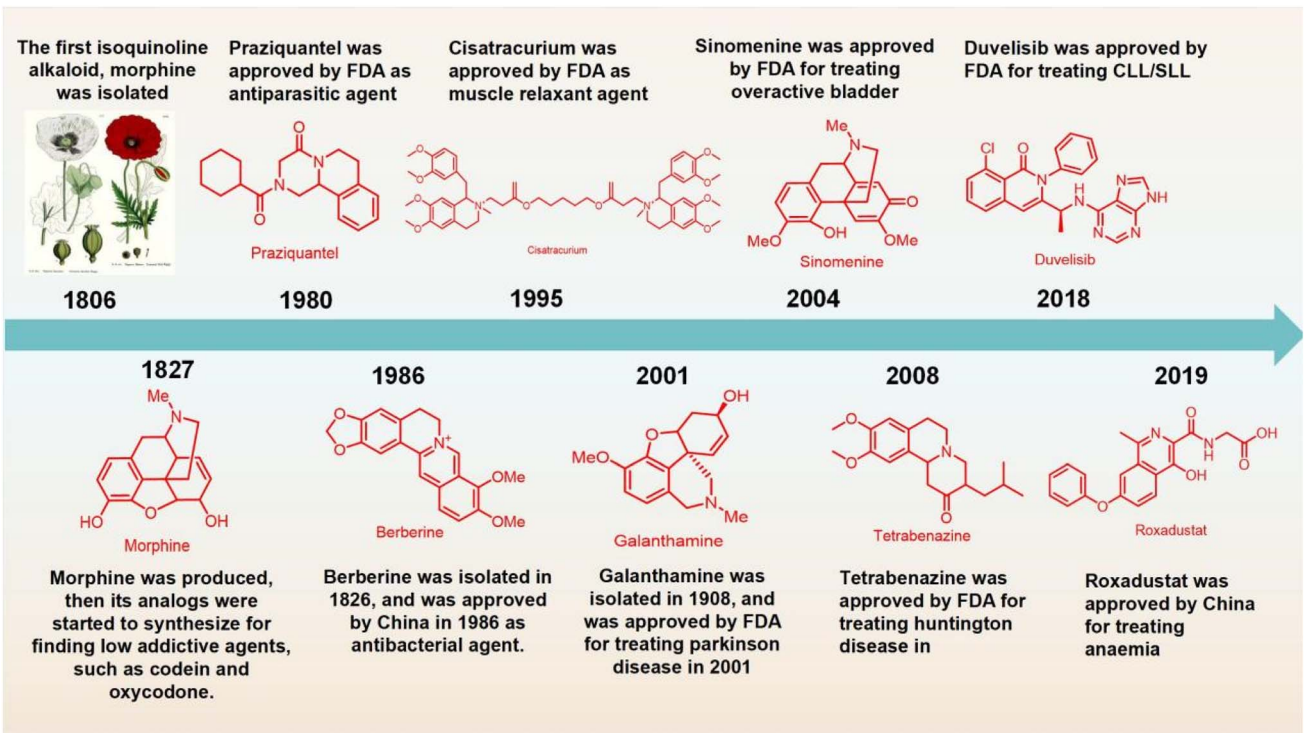

Fig. 2 The development history of some commercially isoquinoline alkaloids and their analogs.

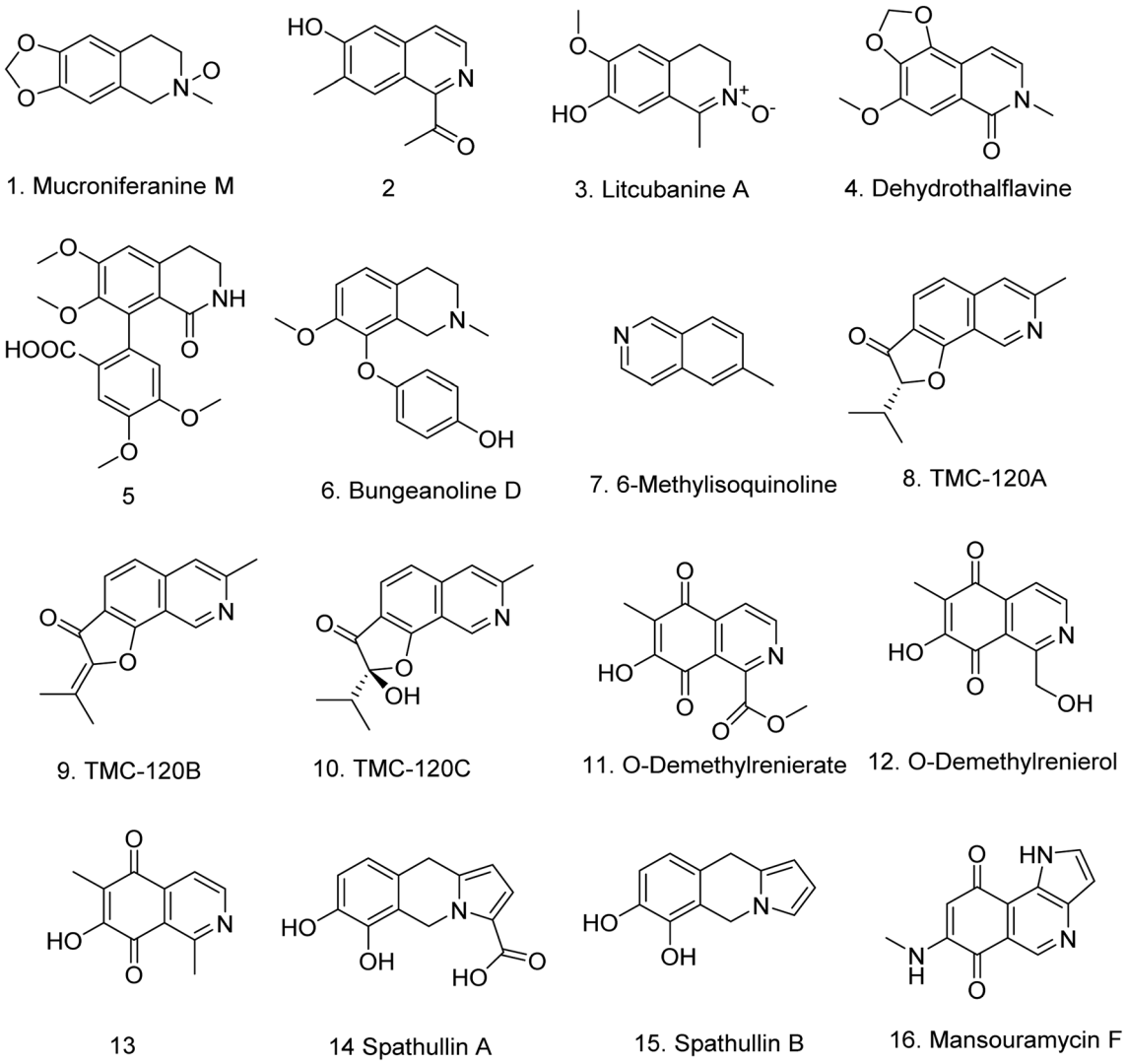

Fig. 3 The chemical structure of compounds 1–16.

these kinds of compounds (**1–30**) were isolated from marine microorganisms and plants from 2019 to the early of 2023 (Fig. 3 and 4).

In 2019, a new simple isoquinoline alkaloid, mucroniferanine M (**1**) was isolated from *Corydalis mucronifera*.[21] In another study conducted in the following year, a new antiviral isoquinoline alkaloid, 1-(6-hydroxy-7-methylisoquinolin-1-yl) ethanone (**2**) from *Thalictrum glandulosissimum*, was found to have prominent anti-tobacco mosaic virus (TMV) activity, with an inhibition rate of 28.4% at 20 μM, which was close to that of the positive control (30.2%).[22] Then, litcubanine A (**3**) with an unusual C-1 methyl group and an N → O group with significant anti-inflammatory activity, was subsequently isolated from *Litsea cubeba*.[23]

More chemicals were found in 2022. From the roots of *Thalictrum cultratum* and *T. baicalense*, a new simple alkaloid, dehydrothalflavine (**4**), was found along with other known compounds.[24] A new 9-phenylisoquinoline alkaloid, (a*S*)-7,8-dimethoxy-9-(2-carboxy-4,5-dimethoxyphenyl)-3,4-dihydroisoquinoline-1(2*H*)-one (**5**), was isolated from the lateral roots of *Aconitum carmichaelii* and was shown to have cardioprotective effects against doxorubicin-induced toxicity in H9c2 cells.[25] Bungeanoline D (**6**), as well as five known benzylisoquinoline alkaloids, namely, (*S*)-norjuziphine, (*S*)-laudanidine, (*S*)-reticuline and (*S*)-armepavine, were isolated from the whole herbs of *Corydalis bungeana*. Among them, (*S*)-reticuline has been shown to have antagonistic effect on the D2 receptor with an IC_{50} value of 2.04 μM [26] (Fig. 3).

Since the first natural isoquinoline isolated from bacteria was reported by Fukum *et al.* in 1977 [27] and then by Kubo *et al.* in 1988,[28] more isoquinoline alkaloids have been found in microorganisms, particularly in marine microorganisms. In 2019, a new isoquinoline alkaloid, 6-methylisoquinoline (**7**), was identified from white button mushrooms (*Agaricus bisporus*),[29] and three compounds TMC-120A (**8**), TMC-120B (**9**) and TMC-120 C (**10**) were isolated from *Aspergillus insuetus*. **8** and **9** were shown to significantly reduce PTZ-induced seizures and epileptiform brain activity.[30] Three new simple

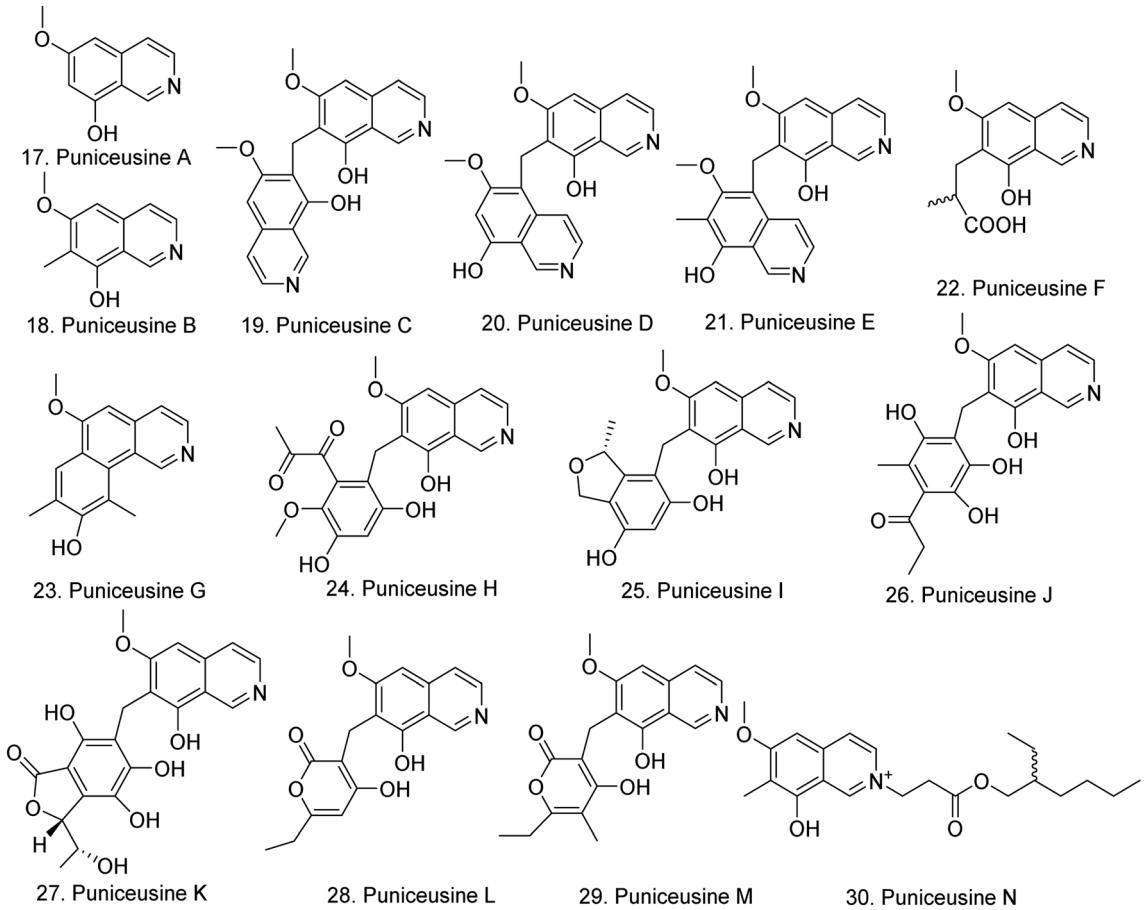

Fig. 4 The chemical structure of compounds 17–30.

isoquinolinequinones containing a 5,8-dioxo-5,8-dihydroisoquinoline moiety, namely, methyl *O*-demethylrenierate (**11**), *O*-demethylrenierol (**12**), and 1,6-dimethyl-7-hydroxy-5,8-dihydroisoquinoline-5,8-dione (**13**), were isolated from the sponge *Haliclona* sp.[31] Moreover, two new compounds, spathullins A (**14**) and B (**15**) were isolated from culture broths of *Penicillium spathulatum* Em19, and are considered promising sources for finding new antibacterial secondary metabolites. In particular, **15** was the most potent against all the tested pathogens, with an MIC as low as 1 μg mL^{-1} (5 μM) against *S. aureus*[32] (Table S3†). Mansouramycin F (**16**), which has significant tumor selectivity against 36 tumor cell lines, was identified from the marine-derived *Streptomyces* sp. isolate B1848[33] (Fig. 3). In the past five years, in the search for find potential antitumor agents from natural products, the cytotoxicities newly isolated isoquinoline alkaloids have been commonly studied (Table S2†).

Puniceusines A–N (**17–30**) (Fig. 4) were subsequently isolated from a deep-sea-derived fungus *Aspergillus puniceus* SCSIO z021. Among them, **19** and **20** showed selective inhibitory activity against the protein tyrosine phosphatase CD45, with IC_{50} values of 8.4 and 5.6 μM (Table S4†), respectively; **20** had moderate cytotoxicity toward H1975 with an IC_{50} value of 11.0 μM (Table S2†); and **30** contained an active center –C=N^+, and exhibited antibacterial activity (Table S3†). The authors also reported that puniceusines C–E and H–M contained an isoquinolinyl, a polysubstituted benzyl or a pyronyl at position C-7 of the isoquinoline nucleus, and substitutions at C-7 of the isoquinoline nucleus will affect their bioactivity.[34]

2.2. Benzylisoquinoline alkaloids

2.2.1 Simple benzylisoquinoline alkaloids. Currently, dereplication strategies involving hyphenated techniques based on liquid chromatography separation and tandem mass spectrometry have been widely applied, and more compounds have been identified from plants. From 2019 to early 2023, twenty-one new benzylisoquinoline alkaloids with significant pharmacological activities were isolated from various plants, and most of these compounds were found in plants of the Lauraceae family, such as the *Ocotea* and *Cryptocarya* species.

In 2020, using HPTLC-DESI-MS^n five known benzylisoquinoline alkaloids, namely, reticuline, magnocurarine, armepavine and coclaurine, were identified from *Ocotea spixiana*.[35] Lima *et al.*[36] identified thirty-one isoquinoline alkaloids from *Annona salzmannii*; however, only *N*,*O*-dimethylcoclaurine *N*-oxide (**31**) is an unprecedented alkaloid that functions as a ligand for acetylcholinesterase. Linderine A (**32**),[37], (+)-*O*,*O*-dimethylautumnaline (**33**),[38] and a new isoquinoline alkaloid

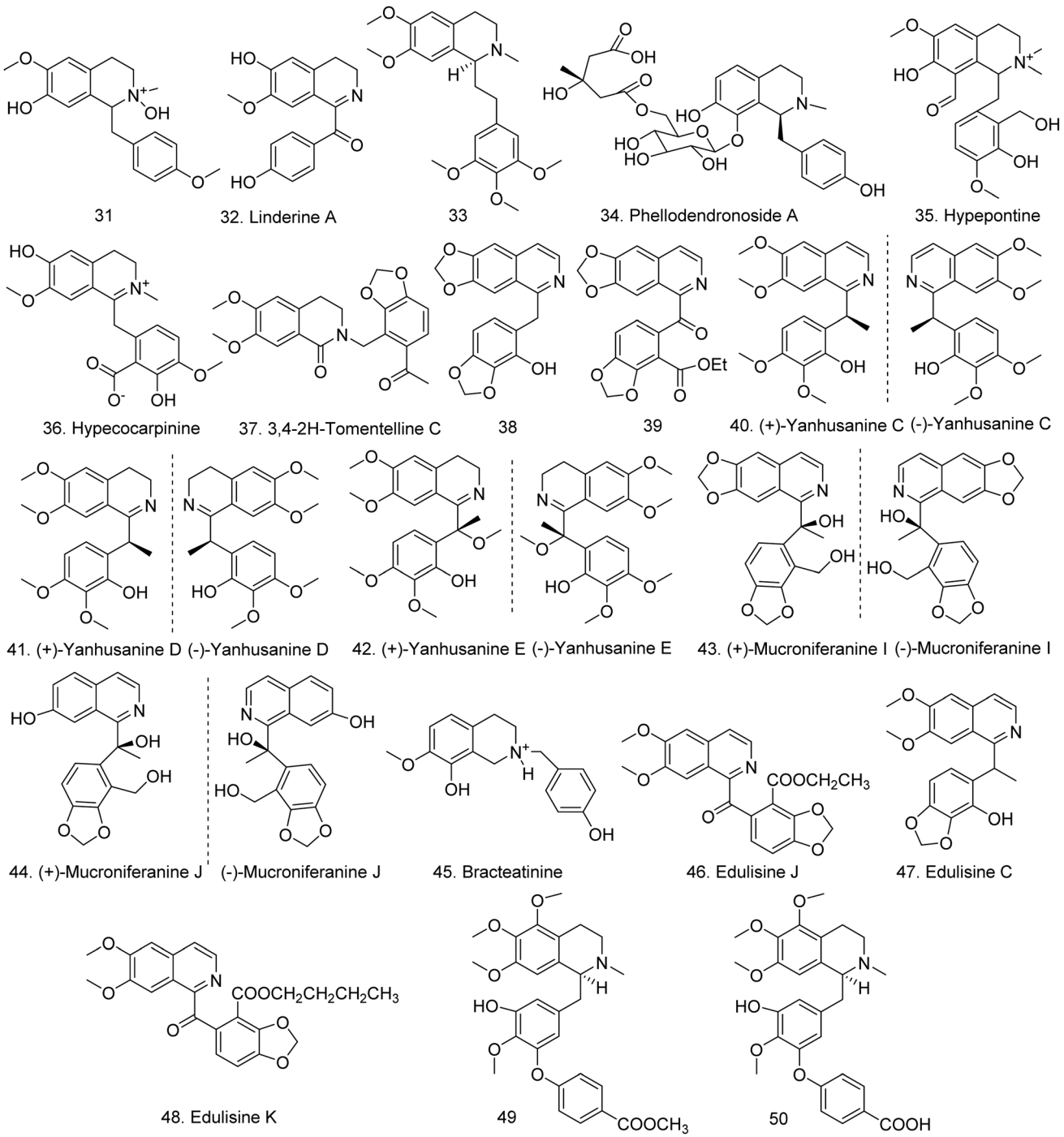

Fig. 5 The chemical structure of compounds **31–50**.

glycoside, phellodendronoside A (**34**)[39] were obtained from *Lindera aggregata*, *Androcymbium palaestinum* and *Phellodendron chinense*. In 2020 and 2022, two new compounds, hypeontine (**35**) and hypecocarpinine (**36**), were identified in *Hypecoum ponticum*,[40,41] respectively, and compound **35** presented an inhibitory effect against *Pseudomonas aeruginosa* (MIC of 64.0 μg mL^{-1}) (Fig. 5).

As noted,[6] the genus *Corydalis* contains many benzyl isoquinoline alkaloids. In 2022, a rare *N*-benzyl isoquinoline alkaloid, 3,4-2*H*-tomentelline C (**37**), was isolated from *C. tomentella* and showed strong cytotoxicity against HepG2 cells, with an IC_{50} value of 7.42 μM.[42] In the same year, 9-demethylmucroniferanine A (**38**) and hendersine B ethyl ester (**39**) were isolated from the Tibetan Medicine *C. hendersonii*; **38** presented the best anti-gastric cancer activity *in vivo* and *in vitro* through topoisomerase I activity, with IC_{50} values of 5.1 μM for MGC-803 cells and 7.6 μM for HGC-27 cells. Further study revealed that it attenuated proliferative capacity, caused G2/M

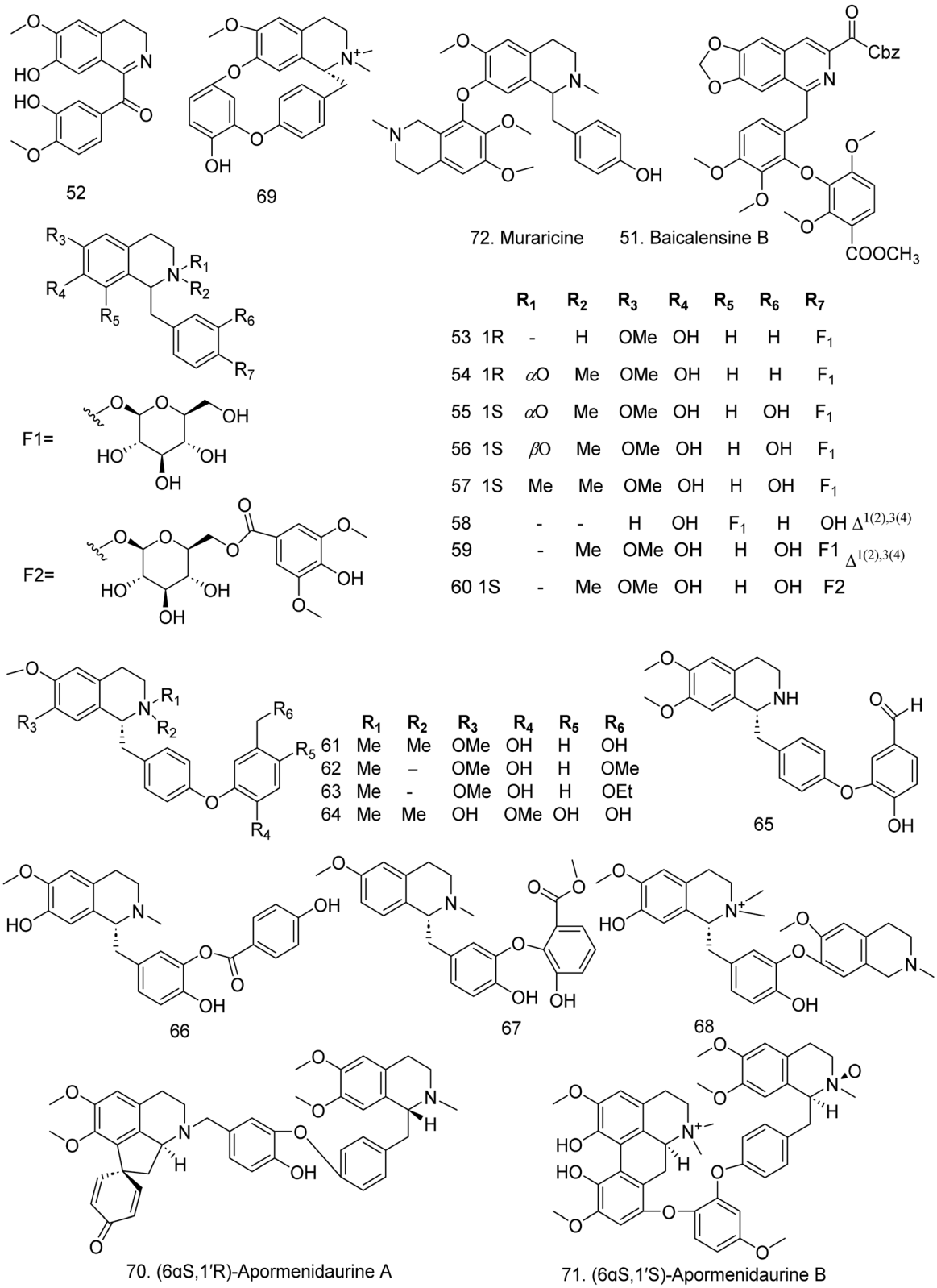

	R_1	R_2	R_3	R_4	R_5	R_6	R_7
53 1R	-	H	OMe	OH	H	H	F_1
54 1R	αO	Me	OMe	OH	H	H	F_1
55 1S	αO	Me	OMe	OH	H	OH	F_1
56 1S	βO	Me	OMe	OH	H	OH	F_1
57 1S	Me	Me	OMe	OH	H	OH	F_1
58	-	-	H	OH	F_1	H	OH $\Delta^{1(2),3(4)}$
59	-	Me	OMe	OH	H	OH	F_1 $\Delta^{1(2),3(4)}$
60 1S	-	Me	OMe	OH	H	OH	F2

	R_1	R_2	R_3	R_4	R_5	R_6
61	Me	Me	OMe	OH	H	OH
62	Me	–	OMe	OH	H	OMe
63	Me	-	OMe	OH	H	OEt
64	Me	Me	OH	OMe	OH	OH

Fig. 6 The chemical structure of compounds 51–72.

phase arrest, inhibited cell migration and invasion, induced cell apoptosis and increased the Bax/Bcl-2 ratio.[43] In addition, from *C. yanhusuo*, five new pairs of isoquinoline alkaloid enantiomers with a rare 9-methyl moiety, designated as yanhusanines B and D–F (**39**, **41–43**), exhibited selective inhibitory activities against human carboxylesterase (hCE2), with IC_{50}

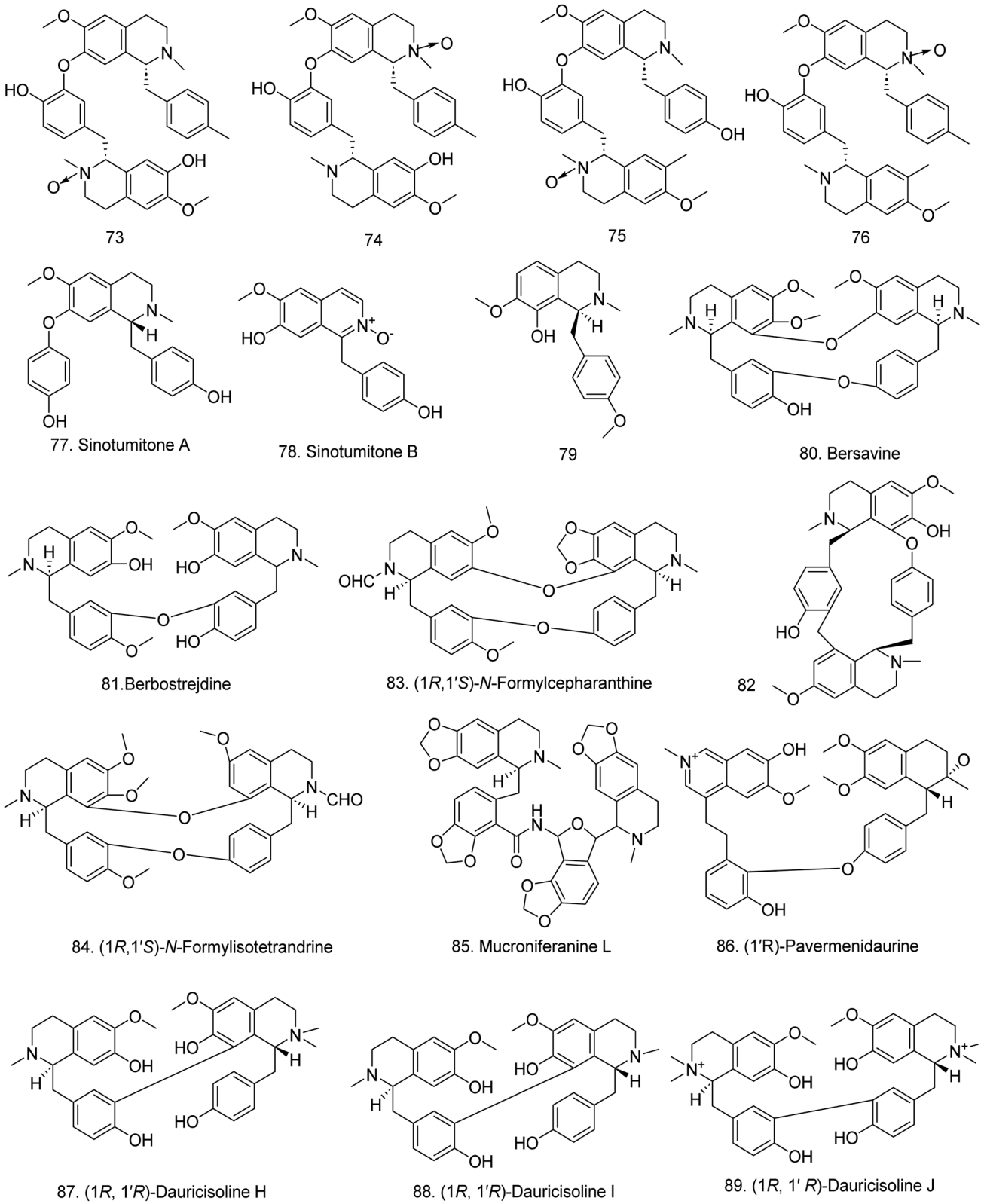

Fig. 7 The chemical structure of compounds 73–89.

values ranging from 2.0–13.2 μM (Table S4†).[44] Mucroniferanines I (**43**) and J (**44**) were isolated from in *C. mucronifera*; however, they do not present cholinesterase inhibition.[21,45] Subsequently, bracteatinine (**45**), which is representative of the rare 2-benzylisoquinoline alkaloid subclass and a close derivative of corgoine, was subsequently isolated from the aerial parts of *C. bracteata*,[46] and edulisine J (**46**), which significantly triggers the secretion of insulin in the HIT-T15 cells at

a concentration of 40 μM, was identified from *C. edulis*, as were edulisines C (**47**) and K (**48**).[47]

From *Thalictrum foliolosum*, Sun and Han isolated 5,6,7,12-tetramethoxy-2-methyl-13-hydroxy-11-(4′-methoxycarbonylphenoxy)-benzylisoquinoline (**49**) and 5,6,7,12-tetramethoxy-2-methyl-13-hydroxy-11-(4′-carbonylphenoxy)benzylisoquin-oline (**50**) (Fig. 5). These compounds exhibited cytotoxic activities against H460, H23, HTB-58, A549, H441, and H2170 cells, with IC_{50} values less than 20 μM.[48] From another species, *T. baicalense*, a benzylisoquinoline bearing a formyl group at C-3, baicalensine B (**51**), was isolated and presented moderate antiproliferative activities against Caco-2 and HL-60 cells.[49] Dehydrooxonorreticuline(3,4-dihydro-7-hydroxy-6-methoxy-1-isoquinoliny-l)(3-hydroxy-4-methoxyphenyl)-methanone (**52**) (Fig. 6) was isolated from *Diclinanona calycina*.[50]

In 2022, from the rhizomes of *Menispermum dauricum*, seventeen benzylisoquinoline alkaloids were isolated and named menisperdaurines A–Q (**53–69**). As glycosidic benzylisoquinolines, menisperdaurines A–E (**53–57**) have glucose moieties attached at the C-12 position. Menisperdaurine H (**60**) is the first example in which benzylisoquinoline and an aromatic unit are connected by a sugar bridge. Menisperdaurine A (**53**) exhibits the highest antagonistic activity (IC_{50} = 1.0 μM).[51] Two aporphine-benzylisoquinoline alkaloids, (6a*S*,1′*R*)-apormenidaurine A (**70**) and (6a*S*,1′*S*)-apormenidaurine B (**71**), were also isolated from this species; the former compound exhibited potent D1 receptor antagonistic activity (IC_{50} = 8.4 μM).[52] Additionally, a new compound, muraricine (**72**) (Fig. 6), was isolated from the root bark of *Berberis vulgaris*.[53] In 2023, Chen *et al.*[54] isolated four new alkaloids, (1*R*,1′*R*) isoliensinine *N*′-oxide (**73**), (1*R*,1′*R*) isoliensinine *N*-oxide (**74**), (1*R*,1′*R*) liensinine *N*′-oxide (**75**), and (1*R*,1′*R*) neferine *N*-oxide (**76**), as well as 10 known compounds from *Plumula nelumbinis*, the green embryo of a lotus seed. **76** at 0.5 μg mL^{-1} significantly reduced melanogenesis in α-MSH-stimulated B16F10 cells, and the tyrosinase (TYR) activity was inhibited by 78.7% at 4 μg mL^{-1}, which was greater than that of α-arbutin (41.3%). Additionally, it exhibited superior antimelanogenic effects compared with α-arbutin in a zebrafish model probably by inhibiting key proteins involved in melanin production, such as the microphthalmia-associated transcription factors TYR, TRP-1, and TRP-2. This result indicates that **76** could be used as a potential drug for treating hyperpigmentation. Two new benzylisoquinoline alkaloids, sinotumitones A (**77**) and B (**78**), were isolated from the stems of *Sinomenium acutum*,[55] (*S*)-1,2,3,4-tetrahydro-7-methoxy-8-hydroxy-2-methyl-13-methoxybenzylisoquinoline (**79**) was obtained from *Fissistigma polyanthum* and exhibited discernible AChE (IC_{50} of 25.6 μM) and BChE (IC_{50} of 33.0 μM) inhibition (Table S4†).[56]

2.2.2 Bisbenzylisoquinoline alkaloids. To date, more than 500 bisbenzyl isoquinoline alkaloids, which contain two benzylisoquinolines linked through diphenyl ether, benzyl phenyl ether, or biphenyl bonds, have been isolated;[7] they widely exist in tropical and subtropical plant families, such as Lauraceae, Menispermaceae, Berberidaceae, and Ranunculaceae.[7]

In addition to muraricine, two new bisbenzylisoquinoline alkaloids, bersavine (**80**) and berbostrejdine (**81**) (Fig. 7) were isolated from *B. vulgaris* in 2019.[53] In addition, Ali *et al.* isolated a novel bisbenzylisoquinoline alkaloid, 13-nitrochondrofoline (**82**), from another species, *B. brevissima*, which showed anti-trypanosomal activity *in vitro*.[57] In the same year, two new bisbenzylisoquinolines, (1*R*,1′*S*)-*N*-formylcepharanthine (**83**) and (1*R*,1′*S*)-*N*-formylisotetrandrine (**84**) were identified from *Stephania cepharantha*. These compounds present the significant inhibitory effects against NO production in overactivated BV2 cells with the IC_{50} values of 12.0 and 12.6 μM, respectively.[58] In the same year, mucroniferanine L (**85**) the first natural amide bond-linked isoquinoline alkaloid dimer from *Corydalis mucronifera*, was reported.[45]

Bisbenzylisoquinoline alkaloids are also found in *Menispermum dauricum*. (1′*R*)-Pavermenidaurine (**86**), consisting of a benzylisoquinoline and a special benzylisoquinoline analog carrying an extra methylene group at C-10, was identified.[52]

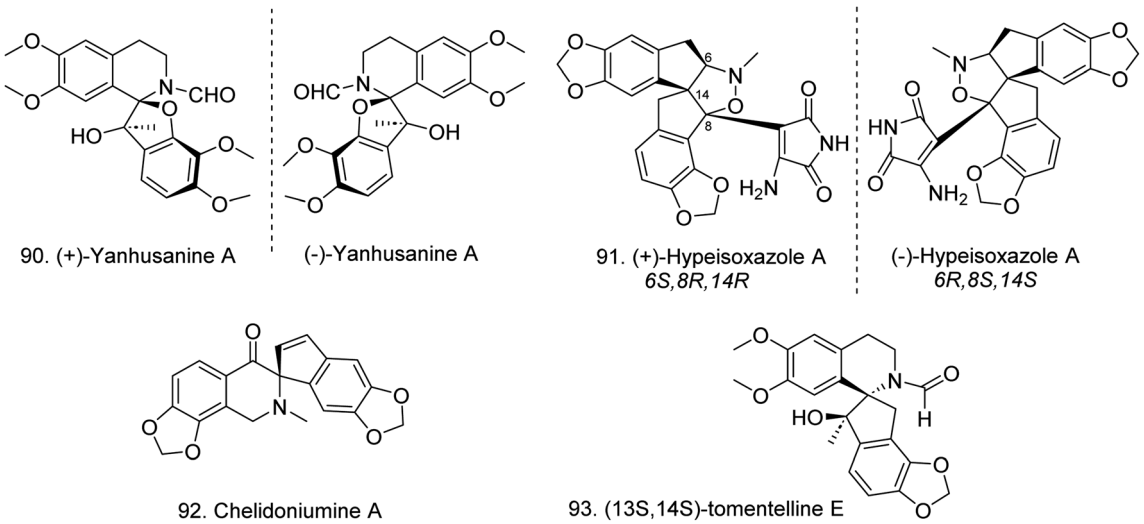

Fig. 8 The chemical structure of compounds **90–93**.

Moreover, three bisbenzylisoquinoline alkaloids with constructed C–C bonds, (1*R*,1′*R*)-dauricisoline H (**87**), (1*R*,1′*R*)-dauricisoline I (**88**) and (1*R*,1′*R*)-dauricisoline J (**89**) (Fig. 7), were isolated.[52]

2.2.3 *Spiro*benzylisoquinoline alkaloids. This type of compound has a unique '*spiro*' structure (Fig. 6) and is distributed in only the plant family Fumariaceae, such as the genera *Corydalis* and *Hypecoum*.

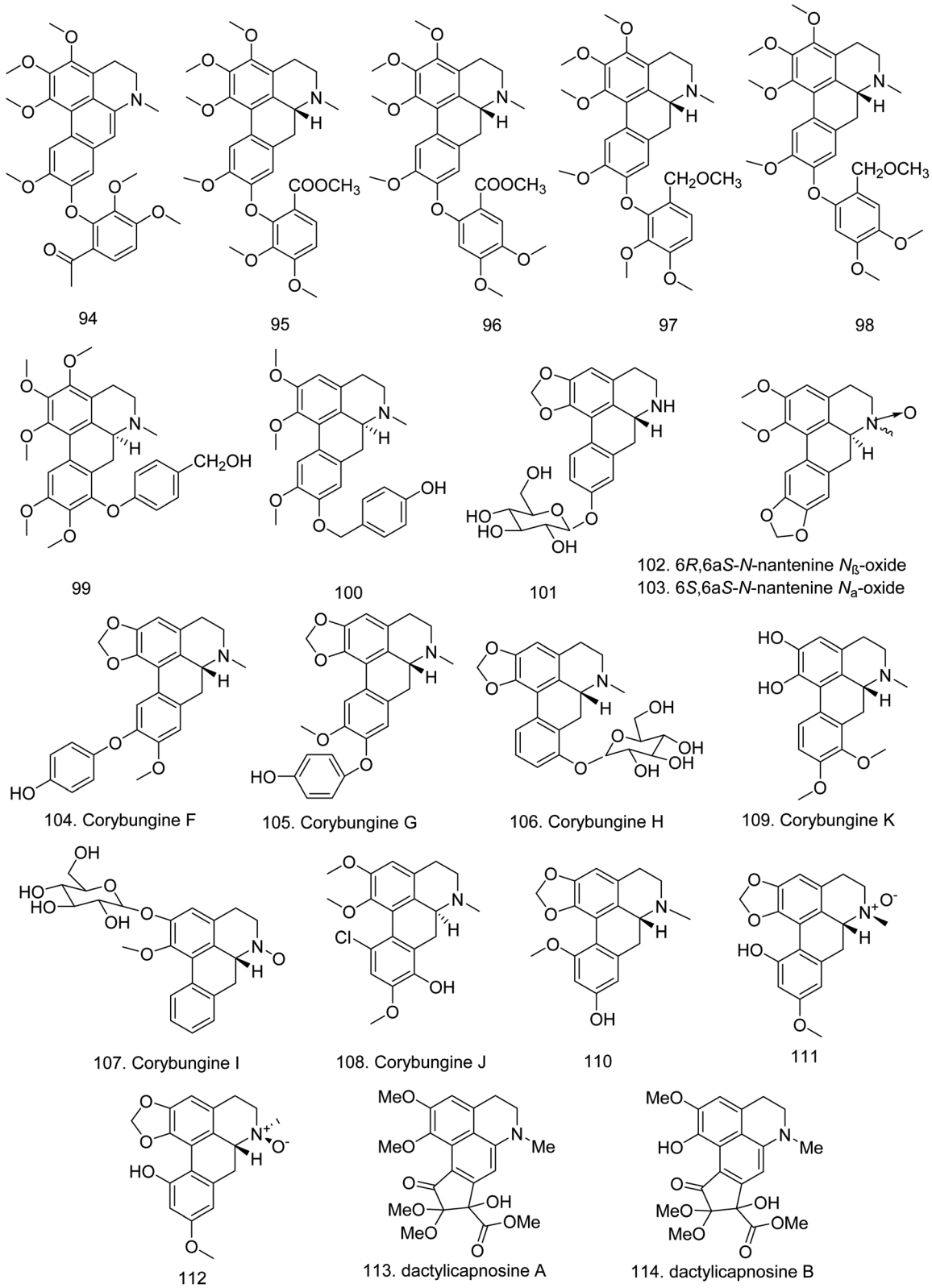

Fig. 9 The chemical structure of compounds **94–114**.

In 2020, from an aqueous extract of *Corydalis yanhusuo* tubers, a *spiro*benzylisoquinoline alkaloid with a rare 1-oxa-6-azaspiro[4.5]decane core containing an *N*-CHO, named groupyanhusanine A, was identified (**90**) (Fig. 8).[44] In 2022, (±)-hypeisoxazole A (**91**), a racemic pair of rearranged alkaloids possessing an unprecedented diindeno [2,1-*c*:2′,1′-*d*] isoxazole scaffold, was subsequently isolated from *Hypecoum erectum*, which presented neuronal excitability activity in a spontaneous calcium oscillation model.[59] Finally, a new alkaloid, chelidoniumine A (**92**), was isolated from the roots and rhizomes of *Hylomecon japonica*,[60] and (13*S*,14*S*)-tomentelline E (**93**) (Fig. 8) from *Corydalis tomentella* showed anti-neuroinflammatory activity at 25 μM against LPS-induced BV2 microglia cells.[61]

2.3. Aporphine isoquinoline alkaloids

Aporphine alkaloids can be classified into subtypes, including simple aporphines, oxoaporphines, dehydroaporphines, proaporphines, and dimeric aporphinoid alkaloids.[62,63]

2.3.1 Simple aporphines. Simple aporphines are the most common type of aporphine isoquinoline alkaloid, they contain a 5,6,6a,7-tetrahydro-4*H*-dibenzo[*de*,*g*]quinoline core substituted primarily with different numbers of hydroxy, methoxy, and methylenedioxy groups.[6] In 2019, five isoquinoline alkaloids, 9-(2′-formyl-5′,6′-dimethoxyphenoxy)-1,2,3,10-tetramethoxy dehydroaporphine (**94**), (−)-9-(2′-methoxycarbonyl-5′,6′-dimethoxyphenoxy)-1,2,3,10-tetramethoxy aporphine (**95**), (−)-2′-methoxycarbonyl thaliadin (**96**), (−)-9-(2′-methoxyethyl-5′,6′-dimethoxyphenoxy)-1,2,3,10-tetramethoxy aporphine (**97**), and (−)-3-methoxy hydroxyhernandalinol (**98**), together with six known alkaloids were isolated from the roots of *Thalictrum foetidum*. **94** and **95** showed selective cytotoxicity against GSC-3# and GSC-18# with IC_{50} values ranging from 2.36 to 5.37 μg mL^{-1} (Table S2†).[64] From another species, *T. tenue*, 3-methoxy-8-(4′-hydroxymethylphenoxy)glaucine(**99**), and 6a*S*-1,10-dimethoxy-natalamine (**100**) (Fig. 9) were isolated from the 90% ethanol extract, and they exhibited some cytotoxic activities against six esophageal carcinoma cell lines (KYSE510, KYSE-180, KYSE-450, EC-109, CEC2, and EC-9706) with IC_{50} values less than 20 μM.[65] In the same year, a new aporphine glycoside, (−)-anolobine-9-*O*-β-D-glucopyranoside (**101**), was obtained from the twigs of the pawpaw (*Asimina triloba*).[66]

In 2020, two oxide isoquinoline alkaloids, 6*R*,6a*S*-*N*-nantenine N_β-oxide (**102**) and 6*S*,6a*S*-*N*-nantenine N_α-oxide (**103**), were subsequently isolated from the seeds of *Nandina domestica*.[67] Six aporphine alkaloids, corybungines F–K (**104–109**) (Fig. 9), have been isolated from *Corydalis bungeana*. Among them, corybungines H presented moderate D2 antagonism in CHO-D2 cells, with an IC_{50} value of 9.12 μM.[26] Additionally, (*R*)-1,2-methylenedioxy-9-methoxy-11-hydroxyaporphine (**110**), (6*S*,6a*R*)-*N*-methylcalycinine-N_α-oxide (**111**), and (6*R*,6a*R*)-*N*-methylcalycinine-N_β-oxide (**112**) were also isolated from *Fissistigma polyanthum*.[56]

In 2019, dactylicapnosines A (**113**) and B (**114**) (Fig. 9), two reconstructed aporphine alkaloids with unprecedented five-membered carbon rings, were isolated from the stems of *Dactylicapnos scandens*.[68] **113** exerts significant *in vivo* anti-inflammatory and analgesic effects by inhibiting the expression of TNF-α, IL-1β, and PGE2, whose activities are superior to those of the control drug isocorydine.

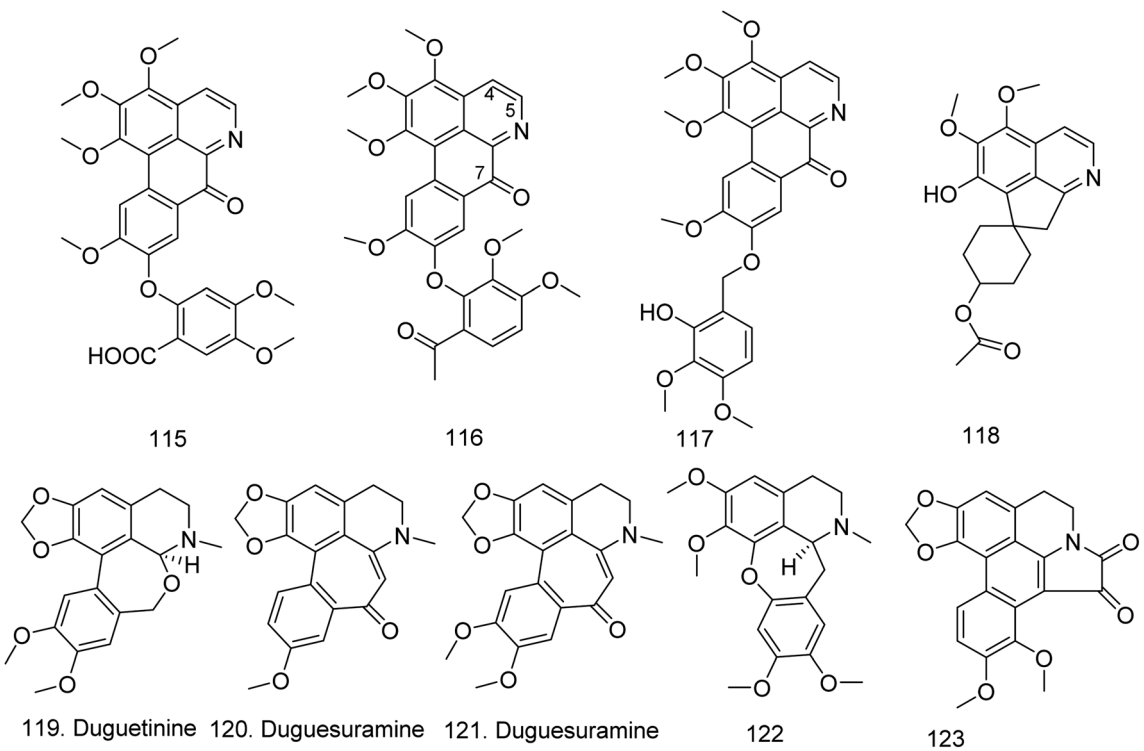

Fig. 10 The chemical structure of compounds **115–123**.

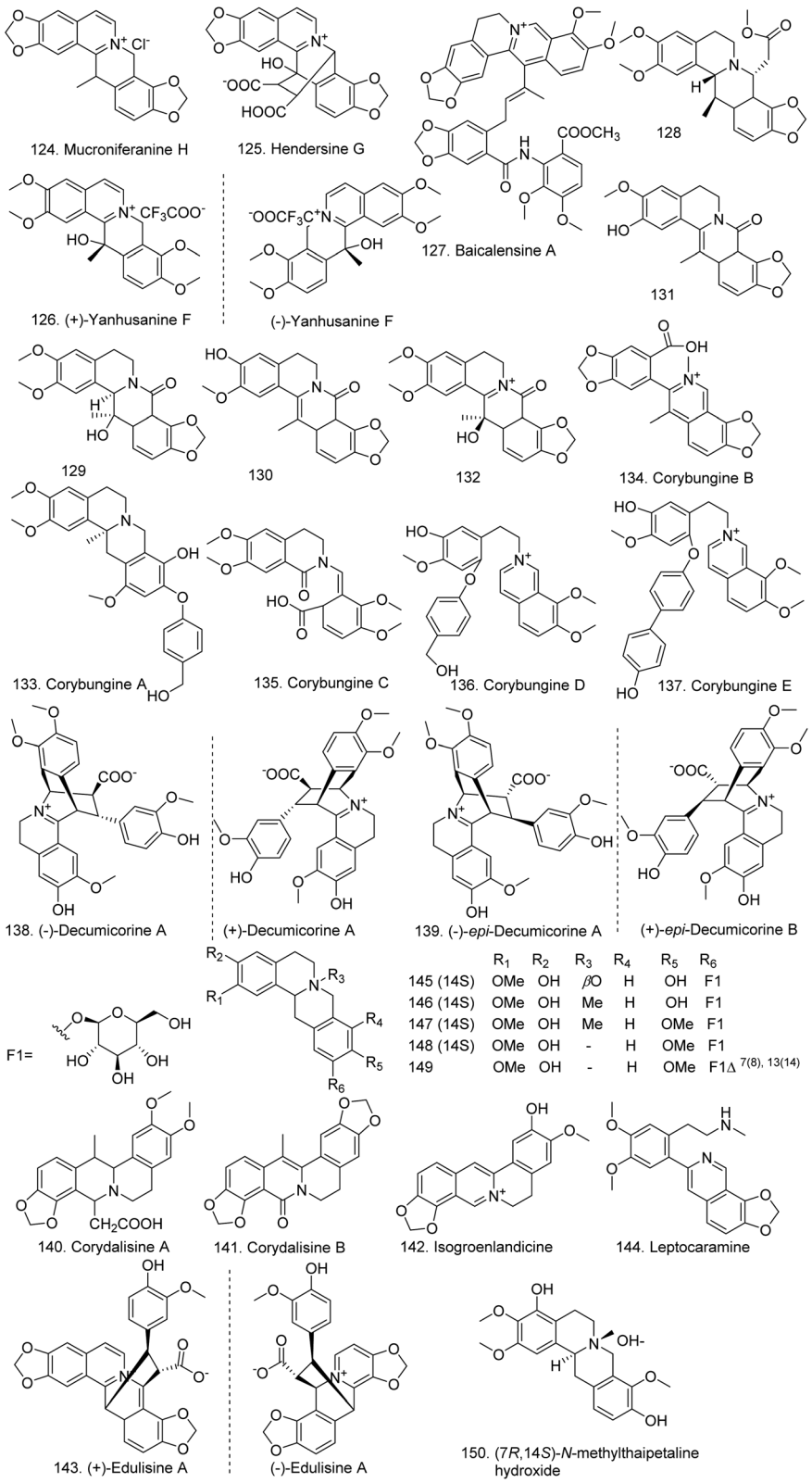

Fig. 11 The chemical structure of compounds **124–150**.

2.3.2. 7-Substituted aporphines and oxoaporphines. 7-Oxygenated aporphines have a hydroxyl or methoxy group at C-7 or two such groups at C-4 and C-7. 7-Methylated aporphines also occur. The oxoaporphines and oxoisoaporphines have an aromatic isoquinoline (aromatic ring B in the tetracyclic structure) and a carbonyl group at C-7.[6,63]

More oxoaporphines, such as 3-methoxy-2′-carbonyl-oxohernandalin (**115**) (from *T. tenue*), were isolated from the

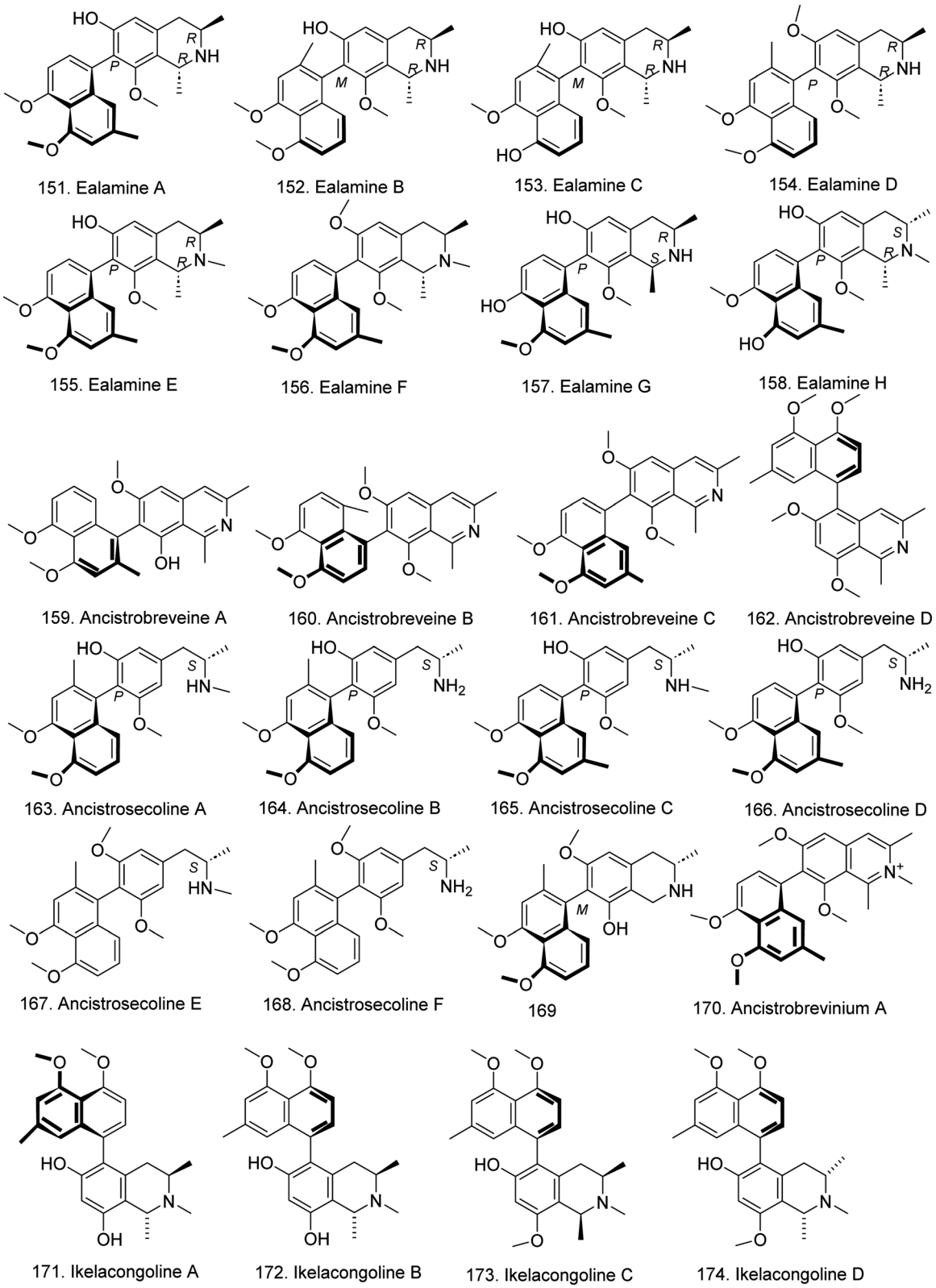

Fig. 12 The chemical structure of compounds 151–174.

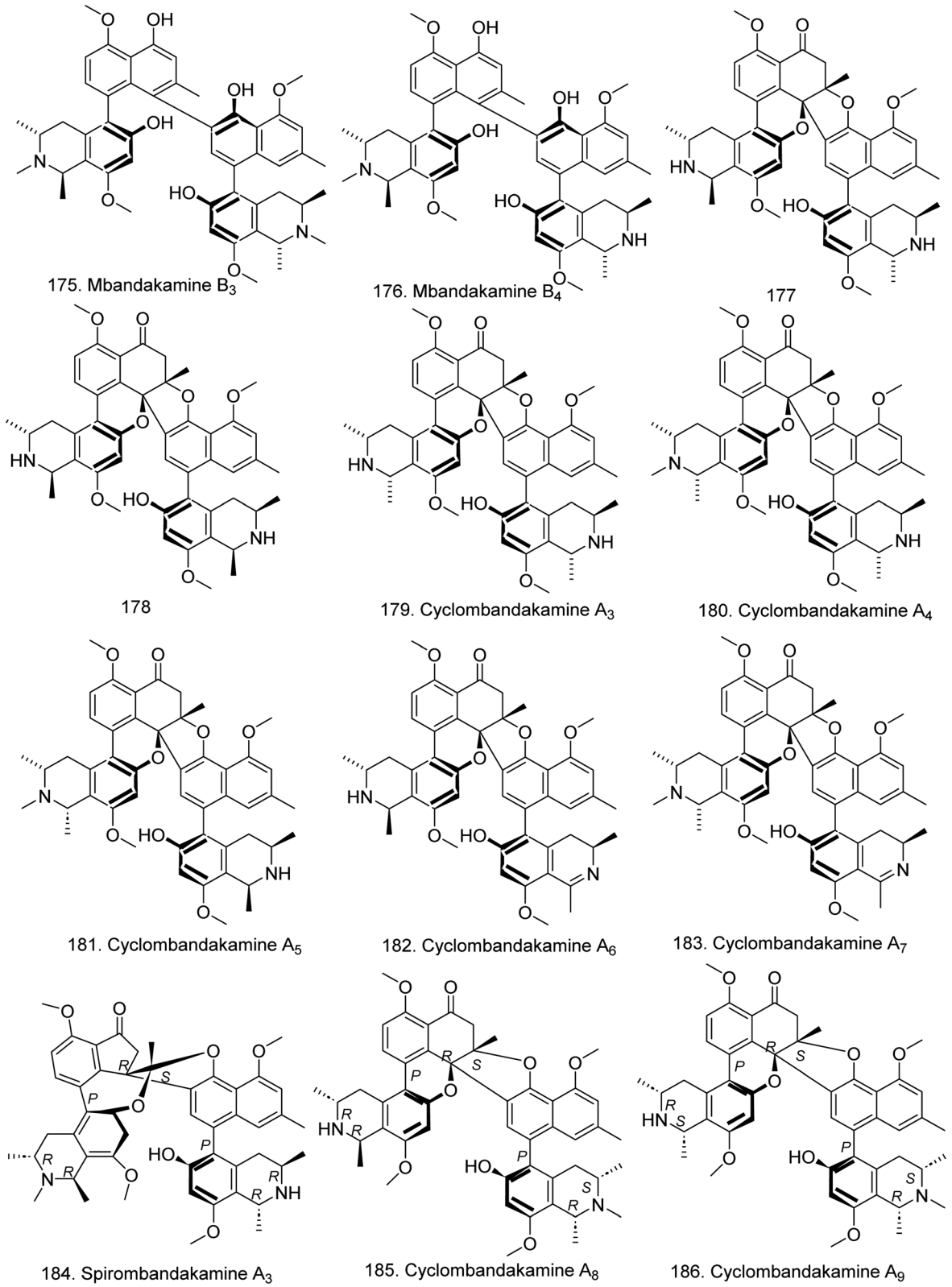

Fig. 13 The chemical structure of compounds 175–186.

genus *Thalictrum*.[65] Two new isoquinoline alkaloids, 9-(2′-formyl-5′,6′-dimethoxyphenoxy)-1,2,3,10-tetramethoxy oxoaporphine (**116**) and 3-methoxy-2′-formyloxohernandalin (**117**), were found in the roots of *T. foetidum*.[64]

2.3.3 Proaporphines and others. The tetracyclic system (2′,3′,8′,8a′-tetrahydro-1′*H*-spiro[cyclohexane-1,7′-cyclopenta[*ij*]isoquinoline]) of proaporphine alkaloids is composed of a bicyclic isoquinoline fused to a five-membered ring that is connected to

a six-membered ring through a spiro carbon.[6] In 2021, a new alkaloid, 3-methoxy-10-*O*-acetylprodensiflorin B (**118**) (Fig. 10), was isolated from *Thalictrum foliolosum*; however, it was not cytotoxic to eight types of cancer cells.[51]

In 2019, three new alkaloids with unprecedented oxahomoaporphine and 8-oxohomoaporphine skeletons were isolated from the bark of *D. surinamensis*, and named duguetinine (**119**), duguesuramine (**120**) and 11-methoxyduguesuramine (**121**) (Fig. 10). Among them, duguetinine has an unusual oxahomoaporphine skeleton bearing an oxepane moiety, and duguesuramine and 11-methoxyduguesuramine contain an extra carbon between the tetrahydroisoquinoline and the pendant aromatic rings.[63] In addition, a newly reported cularine alkaloid (*S*)-2,3,12,12a-tetrahydro-5,6,9,10-tetramethoxy-1-methyl-1*H*-[1]benzoxepino[2,3,4-*ij*]-isoquinoline (**122**), along with four known alkaloids were isolated from the roots of *Stephania cepharantha*; however, they were not cytotoxic to three human cancer cell lines (A549, MCF-7, and SW480).[69] In addition to three simple aporphines, an oxalyl-fused dehydroaporphine alkaloid, 8,9-dimethoxylettowianthine (**123**) (Fig. 10), and the known compound lettowianthine, were isolated from *Fissistigma polyanthum*.[56]

2.4. Berberine and protoberberine isoquinoline alkaloids

These kinds of compounds, such as berberine, exhibit various pharmacological effects. In the past five years, more compounds have been identified from the genus *Corydalis*. In 2019, mucroniferanine H (**124**) from *Corydalis mucronifera* presented the inhibitory effects on AChE and BuChE, with IC_{50} values of 2.31 μM and 36.71 μM, respectively (Table S4†),[45] as a new compound, hendersine G (**125**) was isolated from the whole plant of *C. hendersonii*, as were other known hendersines B–F.[70] In 2020, yanhusanine F (**126**) was identified from an aqueous extract of *C. yanhusuo* tubers.[44] A new class of alkaloid dimer, baicalensine A (**127**) (Fig. 11), which contains berberine conjugated to a ring-opened isoquinoline, was isolated from *Thalictrum baicalense*; it presented moderate antiproliferative activities against Caco-2 and HL-60 cells with IC_{50} values of 9.24 and 10.15 μM, respectively, while those of positive control 5-FU were 20.24 and 3.15 μM, respectively (Table S2†).[49]

Five new isoquinoline alkaloids, (8*R*,13*R*,14*R*)-8-methoxycarbonylmethyl thalictrifoline (**128**), (13*R*,14*R*)-13-hydroxy-13-methyl-8-oxosinactine (**129**), tomentelline F (**130**) and isotomentelline F (**131**) (Fig. 11) were isolated from *Corydalis tomentella*, and **129** showed good anti-neuroinflammatory activity.[61] Additionally, 13*R*-tomentelline (**132**) was also isolated.[42] Moreover, corybungines A–E (**133–137**) including a protoberberine-type alkaloid (**133**), with a unique 6-norprotoberberine skeleton (**134**), one 13,14-*seco*-protoberberine-type alkaloid containing a carboxyl group at C-12 (**135**), and two 1a,14-*seco*-protoberberine-type alkaloids with a 4-(hydroxymethyl)phenoxy moiety (**136**, **137**) have been isolated from the whole herb extract of *C. bungeana*.[71] Subsequently, (±)-decumicorine A (**138**) and

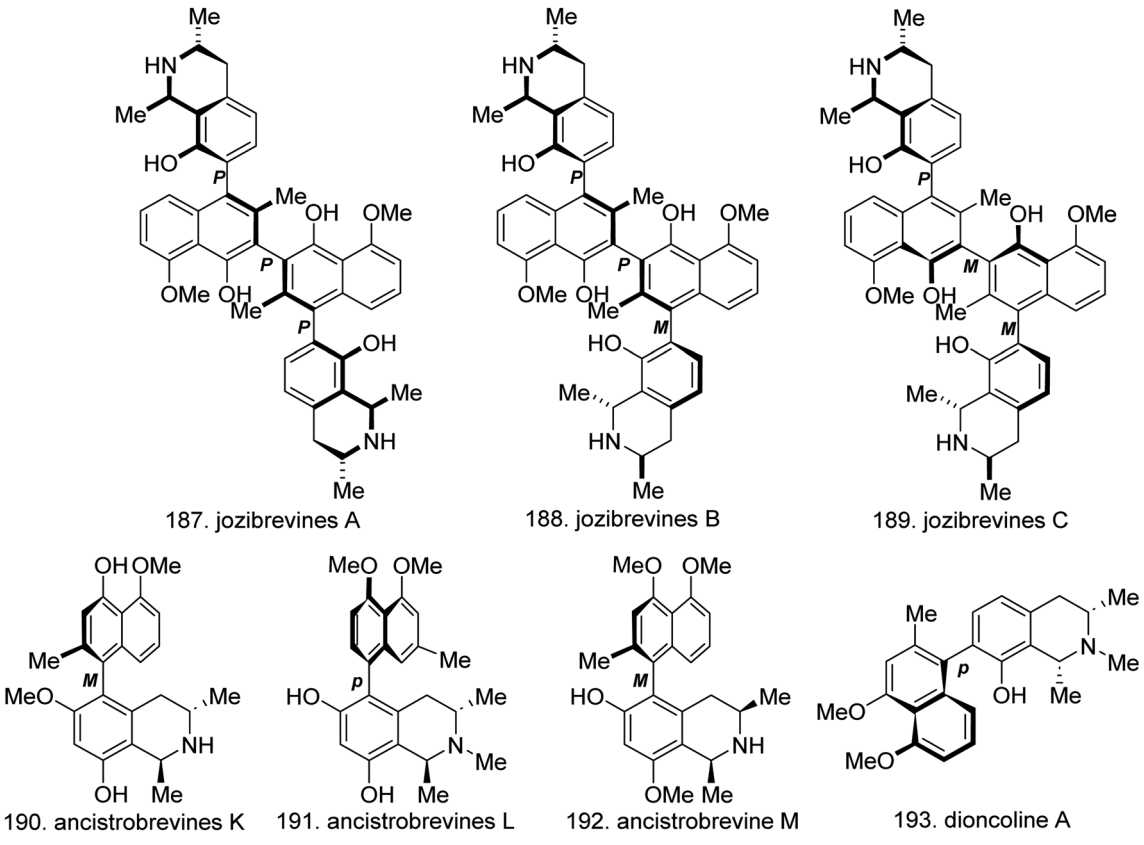

Fig. 14 The chemical structure of compounds **187–193**.

(±)-*epi*-decumicorine A (**139**), two pairs of enantiomeric isoquinoline alkaloids featuring a novel phenylpropanoid-conjugated protoberberine skeleton, were isolated from the rhizomes of *C. decumbens*. **138** exhibited an antiviral entry effect on SARS-CoV-2 pseudovirus by blocking spike binding to the ACE2 receptor on HEK-293T-ACE2^{h} host cells within their maximum nontoxic concentration of 100 μM.[72]

Dai *et al.*,[73] *via* the HSQC-based small molecule accurate recognition technology (SMART) strategy, discovered 19 compounds from *C. saxicola* in 2023, among which corydalisines A (**140**) and B (**141**) were new isoquinoline alkaloids. Unfortunately, none of them presented cytotoxicity against six human cancer cell lines. Isogroenlandicine (**142**), which does not affect platelet function, was isolated from *C. bracteata*.[46] An undescribed isoquinoline alkaloid, edulisine A (**143**), which has a unique coupled pattern of coptisine and ferulic acid *via* Diels–Alder [4 + 2] cycloaddition, was isolated from *C. edulis*.[47]

Moreover, from *Hypecoum leptocarpum*, a new compound leptocaramine (**144**) along with five known compounds, leptopidine, corydamine, protopine, dihydroprotopine and oxohydrastinine, were found, which presented strong activity against A549 cells and moderate cytotoxicity against MGC-803 cells with IC_{50} values of 6.68 and 27.98 μg mL^{-1}, respectively (Table S2†).[41] From the rhizomes of *Menispermum dauricum*, five protoberberine analogs, menisperdaurines R–V (**145–149**) (Fig. 11), were also isolated.[51] Finally, (7*R*,14*S*)-*N*-methylthaipetaline hydroxide (**150**) with a pentaoxygenated *N*-methyltetrahydroprotoberberine core structure was identified from *Fissistigma polyanthum* without anti-AChE and anti-BChE activities.[56]

2.5. Naphthylisoquinoline alkaloids

Naphthylisoquinolines are a group of structurally diverse secondary metabolites containing both naphthalene and isoquinoline bicyclic systems connected by a *C*,*C* or *C*,*N* biaryl axis, and dimeric representatives. These compounds presented outstanding antitumor and antiparasitic activities, especially against leishmaniasis and trypanosomiasis. Since 1970, the first *C*,*C*-coupled alkaloid, ancistrocladine, was discovered from the Indian plant *Ancistrocladus heyneanus*, and more than 250 structurally divergent monomeric and dimeric naphthylisoquinoline alkaloids have been identified. Most of these compounds have been isolated from only the tropical plant families Ancistrocladaceae and Dioncophyllaceae of Asian and African lianas and are classified as dioncophyllaceae-type alkaloids and ancistrocladaceae-type alkaloids. Dioncophyllaceae-type alkaloids have an *R*-configuration at C-3 and lack an oxygen function at C-6. Structurally similar Ancistrocladaceae-type alkaloids have been found in closely related Ancistrocladaceae plant families.[8,74] Over the past two decades, extensive studies on the isolation and bioactivity evaluation of naphthylisoquinoline alkaloids have been carried out by Bringmann's group and other groups.[75–88]

In the past five years, additional compounds have been identified from the tropical liana *Ancistrocladus* sp. by this group, and their antiplasmodial or cytotoxic activities have also been explored. In 2019, from the twigs and leaves of the Central African liana *A. ealaensis*, ten rarely unprecedented 7,8′-coupled naphthylisoquinoline alkaloids were isolated, including eight new compounds, named ealamines A–H (**151–158**) (Fig. 12), and two known compounds, 6-*O*-demethylancistrobrevine A and

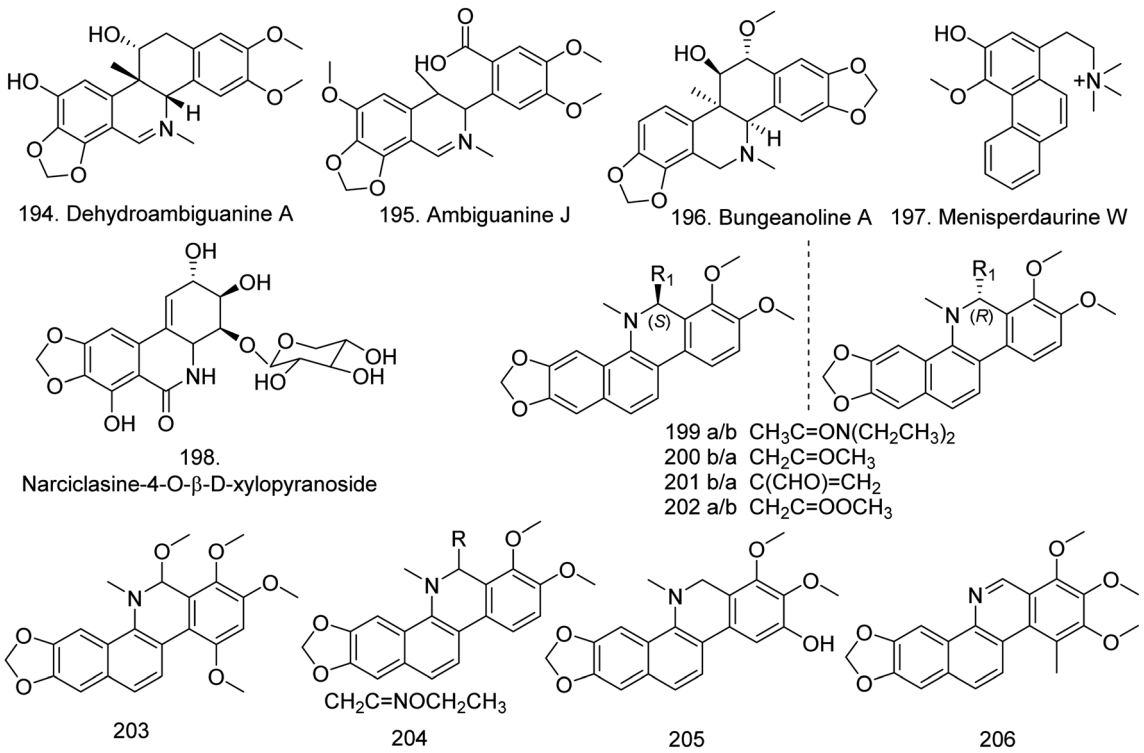

Fig. 15 The chemical structure of compounds **194–206**.

yaoundamine A. Among them, ealamines A–G (**151–157**) are the first 7,8′-linked "hybrid-type" naphthylisoquinoline alkaloids, *i.e.*, 3*R*-configured and 6-oxygenated in the tetrahydroisoquinoline part, and ealamine H (**158**) is a typical Ancistrocladaceae-type alkaloid, with a 3*S*-configuration at C-3 and an oxygen function at C-6. **151–157** exhibited specific antiplasmodial activities against *Plasmodium*, *Trypanosoma* and *Leishmania* and displayed preferential cytotoxic effects toward PANC-1 cells; ealamine C was the most potent agent, with a PC_{50} value of 9.9 μM.[89]

Moreover, ancistrobreveines A–D (**159–162**) (Fig. 12) with five coupling types (5,1′, 7,1′, 7,8′, and 5,8′) were identified from *A. abbreviatus*. **161** is the first example of a 7,8′-linked fully dehydrogenated naphthylisoquinoline discovered in nature that is configurationally stable at the biaryl axis, and that exhibited antiproliferative activities against drug-sensitive acute lymphoblastic CCRF-CEM cells and the multidrug resistant (MDR) subline, CEM/ADR5000.[90] This group subsequently discovered seven new ancistrocladaceae-type *seco*-naphthylisoquinoline alkaloids, ancistrosecolines A–F (**163–168**), along with 1-*nor*-8-*O*-demethylancistrobrevine H (**169**) (Fig. 12). The tetrahydroisoquinoline ring of **163–168** is cleaved, with loss of C-1, and **169** is the first naturally occurring naphthylisoquinoline lacking the otherwise generally present methyl group at C-1. Among them, ancistrosecoline D exhibited strong cytotoxicity against HeLa cells with an IC_{50} value of 11.2 μM.[91] In addition, the first *N*-methylated, cationic naphthylisoquinoline alkaloid, ancistrobrevinium A (**170**) was discovered in the root bark extract of *A. abbreviatus*, and showed weak cytotoxic activity against A549 cells (IC_{50} = 50.6 μM) (Table S2†).[92] Five related 5,8′-linked monomeric alkaloids, named ikelacongolines A–D (**171–174**) (Fig. 12), and two constitutionally unsymmetric dimers, mbandakamines B_3 (**175**) and B_4 (**176**) (Fig. 13), were identified from *A. korupensis* and *A. ealaensis*. The dimers **177** and **176** are structurally unusual quateraryls comprising two 5,8′-coupled monomers linked *via* a sterically strongly constrained 6′,1″-connection between their naphthalene units.[93]

In 2019, a series of unusual dimeric naphthylisoquinoline alkaloids, namely, cyclombandakamine A (**177**), 1-*epi*-cyclombandakamine A (**178**), and cyclombandakamines A_{3-7} (**179–183**) (Fig. 13), were isolated from the leaves of the tropical liana *A. ealaensis* and have a chemically thrilling structural array consisting of a twisted dihydrofuran-cyclohexenone-isochromene system.[94] Then, spirombandakamine A_3 (**184**) and cyclombandakamines A_8

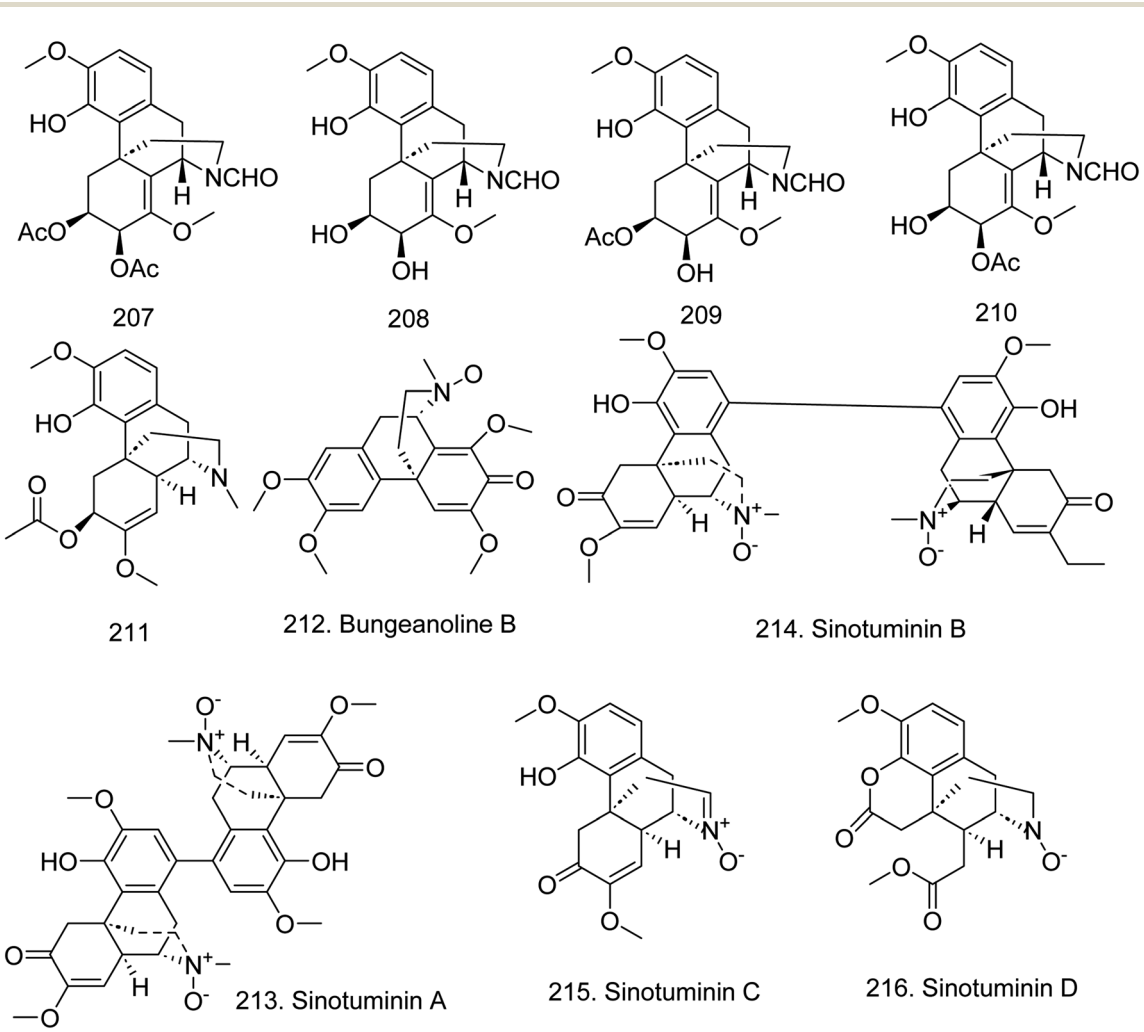

Fig. 16 The chemical structure of compounds **207–216**.

(**185**) and A_9 (**186**) (Fig. 13), three polycyclic naphthylisoquinoline dimers, along with mbandakamines C and D, were found in the leaves of a botanically as of yet unidentified Congolese *Ancistrocladus* plant, which is morphologically closely related to *A. ealaensis*. **184** is only the third known naphthylisoquinoline dimer with a novel *spiro*-fused novel molecular framework and the first such representative to possess a relative *trans*-configuration at the two chiral centers in both tetrahydroisoquinoline subunits.[95]

Three new *Dioncophyllaceae*-type naphthylisoquinoline dimers, jozibrevines A–C (**187–189**) (Fig. 14), were subsequently isolated from *A. abbreviatus*, along with the known dimer jozimine A2. These compounds have the same constitutions and identical absolute configurations at the five stereogenic centers but differ in their axial chirality. Two typical Ancistrocladaceae-type monomeric compounds, ancistrobrevines K (**190**) and L (**191**), with the *S*-configuration at C-3 and an oxygen function at C-6 were identified. A new hybrid-type alkaloid, ancistrobrevine M (**192**) was identified, which is 3*R*-configured and 6-oxygenated, and an "inverse hybrid-type" counterpart, dioncoline A (**193**) (Fig. 14), which is a 3*S*-configured naphthylisoquinoline lacking an O-functionality at C-6, were isolated. They showed the pronounced antiplasmodial activities in the submicromolar range.[96]

2.6. Phenanthridine alkaloids

Phenanthridine isoquinoline compounds occur in higher plants and show a wide spectrum of nonspecific biological activities.[6] Sanguinarine is one of the most famous compounds in this class. In 2020, one benzophenanthridine type, dehydroambiguanine A (**194**) and one isoquinoline type, ambiguanine J (the C ring of a benzophenanthridine-type alkaloid was opened) (**195**) (Fig. 15), were isolated from the *n*-butanol fraction of *Corydalis ambigua* subsp. *amurensis*. Among them, **194** exhibited anti-proliferative activity on HCT 116 cells, with an IC_{50} value of 49.8 μM, and ambiguanine J showed activity against A549 cells with an IC_{50} value of 60.2 μM (Table S2†).[97] Three new compounds, bungeanoline A (**196**), menisperdaurine W (**197**) and narciclasine-4-*O*-β-D-xylopyranoside (**198**), were subsequently isolated from *C. bungeana*,[71] *Menispermum dauricum*,[51] and *Zephyranthes minuta*[6] (Fig. 15), respectively.

Six pairs of enantiomeric isoquinoline alkaloids 6*S*/*R*-(*N*,*N*-diethylacetamido)yl-dihydrochelerythrine (**199**), 6*R*/*S*-acetonyl-9-hydroxy-dihydrochelerythrine (**200**), 6*S*/*R*-acroleinyl-dihydrochelerythrine (**201**), 6*S*/*R*-acetatemethyl-dihydrochelerythrine (**202**), 6,10-dimethoxydihydrochelerythrine (**203**), 6-ethoxy-ethaniminyl dihydroche-landine (**204**), 9-hydroxy-dihydrochelerythrine (**205**), and 9-methoxy-10-hydroxy-norchelerythrine (**206**) (Fig. 15) were isolated from the roots and rhizomes of *Hylomecon japonica*. Among them, **201**, **203**, **204**, **206** and the known alkaloids 6-methoxydihydrosanguinarine, 6-acetaldehyde-dihyrochelerythrine, dihydrosanguina-line and 10-methoxy boconoline presented inhibitory effects on MCF-7 cells, with IC_{50} values lower than 20 μM (Table S2†).[60]

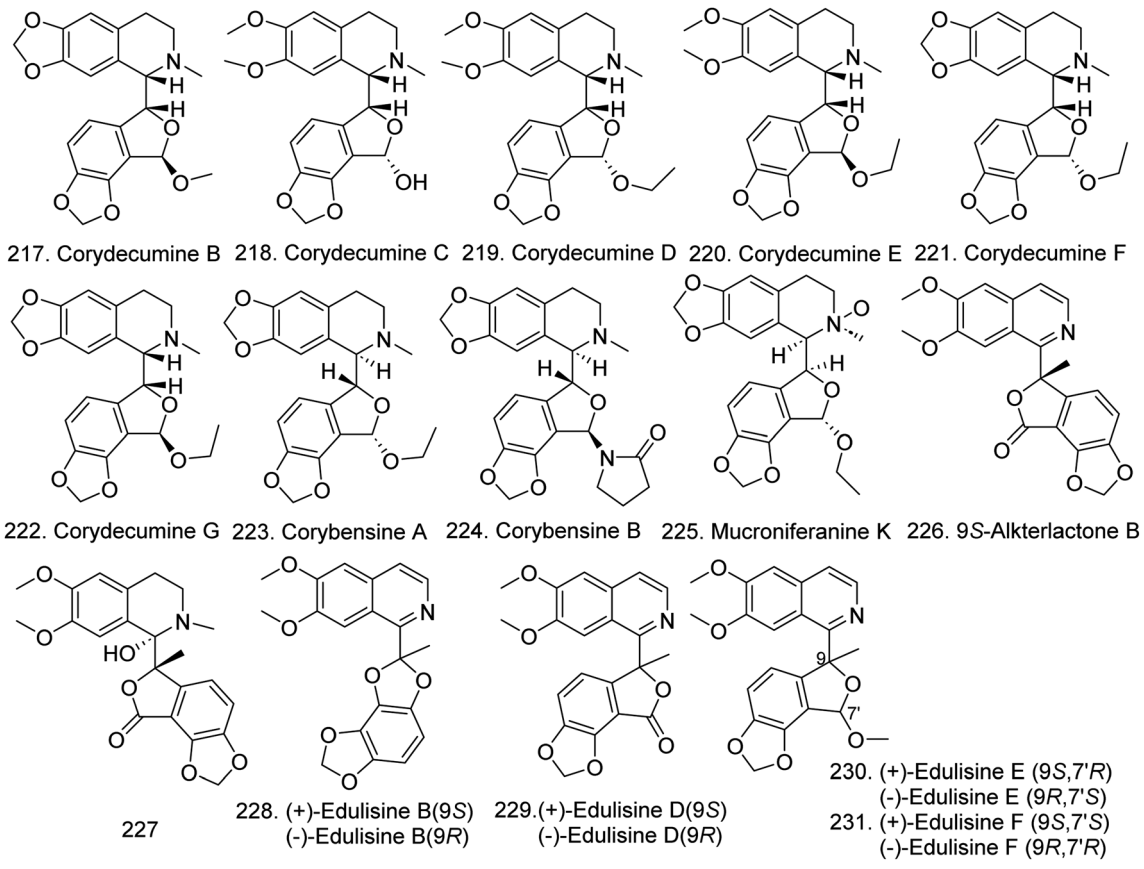

Fig. 17 The chemical structure of compounds **217–231**.

2.7. Morphine isoquinoline alkaloids

Morphine alkaloids have a 1-benzylisoquinoline skeleton with one additional ring closure. In 2020, four new isoquinoline alkaloids, (6*S*,7*S*,9*R*,13*S*)-6,7-di-*O*-acetyl-*N*-formylsinococuline (**207**), (6*S*,7*S*,9*R*,13*S*)-*N*-formylsinococuline (**208**), (6*S*,7*S*,9*R*,13-*S*)-6-*O*-acetyl-*N*-formylsinococuline (**209**), (6*S*,7*S*,9*R*,13*S*)-7-*O*-acetyl-*N*-formylsino-coculine (**210**)[58] and (6*S*,9*S*,13*R*,14*S*)-6-*O*-acetyl-7,8-didehydro-4-hydroxy-3,7-dimethoxymorphinan-6-ol (**211**)[69] (Fig. 16), were identified from *Stephania cepharantha*; however, they did not present the anti-inflammatory activity against NO production or cytotoxicity in three human cancer cell lines (A549, MCF-7, SW480). In 2022, a new morphine derivative, bungeanoline B (**212**) together with three known compounds, protostephanone, salutaridine, and salutaridine *N*-oxide, were isolated from the whole herb extract of *Corydalis bungeana*.[71] In 2023, Zeng *et al.*[55] isolated four new morphine isoquinoline alkaloids from *Sinomenium acutum*, including three *N*-oxide alkaloids, sinotuminins A (**213**), B (**214**) and C (**215**), and sinotuminin D; however, they did not have NO or AChE production inhibitory effects.

2.8. Phthalideisoquinoline alkaloids

Since the first prototypical phthalideisoquinoline hemiacetal alkaloid, (+)-egenine, was isolated from *Fumaria vaillantii* in 1983, this kind of compound has attracted considerable scientific attention, more than 30 compounds with two asymmetric centers in the molecule at C-1 and C-9 have been identified from the families Fumariaceae, Papaveraceae, Berberidaceae, and Ranunculaceae. They can be divided into two classes according to their chemical features: typical phthalideisoquinoline alkaloids with an intact tetracyclic skeleton and *seco*-phthalideisoquinoline alkaloids with a cleaved B ring that results in the formation of a dimethylaminoethyl side chain.[98,99]

In 2019, six new phthalideisoquinoline hemiacetal alkaloids, namely corydecumines B–G (**217–222**) (Fig. 17), as well as the known compounds corydecumine A and corydecumbine, were isolated from the bulbs of *Corydalis decumbens*. All new compounds inhibited neuron excitability at low micromolar concentrations.[100] This group subsequently isolated two new phthalideisoquinoline hemiacetal alkaloid derivatives, corybensines A (**223**) and B (**224**). **224** inhibited neuron excitability with an IC_{50} value of 10.0 μM in the suppression of SCO

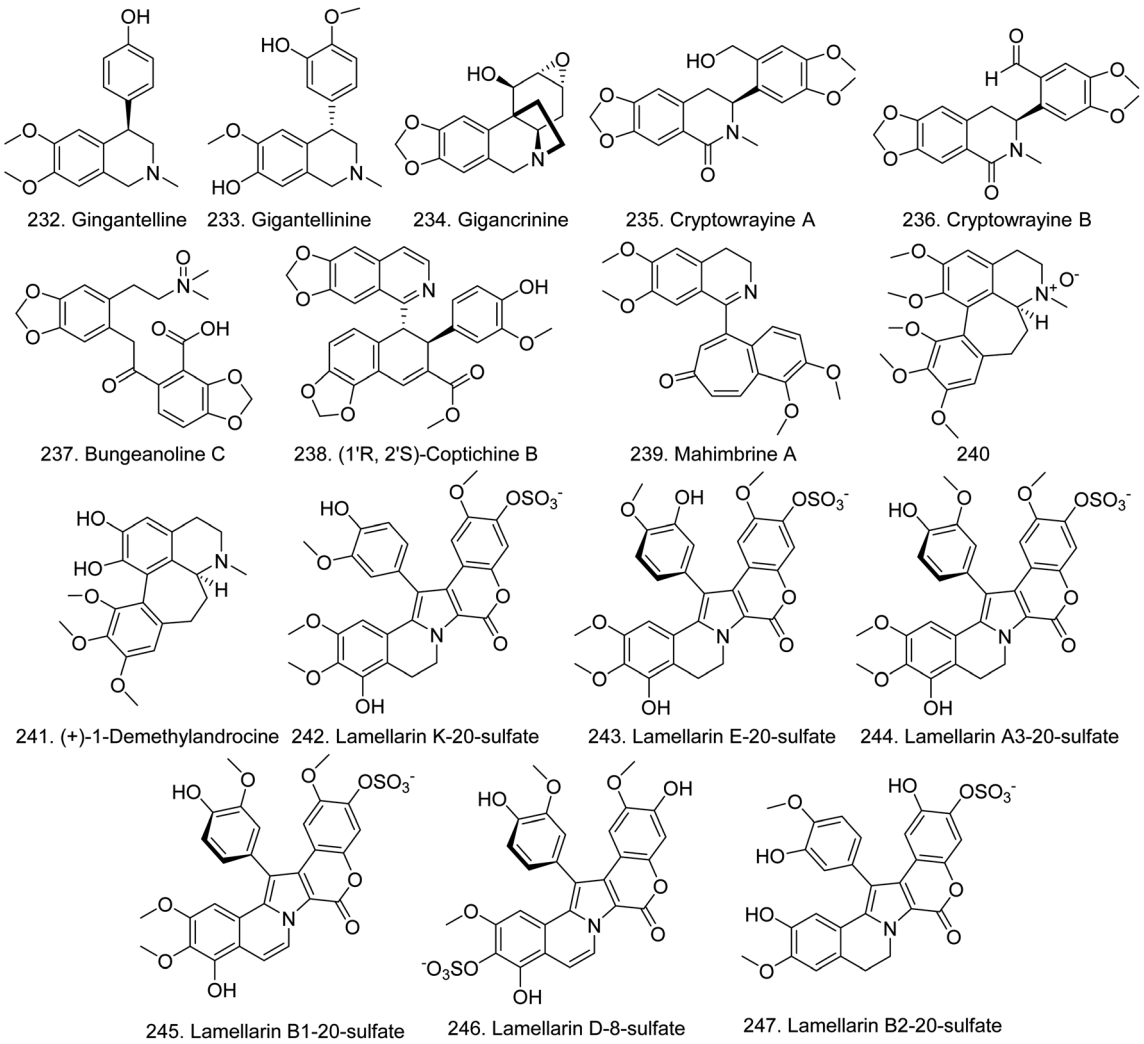

Fig. 18 The chemical structure of compounds **232–247**.

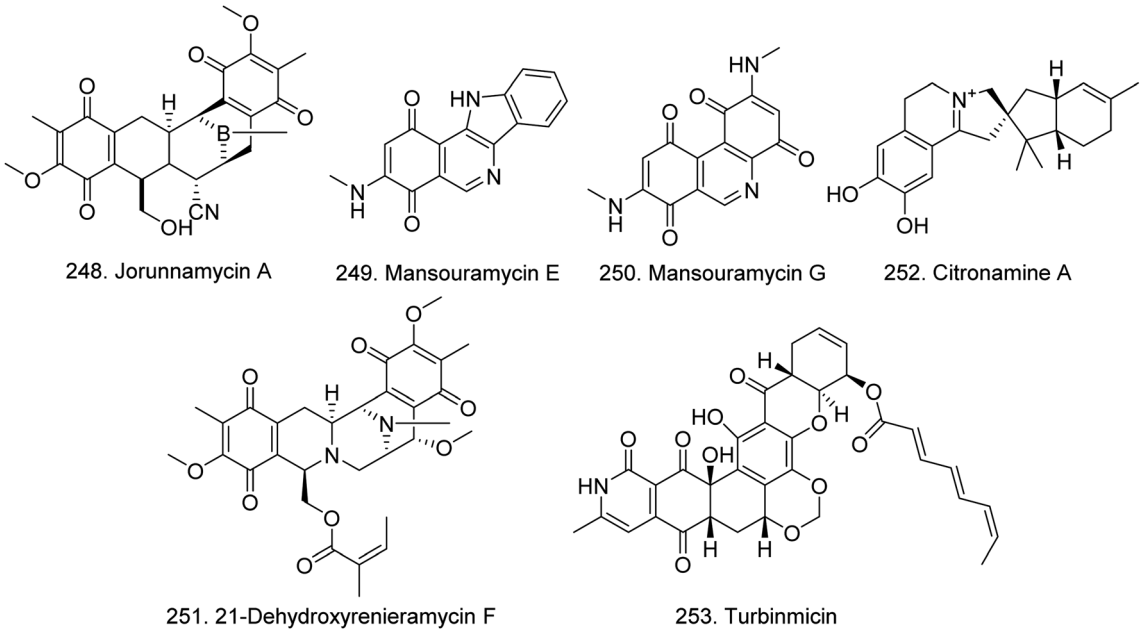

Fig. 19 The chemical structure of compounds 248–253.

frequency, indicating its antiepileptic and analgesic properties, and the methylenedioxy group at the at C-5 and C-6 and the oxygen-containing substituent at C-7 are important contributors to its activity.[101] Mucroniferanine K (**225**) was isolated from *C. mucronifera*.[45] Two novel benzylisoquinoline alkaloids, namely, 9*S*-alkterlactone B (**226**) and (1*S*,9*S*)-1-hydroxy-9-methyl-corlumine (**227**) (Fig. 17), were isolated from *C. tomentella*.[42] Moreover, four undescribed phthalideisoquinoline alkaloids, namely, edulisine B (**228**) with a benzo [1,2-*d*:3,4-*d*]bis [1,3]dioxole moiety, and edulisines D–F (**229–231**) (Fig. 17), were isolated from the whole plants of *C. edulis*, and (+)-edulisine B, (−)-edulisine B and (−)-edulisine F all exhibited insulinotropic action *in vitro*.[47]

2.9. Various isoquinoline alkaloids

In 2020, three undescribed alkaloids, namely, gingantelline (**232**), gigantellinine (**233**), and gigancrinine (**234**) (Fig. 18), together with the well-known sanguinine, cherylline, lycorine, crinine and flexinine, were isolated from *Crinum jagus*. However, only sanguinine was remarkably effective against AChE, with an IC_{50} value of 1.83 μM.[102] Cryptowrayines A (**235**) and B (**236**) (Fig. 18), which have approximately 1.4-fold and 1.2-fold quinone reductase-inducing activity in Hepa 1c1c7 cells at 3.125 μM, respectively, were subsequently isolated from the twigs of *Cryptocarya wrayi* (Table S2†).[103] A new narceine-type alkaloid, bungeanoline C (**237**), was obtained from the whole herb extract of *Corydalis bungeana*.[26]

(1′*R*,2′*S*)-Coptichine B (**238**) from *C. tomentella* exhibited strong antibacterial activities against two Gram-positive bacteria, *Staphylococcus aureus* and *Bacillus subtilis*, and two negative bacteria, *Escherichia coli* and *Pseudomonas aeruginosa* with MIC values of 3.12, 3.12, 12.5 and 6.25 μg mL^{-1}, respectively[42] (Table S3†). Moreover, mahimbrine A (**239**), which possesses a rare benzotropolone framing scaffold, was isolated from the endemic plant of *Mahonia imbricata*. However, it did not have antimicrobial activity at 1 mg mL^{-1}.[104] Two phenethyisoquinoline alkaloids, (+)-*O*-methylkreysigine-*N*-oxide (**240**) and (+)-1-demethylandrocine (**241**) (Fig. 18), were subsequently isolated from the leaves of *Androcymbium palaestinum*.[38]

Six new lamellarin sulfates, lamellarin K-20-sulfate (**242**), lamellarin E-20-sulfate (**243**), lamellarin A3-20-sulfate (**244**), lamellarin B1-20-sulfate (**245**), lamellarin D-8-sulfate (**246**), and lamellarin B2-20-sulfate (**247**) (Fig. 18), were isolated from the methanolic extract of the Pacific tunicate *Didemnum ternerratum*, and **245** exhibited moderate cytotoxicity against HCT-116 with an IC_{50} of 9.7 μM (Table S2†).[105]

Among sponges, more isoquinoline alkaloids were found. In 2019, a new bistetrahydroisoquinolinequinone, jorunnamycin A (**248**), with antimetastatic activity, was isolated from a Thai blue sponge *Xestospongia* sp.[106] Mansouramycins E (**249**) and G (**250**) (Fig. 19) were found in the marine-derived *Streptomyces* sp. isolate B1848.[33] A new isoquinolinequinones, 21-dehydroxyrenieramycin F (**251**), was isolated from the sponge *Haliclona* sp.[31] Citronamine A (**252**) (Fig. 19), an isoquinoline alkaloid containing an unprecedented pentacyclic ring system was isolated from the Australian marine sponge *Citronia astra*.[107] Turbinmicin (**253**) (Fig. 19), which has antibacterial activity, was identified from the marine microbiome (Table S3†).[108]

3. Synthesis of isoquinoline alkaloids

3.1. Chemical syntheses of isoquinoline alkaloids

Isoquinoline alkaloids are natural products with complex and diverse chemical structures that are widely used in medicine, pesticides, and other fields. However, the direct extraction and separation of these alkaloids from nature are often costly and

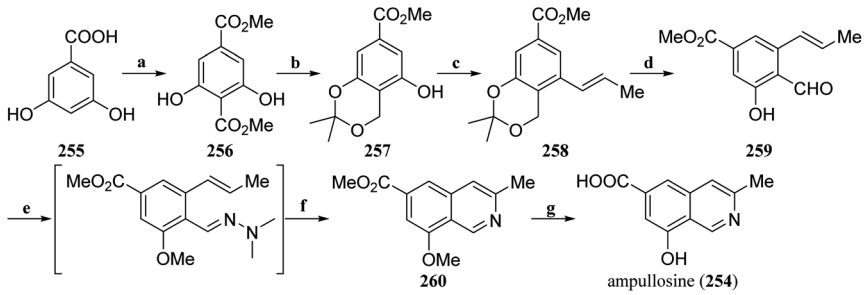

Scheme 1 Total synthesis of ampullosine (**254**) by Kaufman's group. Reagents and conditions: (a) (i) CO_2, $KHCO_3$, 1,2-propanediol, 180 °C, (ii) Me_2SO_4, $KHCO_3$, acetone, reflux; (b) (i) $NaBH_4$, THF/H_2O, 0.1 M phosphate buffer pH 7.5, 0 °C-rt, (ii) 2,2-DMP, TsOH, rt; (c) (i). $PhNTf_2$, DMAP, NEt_3, DCM, rt, (ii) $PdCl_2(PPh_3)_2$, DavePhos, THF/H_2O, 80 °C; (d) (i) TsOH, THF/H_2O, 60 °C, (ii) MnO_2, EtOAc, 78 °C; (e) (i) MeI, K_2CO_3, DMF, 0 °C-rt, (ii) Me_2N-NH_2, AcOH, $PhCF_3$, rt; (f) MW, 160 °C; (g) Al^0, I_2, DMSO, MeCN, 80 °C.

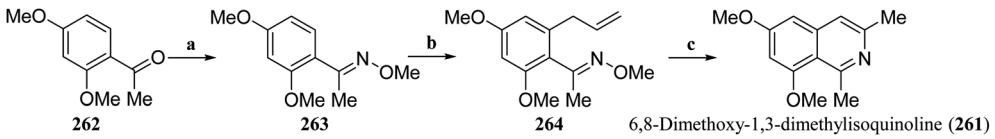

Scheme 2 Total synthesis of 6,8-dimethoxy-1,3-dimethylisoquinoline (**261**) by Kaufman's group. Reagents and conditions: (a) $MeONH_2 \cdot HCl$, $CeCl_3 \cdot 7H_2O$, NaOAc, EtOH, 50 °C; (b) allyl acetate, $[RuCl_2(p\text{-cymene})]_2$, $AgSbF_6$, DCE, rt; (c) (i) $RuHCl(CO)(PPh_3)_3$, 90 °C, (ii) PhMe, 150–160 °C.

inefficient, making synthetic methods a promising alternative. Developing new synthetic strategies to increase the efficiency of isoquinoline alkaloid synthesis is crucial for advancing the research and application of these compounds.[109–111] As global environmental and energy issues become increasingly prominent, the development of green, efficient, and economically sustainable synthetic strategies has taken on particular importance. In recent years, photoredox catalysis,[112–116] electrochemical synthesis,[117] and continuous flow reaction[118–120] strategies have garnered significant attention in the field of organic synthetic chemistry, and are seen as key technologies driving the transformation of organic synthesis. Here, the first total synthesis of isoquinoline alkaloid natural products, new synthetic strategies, and the application of new technologies in the synthesis of isoquinoline alkaloids will be introduced.

3.1.1 Simple isoquinoline alkaloids. Kaufman's group have developed a method using 6π-azaelectrocyclization as an effective atom-economic strategy for synthesizing natural products or analogs containing a 3-methylisoquinoline structure.[121] Based on this synthetic strategy, the first total synthesis of ampullosine (**254**), which has a unique structure was achieved.[122] Starting from 3,5-dihydroxybenzoic acid (**255**) as the raw material, **256** was obtained after a Kolbe-Schmitt carboxylation and methylation. Following selective reduction of **256**, protection of the ketal and activation of phenolic hydroxyl groups produced **257**. Then, **258** was obtained *via* Suzuki–Miyaura coupling reaction between **257** and potassium propenyl trifluoroborate. After hydrolysis and deprotection, the oxidation of benzyl alcohol produced the key intermediate **259**, which underwent *O*-methylation, and according to the established conditions of hydrazonetion/6π-azaelectrocyclization/

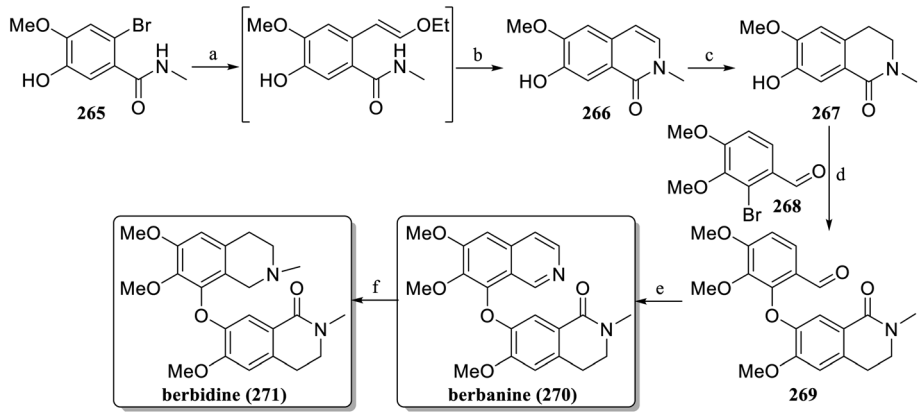

Scheme 3 Total synthesis of berbanine (**270**) and berbidine (**271**) and by Bracher's group. Reagents and conditions: (a) *trans*-2-ethoxyvinylboronic acid pinacol ester, $Pd(Ph_3P)_4$, Cs_2CO_3; (b) TFA; (c) H_2, Pd/C, 20–40 bar; (d) $CuBr \cdot Me_2S$, Cs_2CO_3; (e) (i) aminoacetaldehyde dimethyl acetal, (ii) TFAA, $BF_3 \cdot (AcOH)_2$; (f) (i) MeI, (ii) $NaBH_4$.

elimination,[123] permethyl ampullosine (**260**) was obtained. Finally, treatment with a strong Lewis acid simultaneously removed two methyl groups, completing the first total synthesis of ampullosine (**254**) with a total yield of 3.2% (Scheme 1).

6,8-Dimethoxy-1,3-dimethylisoquinoline (**261**) is a simple isoquinoline alkaloid natural product and a fragment of many complex natural products or drugs. In 2019, Kaufman *et al.* reported a concise and efficient synthesis strategy that achieved a total synthesis of **261** in just three steps with a total yield of 27.3% (Scheme 2).[124] First, Ce-catalyzed methoximation of acetophenone (**262**) was used to obtain **263**, and a ruthenium-catalyzed allyl reaction with methyloxime as the guide group was carried out to generate **264**. Finally, ruthenium-catalyzed allyl isomerization and microwave-facilitated 6π-azaelectrocyclization were carried out *via* a one-pot method to complete the total synthesis of 6,8-dimethoxy-1,3-dimethylisoquinoline (**261**).

In 2020, Bracher *et al.* refined the total synthesis strategy for 1-oxoisoquinoline alkaloids, introducing the C-3 and C-4 units

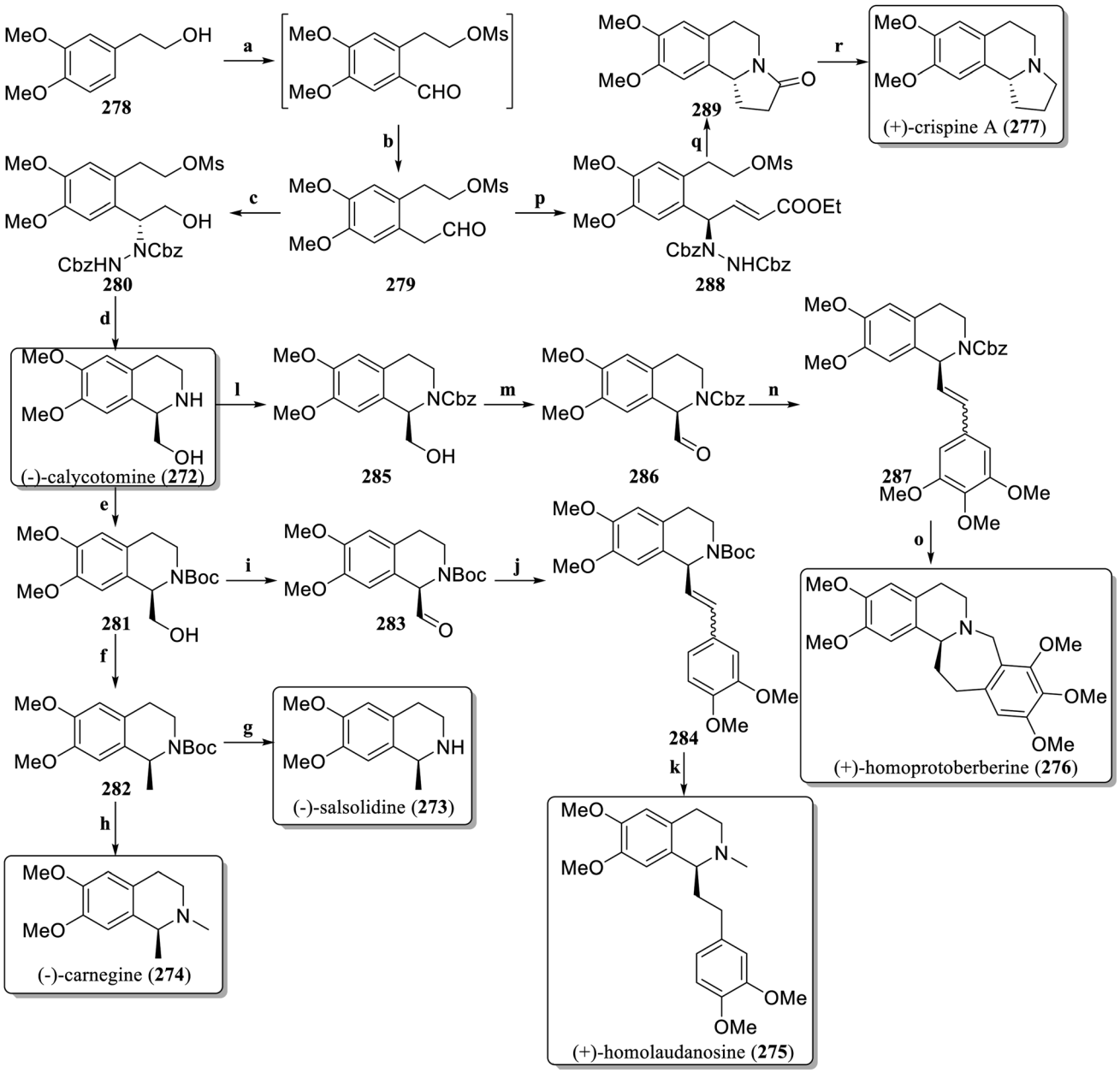

Scheme 4 Total synthesis of C-1 substitutes tetrahydroisoquinoline alkaloids by Ramapanicker's group. Reagents and conditions: (a) (i) MsCl, Et_3N, DCM, 0 °C to rt, (ii) dichloromethyl methyl ether, $SnCl_4$, CH_2Cl_2, −20 °C-rt; (b) (i). $MeOCH_2PPh_3Br$, *t*-BuOK, THF, 0 °C to rt, (ii) THF, 2 N HCl, 0 °C-rt; (c) (i) DBAD, L-proline, CH_3CN, 0 °C-rt, (ii) $NaBH_4$, EtOH; (d) RANEY®-Ni, MeOH, H_2, rt; (e) Boc_2O, $NaHCO_3$, THF, rt; (f) (i) TsCl, pyridine, CH_2Cl_2, 0 °C-rt, (ii) $LiAlH_4$, THF, 0 °C-rt; (g) TFA, CH_2Cl_2, 0 °C; (h) $LiAlH_4$, THF, reflux; (i) IBX, DMSO, rt; (j) (3,4-dimethoxybenz-yl)triphenyl-phosphonium bromide, *t*-BuOK, THF, 0 °C; (k) (i) Pd/C, EtOAc, H_2, rt, (ii) $LiAlH_4$, THF, reflux; (l) CbzCl, $NaHCO_3$, THF, 0 °C; (m) IBX, DMSO, rt; (n) triphenyl(3,4,5-trimethoxybenzyl)phosphonium bromide, *t*-BuOK, THF, 0 °C; (o) (i) Pd/C, EtOAc, H_2, rt, (ii) HCHO, HCl, EtOH, reflux; (p) (i) DBAD, L-proline, CH_3CN, 0 °C to rt, (ii) Ph_3PCHCO_2Et, 0 °C to rt; (q) (i) H_2, RANEY®-Ni, MeOH, rt, (ii) K_2CO_3, MeOH, reflux; (r) $LiAlH_4$, THF, reflux.

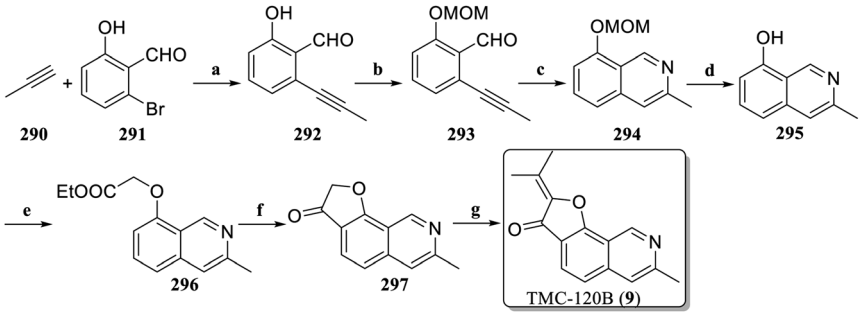

Scheme 5 Total synthesis of TMC-120B (**9**) by Clausen's group. Reagents and conditions: (a) $PdCl_2(PPh_3)_2$, Et_3N, CuI, 55 °C, 24 h; (b) MOMCl, DIPEA, CH_2Cl_2, 40 °C, 16 h; (c) NH_3, 80 °C, 7 h; (d) HCl, MeOH, reflux, 3 h; (e) ethyl bromoacetate, NaOEt, DMF, 12 h; (f) (i) NaOH, EtOH, 1 h, (ii) $SOCl_2$, reflux, 1 h, (iii) $AlCl_3$, 1 h; (g) *p*-TsOH·H_2O, acetone, DCE, reflux, 5 h.

of the isoquinoline core using 2-ethoxyvinyl boronate as the C_2 structural unit. Starting with commercially available *ortho*-bromobenzoic acid, which is activated with thionyl chloride and then amidated with ammonia or aqueous methylamine solution to obtain benzamide derivatives, only two to three convenient operations are needed to construct 1-oxo-, 1-oxo-3,4-dihydro-, and 1,3,4-trioxoisoquinoline alkaloids, establishing a concise and efficient general synthetic method. Based on this synthetic strategy, the first total synthesis of the dimer alkaloids berbanine and berbidine was completed (Scheme 3).[125] Starting from *N*-methylbenzamide **265**, the 1-oxoisoquinoline alkaloid **266** was constructed according to an established synthetic method, followed by Pd/C reduction to obtain 1-oxo-3,4-dihydroisoquinoline alkaloid **267**. Subsequently, it was combined with **268** *via* the Ullman coupling reaction to generate the intermediate **269**, and then the berbanine (**270**) was obtained through the Pomeranz–Fritsch reaction, followed by *N*-methylation and reduction to give the berbidine (**271**).

In 2021, Ramapanicker *et al.* designed a new method for the synthesis of enantioselective C-1-substituted tetrahydroisoquinoline natural products with proline-catalyzed asymmetric α-hydrazination as a key step,[126] achieving asymmetric total synthesis of six different natural products (Scheme 4). The commercially available 2-(3,4-dimethoxyphenyl)ethan-1-ol **278** was converted into the aldehyde **279** through a simple two-step process. The aldehyde **279** was subjected to asymmetric α-hydrazination *via* dibenzyl azodicarboxylate (DBAD) in the presence of L-proline, and after reduction with $NaBH_4$, β-hydrazino alcohol **280** was obtained. RANEY®-Ni was used to hydrogenate **280**, followed by *in situ* cyclization to produce (−)-calycotomine (**272**). The hydroxyl group in Boc-protected **281** was converted to an unstable toluenesulfonyl derivative and then reduced to **282** *via* $LiAlH_4$. Deprotection afforded (−)-salsolidine (**273**) and methylation produced (−)-carnegine (**274**). The hydroxyl group in **281** was oxidized to form the aldehyde **283**, followed by a Wittig reaction to generate the olefin **284**. Hydrogenation reduced the number of double bonds, deprotection and methylation to obtain (+)-homolaudanosine (**275**). Cbz protected **272** to obtain **285**, which was oxidized to the aldehyde **286**, and then reacted by Wittig reaction to obtain the olefin **287**. Hydroreduction followed by a Pictet–Spengler reaction produced (+)-homoprotoberberine (**276**). Aldehyde **279** was treated with dibenzyl azodicarboxylate in the presence of D-proline, followed by a Wittig reaction to obtain the unsaturated ester **288**. The one-pot method reduced and cyclized to produce **289**. Finally, the lactam **289** was reduced to obtain (+)-crispine A (**277**).

In 2022, Clausen *et al.* optimized the synthesis method of TMC-120B (**9**) to achieve its total synthesis with only a 7-step reaction (9% overall yield),[127] a significant improvement over the previously reported 11-step reactions (2.9% overall yield)[128] (Scheme 5). Starting from the commercially available 2-bromo-6-hydroxybenzaldehyde **291**, **292** was obtained through Sonogashira coupling with **290**. The MOM protected the phenolic hydroxyl group to generate **293**, which constructed the isoquinoline scaffold **294** through imination and intramolecular ethynyl-imino cyclization. Deprotection under acidic conditions led to the formation of **295**, which subsequently underwent alkylation with ethyl bromoacetate to generate **296**. In contrast to previous synthesis strategies, the core scaffold **297** was constructed *via* intramolecular Friedel–Crafts acylation. Finally, under acidic conditions, an aldol condensation reaction occurred between **297** and acetone to form TMC-120B (**9**).

3.1.2 Benzylisoquinoline alkaloids. In 2020, Bracher *et al.* completed the first total synthesis of *rac*-muraricine (**72**).[129] The key to this synthetic strategy was the *N*-acyl Pictet–Spengler condensation reaction to form the tetrahydroisoquinoline skeleton, as well as the copper-catalyzed Ullmann coupling reaction to construct the diaryl ether bridge. Starting from commercially available 4-benzyloxybenzaldehyde (**298**), 3-bromo-4,5-dimethoxybenzaldehyde (**299**), and 4-hydroxy-3-methoxyphenethylamine (**300**), through multiple transformations, as well as the Pictet–Spengler condensation reaction and Ullmann coupling reaction, the key intermediate **301** was obtained. Under the action of trifluoroacetic acid, **301** underwent an *N*-acyl Pictet–Spengler reaction with paraformaldehyde to obtain the ethoxycarbonyl-protected compound **302**. Finally, after $LiAlH_4$ reduction, the target product *rac*-muraricine (**72**) was obtained with a total yield of 3.8% (Scheme 6). Moreover, biological activity studies have shown that *rac*-muraricine can serve as a potential lead structure for the development of novel nontoxic P-gp inhibitors. Based on this synthetic strategy, a series of muraricine

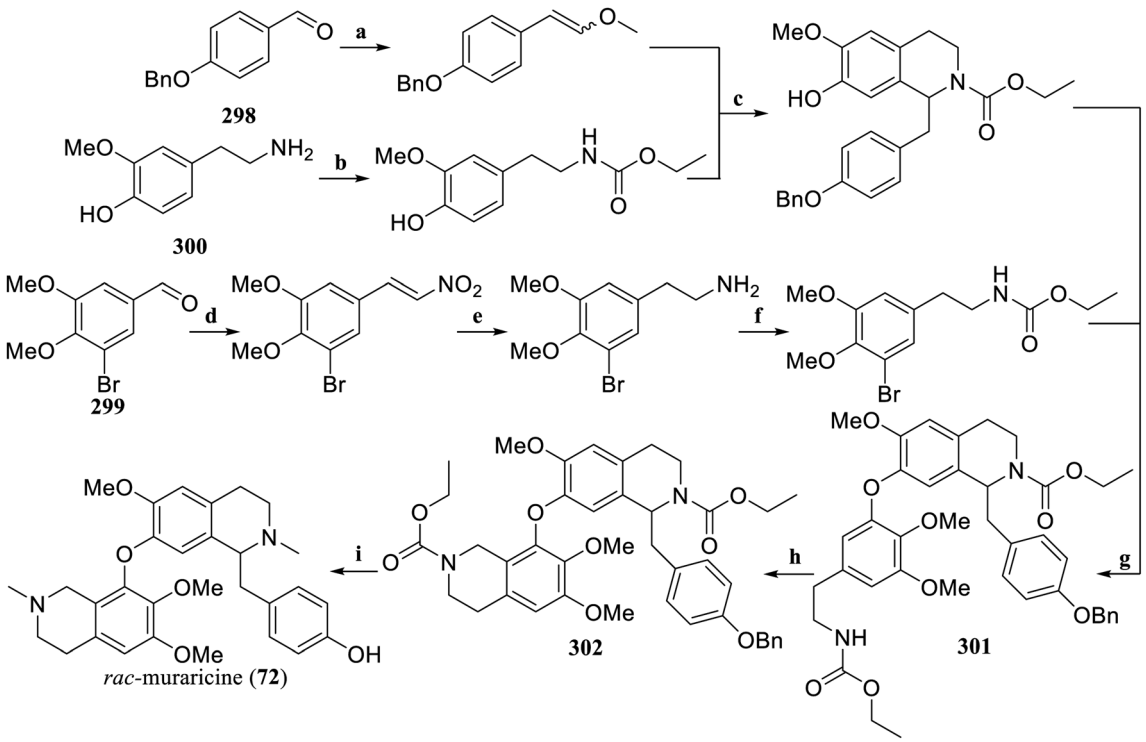

Scheme 6 Total synthesis of *rac*-muraricine (**72**) by Bracher's group. Reagents and conditions: (a) (methoxymethyl)triphenylphosphonium chloride, LDA; (b) ethyl chloroformate, Et_3N, NaOH; (c) TFA, CH_2Cl_2; (d) CH_3NO_2, NH_4AcO, CH_3COOH; (e) Zn, HCl, MeOH; (f) ethyl chloroformate, Et_3N, CH_2Cl_2; (g) (i) $CuBr{\cdot}Me_2S$, Cs_2CO_3, (ii) Pd/C, H_2, MeOH; (h) paraformaldehyde, TFA, CH_2Cl_2, 0 °C-rt; (i) $LiAlH_4$, THF, 50 °C.

derivatives are expected to be synthesized, laying a compound foundation for future drug development.

Bracher and coworkers improved the *N*-acyl-Pictet–Spengler condensation reaction in 2021, enabling the efficient synthesis of 1-benzyltetrahydroisoquinolines.[130] This strategy uses ω-methoxystyrene (**303**) as a convenient alternative to aryl acetaldehyde to rapidly construct the compound skeleton *via* an *N*-acyl-Pictet–Spengler reaction with *N*-ethoxycarbonyl phenethylamines (**304**). After removing the ethoxycarbonyl groups from **305**, *N*-methylated isoquinoline alkaloids could be obtained *via* route A, or the corresponding alkaloids with free N–H could be generated *via* route B. In this synthetic strategy, the dual utilization of ethoxycarbonyl significantly simplified the synthesis of hydroxylated 1-benzyltetrahydroisoquinolines. Through this strategy, 10 racemic benzyl isoquinoline alkaloids were efficiently synthesized (Scheme 7).

The asymmetric catalytic Pictet–Spengler reaction represents an ideal strategy for the synthesis of tetrahydroisoquinoline (THIQ) and related natural products. In 2022, List *et al.* employed imidodiphosphorimidate (IDPi) as the asymmetric organocatalyst to promote the asymmetric Pictet–Spengler reaction between the aldehydes **307** and the *N*-methoxycarbonyl phenethylamines **306** (Scheme 8).[131] This approach efficiently afforded the tetrahydroisoquinoline derivatives **308** with excellent enantioselectivity. Through this strategy, key intermediates for the synthesis of isoquinoline alkaloid natural products could be obtained in a concise and efficient manner. Simple chemical transformations then allow for the efficient synthesis of natural products. By reducing or removing the carbamate functional group, asymmetric THIQs such as laudanosine, romneine, and lophocerine with *N*-methylation or *N*–H could be obtained. Removing the carbamate and treating it with a base could effectively cyclize it to form the corresponding γ-lactam, which could be further synthesized into the tetrahydroisoquinoline alkaloids oleracein E and crispine A. After reductive methylation, oxidative phenol–phenol coupling could construct an androcymbine skeleton. The intermediate with the carbamate functional group removed could undergo a Pictet–Spengler reaction with formaldehyde to construct the tetrahydroberberine natural product xylopinine. The transition metal-promoted intramolecular coupling reaction efficiently synthesized the aporphine natural product glaucine. Through the constant current electrolysis (CCE) conditions developed by Opatz and Waldvogel,[132] the morphinan skeleton amurine could be efficiently obtained.

In 2022, Baskar's group established a visible light-mediated organophoto-redox catalyzed method for the α-benzylation of tertiary amines (Scheme 9a).[133] The organic nonmetallic photocatalyst 4-CzIPN was used to achieve the green and efficient synthesis of compound *N*-aryl-substituted tertiary amines and benzyl bromide under visible light irradiation, and a series of tetrahydroisoquinoline derivatives were constructed. Furthermore, this method could be used to synthesize biologically active natural products of isoquinoline alkaloids (Scheme 9b). The tetrahydroisoquinoline derivative (**309**) obtained as the photocatalysis reaction product was converted to important

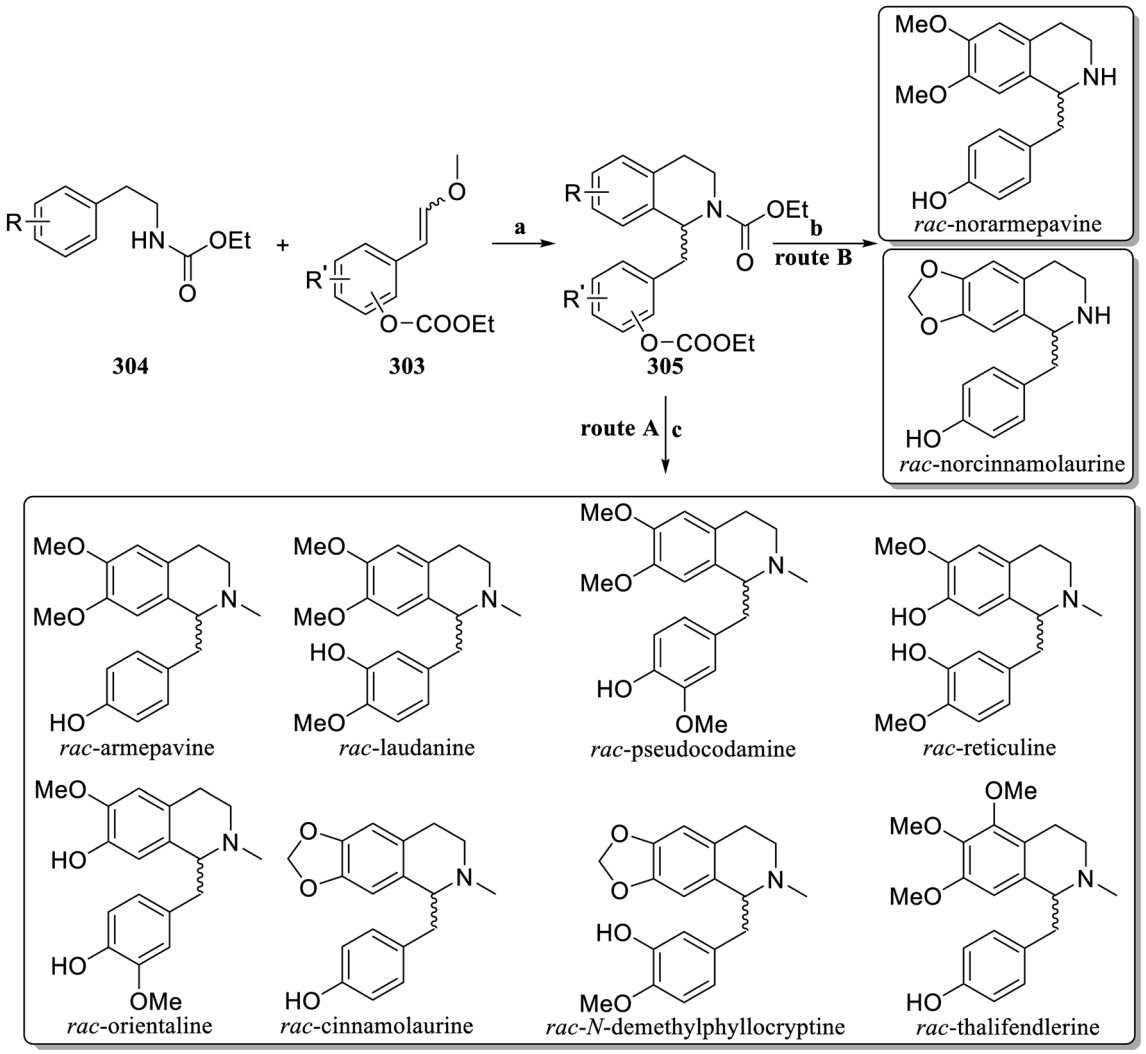

Scheme 7 Total synthesis of racemic 1-benzyltetrahydroisoquinoline alkaloids by Bracher's group. Reagents and conditions: (a) TFA, DCM; (b) CH_3Li, THF, 0 °C; (c) $LiAlH_4$, THF, reflux.

alkaloids *rac*-norlaudanosine (**310**), *rac*-laudanosine (**311**) and *rac*-xylopinine (**312**) through simple chemical transformations.

The enantioselective C–H functionalization strategy catalyzed by transition metals has provided a new approach for the retrosynthetic analysis of natural products, revolutionizing the traditional logic of synthesizing natural compounds.[134] Recently, Shi and Yao *et al.* established a cobalt-catalyzed enantioselective C–H/*N*–H cyclization reaction between picolinamides (**313**) and alkynes (**314**), providing a direct and efficient synthetic strategy to prepare C1-chiral 1,2-dihydroisoquinolines (**315**) with good yields and excellent enantioselectivity (Scheme 10).[135] Based on this method, the *N*-benzhydrylpicolinamide **316** underwent enantioselective C–H/*N*–H cyclization with trimethylsilylacetylene to produce **317**. After the TMS was removed and the dihydroisoquinoline was hydrogenated and deprotected, (*S*)-1-phenyl-1,2,3,4-tetrahydroisoquinoline (**318**), which is the key intermediate for the synthesis of (+)-solifenacin and FR115427, was obtained. According to this strategy, picolinamides **319** and **320** underwent kinetic resolution reactions with trimethylsilylacetylene to produce the enantioselective C–H/N–H cyclization products **321** and **322**, respectively. After the TMS was removed, the dihydroisoquinolines were hydrogenated and deprotected, and (*S*)-norlaudanosine (**324**) and **323** were formed. **324** could be further converted into (*S*)-laudanosine (**325**), (*S*)-xylopinine (**326**), and (*S*)-sebiferine (**327**) with excellent enantioselectivity. After *N*-methylation, **323** was converted to (*S*)-cryptostyline II (**328**). The synthesis of the above natural products can be carried out on a gram scale, efficiently obtaining hundreds of milligrams of target natural products or drug candidate molecules, which further demonstrates the important application value of this strategy in the field of synthesis chiral isoquinoline alkaloids.

Lumb's group has established a new method for the selective catalytic aerobic cross-dehydrogenative coupling reaction of phenols and catechols to construct aryl ether compounds, which are difficult to synthesize *via* traditional Ullman coupling. Based on this method, the simple and efficient total synthesis of the tetrahydroisoquinoline alkaloid natural

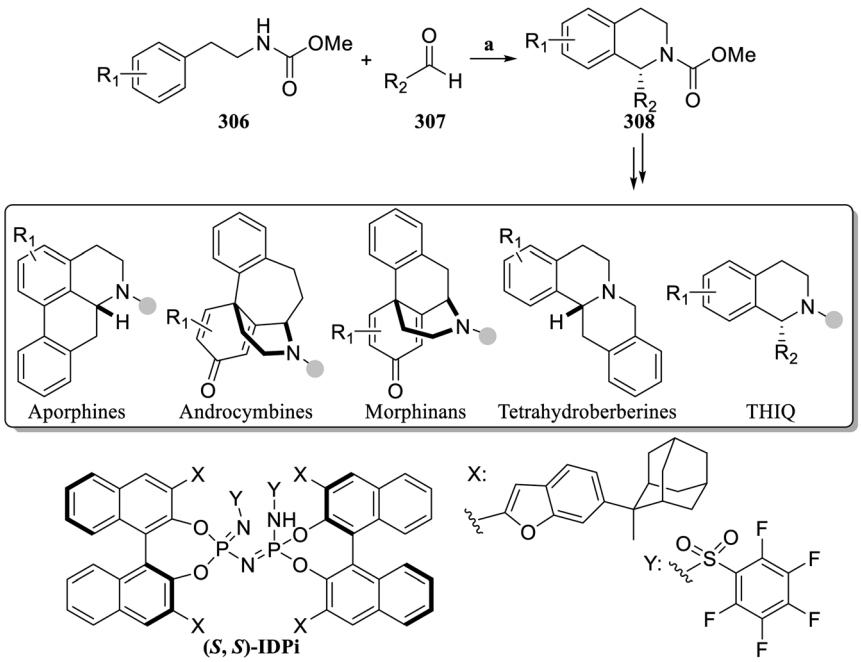

Scheme 8 Catalytic asymmetric Pictet–Spengler platform and application by List's group. Reagents and conditions: (a) (*S*,*S*)-IDPi, $CHCl_3$, rt.

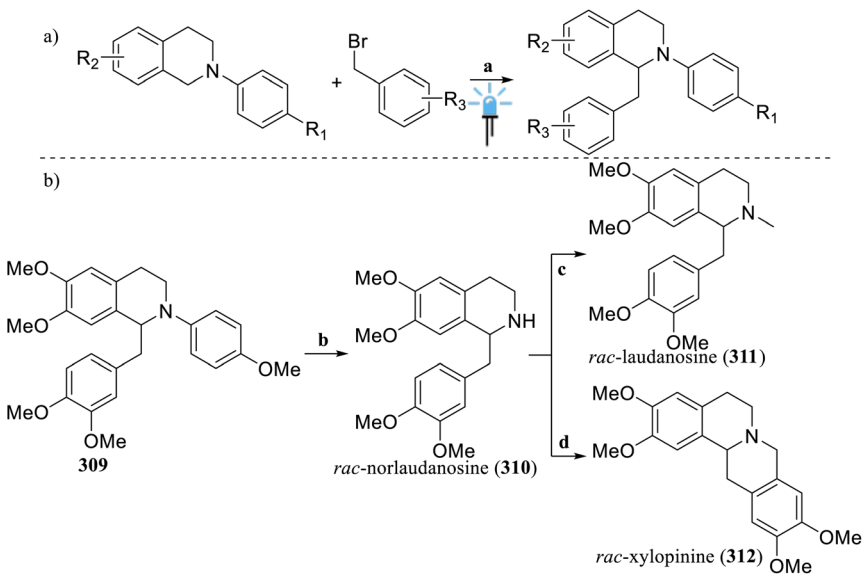

Scheme 9 Metal-free photoredox catalyzed α-benzylation and application by Baskar's group. Reagents and conditions: (a) 4-CzIPN, K_2CO_3, MeCN, Ar, rt, blue LED; (b) CAN, $MeCN/H_2O$, 0 °C; (c) HCHO, $NaBH_4$, $MeCN/H_2O$, rt; (d) HCHO, HCOOH, H_2O, 90 °C.

products (*S*,*S*)-thalicarpine (**329**)[136] and (*S*,*S*)-tetramethylmagnolamine (**330**)[137] could be achieved in total yields of 20% and 21%, respectively. Compared with the previous synthesis methods (with total yields of 1.5% for **329** and 14% for **330**), the new method can synthesize hundreds of milligrams of natural products in a single batch, which holds higher application value for studying their biological activities or synthesizing analogs.

Through the amidation of 3,4-dimethoxyphenethylamine (**331**) with 3-hydroxy-4-methoxyphenylacetic acid (**332**) and 4-hydroxyphenylacetic acid (**333**) respectively, followed by Bischler–Napieralski cyclization, the asymmetric tetrahydroisoquinoline skeletons **334** and **335** were constructed *via* asymmetric Noyori hydrogenation. Based on Fagnou's aporphine synthesis method,[138] **334** was further converted into aporphine **336**. Boc protected **335** and further oxidized it to obtain **337**. Finally, under the established standard conditions, catalytic aerobic CDC reaction was performed on **336** and **337** to generate the aryl ether **338**. After deprotection and methylation, (*S*,*S*)-thalicarpine (**329**) was obtained (Scheme 11). After Boc

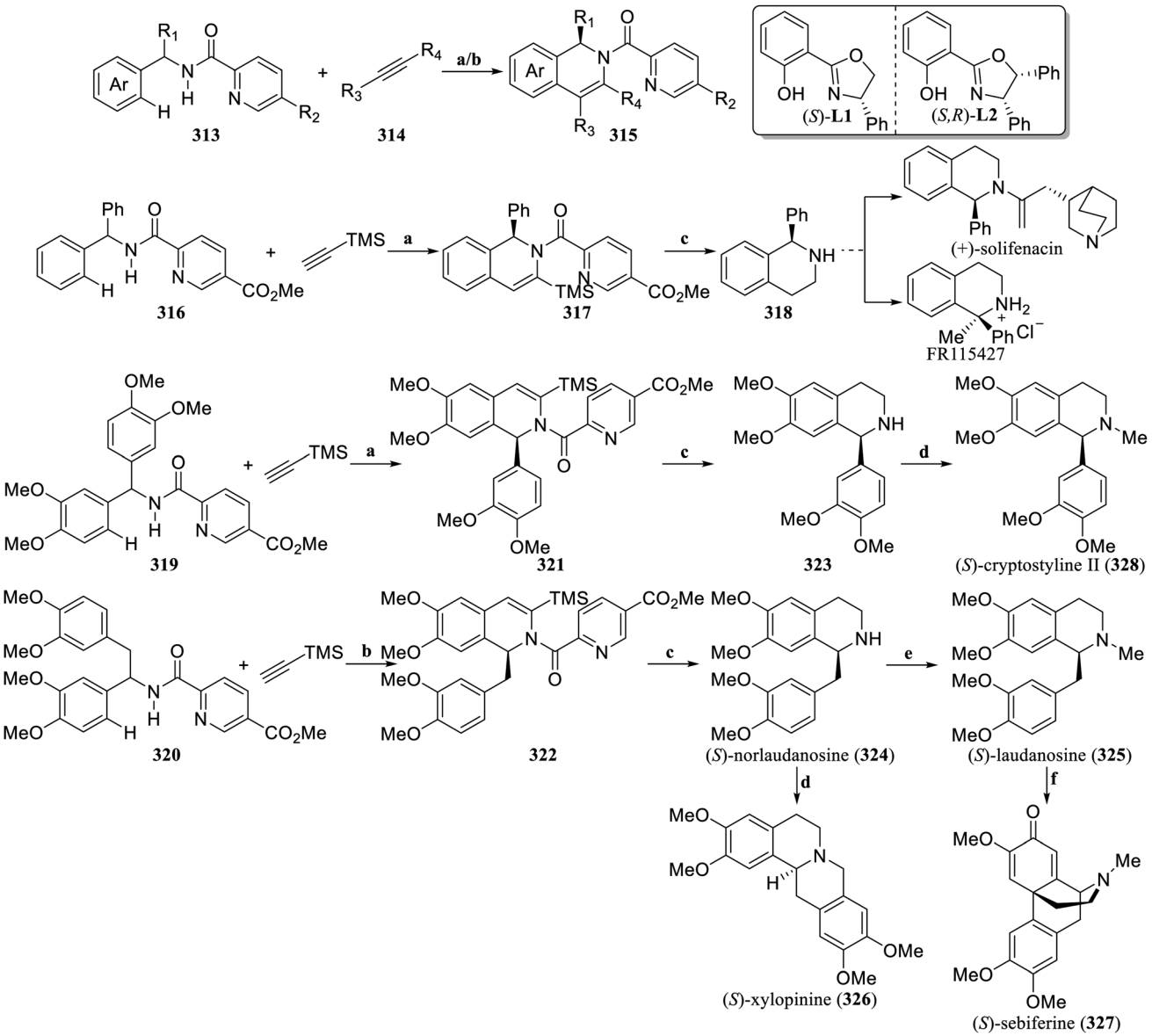

Scheme 10 Cobalt-catalyzed enantioselective C–H/N–H cyclization by Shi's group. Reagents and conditions: (a) $Co(OAc)_2 \cdot 4H_2O$, (*S*)-L1, $Mn(OAc)_2 \cdot 4H_2O$, $PivONa \cdot H_2O$, MeOH, O_2, 90 °C; (b) $Co(OAc)_2 \cdot 4H_2O$, (*S*,*R*)-L2, $Mn(OAc)_2 \cdot 4H_2O$, $PivONa \cdot H_2O$, MeOH, O_2, 90 °C; (c) (i) CF_3-COOH, DCM, −5 °C-rt, (ii) Pd/C, H_2, MeOH, 50 °C, (iii) $LiAlH_4$, THF, −78 °C-rt; (d) HCHO, HCO_2H, 90 °C; (e) HCHO, MeOH, then $NaBH_4$, rt; (f) PIFA, HPA, $BF_3 \cdot Et_2O$, MeCN, −20–0 °C.

protection of **335**, aerobic oxidative coupling was achieved under the established standard reaction conditions, and the corresponding aryl ether **339** was obtained after reduction. After methylation of the phenolic hydroxyl groups and reduction of *N*-Boc, (*S*,*S*)-tetramethylmagnolamine (**330**) was subsequently obtained (Scheme 12).

In 2020, Bracher's group established a new method for the synthesis of bisbenzylisoquinoline alkaloids,[139] which could efficiently construct *rac*-tetrandrine (**340**) and its diastereomer isotetrandrine (**341**) by replacing the Bischler–Napieralski reaction with the *N*-acyl Pictet–Spengler cyclization and combined with the Ullmann reaction (Scheme 13).

The *N*-acyl Pictet–Spengler cyclization reaction directly provides a tetrahydroisoquinoline skeleton, and the required *N*-methyl group can be obtained simply by reducing the carbamate group, significantly reducing the number of synthetic steps. In routes 1a and 1b, the two 1-benzyl tetrahydroisoquinoline moieties were constructed in the early stages through an intermolecular *N*-acyl Pictet–Spengler reaction, and the macrocycle was subsequently constructed through intramolecular diaryl ether synthesis. Conversely, in routes 1c and 1d, the intramolecular *N*-acyl Pictet–Spengler cyclization was the core step for constructing the macrocycle in the later stages. All four routes enable the total synthesis of *rac*-tetrandrine (**340**) and its diastereomer isotetrandrine (**341**) through more

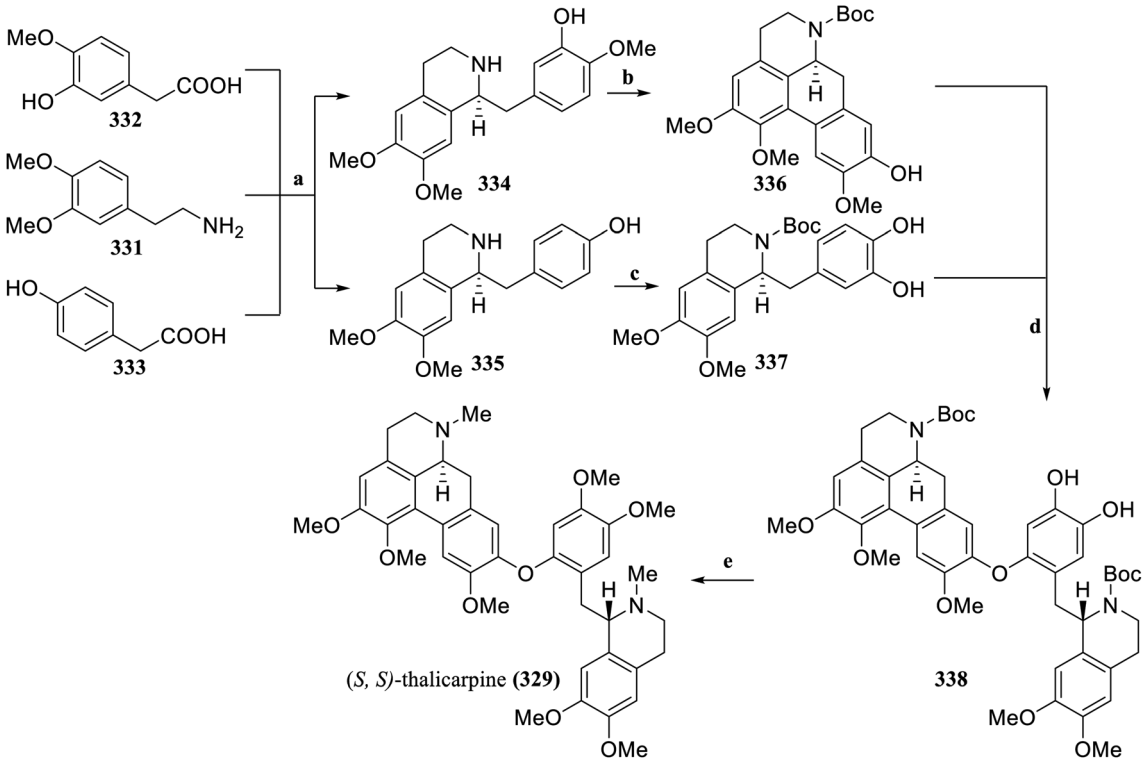

Scheme 11 Total synthesis of (*S*,*S*)-thalicarpine (**329**) by Lumb's group. Reagents and conditions: (a) (i) neat, 200 °C, (ii) $POCl_3$, MeCN, reflux, (iii) (*R*,*R*)-Ru(Ts-DPEN)(*p*-cymene)Cl, HCO_2H/Et_3N (5 : 2), DMF, rt; (b) (i) Br_2, HCl, AcOH, then Boc_2O, MeOH, (ii). BnBr, Cs_2CO_3, DMSO, (iii) $Pd(OAc)_2$, K_2CO_3, PhDavePhos, DMA, 130 °C, then Pd/C, MeOH, H_2; (c) (i) Boc_2O, MeOH, (ii) IBX, DMF; (d) (i) O_2, CuCl, 4-MeO-Py, rt, (ii) $NaBH_4$, MeOH; (e) (i) Cs_2CO_3, MeI, DMSO, (ii) $LiAlH_4$, THF, reflux.

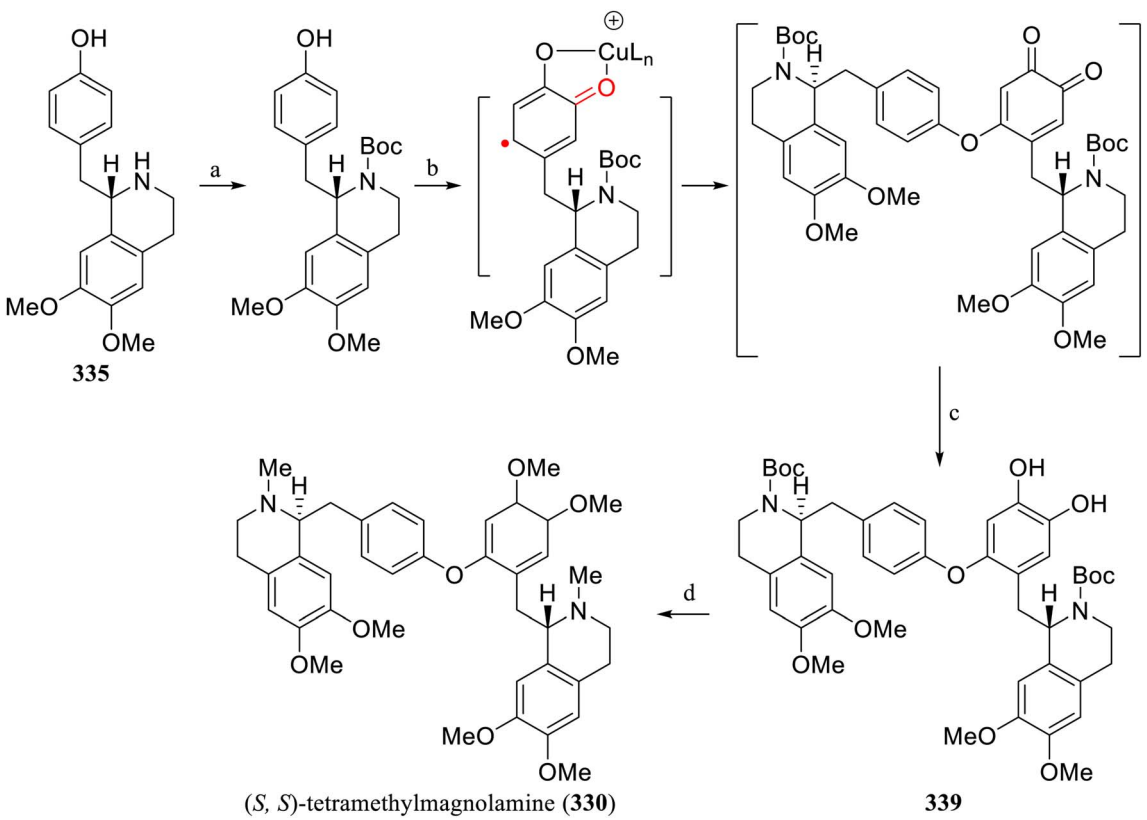

Scheme 12 Total synthesis of (*S*,*S*)-tetramethylmagnolamine (**330**) by Lumb's group. Reagents and conditions: (a) Boc_2O, MeOH, rt; (b) $[Cu(MeCN)_4](PF_6)$, DBED, 4 Å MS, DCM, O_2, rt; (c) $Na_2S_2O_4$ workup; (d) (i) MeI, Cs_2CO_3, DMSO, (ii) $LiAlH_4$, THF, reflux.

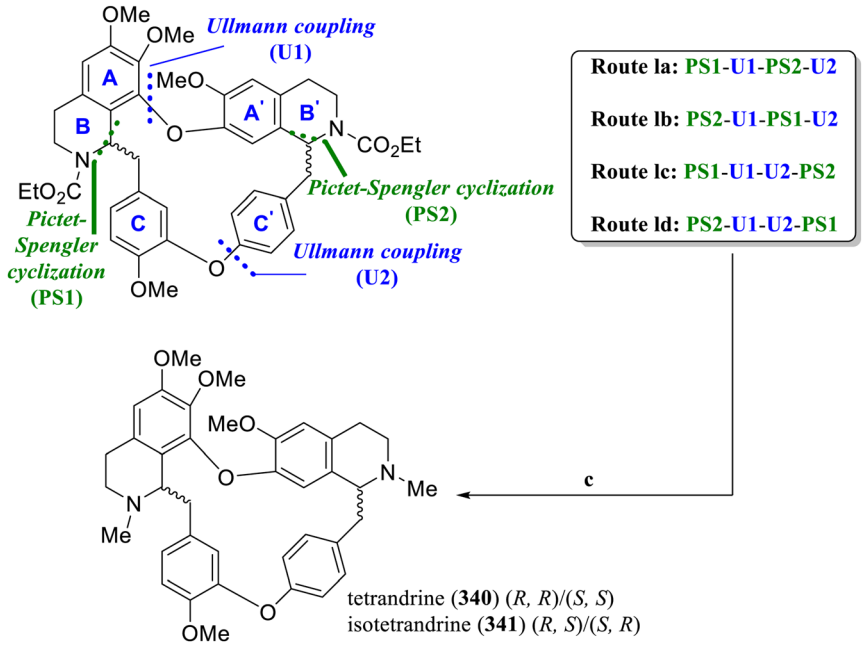

Scheme 13 Total synthesis of tetrandrine (340) and isotetrandrine (341) by Bracher's group. Reagents and conditions: (a) Ullmann coupling: CuBr·Me_2S, Cs_2CO_3, pyridine, 110 °C; (b) Pictet–Spengler cyclization: TFA, CH_2Cl_2, 0 °C-rt; (c) $LiAlH_4$, THF, 80 °C.

efficient synthetic steps (12 steps), with route 1d achieving the highest total yield of 19.2% among the four routes. In terms of stereoselectivity, routes 1a and 1b do not result in good stereoselectivity, producing an almost equimolar mixture of diastereomers, whereas routes 1c and 1d show good stereoselectivity for one or the other diastereomer.

3.1.3 Aporphine isoquinoline alkaloids. In 2019, Zhang and Luo *et al.* first isolated and identified the reconstructed aporphines isoquinoline alkaloids dactylicapnosine A (**342**) and dactylicapnosine B (**343**).[68] Based on the postulated biosynthetic pathway of dactylicapnosine A, they designed a synthetic strategy that involves oxidizing the precursors isocorydine/

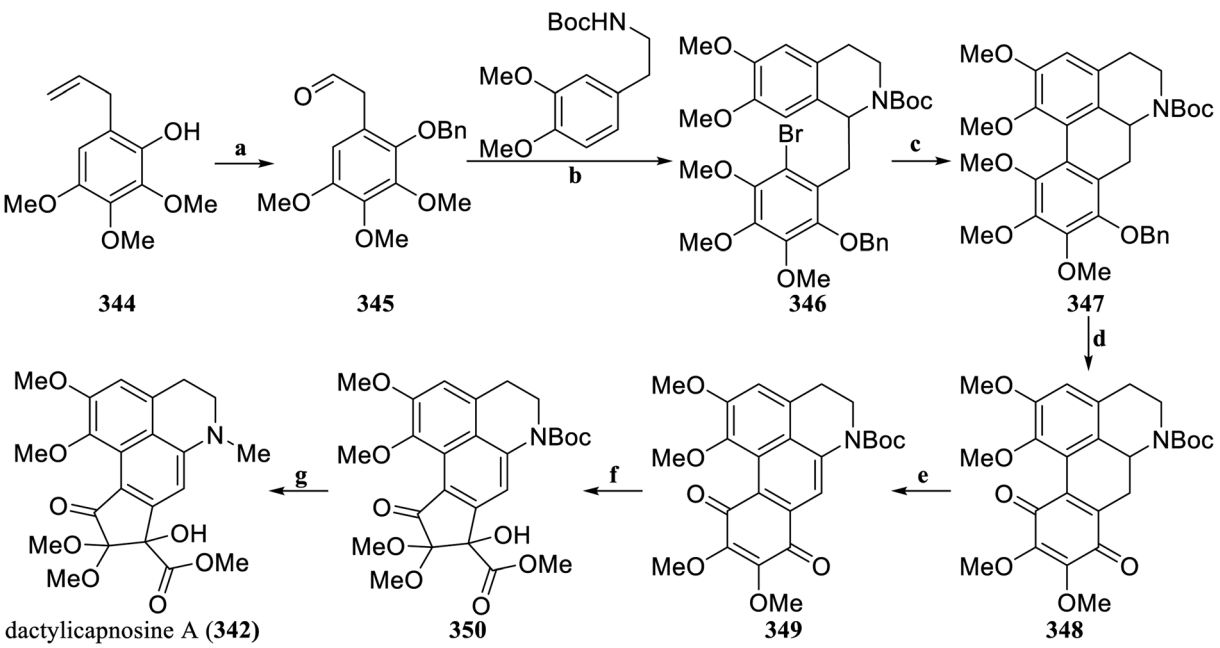

Scheme 14 Total synthesis of dactylicapnosine A (342) by Zhang's group. Reagents and conditions: (a) (i) BnBr, K_2CO_3, acetone, 65 °C, (ii) O_3, DCM-MeOH, then Me_2S, −78 °C; (b) (i) NBS, AcOH, DCM, rt, (ii) CF_3COOH, DCM, rt, (iii) NaOH, $(Boc)_2O$, rt; (c) $Pd(OAc)_2$, PPh_3, K_2CO_3, DMA, 150 °C, MW; (d) (i) Pd/C, H_2, MeOH-EtOAc, rt, (ii) IBD, HFIP-H_2O, 0 °C; (e) O_2, K_2CO_3, THF-MeOH, rt; (f) $NaIO_4$, MeOH, 100 °C; (g) (i) MeCN, 170 °C, MW, (ii) MeI, K_2CO_3, THF, 100 °C.

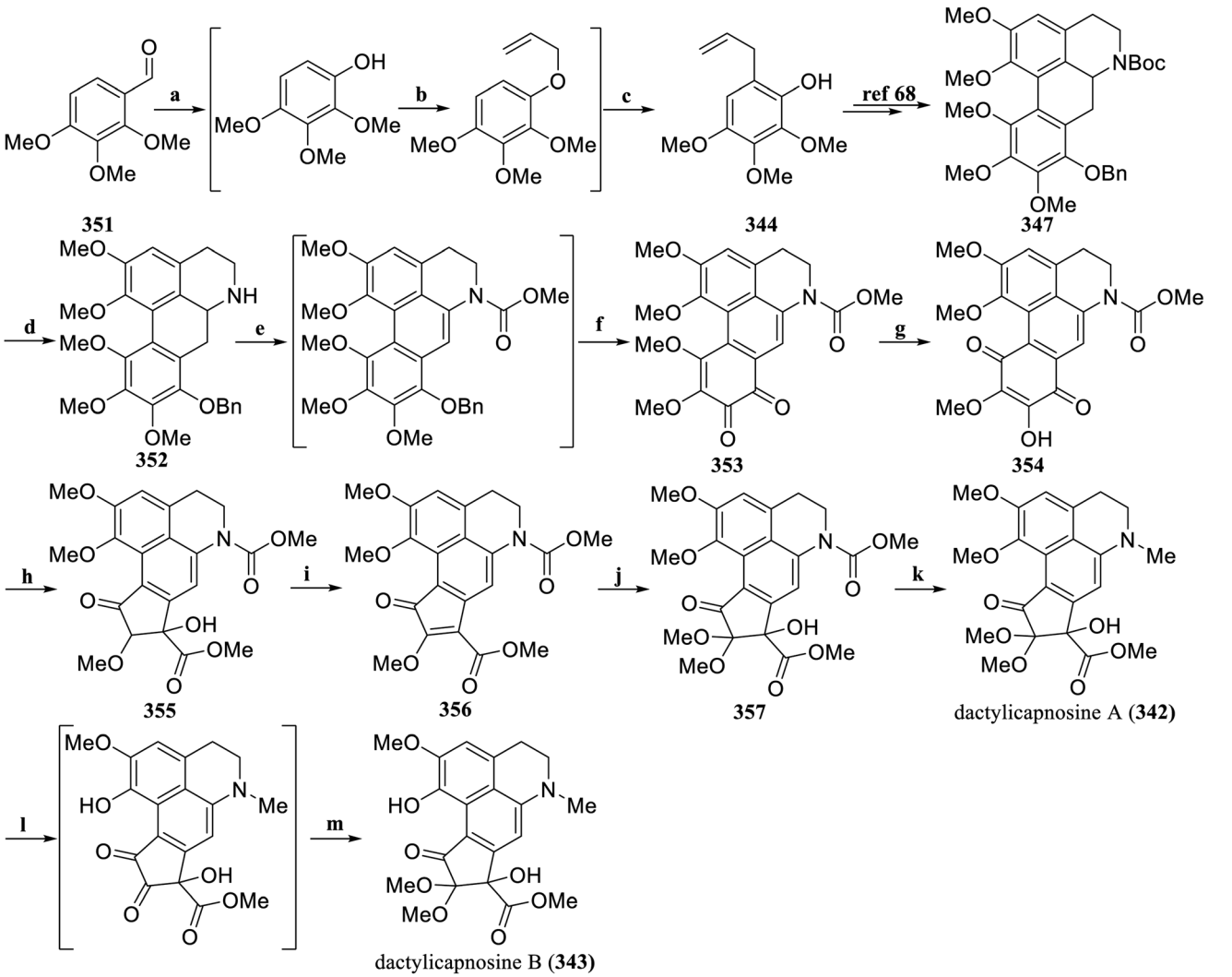

Scheme 15 Total synthesis of dactylicapnosine A (**342**) and dactylicapnosine B (**343**) by Zhang's group. Reagents and conditions: (a) H_2O_2, H_2SO_4, MeOH, rt; (b) allyl bromide, K_2CO_3, acetone, reflux; (c) DMF, 190 °C; (d) TFAA, DCM, rt; (e) (i) NCS, THF, rt, (ii) *t*-BuONa, $ClCO_2Me$, rt; (f) (i) Pd/C, H_2, MeOH, rt, (ii) IBX, DMSO, rt; (g) H_2SO_4, MeCN, rt; (h) $CoCl_2$, MeOH-THF, 80 °C; (i) Et_3N, $(CF_3CO)_2O$, DCM, rt; (j) H_2O_2, Na_2CO_3, MeOH, rt; (k) (i) CH_3ONa, MeOH, rt, (ii) MeI, K_2CO_3, THF, 100 °C; (l) BCl_3, DCM, −78 °C; (m) DMP, TsOH, MeOH, 80 °C.

corytuberine, followed by a rearrangement reaction akin to that of benzilic acid, ultimately yielding the target product.[68] Starting from the 2-allylphenol **344** as the initial material, the phenolic hydroxyl group was protected with benzyl, followed by ozone cleavage of the double bond to obtain aldehyde **345**. After bromination with NBS, the Pictet–Spengler cyclization reaction was performed to construct the tetrahydroisoquinoline skeleton **346**. Subsequently, a palladium-catalyzed C–H activation coupling reaction was employed to produce the aporphine derivative **347**. Following deprotection and oxidation, the *p*-quinone **348** was obtained. With the aid of K_2CO_3, oxygen was used to oxidize **348**, producing the crucial intermediate **349**. Sodium periodate then facilitated a key biomimetic oxidative rearrangement reaction, resulting in the desired product **350**. Under microwave (MW) conditions, the Boc protection was removed, followed by methylation, achieving the first biomimetic total synthesis of dactylicapnosine A (**342**) (Scheme 14).

Later, in 2020, Zhang and Luo *et al.* reported a new synthetic method that employed acid-induced *ortho*-quinone isomerization, cobalt-mediated regioselective cyclocontraction of *p*-quinone, and oxidative methoxylation of enone as key steps. This strategy enabled a more efficient synthesis of dactylicapnosine A and achieved the first total synthesis of dactylicapnosine B.[140] This approach may also provide new insights for the synthesis of other medicinally valuable dactylicapnosine-like analogs (Scheme 15). Starting from 2,3,4-trimethoxybenzaldehyde **351**, the corresponding phenol was obtained through Baeyer–Villiger oxidation. The subsequent allyl ether compound underwent a Claisen rearrangement to produce **344**, which followed the same synthetic path to obtain the aporphine derivative **347**. After removal of the Boc-protecting group, the amine **352** was oxidized to the *ortho*-quinone **353**. Acid-induced isomerization of the *ortho*-quinone gave the *p*-quinone **354**. Then, through cobalt-mediated regioselective cyclocontraction

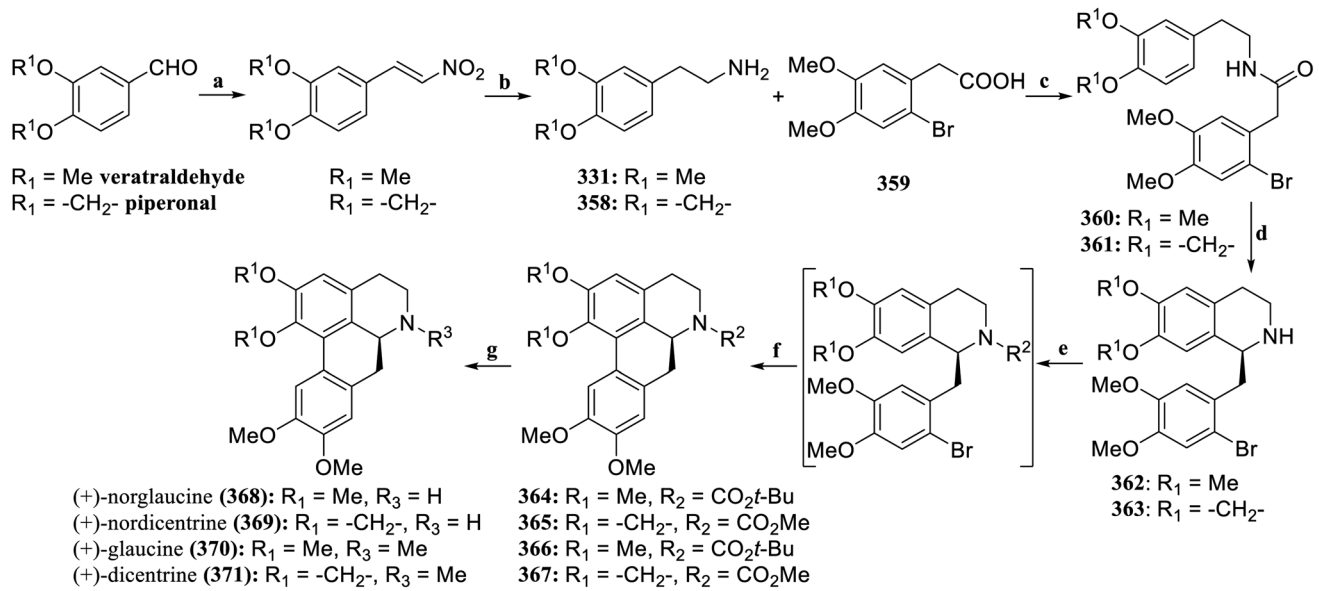

Scheme 16 Total synthesis of (+)-norglaucine (**368**), (+)-nordicentrine (**369**), (+)-glaucine (**370**) and (+)-dicentrine (**371**) by Anderson's group. Reagents and conditions: (a) CH_3NO_2, ethylenediamine, AcOH, 70 °C; (b) $LiAlH_4$, THF, 70 °C; (c) EDC·HCl, NMM, HOBt, DMF, 0 °C to rt; (d) (i) 2-chloropyridine, Tf_2O, DCM, −78 °C to 0 °C, (ii) (*R*,*R*)-Ru(Ts-DPEN)(*p*-cymene)Cl, HCO_2H/Et_3N (5 : 2), 0 °C to rt; (e) (i) Boc_2O, i-Pr_2EtN, DMAP, CH_2Cl_2, rt, or (ii) MeOCOCl, i-Pr_2EtN, DMAP, CH_2Cl_2, rt; (f) $Pd(OAc)_2$, (*t*-Bu)$_2$PMeHBF$_4$, K_2CO_3, DMA, 130 °C; (g) (i) $ZnBr_2$, CH_2Cl_2, rt, or (ii) $LiAlH_4$, THF, 0 °C to rt.

of *p*-quinone, the key intermediate **355** was obtained. After dehydration to obtain **356**, oxidative methoxylation of the enone was performed to obtain the key precursor **357**. Finally, deprotection and methylation afforded dactylicapnosine A (**342**) with a 12% overall yield. By using boron trichloride for demethylation, an unstable diketone intermediate was obtained. After methoxylation with DMP, the first total synthesis of dactylicapnosine B (**343**) was achieved.

In 2020, Anderson *et al.* established a modular strategy for synthesizing enantioselective aporphine (Scheme 16).[141] The phenylethylamine **331** and **358**, which obtained from vanillin and piperonal through Henry reaction and reduction, were coupled with the carboxylic acid **359** to prepare the amides **360** and **361**. Bischler–Napieralski cyclization followed by direct reduction by Noyori asymmetric transfer hydrogenation produced the chiral tetrahydroisoquinolines **362** and **363**, respectively. After the amino group was protected, palladium

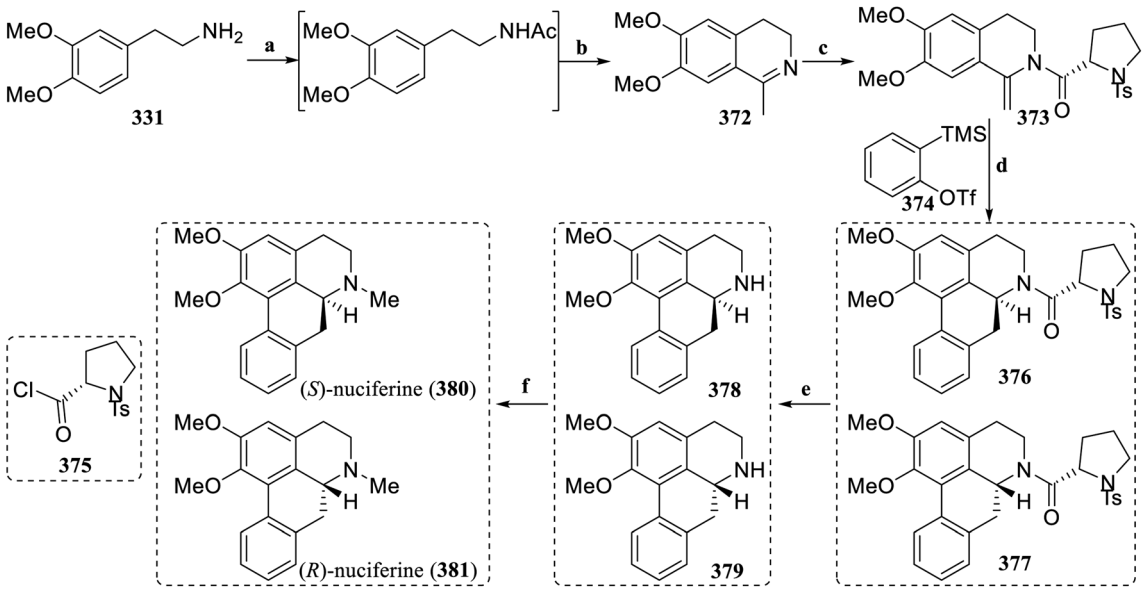

Scheme 17 Total synthesis of (*S*)-nuciferine (**380**) and (*R*)-nuciferine (**381**) by Raminelli's group. Reagents and conditions: (a) Ac_2O, pyridine, 90 °C; (b) (i) $POCl_3$, toluene, reflux, (ii) 40% NaOH, H_2O, rt; (c) **375**, Et_3N, DCM, 0 °C to rt; (d) CsF, MeCN, rt; (e) LiOH, EtOH/H_2O (2 : 1), MW 180 °C; (f) (i) 37% CH_2O, DCM, rt, (ii) $NaBH_4$, rt.

catalyzed the *ortho*-arylation reaction to construct the aporphine backbone **364–367**. The synthesis of (+)-norglaucine (**368**) and (+)-nordicentrine (**369**) was achieved through the deprotection of the Boc group. (+)-glaucine (**370**) and (+)-dicentrine (**371**) were obtained through reductive methylation.

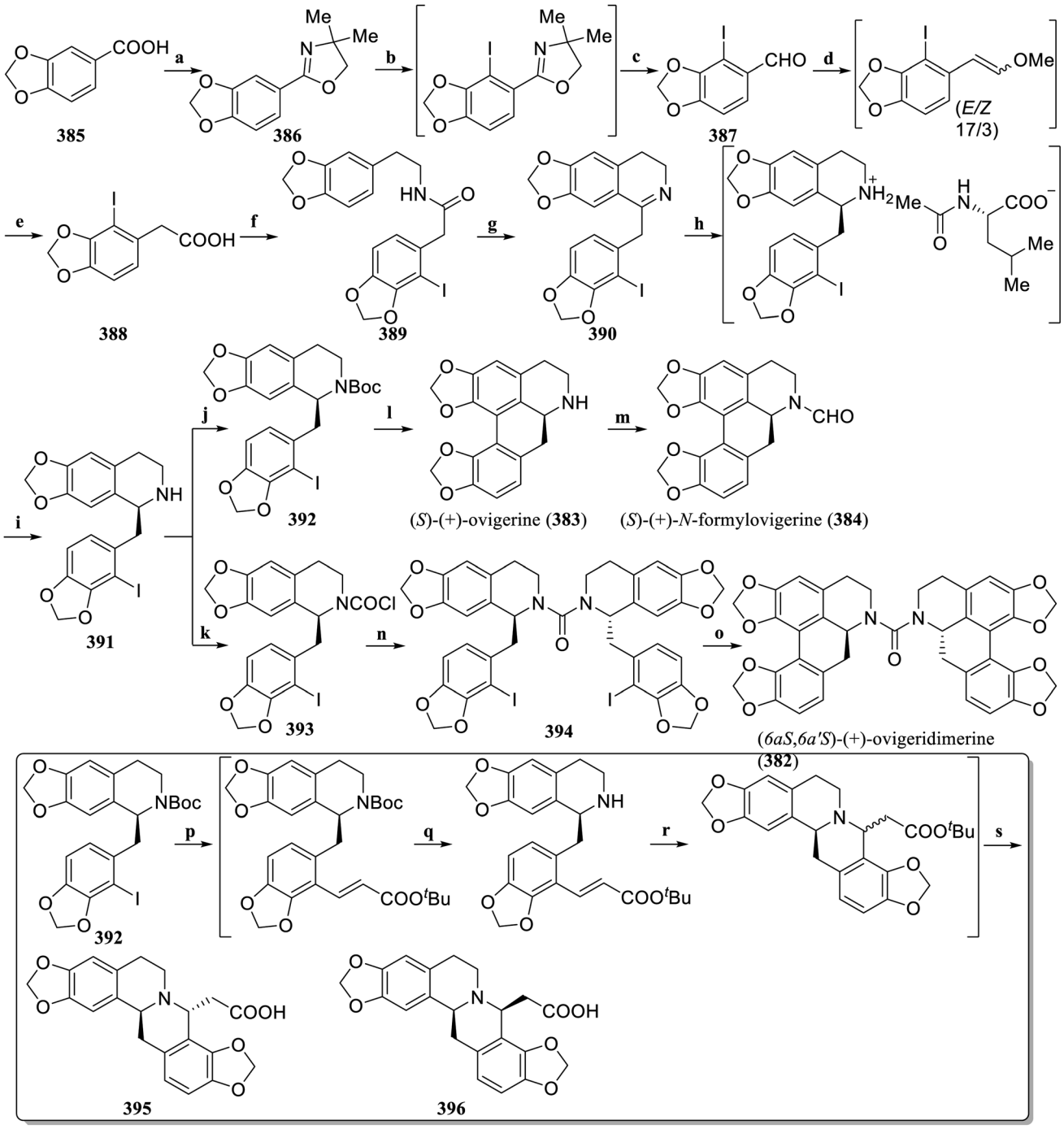

Scheme 18 Total synthesis of (*S*)-(+)-ovigerine (**383**), (*S*)-(+)-*N*-formylovigerine (**384**) and (6a*S*,6a′*S*)-(+)-ovigeridimerine (**382**) by Qin's group. Reagents and conditions: (a) (i) HATU, 2-amino-2-methylpropan-ol, DMF, rt, (ii) *p*-TsCl, Et_3N, DMAP, CH_2Cl_2, rt, (iii) NaOH, MeOH, rt; (b) (i) *n*-BuLi (2.4 M), THF, −50 °C, (ii) I_2, THF, −78 to −50 °C; (c) oxalic acid, THF/H_2O (4/1), rt; (d) NaHMDS (1 M), $Ph_3P^+CH_2OMeCl^-$, THF, 0 °C to rt; (e) (i) TsOH·H_2O, THF, reflux, (ii) $NaClO_2$, NaH_2PO_4, 2-methyl-2-butene, 0 °C; (f) homopiperonylamine, EDCI, HOBt, DIPEA, DMF, 0 °C to rt; (g) $POCl_3$, MeCN, reflux; (h) (i) RuCl[(*R*,*R*)-TsDPEN](*p*-cymene), HCO_2H/Et_3N (5/2), DMF, 0 °C to rt, (ii) *N*-acetyl-L-leucine, i-Pr_2O/MeOH (1/2), reflux; (i) 10% NaOH, pH = 12–13, rt; (j) $(Boc)_2O$, DIPEA, THF, 40 °C; (k) triphosgene, Et_3N, CH_2Cl_2, 0 °C; (l) (i) K_2CO_3, $Pd(OAc)_2$, PhDave-Phos, DMF, 110 °C, (ii) $ZnBr_2$, CH_2Cl_2, rt; (m) ethyl formate, Ar, 75 °C; (n) **391**, DIPEA, MeCN, 40 °C; (o) K_2CO_3, $Pd(OAc)_2$, X-Phos, DMF, 110 °C; (p) $Pd(OAc)_2$, TBAC, *tert*-butyl acrylate, DMF, 120 °C; (q) $MeSO_3H$, CH_2Cl_2/*t*-BuOAc (1/3), 0 °C to rt; (r) *t*-BuOH, reflux; (s) $ZnBr_2$, CH_2Cl_2, rt.

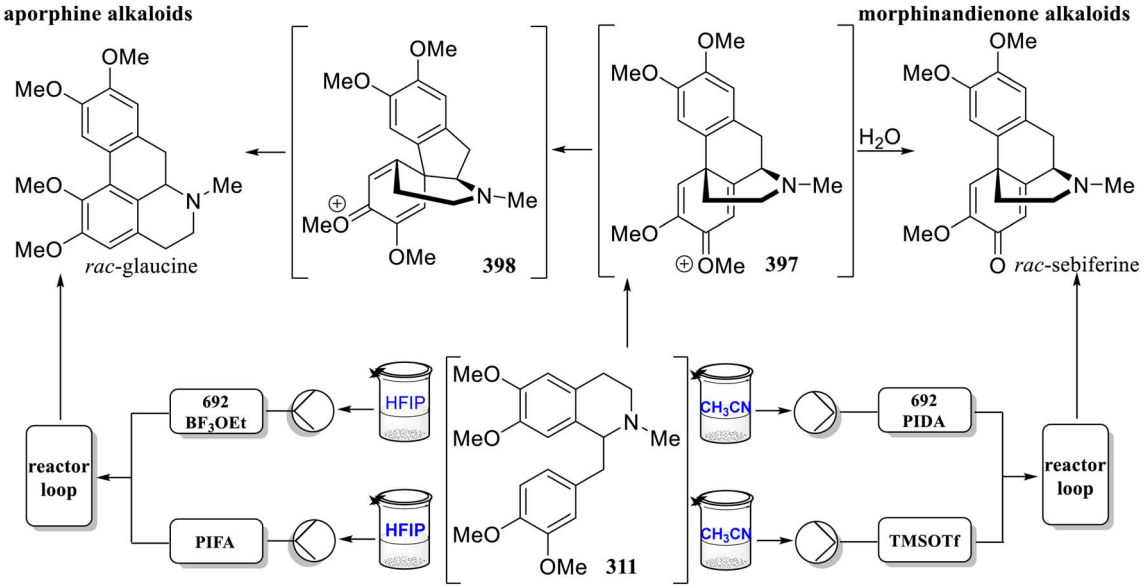

Scheme 19 Flow chemistry divergency between aporphine and morphinandione alkaloids by Felpin's group.

In 2020, Raminelli's group described the stereoselective total synthesis of (*S*)- and (*R*)-nuciferine (Scheme 17).[142] The key to this synthesis was the preparation of the chiral intermediate **373** *via* the triethylamine-mediated coupling of the dihydroisoquinoline **372** and the chiral acid chloride **375**. The dihydroisoquinoline **372** was obtained from the 3,4-dimethoxyphenethylamine **331** by acetylation, Bischler–Napieralski cyclization, and enamidation reactions. Subsequently, the intermediate **373** underwent a [4 + 2] cyclization reaction with the benzyne precursor **374** to obtain diastereoselective intermediates **376** and **377**. Then, the hydrolysis reaction was carried out under microwave heating conditions, and **378** and **379** were obtained. Finally, the *N*-methylation reaction achieved (*S*)-nuciferine (**380**) and (*R*)-nuciferine (**381**) with total yields of 13% and 4%, respectively, in the 6-step reaction.

Qin's group unified the total synthesis routes for benzo[*d*][1,3]dioxole-type aporphines, coptisines, and dibenzopyrrocolines. By utilizing Noyori asymmetric hydrogenation and diastereoselective resolution to achieve excellent enantioselectivity, and combining palladium-catalyzed arylation as a key step, they accomplished the first asymmetric total synthesis of benzo[*d*][1,3]dioxole aporphine alkaloids (6a*S*,6a′*S*)-(+)-ovigeridi-merine (**382**), (*S*)-(+)-ovigerine (**383**), and (*S*)-(+)-*N*-formylovigerine (**384**) (Scheme 18).[143] With slight modifications to the synthetic route, and by combining it with aza-Michael addition, the Bischler–Napieralski reaction, and *N*-arylation, the total synthesis of benzo[*d*][1,3]dioxole-type benzylisoquinoline alkaloids of coptisines and dibenzopyrrocolines was also achieved. The key intermediate, substituted phenylacetic acid, was constructed starting from commercially available piperonylic acid (**385**). Through a series of reactions, which encompassed the

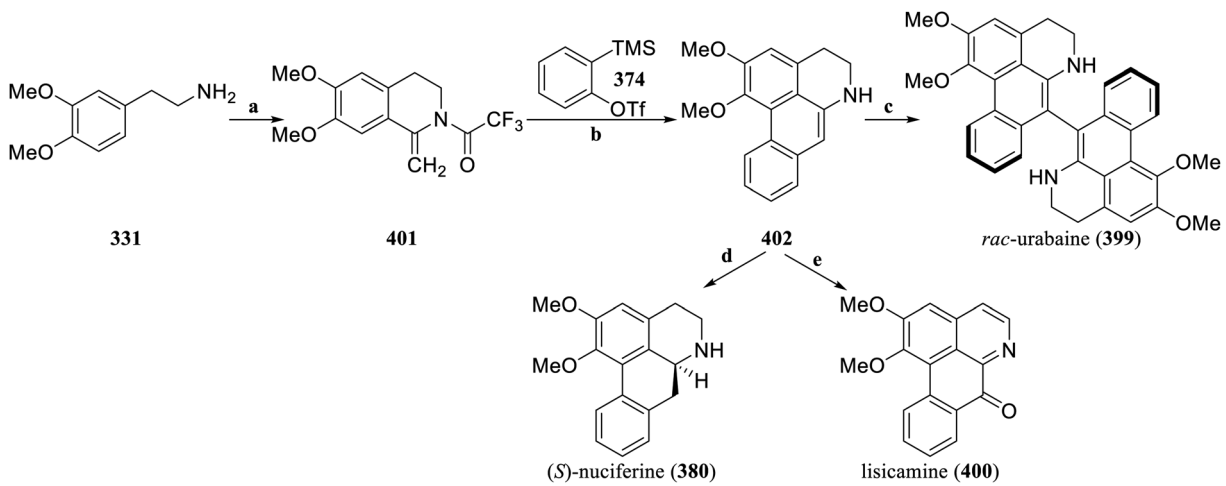

Scheme 20 Total synthesis of *rac*-urbaine (**399**), (*S*)-nuciferine (**380**) and lisicamine (**400**) by Raminelli's group. Reagents and conditions: (a) (i) $(MeCO)_2O$, pyridine, 90 °C, (ii) $POCl_3$, PhMe, NaOH (40%), H_2O, rt, (iii) $(CF_3CO)_2O$, pyridine, DCM, −50 °C; (b) CsF, MeCN, 80 °C, (ii) $NaBH_4$, EtOH, rt, (iii) NCS, DCM, rt; (c) N_2, DCM, 50 °C; (d) $[Ir(COD)Cl]_2$, (S_a,*R*,*R*)-MomoPhos, I_2, H_2, 50 °C; (e) Fremy's salt, Na_2CO_3, MeOH, rt.

formation of precursor oxazoline (**386**), aryl modification, and hydrolysis of the oxazoline to obtain the aldehyde **387**, followed by a Wittig reaction, hydrolysis, and Pinnick oxidation, the key carboxylic acid **388** was synthesized. The **388** was amidated with homopiperonylamine to give **389**, which underwent Bischler–Napieralski cyclization to generate the air-sensitive **390**. The enantiomer **391** was obtained *via* Noyori asymmetric hydrogenation.

After Boc protection and *N*-acylation, **392** and **393** were generated, and **393** was further acylated to give the intermediate **394**. Palladium-catalyzed intramolecular arylation of **392** and **394** produced (*S*)-(+)-ovigerine (**383**), (*S*)-(+)-*N*-formylovigerine (**384**), and (6a*S*, 6a′*S*)-(+)-ovigeridimerine (**382**). In addition, based on this synthesis strategy, the first asymmetric total synthesis of the impatiens **395** and **396** was completed, but the compound spectra were different from those of impatien B.

Through detailed analysis of the reaction mechanism[144] of **311** radical cyclization intermediate **397** rearranged to *rac*-glaucine by erythrinadienone intermediate **398** and hydrolyzed into *rac*-sebiferine, Felpin's group established a flow-controlled divergent synthesis of aporphine and morphinandienone alkaloids based on biomimetic oxidative cyclization using a high-valent iodine(III) reagent in 2022 (Scheme 19).[145] To stabilize the aromatic radical cations formed by PIFA and BF_3-$\cdot Et_2O$, hexafluoroisopropanol (HFIP) was used as the mobile phase solvent to selectively generate aporphine-type natural

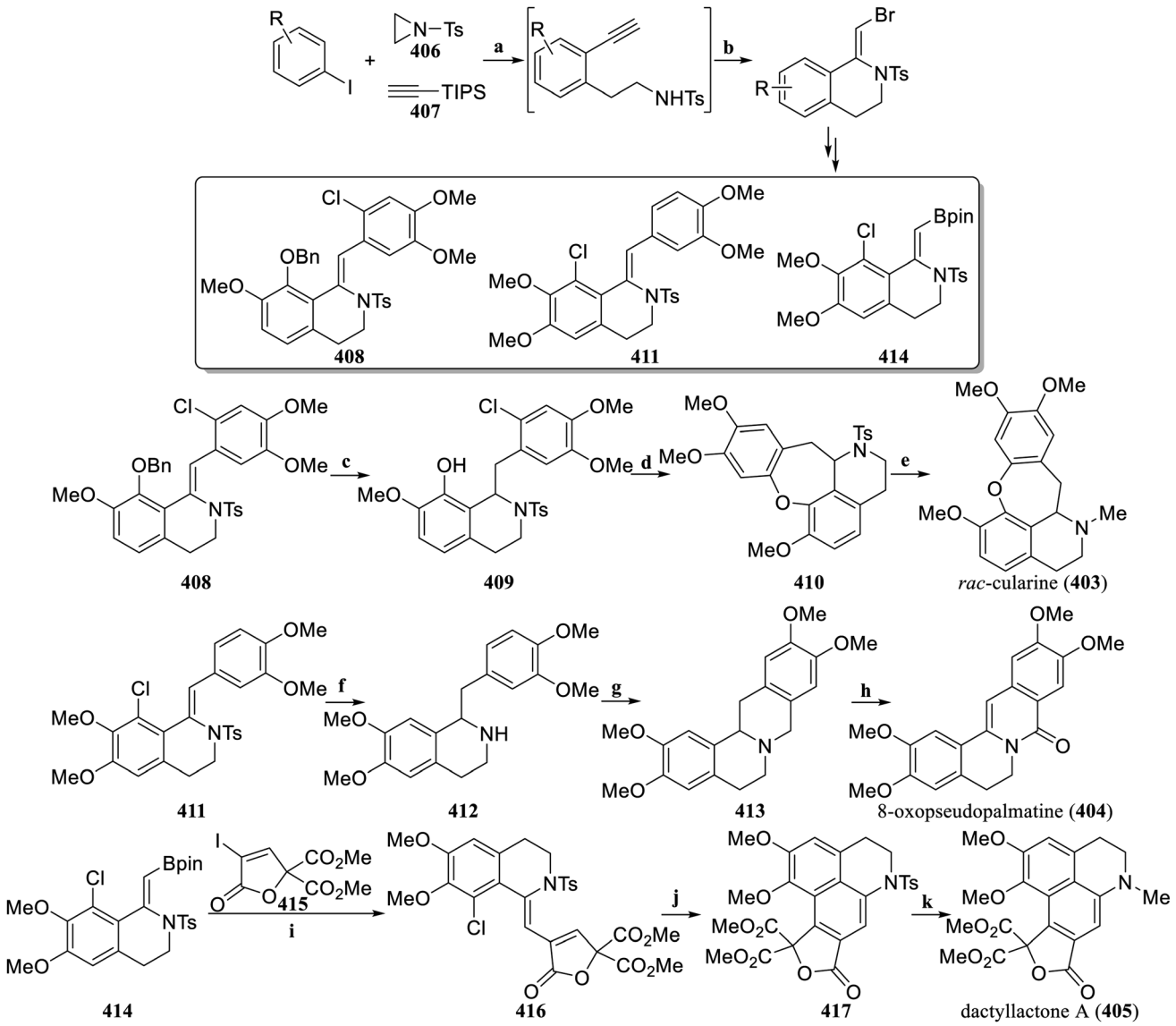

Scheme 21 Total synthesis of *rac*-cularine (**403**), 8-oxopseudopalmatine (**404**) and dactyllactone A (**405**) by Zhou's group. Reagents and conditions: (a) (i) K_2CO_3, $Pd(OAc)_2$, Dave-Phos, NBE derivative, MeCN, 60 °C, (ii) TBAF, THF, rt; (b) NBS, DBU, MeCN, rt; (c) PtO_2, H_2, MeOH : DCM = 1 : 1, TFA, Et_3SiH, DCM, rt; (d) $Pd(OAc)_2$, *tert*-butyl-XPhos, NaOH, toluene, 140 °C; (e) (i) Na, naphthalene, DME, −78 °C, (ii) HCHO (37%), $NaBH_3CN$, acetic acid, MeCN, 0 °C; (f) Pd/C (10%), H_2, MeOH/DCM (1 : 1), Mg powder, MeOH, sonication, rt; (g) HCHO (37%), acetic acid, 100 °C; (h) $Pd(OAc)_2$, $Cu(OAc)_2$, O_2, toluene, 120 °C; (i) $Pd_2(dba)_3$, $AsPh_3$, Ag_2O, THF, rt; (j) *hv* 365 nm, MeOH, rt; (k) (i) H_2SO_4, DCM, rt, (ii) HCHO (37%), $NaBH_3CN$, acetic acid, MeCN, 0 °C.

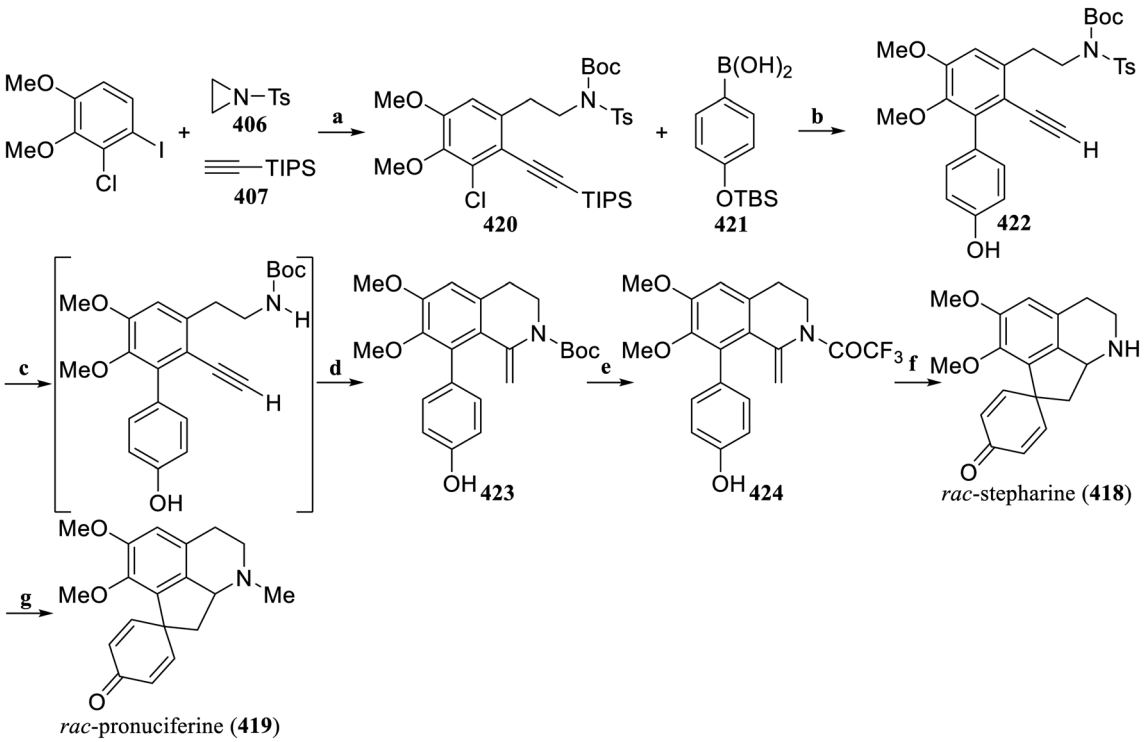

Scheme 22 Total synthesis of *rac*-stepharine (**418**) and *rac*-pronuciferine (**419**) by Zhou's group. Reagents and conditions: (a) (i) K_2CO_3, $Pd(OAc)_2$, Dave-Phos, 5-norbornene-2-carbonitrile, MeCN, 60 °C, (ii) $(Boc)_2O$, DMAP, CH_2Cl_2, rt; (b) (i) NaOH, $Pd(OAc)_2$, SPhos, toluene, 95 °C, (ii) TBAF, THF, 50 °C; (c) Mg powder, MeOH, sonication; (d) $AuPPh_3Cl$, $AgNTf_2$, 4 Å molecular sieves, EtOH, CH_2Cl_2, 30 °C; (e) (i) CF_3COOH, rt, (ii) $(CF_3CO_2)_2O$, Et_3N, CH_2Cl_2, 0 °C; (f) CF_3CH_2OH, PIDA, $NaBH_4$, 0 °C; (g) HCHO (37%), $NaBH_3CN$, AcOH, MeCN, 0 °C.

products. The use of PIDA and TMSOTf in wet CH_3CN allowed the synthesis to diverge into morphinedienone-type natural products. Mixing the two streams in a T-mixer significantly improved mixing efficiency due to the high viscosity of HFIP. Under optimized conditions, this method could provide five natural aporphine products in good to moderate yields depending on the substrate used. Changing the solvent to wet CH_3CN could effectively provide five morphinedienone alkaloids. This strategy offers a new approach for the large-scale production of such natural products.

Based on the benzyne cyclization strategy[146] combined with an oxidative dehydrogenation reaction, Raminelli's group successfully constructed the key dehydroaporphine intermediate, achieving the first total synthesis of (±)-urbaine (**399**), the asymmetric total synthesis of (*S*)-nuciferine (**380**), and the second-generation total synthesis of lisicamine (**400**).[147] Isoquinoline **401** was obtained from the 3,4-dimethoxyphenethylamine **331** by acetylation, Bischler–Napieralski cyclization, and enamidation reactions. Then, the isoquinoline **401** underwent a [4 + 2] cyclization reaction with the benzyne precursor **374** to construct the aporphine skeleton, which was selectively oxidized to obtain the key dehydroaporphine intermediate **402**. The first total synthesis of the bisaporphine alkaloid *rac*-urbaine (**399**) was completed with a total yield of 11% after dimerization of **402** (Scheme 20). After asymmetric hydrogenation and *N*-methylation, (*S*)-nuciferine (**380**) was obtained. Oxidation with Fremy's salt produced lisicamine (**400**).

Based on the previously established strategy of using three components to construct the 1-methylene-THIQ skeleton,[148,149] Zhou's group optimized the Catellani reaction conditions involving aryl iodide, azetidine, and terminal alkynes, and established NBS-mediated cyclization reaction conditions. The modular synthesis of 1-bromomethylene-THIQ scaffold for the multipurpose intermediate in synthetic chemistry was realized. Suzuki–Miyaura coupling reactions and the Heck reaction, among others, could quickly convert 1-bromomethylene-THIQ scaffolds into synthetic intermediates with various structures (Scheme 21).[150] On the basis of this new method, the concise synthesis of *rac*-cularine (**403**), and 8-oxopseudopalmatine (**404**) was completed, and dactyllactone A (**405**) was total synthesized for the first time. The intermediate compound **408** was hydrogenated to remove the benzyl protecting groups and simultaneously reduce enamide to obtain **409**. Palladium-catalyzed intramolecular coupling produced **410**. Removal of Ts, followed by reductive amination with formaldehyde solution generated *rac*-cularine (**403**). Starting from the intermediate compound **411**, catalytic hydrogenation and a detoluenesulfonyl group were used to obtain **412**. Subsequently, **412** was reacted with formalin in AcOH *via* the Mannich reaction to yield the lutenine **413**. According to the reported procedure,[151] 8-oxopseudopalmatine (**404**) was obtained by oxidation. The intermediate compound **414** and the alkenyliodide **415** were coupled *via* Suzuki–Miyaura coupling to obtain the key intermediate **416**. Photocyclization of **416** with a 365 nm UV lamp at room

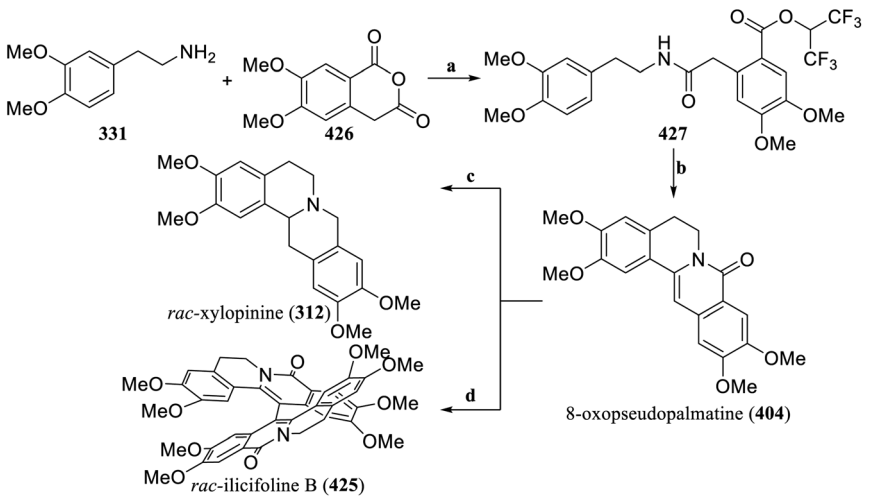

Scheme 23 Total synthesis of 8-oxopseudopalmatine (**404**), *rac*-ilicifoline B (**425**) and *rac*-xylopinine (**312**), by Christmann's group. Reagents and conditions: (a) EDC, DMAP, HFIP, DCM; (b) (i) $POCl_3$, toluene, 110 °C, (ii) K_2CO_3, nBu_4NBr, MeOH, 80 °C; (c) (i) $LiAlH_4$, $AlCl_3$, Et_2O, reflux, (ii) RuCl[(*S*,*S*)-TsDPEN](mesitylene), HCOOH, Et_3N, rt; (d) PIFA, $BF_3{\cdot}Et_2O$, DCM, −78 °C.

temperature to obtain **417**. Finally, after removal of Ts, followed by simple reductive *N*-methylation, the first total synthesis of dactyllactone A (**405**), was realized.

Zhou's group subsequently reported a concise total synthesis method for *rac*-stepharine (**418**) and *rac*-pronuciferine (**419**) (Scheme 22).[152] Through the established Pd/NBE cooperative catalysis of a three-component Catellani reaction and the Suzuki–Miyaura coupling reaction, the key intermediate **420** was prepared, and then coupled with **421** *via* the Suzuki–Miyaura reaction to produce **422**. The *N*-tosyl group was removed, and Au/Ag-catalyzed 6-*exo*-dig cyclization was performed to produce 1-methylene-THIQ **423**. The *N*-protecting group was replaced, and then **424** underwent oxidative dearomatization promoted by PIDA, followed by reduction with $NaBH_4$ to obtain *rac*-stepharine (**418**). Finally, *rac*-pronuciferine (**419**) was generated through reductive amination.

3.1.4 Berberine isoquinoline alkaloids. In 2021, Christmann *et al.* developed a complementary di-carbonyl activation strategy for the synthesis of polycyclic alkaloids, enabling the rapid construction of the polycyclic skeletons of biologically active alkaloids.[153] This method facilitated the efficient total synthesis of berberine alkaloids such as 8-oxopseudopalmatine (**404**), *rac*-ilicifoline B (**425**), and *rac*-xylopinine (**312**) (Scheme 23). First, the key reaction intermediate **427** was synthesized through an amidation reaction between the 3,4-dimethoxyphenylethylamine **331** and the 6,7-dimethoxyvarie-1,3-dione **426**. Then, under standard reaction conditions, a cyclization reaction was performed, which directly produced 8-oxopseudopalmatine (**404**). Subsequently, using Opatz's dimerization conditions,[154] *rac*-ilicifoline B (**425**) was subsequently synthesized. According to the reported method,[155] **404** can be converted into the tetracyclic protoberberine alkaloid *rac*-xylopinine (**312**). Furthermore, this strategy can also be applied to the synthesis of different types of polycyclic alkaloids and their analogs, such as tetracyclic alkaloids and pentacyclic indoquinoline alkaloids with significant application value.

Yamamoto *et al.* achieved the asymmetric total synthesis of the C8-substituted tetrahydroproberberine natural product (−)-javaberine A (**428**) and its epimer through asymmetric hydroamination and Bischler–Napieralski cyclization in 2021.[156] First, the cyclization precursor was constructed, which obtained **432** by the Heck reaction of 2-bromo-4,5-dimethoxybenzaldehyde (**430**) and 3,4-dimethylstyrene (**431**), and then **433** was obtained *via* the Henry reaction, reduction and methylation reaction. The lithium amide-chiral bisoxazoline catalyzed the intramolecular asymmetric hydroamination reaction of **433**, which was demethylated by Polonovski-type reaction to obtain **434**. Condensation of **434** with homoveratric acid afforded the amide **435**. Bischler–Napieralski cyclization of **435** produced **436**, followed by $LiAlH_4$ reduction and BBr_3 demethylation to afford (−)-javaberine A (**428**) and *epi*-javaberine A (**429**) (Scheme 24).

In 2021, Chen's group completed the asymmetric total synthesis of tetrahydro-protoberberine alkaloids (Scheme 25).[157] First, the efficient and sustainable synthesis of the secondary amine hydrochlorides **437a–d** was realized by using disubstituted phenethylamine **331**, **358** and disubstituted benzaldehyde as raw materials through a continuous flow system. The key Pictet–Spengler reaction/Friedel–Crafts hydroxyalkylation/dehydration cascade cyclization reaction conditions were subsequently optimized to further convert **437a–d** to dihydroprotoberberines **438a–d**. By screening the chiral ligands, the Ir-catalyzed enantioselective hydrogenation was successfully realized, the chiral center of C-14 was constructed, the efficient asymmetric total synthesis of (−)-canadine (**439**), (−)-rotundine (**440**), (−)-sinactine (**441**), and (−)-xylopinine (**326**) were completed.

Subsequently, based on this synthetic strategy,[157] Chen's group achieved the first fully continuous flow asymmetric synthesis method for natural tetrahydroproto-berberine alkaloids in 2022 (Scheme 26).[158] Using commercialized homopiperony-lamine and disubstituted benzaldehyde as

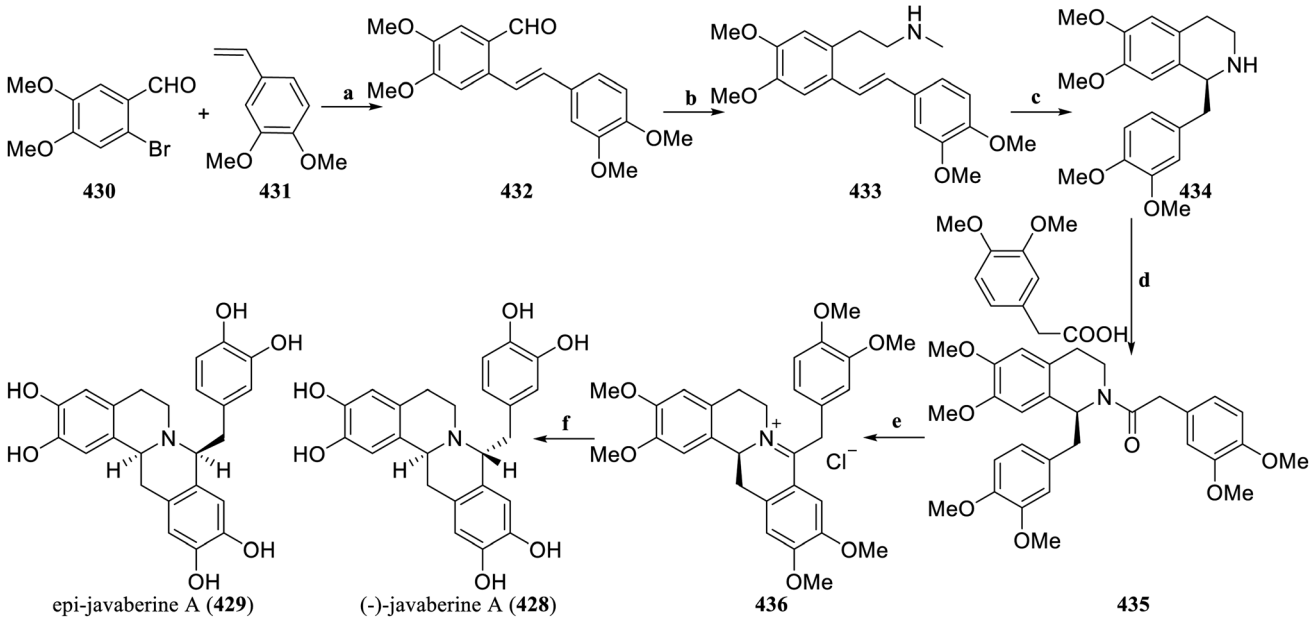

Scheme 24 Total synthesis of (−)-javaberine A (**428**) and *epi*-javaberine A (**429**), by Yamamoto's group. Reagents and conditions: (a) $Pd(OAc)_2$, K_3PO_4, DMA, 140 °C; (b) (i) $MeNO_2$, NH_4OAc, 100 °C, (ii) $LiAlH_4$, THF-Et_2O, rt, (iii) HCOOH, Ac_2O, rt, (iv) $LiAlH_4$, THF, rt; (c) (i) chiral box ligand, *n*-BuLi, i-Pr_2NH, toluene, −30 °C, (ii) *m*CPBA, DCM, rt, (iii) HCl, $FeSO_4 \cdot 7H_2O$, rt; (d) EDC, HOBt, Et_3N, DCM, rt; (e) $POCl_3$, MeCN, reflux; (f) $LiAlH_4$, THF, −78 °C, (ii) BBr_3, DCM, 0 °C.

starting materials, four reaction steps and work-up processing were realized through six different continuous flow devices integrated in a flow platform, including the reductive amination of secondary amines, the formation of secondary amine hydrochlorides, Pictet–Spengler reaction/Pomeranz–Fritsch reaction cascade cyclization to form the dihydroprotoberberine core skeleton, and enantioselective catalytic hydrogenation. Without any intermediate purification, this new fully continuous process ultimately synthesized (−)-isocanadine (**442**), (−)-tetrahydropseudocoptisine (**443**), (−)-stylopine (**444**) and (−)-nandinine (**445**) with an enantiomeric excess (ee) of over 84% and a total yield of over 43%. Moreover, the total reaction residence time was reduced from 100 hours to 32.5 minutes. Compared with traditional batch operations, this fully continuous flow synthesis process offers advantages such as high production efficiency, good time economy, and high route sustainability; this provides a new scalable and efficient continuous production technology for the total synthesis of tetrahydroprotoberberine alkaloids. This further demonstrates the potential application of continuous flow reaction technology in the total synthesis of natural products.

In 2022, Cuny's group achieved the first total synthesis of pallimamine (**446**) and its epimer (**447**) (Scheme 27).[159] Vanillin (**448**) was selectively iodinated and hydroxylated at the 5-

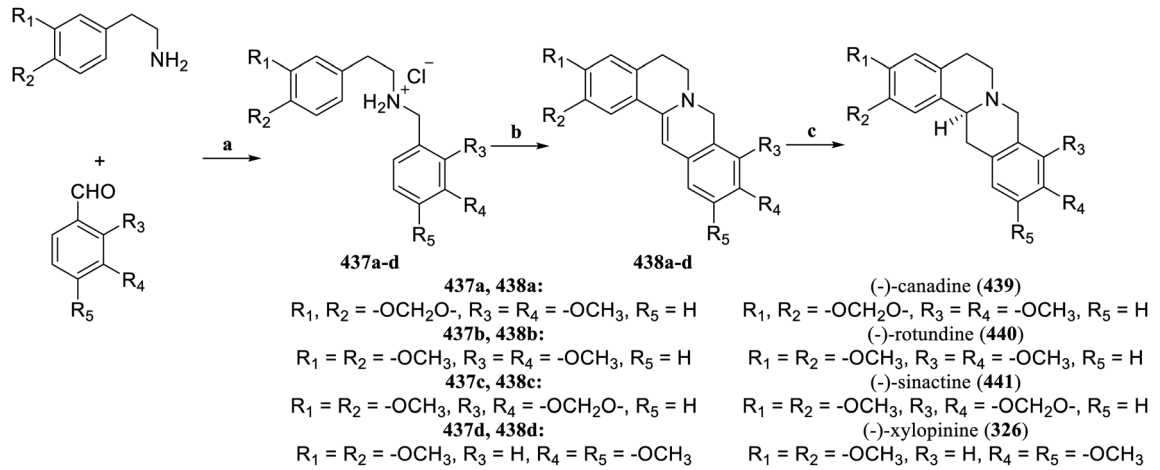

Scheme 25 Total synthesis of (−)-canadine (**439**), (−)-rotundine (**440**), (−)-sinactine (**441**) and (−)-xylopinine (**326**) by Chen's group. Reagents and conditions: (a) 4 Å MS powder, 10% $Pd(OH)_2$/C-SiO_2, H_2, MeOH, continuous flow synthesis; (b) $B(OH)_3$, NaCl, 98% HCOOH, 80 °C; (c) $[Ir(COD)Cl]_2$, (*S*,*S*)-*f*-BINAPHANE, KBr, H_2, DCM : AcOH = 9 : 1, rt.

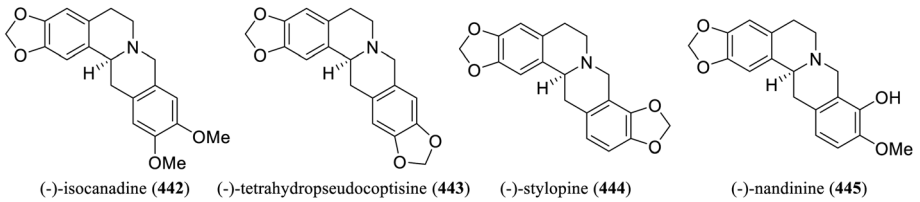

Scheme 26 Continuous-flow total synthesis of (−)-isocanadine (**442**), (−)-tetrahydropseudocoptisine (**443**), (−)-stylopine (**444**) and (−)-nandinine (**445**) by Chen's group.

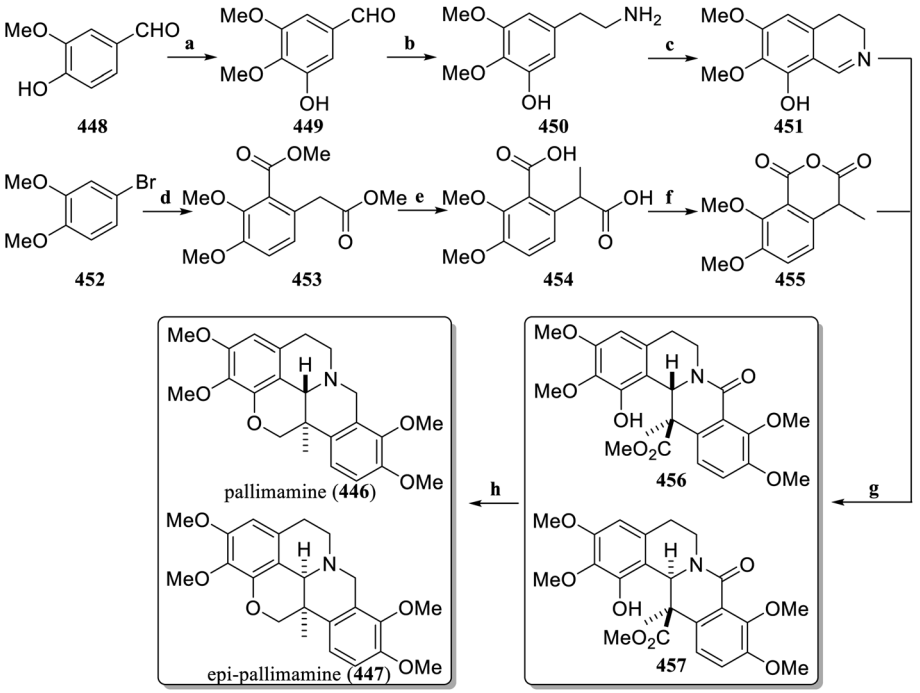

Scheme 27 Total synthesis of pallimamine (**446**) and *epi*-pallimamine (**447**), by Cuny's group. Reagents and conditions: (a) (i) I_2, KI, $NaHCO_3$, H_2O, rt, (ii) $CuSO_4 \cdot 5H_2O$, 20% NaOH, reflux, (iii) Me_2SO_4, Na_2CO_3, acetone, reflux; (b) (i) $MeNO_2$, NH_4OAc, AcOH, 90 °C, (ii) $NaBH_4$, MeOH, 0 °C, (iii) Pt/C, H_2, EtOAc, rt; (c) (i) HCO_2Et, Et_3N, reflux, (ii) $POCl_3$, $CHCl_3$, 55 °C; (d) $MeO_2CCH_2CO_2Me$, TMP, *n*-BuLi, THF, −78 °C; (e) (i) LDA, MeI, THF, −78 °C-rt, (ii) KOH, MeOH : H_2O (1 : 2), reflux; (f) AcCl, reflux; (g) (i) DCM, 0 °C-rt, (ii) $SOCl_2$, MeOH, reflux; (h) (i) LAH, THF, 0 °C-rt, (ii) DIAD, *n*-Bu_3P, DCM, rt.

position, followed by the method of Banwell *et al.*[160] to obtain **449**. The benzaldehyde **449** was condensed with nitromethane, and after reduction of the olefin and nitro groups, the desired phenylethylamine derivative **450** was obtained. The Bischler–Napieralski cyclization then gave the key fragment imine **451**. The reaction of the 4-bromo-1,2-dimethoxybenzene (**452**) with dimethylmalonic acid in the presence of 2,2,6,6-tetramethylpiperidine lithium (TMP) gave the diester **453**, followed by methylation and ester hydrolysis to obtain **454**. Dehydration cyclization gave another key fragment, anhydride **455**. The formal [4 + 2] cycloaddition reaction of **451** and **455** obtained the epimers **456** and **457**. After $LiAlH_4$ reduction, intramolecular Mitsunobu reaction achieved the first total synthesis of the pallimamine (**446**) and *epi*-pallimamine (**447**) with total yields of 0.19% and 1.1%, respectively, laying the foundation for pharmacological studies of this interesting and unique tetrahydroberberine natural product.

In 2023, Chen's group established an efficient and environmentally friendly green dehydrogenation reaction method. Through I_2-mediated electrochemical acceptorless

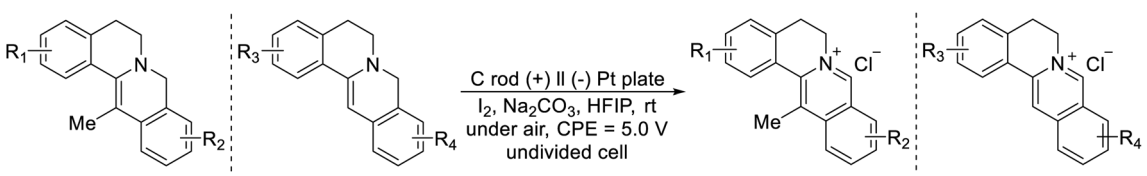

Scheme 28 Synthesis of protoberberine (PB) and 13-methylprotoberberine (13-MePB) by Chen's group.

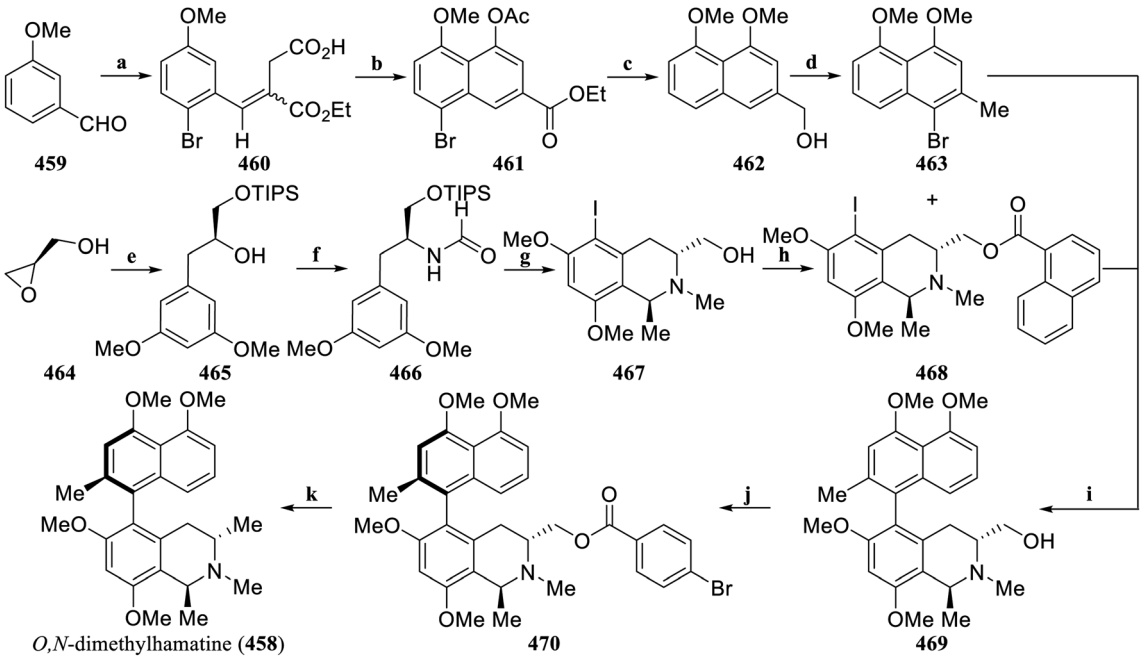

Scheme 29 Total synthesis of *O*,*N*-dimethylhamatine (**458**) by Lipshutz's group. Reagents and conditions: (a) (i) NBS, acetone, rt, (ii) diethoxyphosphorylacetic acid ethyl ester, DBU, MeCN, rt, (iii) 90/10 TFA/H_2O, rt; (b) Ac_2O, NaOAc, rt; (c) (i) NaOH, EtOH, rt, (ii) Pd/C, H_2, EtOH, rt, (iii) MeI, K_2CO_3, acetone, reflux, (iv) LAH, THF, rt; (d) (i) TBAB, DCM, rt, (ii) PPh_3, 1,2-dibromotetrachloroe-thane, DCM, rt, (iii) L-selectride, 0 °C; (e) (i) triisopropylsilyl chloride (TIPSCl), imidazole, DCM, 0 °C, (ii) 3,5-dimethoxybromobenzene, Mg, CuI, THF, −35 °C; (f) (i) PPh3, diisopropyl azodicarboxy-late (DIAD), phthalimide, THF, 0 °C, (ii) $(H_2N)_2$, EtOH, reflux, (iii) methyl formate, CH_3CO_2H, rt; (g) (i) $POCl_3$, 2-methylpyrazine, DCM, 0 °C, (ii) MeMgCl, Et_2O, −78 °C, (iii) *N*-iodosuccinimide, TFA, MeCN, rt, (iv) paraformaldehyde, HCO_2H, MeOH, reflux, (v) tetrabutylammonium fluoride (TBAF), THF, rt; (h) dicycloheylcarbodiimide (DCC), 1-naphthoic acid, 4-dimethylaminopyridine (DMAP), DCM, rt; (i) (i) Pd(IPr*)(cinnamyl) Cl, $ZnCl_2$, THF, rt, (ii) NaOH, MeOH, rt; (j) DCC, DMAP, *p*-bromobenzoic acid, DCM, rt; (k) (i) NaOH, MeOH, rt, (ii) *n*-BuLi, tosyl chloride (TosCl), −78 °C, H_2O, 0 °C, (iii) $LiBEt_3H$, THF, 0 °C-rt.

dehydrogenation (ECAD) could eco-efficiently construct aromatized of protoberberine (PB) and 13-methyl-protoberberine (13-MePB) in last-stage (Scheme 28).[161] This new method for aromatization of the tetracyclic framework was applied to divergent syntheses of ten PBs and eight 13-MePBs in high yields. Importantly, this I_2-ECAD protocol can be conducted on a gram scale and applied successfully in a continuous flow microreactor successfully.

3.1.5 Naphthylisoquinoline alkaloids. The Lipshutz's group achieved the first total synthesis of an axially chiral, tetra-*ortho*-substituted, sterically congested *O*,*N*-dimethylhamatine (**458**) through a late-stage biaryl bond-forming strategy

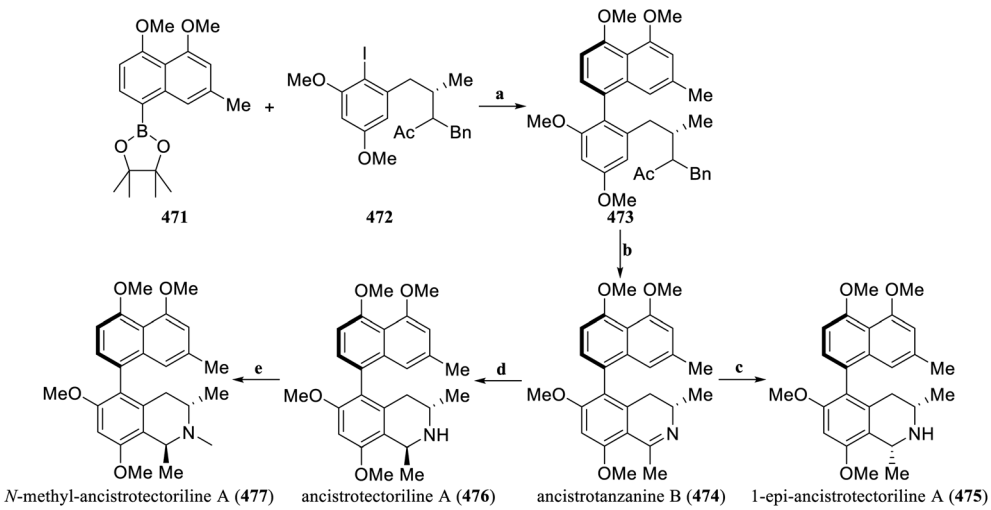

Scheme 30 Total synthesis of ancistrotanzanine B (**474**), 1-*epi*-ancistrotectoriline A (**475**), ancistrotectoriline A (**476**) and *N*-methyl-ancistrotectoriline A (**477**) by Cheon's group. Reagents and conditions: (a) $Pd(OAc)_2$, *t*-BuXPhos, K_3PO_4, BHT, DMF, 100 °C; (b) (i) Pd/C, H_2, MeOH, rt, (ii) $POCl_3$, MeCN, 80 °C; (c) $NaBH_4$, MeOH, rt; (d) $AlEt_3$, $LiAlH_4$, THF, −78 °C-rt; (e) (i) Boc_2O, TEA, DCM, rt, (ii) $LiAlH_4$, THF, 60 °C.

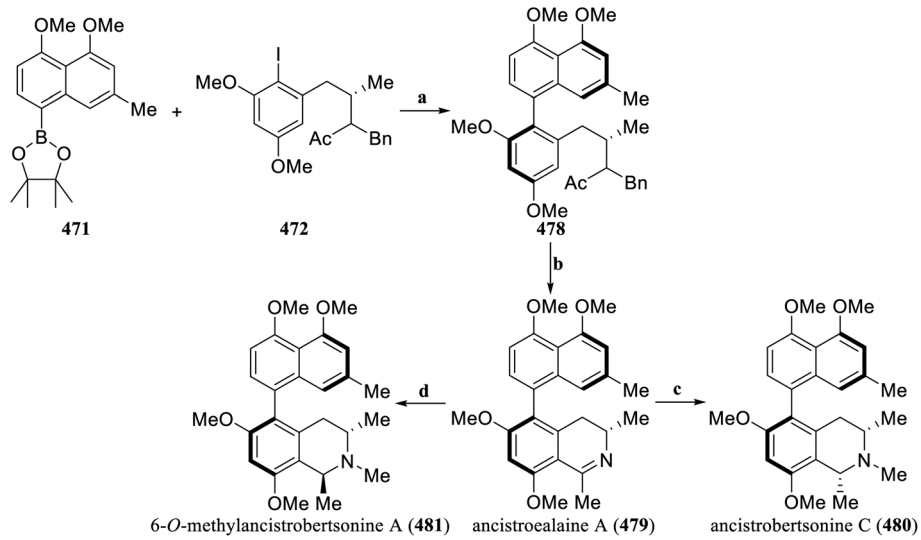

Scheme 31 Total synthesis of ancistroealaine A (**479**), ancistrobertsonine C (**480**) and 6-*O*-methyl-ancistrobertsonine A (**481**) by Cheon's group. Reagents and conditions: (a) $Pd(OAc)_2$, SPhos, $Ba(OH)_2$, BHT, DMF, 100 °C; (b) (i) Pd/C, H_2, MeOH, rt, (ii) $POCl_3$, MeCN, 80 °C; (c) (i) $NaBH_4$, MeOH, rt, (ii) $ClCO_2Me$, TEA, DCM, 0 °C, (iii) $LiAlH_4$, THF, 60 °C; (d) (i) $AlEt_3$, $LiAlH_4$, THF, −78 °C-rt, (ii) $ClCO_2Me$, TEA, DCM, 0 °C, (iii) $LiAlH_4$, THF, 60 °C.

(Scheme 29).[162] Initially, 3-methoxybenzaldehyde (**459**) underwent *ortho*-bromination, followed by conversion *via* the Horner–Wadsworth–Emmons (HWE) reaction to obtain a mixture of *E*- and *Z*-alkenes. The *tert*-butyl ester was then hydrolyzed to give **460**. Cyclization with acetic anhydride produced **461**. Subsequently, alkaline hydrolysis, and Pd/C hydrogenation were performed to remove the Ac protecting group and bromine, followed by *O*-methylation and reduction to obtain the alcohol **462**. After selective bromination of TBAB, the Appel reaction converted it to dibromide, which was then reduced by L-selectride to obtain the fragment **463**. After the hydroxyl group of (*R*)-glycerol **464** was protected by TIPS, the aryl Grignard reagent was used for ring-opening to obtain **465**. Subsequently, Mitsunobu inversion and hydrazinolysis were performed to produce free amine, which, upon formylation, generated **466**. After Bischler–Napieralski cyclization and methylation, selective aryl iodination, *N*-methylation, and deprotection of hydroxyl group afforded **467**. After esterification, the coupling fragment **468** was obtained. Under optimized Negishi coupling conditions, the fragment **468** was coupled with the Grignard reagent prepared *in situ* from **463**, constructing the biaryl structure. Ester hydrolysis gave a mixture **469**, which was then converted to the corresponding *p*-bromobenzoate. Chromatographic separation on silica gel provided the pure isomer **470**. Finally, SuperHydride reduction afforded *O*,*N*-dimethylhamatine (**458**).

In 2020, Cheon's group established a new method to construct biaryl products with high atroposelectivity through the atroposelective aryl coupling reaction based on the chirality of the existing center.[163] This new method does not require the use of an external chiral source, but utilizes a central chirality group for atroposelectivity control. The total synthesis of C5–C8′ coupled naphthylisoquinoline alkaloids with *M*-configuration was achieved (Scheme 30). By adjusting the types of ligands and bases, the Suzuki–Miyaura coupling conditions for the naphthyl pinacol boronic acid ester **471** and the chiral aryl iodide **472** were optimized to obtain biaryl coupling product **473** with the *M*-configuration. After debenzyl protection, ancistrotanzanine B (**474**) was obtained *via* the Bischler–Napieralski reaction. Reduction of **474** with $NaBH_4$ gave the *cis*-product 1-*epi*-ancistrotectoriline A (**475**). In the presence of $AlEt_3$, the reduction of **474** with $LiAlH_4$ resulted in the corresponding *trans*-product ancistrotectoriline A (**476**), which was then *N*-methylated to obtain *N*-methyl-ancistrotectoriline A (**477**).

In the same year, the total synthesis of naphthylisoquinoline alkaloids with (*P*)-configurations, including ancistroealaine A (**479**), ancistrobertsonine C (**480**) and 6-*O*-methyl-ancistrobertsonine A (**481**), were achieved by adjusting the ligand and base species *via* the same synthesis strategy used by Cheon's group (Scheme 31).[164]

Zhou *et al.* established a novel modular method for efficiently constructing 1,3-*trans*-disubstituted tetrahydroisoquinolines through a three-component Catellani reaction and an Au-catalyzed cyclization/reduction cascade reaction, providing a new synthetic strategy for the total synthesis of naphthylisoquinoline alkaloids and related drugs.[149] In this method (Scheme 32), simple aryl iodide **482**, aziridine **483** and (triisopropylsilyl)acetylene **407** were used as the building blocks to promote the Catellani reaction through a Pd-ligand/NBE derivative catalytic system, and the Au-catalyzed intramolecular 6-*exo*-dig cyclization and reduction reaction was used in tandem to construct the 1,3-*trans*-disubstituted tetrahydroisoquinoline **484** in a concise and efficient manner. The iodo product **485** was then coupled with naphthalene boronic acid **486** *via* a Suzuki–Miyaura coupling reaction to assemble the axially chiral intermediate **487**(*M* + *P*). Catalytic hydrogenation simultaneously removed benzyl protection and Cbz protection, completing the total synthesis of korupensamine A (**488**) and B

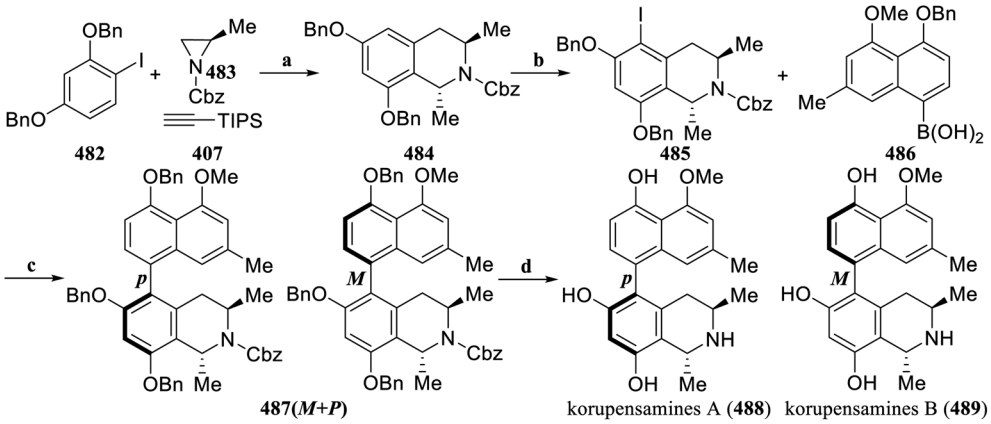

Scheme 32 Total synthesis of korupensamine A (**488**) and B (**489**) by Zhou's group. Reagents and conditions: (a) (i) $Pd(OAc)_2$, DavePhos, NBE derivative, K_2CO_3, MeCN, 70 °C, TBAF, rt, (ii) $AuCl(PPh_3)$, $AgSbF_6$, THF, reflux, (iii) Et_3SiH, TFA, 4A MS, DCM, rt; (b) I_2, CF_3CO_2Ag, $CHCl_3$, rt; (c) $Pd(OAc)_2$, XPhos, K_3PO_4, THF/H_2O, 80 °C; (d) Pd/C, H_2, EtOH/DCM, rt.

(**489**). This is the shortest (requiring only five reaction steps) and most efficient (with a total yield of 30%) synthetic route to date.

Under the action of TFA, *N*-iodosuccinimide (NIS) iodized the key intermediate **487** (*M* + *P*) to obtain the aryl iodides **492a** and **492b**, respectively. Subsequently, Turbo Grignard reagent (iPrMgCl·LiCl) was used to treat **492a**, forming the aryl zinc reagent **493** *in situ* through metal transfer. It then underwent Negishi coupling with **492a** and **492b**, respectively. After catalytic hydrogenation to simultaneously remove benzyl and Cbz protections, the more challenging target products, namely, michellamines B (**490**) and C (**491**), were efficiently synthesized (Scheme 33).

In 2023, van Otterlo's group established the first catalyst-controlled atroposelective cross-coupling reaction that enabled the direct synthesis of different naphthylisoquino-line alkaloids from their respective precursors (Scheme 34).[165] First, northern naphthalene building blocks started with commercially available 1,8-dihydroxynaphthalene (**494**), naturally occurring methyl groups were selected for protection of phenol functional groups, and then regioselective OH-directed

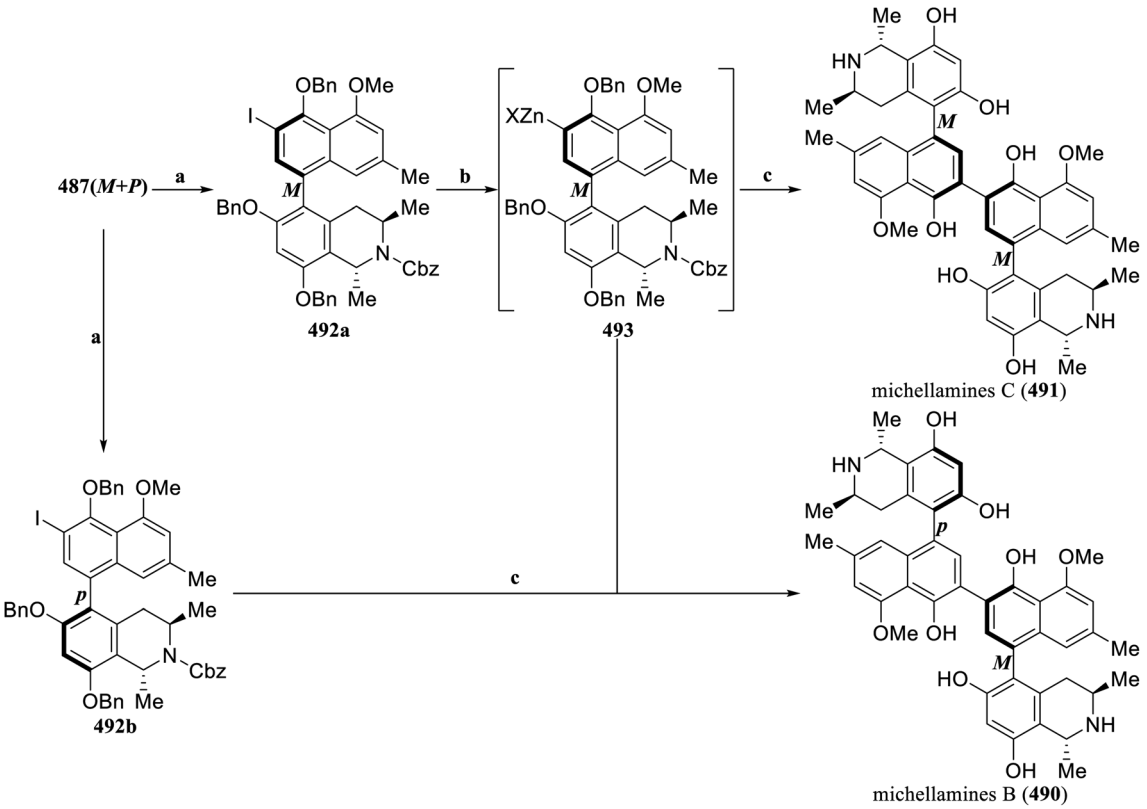

Scheme 33 Total synthesis of michellamines B (**490**) and C (**491**) by Zhou's group. Reagents and conditions: (a) NIS, TFA, MeCN, rt, dark; (b) $^{i}PrMgCl·LiCl_2$, $ZnCl_2$, THF, rt; (c) (i) $Pd(PPh_3)_4$, THF, 80 °C, (ii) Pd/C, H_2, EtOH/DCM, rt.

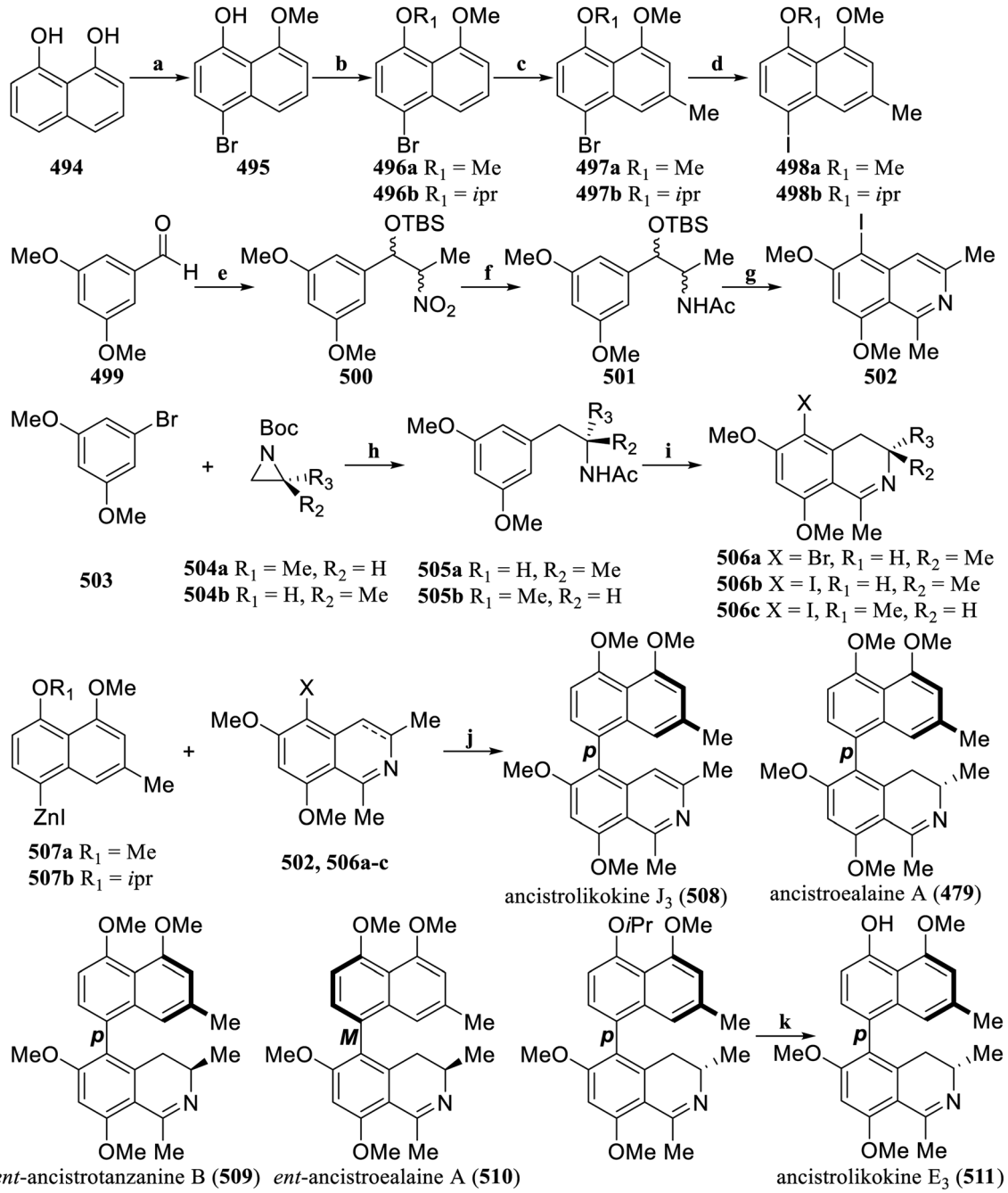

Scheme 34 Total synthesis of 5,8′-naphthylisoquinoline alkaloids (**479**, **508**–**511**) by van Otterlo's group. Reagents and conditions: (a) (i) MeI, K_2CO_3, acetone, rt, (ii) NBS, MeCN, rt; (b) iPrI, K_2CO_3, acetone, 80 °C; (c) (i) HBpin, [{Ir(cod)OMe}2], dtbpy, THF, 80 °C, (ii) $(MeO)_3PO$, LiO*t*Bu, CuI, LiI, DMI, 50 °C; (d) *n*BuLi, Et_2O, I_2, −78 °C-rt; (e) (i) $EtNO_2$, $LiAlH_4$, THF, 0 °C-rt, (ii) TBSCl, imidazole, DCM, 45 °C; (f) (i) $CoCl_2$, $NaBH_4$, MeOH, 0 °C-rt, (ii) AcCl, DMAP, NEt_3, DCM, 0 °C-rt; (g) (i) $POCl_3$, MeCN, 85 °C, (ii) NIS, TfOH, 0 °C; (h) (i) Mg, THF (0.5 m), rt-70 °C, then **505a,b**, CuBr, THF, 0 °C-rt, (ii) TFA, DCM, 0 °C-rt, then AcCl, DMAP, NEt_3, DCM, 0 °C-rt; (i) (i) NIS, TFA, MeCN, 0 °C-rt, (ii) Tf_2O, 2-Cl-pyridine, DCM, −78 °C-rt; (j) $NiCl_2$(DME), Lassaletta's *N*,*N*-ligand, THF/DMF, 60 °C; (k) BCl_3, DCM, −30 °C.

bromination at the 8′-position of the naphthalene core were performed using NBS. The naturally occurring methyl and synthetically more labile isopropyl group was then selected as the protective group of the phenol functional group in **495**, and gave **496a,b**. Hartwig's CuI-catalyzed methylation reaction was used to achieve regioselective methylation, and then the bromide **497a,b** was converted to northern naphthalene building blocks **498a,b**. From the Henry reaction of 3,5-dimethoxybenzal-dehyde (**499**) catalyzed by $LiAlH_4$ with nitroethane, and then the TBS protection of free alcohols, **500** in *cis*/*trans* configuration was obtained. The secondary nitro group was then converted to an amine. The acylation of the amine provides the amide **501**, which then undergoes a Bischler–Napieralski reaction to obtain one of the southern isoquinoline building block **502**.

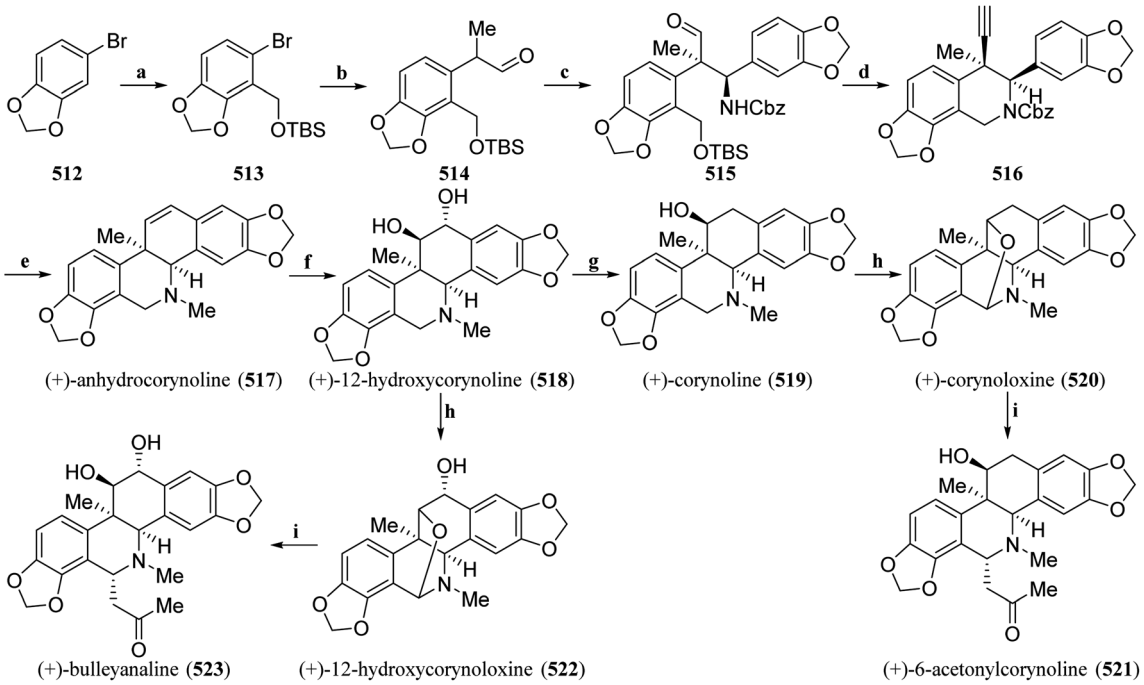

Scheme 35 Total synthesis of isoquinoline alkaloids (517–523) from genus *Corydalis* by Trost's group. Reagents and conditions: (a) (i) LDA, THF, −78 °C, DMF, rt, (ii) $NaBH_4$, MeOH, rt (iii) TBSCl, imidazole, rt; (b) (i) $Pd(OAc)_2$, DavePhos, LiHMDS, PhMe, 70 °C, (ii) DIBAL-H, DCM, −78 °C; (c) imine, Zn-(*S*,*S*)-ProPhenol, PhMe, 3A MS, 4 °C; (d) (i) K_2CO_3, Ohira–Bestmann reagent, MeOH, rt, (ii) CSA, MeOH, sulfonyldiimidazole, Cs_2CO_3, MeCN, rt; (e) IPrAuNTf$_2$, PhMe, rt, then Red-Al, rt-80 °C; (f) H_2O_2, HCOOH, then $Na_2S_2O_5$, NaOH, rt; (g) Et_3SiH, $BF_3\cdot Et_2O$, DCE, rt; (h) I_2, KOAc, K_2CO_3, EtOH, reflux; (i) KOH, MeOH, 50 °C.

The format reagent generated *in situ* from **503** attacks the Boc-protected chiral aziridine **504a,b**, and then the Boc is deprotected and acetylated to obtain the chiral amide **505a,b**, followed by a iodination and a final Bischler–Napieralski reaction to obtain the southern isoquinoline building blocks **506a–c**. Based on the Lassaletta's second-generation *N*,*N*-ligand, a catalyst-controlled Pd-catalyzed Suzuki cross-coupling reaction system was established, and a series of naphthalene isoquinoline alkaloids **479**, **508–511** were obtained.

3.1.6 Phenanthridine alkaloids. In 2019, Trost *et al.* established a novel synthetic strategy based on asymmetric Mannich reactions and cationic Au-catalyzed cycloisomerization as the key steps, achieving efficient asymmetric total synthesis of natural isoquinoline alkaloid products from the genus *Corydalis* with atom and step economies (Scheme 35).[166] A ten-gram scale of known **513** was prepared using the aryl bromide **512** as the starting material. Then, palladium catalyzed the α-arylation reaction of **513** with *tert*-

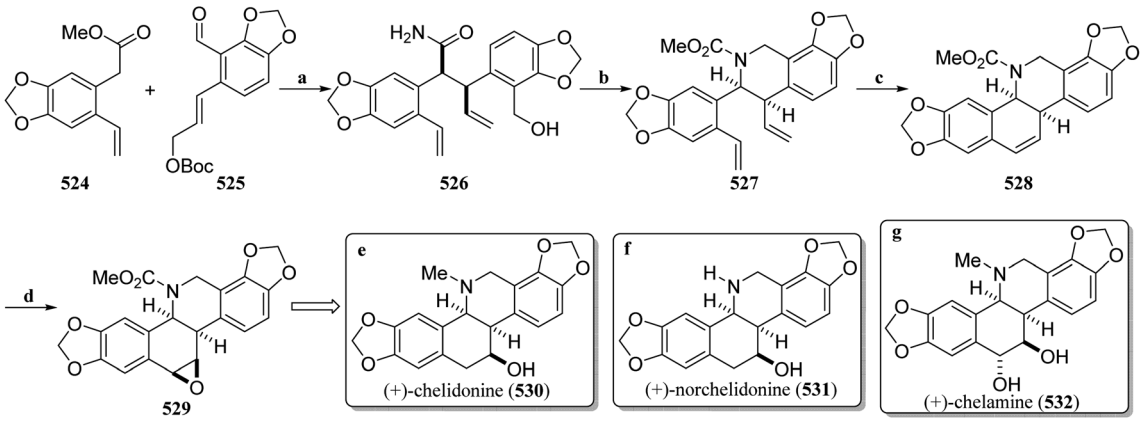

Scheme 36 Total synthesis of (+)-chelidonine (530), (+)-norchelidonine (531) and (+)-chelamine (532) by Snaddon's group. Reagents and conditions: (a) (i) (*S*)-BTM, Hartwig's (*R*,*R*,R_a)-Ir catalyst, iPr_2NEt, THF, NH_4OH, rt, (ii) $NaBH_4$, MeOH, rt; (b) (i) $PhI(OAc)_2$, KOH, MeOH/THF, rt, (ii) PPh_3, CBr_4, then NaH, DMF, rt; (c) Grubbs second generation catalyst, PhMe, rt; (d) (i) NBS, H_2O, rt, (ii) KO*t*Bu, THF, −78 °C; (e) $LiAlH_4$, 1,4-dioxane, reflux; (f) L-selectride, THF, 40 °C; (g) (i) $BiCl_3$, MeCN/H_2O, 0 °C, (ii) $LiAlH_4$, 1,4-dioxane, reflux.

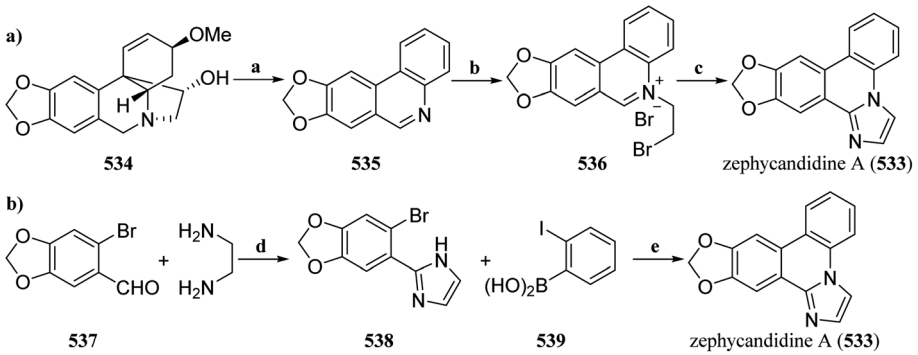

Scheme 37 Total synthesis of zephycandidine A (**533**) by Murphy's and Banwell's group. Reagents and conditions: (a) heat, 190–195 °C; (b) 1,2-dibromoethane, 90 °C; (c) (i) NH_3 (liq.), −78 to −33 °C, (ii) MnO_2, Na_2CO_3, −78 °C-rt, (iii) toluene, 111 °C; (d) (i) I_2, K_2CO_3, *t*-BuOH, 70 °C, (ii) $PhI(OAc)_2$, K_2CO_3, DMSO, rt; (e) $Pd(OAc)_2$, NaOAc, DMF, 110 °C.

butylpropionate, and after the reduction of DIBAL-H, the aldehyde **514** was generated. Based on the research of Trost's team on Zn-ProPhenol-catalyzed asymmetric Mannich reactions,[167,168] the reaction conditions of the critical asymmetric Mannich reaction were established, which produced the crucial chiral synthetic intermediate **515**. The aldehyde **515** underwent homologation *via* the Ohira–Bestmann reagent, and after deprotection of the benzylic alcohol, an *in situ* intramolecular SN_2 cyclization was facilitated by sulfonyl diimidazole to obtain compound **516**. By optimizing the conditions for cationic Au-catalyzed oxidative cyclization, **516** was directly converted into the phenanthridine alkaloid backbone in one step. A one-pot addition of Red-Al resulted in the first asymmetric total synthesis of (+)-anhydrocorynoline (**517**) with a 25% overall yield. Following the reaction conditions established by Ninomiya *et al.*,[169] **517** underwent epoxidation and subsequent hydrolysis to achieve the first asymmetric total synthesis of (+)-12-hydroxycorynoline (**518**). Compared with previously reported methods, the treatment of **518** with Et_3SiH and BF_3-Et_2O provided (+)-corynoline (**519**) at a higher yield than previously reported methods. Under optimized conditions for selective oxidation at C-6, both **518** and **519** were quantitatively converted into (+)-12-hydroxycorynoloxine (**522**) and (+)-corynoloxine (**520**), respectively, achieving their first total synthesis. Treatment of **520** and **522** with KOH in a mixture of methanol and acetone at elevated temperatures produced (+)-6-acetonylcorynoline (**521**) and (+)-bulleyanaline (**523**) as single diastereomers, respectively. The high overall yield and atom-economy of this novel synthetic strategy open up new avenues for the preparation and biological activity studies of these natural products and related analogs.

In 2020, Snaddon's group achieved enantioselective synthesis of chelidonium alkaloids (Scheme 36) by establishing asymmetric allylic alkylation reaction conditions catalyzed by a Lewis base and transition metal,[170] combined with Hofmann rearrangement.[171] Under the optimized reaction conditions, the electrophile **525** underwent asymmetric allylic alkylation with **524**, followed by ammonolysis of the ester using ammonium hydroxide and reduction of the aldehyde to obtain the corresponding alcohol **526**. PIDA was used to facilitate Hofmann rearrangement of **526**, and then the primary alcohol was converted into the corresponding bromide before treatment with sodium hydride to promote intramolecular *N*-alkylation, resulting in **527**. The second-generation Grubbs catalyst facilitated ring-closing metathesis, resulting in benzo[*c*]phenanthridine skeleton **528**. *N*-Bromosuccinimide (NBS) mediated regioselective bromonium ion hydrolysis to obtain bromohydrin, which was then treated with potassium *tert*-butoxide at low temperature to obtain the critical epoxide **529**. $LiAlH_4$ reduced the epoxide **529** to give (+)-chelidonine (**530**). (+)-Norchelidonine (**531**) was prepared by treating **529** with L-selectride. Bismuth trichloride catalyzed the hydrolytic ring-opening of epoxide **529**, followed by reduction with $LiAlH_4$ to produce (+)-chelamine (**532**). In addition, the efficient synthesis of *strychnos* alkaloids and pharmaceutical lead compounds was achieved by combining Lewis base/transition metal-catalyzed asymmetric allyl alkylation with Hoffman rearrangement, indicating that this strategy has important application value in the synthesis of other alkaloids and analogs designed for drug development.

Murphy's group and Banwell's group completed the total synthesis of zephycandidine A (**533**) in 2020 and 2021, respectively. Murphy's group used haemanthamine (**534**), which can be obtained in large quantities, as a raw material, which can be directly converted into trispheridine (**535**) at high temperatures, and then placed in 1,2-dibromoethane to heat, and the key intermediate **536** can be obtained. Finally, according to the method reported by Cronin and coworkers,[172] the target compound **533** was obtained by reacting with liquid ammonia to close the ring (Scheme 37a).[173]

Banwell's group achieved the total synthesis of **533** from readily available starting materials *via* Buchwald–Hartwig and Heck reactions (Scheme 37b).[174] According to the method reported by Ishihara and Togo, the 2-imidazoline derivative **538** could be synthesized using **537** and ethylenediamine as raw materials. The total synthesis of **533** was subsequently achieved *via* palladium-catalyzed cross-coupling of **538** with *o*-iodophenylboronic acid (**539**).

Jeganmohan's group had established a series of new methods for the synthesis of benzophenanthridines **544**, *cis*-

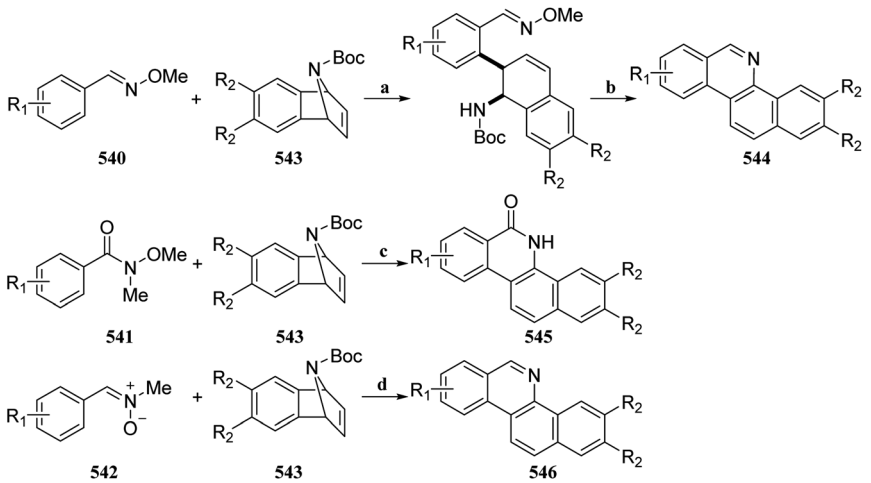

Scheme 38 Synthesis methods of benzophenanthridines (**544**), *cis*-fused dihydrobenzo[*c*]phenanth-ridinones (**545**) and benzo[*c*]phenanthridine alkaloids (**546**) by Jeganmohan's group. Reagents and conditions: (a) $[\{Rh(CH_3CN)_3(Cp^*)\}\{SbF_6\}_2]$, NaOAc, DCE, 100 °C; (b) 6 N HCl, 1,4-dioxane, 80 °C; (c) $[Ru(p\text{-cymene})Cl_2]_2$, $AgSbF_6$, AgOTf, DCE, 100 °C; (d) $[Cp^*RhCl_2]_2$, $AgSbF_6$, Ag_2O, 4A MS, DCE, 120 °C.

fused dihydrobenzo[*c*]phenanthridinones **545** and benz-o[*c*]phenanthridine alkaloids **546** by a metal-catalyzed reaction of 7-azabenzonorborna-dienes **543** with the aromatic aldoximes **540**,[175] aryl amides **541**[176] and the aryl nitrones **542**,[177] and applied them to the synthesis of natural products (Scheme 38).

In 2022, Liu *et al.* established a novel strategy for the efficient construction of benzo[*c*]phenanthridine structures through sequential transition metal-catalyzed reactions and condition-controlled Mannich reactions,[178] achieving efficient total synthesis of eight benzo[*c*]phenanthridine alkaloids and two derivatized molecules (25–34% total yield).

The strategy began with the preparation of diaryl acetylenes using readily available building blocks **547** and **548** *via* the Sonogashira coupling reaction, and then the key 1,5-enynes **549** was synthesized *via* a one-pot Wittig reaction. Subsequently, the 1-iodo-2-phenylnaphthalenes **550** was synthesized under the optimal reaction conditions of one-pot Au/Ag-catalyzed cyclization tandem *in situ* iodination. The copper-catalyzed cross-coupling reaction between **550** and methylamine was used to construct the C–N bond, and the total synthesis of benzo[*c*]phenanthridine alkaloids was completed through a one-pot Mannich reaction under different reaction atmospheres. The

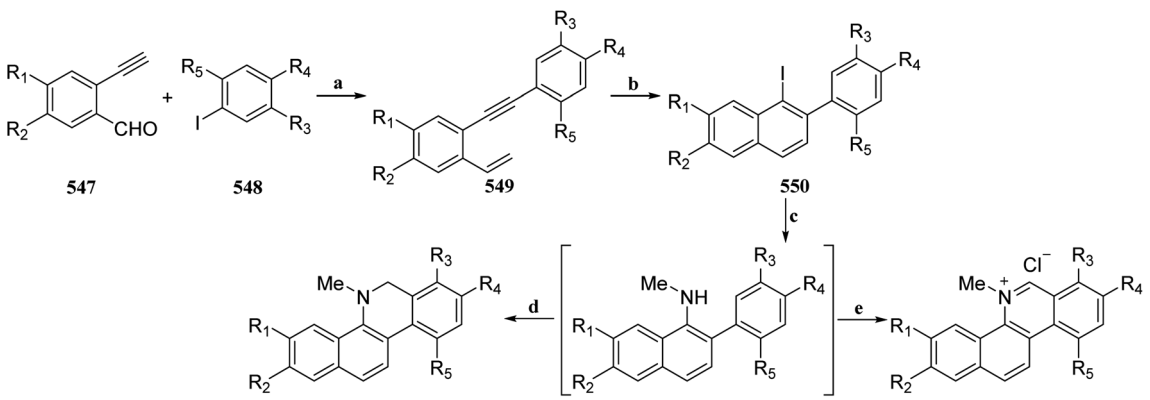

552a, **dihydrochelilutine**,
$R_1 + R_2 = OCH_2O$, R_3,R_4,R_5= OMe;
552b, **dihydrobocconine**,
$R_1 + R_2 = OCH_2O$, $R_3 + R_4 = OCH_2O$, R_5= OMe;
552c, **dihydrosanguilutine**,
R_1,R_2,R_3,R_4,R_5= OMe;
552d, **dihydrosanguirubine**,
R_1,R_2 = OMe, $R_3 + R_4 = OCH_2O$, R_5= OMe;
552e, **10-isopropoxydihydrosanguinarine**,
$R_1 + R_2 = OCH_2O$, $R_3 + R_4 = OCH_2O$, R_5= O^{i}Pr;

551a, **chelilutine**,
$R_1 + R_2 = OCH_2O$, R_3,R_4,R_5= OMe;
551b, **bocconine**,
$R_1 + R_2 = OCH_2O$, $R_3 + R_4 = OCH_2O$, R_5= OMe;
551c, **sanguilutine**,
R_1,R_2,R_3,R_4,R_5= OMe;
551d, **sanguirubine**,
R_1,R_2 = OMe, $R_3 + R_4 = OCH_2O$, R_5= OMe;
551e, **10-isopropoxy-sanguinarine**,
$R_1 + R_2 = OCH_2O$, $R_3 + R_4 = OCH_2O$, R_5= O^{i}Pr;

Scheme 39 Total synthesis of benzo[*c*]phenanthrene alkaloids by Liu's group. Reagents and conditions: (a) (i) $Pd(Ph_3P)_2Cl_2$, CuI, Et_3N, THF, rt, (ii) methyltriphenylphosphonium bromide, NaHMDS, THF, −78 °C-rt; (b) IPrAuCl, $AgSbF_6$, NIS, DCM, rt; (c) Cu (powder), $MeNH_2$ (H_2O), EtOH, 110 °C; (d) $(HCHO)_n$, TFA, N_2, $MgSO_4$, EtOH, 65 °C; (e) $(HCHO)_n$, TFA, O_2, $MgSO_4$, EtOH, 65 °C.

oxidative products **551a–e** were synthesized under an oxygen atmosphere, whereas the reductive products **552a–e** were synthesized under a nitrogen atmosphere (Scheme 39). This efficient and economical new synthetic strategy is expected to further expand the research and application of benzo[*c*]phenanthridine alkaloids and their derivatives.

Amaryllidaceae alkaloids such as γ-lycorane have gained great attention in the field of total synthesis.[179] In recent years, many studies have investigated different synthesis strategies. In 2020, Prasad's group accomplished the total synthesis of γ-lycorane is accomplished from (*S*)-lactic acid (Scheme 40a).[180] The known phosphonate **553** derived from (*S*)-lactic acid was used as the raw material and converted into the Weinreb amide **554** by Horner–Wittig olefination, Claessen rearrangement, *etc.* The Weinreb amide **554** reacts with vinylmagnesium bromide, and then undergoes Luche reduction, hydroxyl protection and deprotection to obtain **555**. By Overman rearrangement, RCM ring closure, deprotection, oxidation and stereoselective reduction, the allyl alcohol **555** was converted to cyclohexene **556**. After Claessen rearrangement, the ring was closed to obtain lactam **557**, and finally, the Pictet–Spengler reaction was used to form an isoquinoline backbone, and the lactam was reduced to obtain (+)-γ-lycorane (**558a**).

Chuang *et al.* developed a Pd-catalyzed aza-Wacker-Heck cyclization reaction to construct the galanthan skeleton.[181] Through this one-pot sequential C–N and C–C bond-forming process, fused aza-tetracyclic compounds can be efficiently synthesized. Based on this synthetic strategy, using compound **559** as the starting material, galanthan-7-one and its isomer were concisely synthesized *via* a one-pot method. Subsequent reduction of the olefins and carbonyl groups produced (±)-γ-lycorane (**558c**) (Scheme 40b).

Wang and coworkers have successfully established a synthetic strategy with palladium-catalyzed aryl C–H

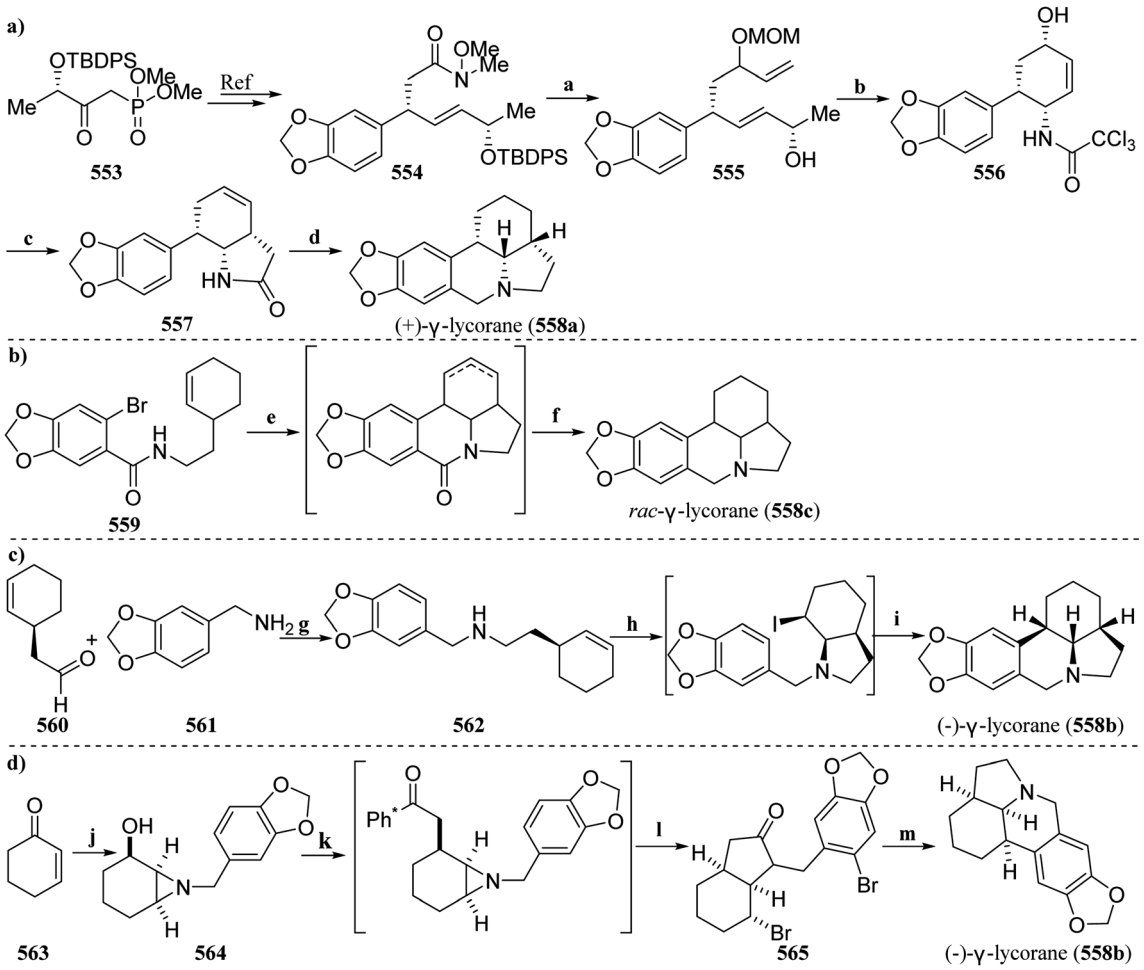

Scheme 40 Total synthesis of γ-lycorane. Reagents and conditions: (a) (i) vinylmagnesium bromide, THF, 0 °C, (ii) $CeCl_3 \cdot 7H_2O$, $NaBH_4$, MeOH, rt, (iii) MOMCl, DIPEA, DMAP, DCM, reflux, (iv) TBAF, THF, 0–50 °C; (b) (i) Cl_3CCN, DBU, DCM, 0 °C, then xylene, MW 160 °C, (ii) Grubbs' 2nd generation catalyst, DCM, reflux, (iii) PPTS, $MeOH/H_2O$, 80 °C, (iv) DMP, $NaHCO_3$, DCM, 0 °C-rt, then $NaBH_4$, $CaCl_2$, MeOH, 0 °C; (c) (i) CH_3-$C(OEt)_2$, EtCOOH, toluene, seal tube, 150 °C, (ii) Cs_2CO_3, DMSO, 100 °C; (d) (i) $(HCHO)_n$, TFA, DCE, rt, (ii) H_2, Pd/C, MeOH, rt, (iii) $LiAlH_4$, THF, reflux; (e) (i) $Pd(OAc)_2$, DMSO, O_2, 65 °C, (ii) *n*-Bu_3P, DIPEA, 110 °C; (f) (i) H_2, PtO_2, EtOH, rt, (ii) $LiAlH_4$, THF, reflux; (g) (i) MeOH, r.t, (ii) $NaBH_4$, 0 °C; (h) I_2/K_2CO_3, DCM, 0 °C-rt; (i) $Pd(PPh_3)_4$, Cs_2CO_3, 1,4-dioxone, 100 °C; (j) Br_2, DCM, −17 °C; (k) (i) KO*t*-Bu, THF, rt, (ii) $Pd(OAc)_2$, PPh_3, i-Pr_2NEt, DMF, reflux, (iii) H_2, Pd/C, MeOH, rt, (iv) $LiAlH_4$, THF, reflux.

alkylation as the key reaction,[182] achieving the concise and efficient total synthesis of (−)-γ-lycorane (**558b**) (Scheme 40c). The benzylamine **561** underwent reductive amination with the aldehyde **560**, and the intermediate product **562** was generated. The intermediate products underwent intramolecular iodine cyclization under the action of I_2/K_2CO_3 to construct a *cis*-5,6-ring structure, and then palladium-catalyzed aryl C–H alkylation was carried out to obtain (−)-γ-lycorane (**558b**).

In 2022, Donohoe's group, for the first time, applied hydrogen-borrowing C–C bond formation as a key step in total synthesis (Scheme 40d), developing a hydrogen-borrowing alkylation of aziridinyl alcohol combined with Ph* (Me_5C_6) deprotection/cyclization reaction, which efficiently constructed fused 6,5 heterocyclic structures.[183] Initially, chiral aziridine was synthesized from the cyclohexenone **563** according to the method reported in the literature.[184] After reduction, deprotection, and nucleophilic substitution reactions, the key aziridinyl alcohol **564** was obtained. Research on hydrogen-borrowing C–C bond formation reactions has revealed that the hydrogen-borrowing catalytic alkylation of Ph*COMe with the aziridinyl alcohol **564** was achieved. Treatment with liquid bromine produced the dibrominated lactam **565**, which was used to construct the 6,5 heterocyclic. Following regioselective elimination of the alkyl bromide, an intramolecular Heck reaction was used for cyclization to construct the galanthan skeleton. Reduction of the double bond and carbonyl group afforded (−)-γ-lycorane (**558b**). This synthetic strategy has potential application value in the construction of various complex polycyclic nitrogen-containing natural products and their derivatives.

Recently, Yang's group achieved the collectively asymmetric total synthesis of all members of lycorane, including (+)-α, (+)-β, (+)-γ, and (−)-δ, using Carreira's dual Ir/amine-catalyzed α-allylation of the 2-phthalimidoacetaldehyde (**567**) with allylic alcohol **566** as a key reaction (Scheme 41).[185] Through the regulation of chiral ligands, **568a,b** with different

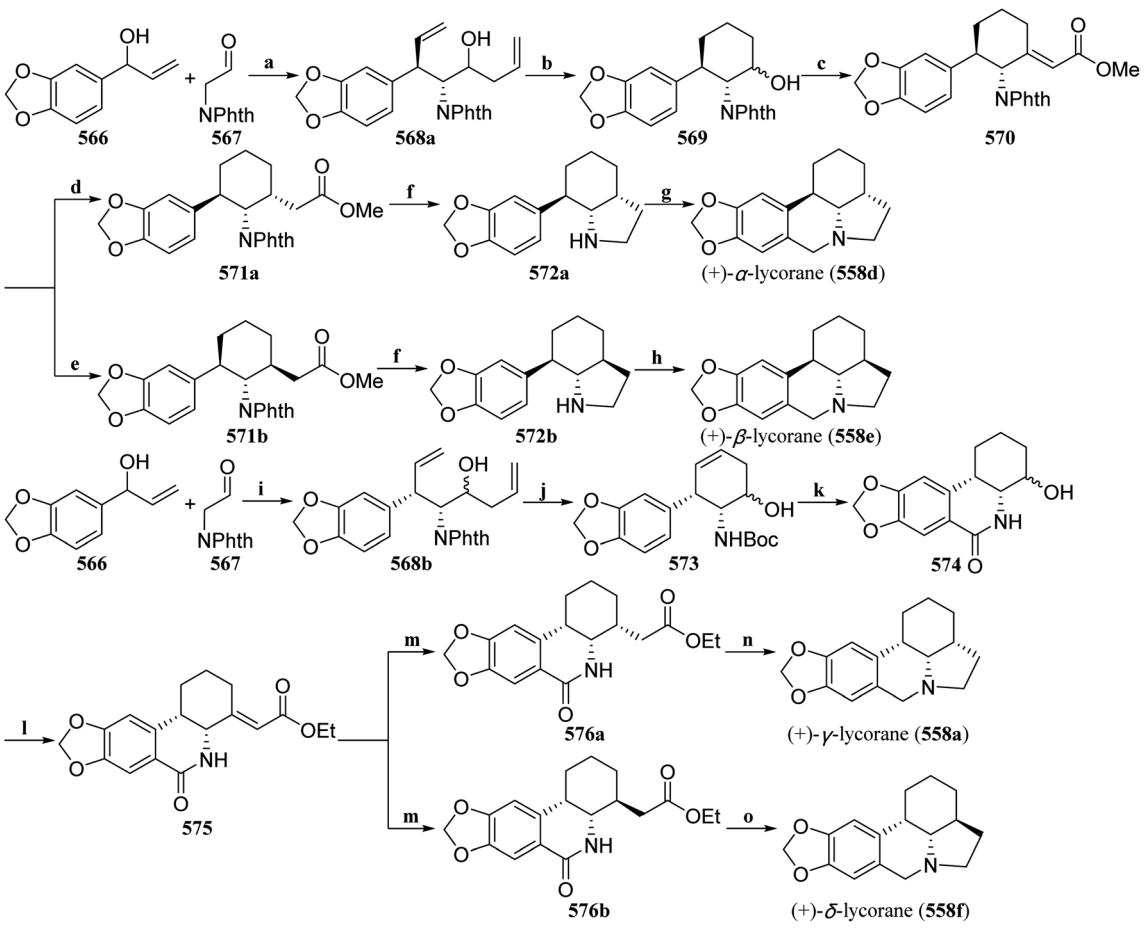

Scheme 41 Total synthesis of γ-lycorane by Yang's group. Reagents and conditions: (a) (i) $[Ir(cod)Cl]_2$, Carreira ligand (*R*)-L, proline-derived amine (*S*)-A, maleic acid, DCE, 0 °C, (ii) allyltrimethylsilane, $BF_3{\cdot}Et_2O$, DCM, −78–0 °C; (b) (i) Grubbs' 2nd generation catalyst, DCM, reflux, (ii) H_2, Pd/C, EtOH, rt; (c) (i) DMP, DCM, rt, (ii) trimethyl phosphonoacetate, *t*-BuOk, THF, 0 °C-rt; (d) H_2, Pd/C, EtOH, rt; (e) $NiBr_2$(DME), (*S*)-Me-DuPhoS, $ZnCl_2$, DMF/H_2O, 110 °C; (f) (i). $NaBH_4$, i-PrOH/H_2O, 100 °C, (ii) DIAD, PPh_3, THF, 0 °C-rt; (g) Eschenmoser's salt, THF, 40 °C; (h) (i). $ClCO_2Me$, Et_3N, DCM, rt, (ii) $POCl_3$, 90 °C, (iii) $LiAlH_4$, THF, rt; (i) (i) $[Ir(cod)Cl]_2$, Carreira ligand (*S*)-L, proline-derived amine (*S*)-A, $Bi(OTf)_3$, DCE, 0 °C, (ii) ethylenediamine, MeOH/DCM, 40 °C, (iii) $(Boc)_2O$, Na_2CO_3, THF/H_2O, rt; (j) (i) Grubbs' 2nd generation catalyst, DCM, reflux, (ii) H_2, Pd/C, EtOH, rt; (k) (i) H_2, Pd/C, EtOH, rt, (ii) Ac_2O, Et_3N, DMAP, DCM, rt, (iii) PPh_3O, $BF_3{\cdot}Et_2O$, Tf_2O, DCM, rt, (iv) K_2CO_3, MeOH, rt; (l) (i) DMP, DCM, rt, (ii) ethyl (triphenylphosphoranylidene)-acetate, DCM, rt; (m) H_2, Pd/C, EtOH, rt; (n) (i) DIBAL-H, DCM, −78 °C (ii) $LiAlH_4$, THF, 50 °C; (o) (i) $LiAlH_4$, THF, reflux, (ii) MsCl, Et_3N, DCM, 0 °C.

stereoselectivities could be obtained after Sakurai allylation. **568a** underwent RCM cyclization and catalytic hydrogenation to obtain the alcohol **569**, followed by DMP (Dess–Martin periodinane) oxidation and the Horner–Wadsworth–Emmons reaction to produce the α,β-unsaturated ester **570**. Under different reduction conditions, the stereoselective products **571a** and **571b** are generated. Then, intramolecular nucleophilic substitution was carried out *via* the Mitsunobu reaction to give **572a** and **572b**. Pictet–Spengler cyclization of **572a** with eschenmoser salt gave (+)-α-lycorane (**558d**). The amine **572b** was converted to carbamate and then subjected to the Bischler–Napieralski reaction, followed by the reduction of the oxolycorane intermediate to obtain (+)-β-lycorine (**558e**).

On the other hand, **568b** underwent RCM cyclization, and the phthalimide was replaced with a Boc group to give **573**. The catalytic hydrogenation of **573** afforded cyclohexane, which was acetylated with Ac_2O. Upon treatment with Hendrickson's reagent, the Bischler–Napieralski reaction was performed, resulting in an acetylated intermediate that was converted to **574**. After DMP oxidation and then Wittig reaction, **575** was obtained. Under different reduction conditions, the stereoselective products **576a** and **576b** were produced. Dibal-H was added to reduce **576a**, quickly close the ring, and then reduce the lactam, giving (+)-γ-lycorane (**558a**). **576b** was reduced to an amino alcohol, which was then converted to (−)-δ-lycorane (**558f**) by the intramolecular displacement of methanesulfonate.

In 2022, Waldvogel and Opatz *et al.* efficiently constructed spirodienones *via* an electrochemical method with simple starting materials.[186] Based on this versatile key transformation (Scheme 42), they designed a general biomimetic synthetic strategy for Amaryllidaceae alkaloids. Different aldehydes react with **577** to obtain the key reaction precursor **578**, which is then converted into the corresponding spirodienone **579** through an electrocatalytic reaction. This key reaction could achieve excellent yields in both batch and continuous flow reactors. After the deprotection of **579** under alkaline conditions, the intramolecular azaza-Michael addition reaction occurred to generate the tetracyclic cores **580a–c**. After removing the benzyl protection from **580b**, it along with **580a** and **580c**, was reduced by an L-selective reducing agent to produce *rac*-siculine (**581**), *rac*-maritidine (**582a**), *rac*-epimaritidine (**582b**), *rac*-crinine (**583a**), and *rac*-epicrinine (**583b**).

3.1.7 Morphine isoquinoline alkaloids. Opatz *et al.* had developed a regioselective and diastereoselective anodic coupling of 3′,4′,5′-trioxygenated laudanosine derivatives, achieving the first electrochemical synthesis of (−)-thebaine (Scheme 43).[187] The inexpensive and easily obtainable homoveratrylamine and methyl gallate were used as raw materials, which were then converted into the α-aminonitrile **584** and the benzyl bromide **585** through a multistep reaction. Through deprotonation, alkylation, and Noyori asymmetric transfer hydrogenation in one pot, **584** and **585** generated the 1-benzyl tetrahydroisoquinoline **586**. After installing a suitable protecting group, **587** underwent electrocatalytic coupling to obtain **588**. After debenzylation, the corresponding trifluoromethanesulfonate was generated, and Pd-catalyzed transfer hydrogenation removed excess hydroxyl groups to obtain **589**. After removing the Ac protection, the carbonyl group was selectively reduced, and then the full synthesis of (−)-thebaine (**590**) was completed through biomimetic

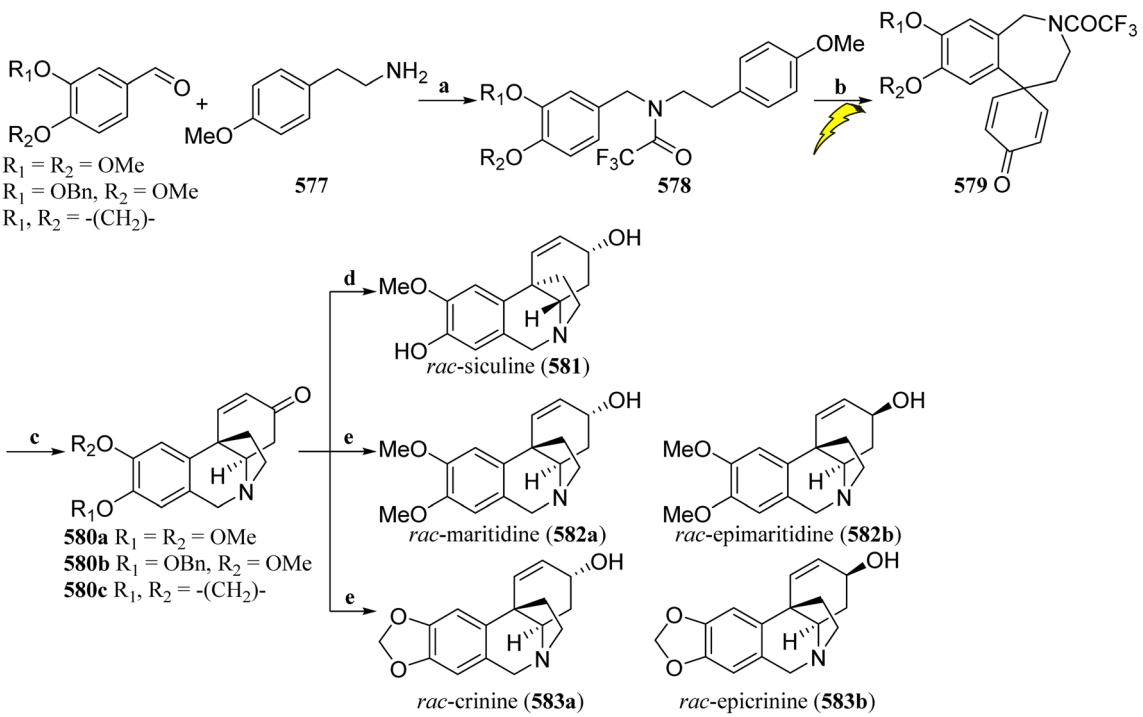

Scheme 42 Total synthesis of Amaryllidaceae alkaloids (**581**, **582a,b**, **583a,b**) by Waldvogel and Opatz's group. Reagents and conditions: (a) (i) MeOH, 80 °C, (ii) $NaBH_4$, 0 °C, (iii) TFAA, pyridine, 0 °C; (b) BDD/Pt, MeCN, aq. HBF_4, −20 °C, 2.0 F, 1.0 mA cm^{-2}, 200 rpm; (c) 10% KOH, MeCN, r.t; (d) (i) BCl_3, DCM, −78 °C, (ii) L-selectride, THF, −78 °C; (e) L-selectride, THF, −78 °C.

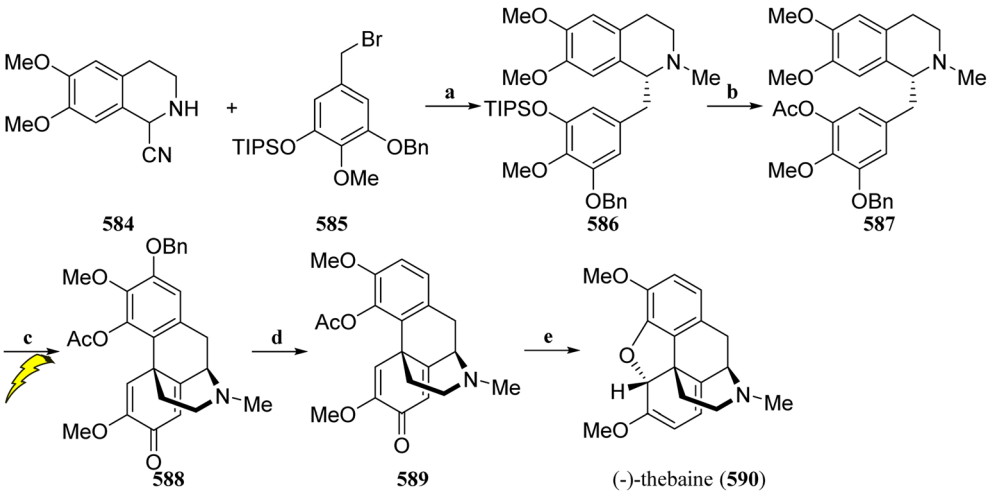

Scheme 43 Total synthesis of (−)-thebaine (**590**) by Opatz's group. Reagents and conditions: (a) (i) KHMDS, THF, −78 °C, then bromide **585**, −78 °C-rt, (ii) RuCl(*p*-cymene)[(*S*,*S*)-Ts-DPEN], HCOOH, Et_3N, DMF, 0 °C-rt, (iii) HCHO, $NaBH_4$, MeOH, 0 °C; (b) (i) TBAF, THF, rt, (ii) AcCl, Et_3N, DMAP, DCM, rt; (c) constant current electrolysis, undivided cell, Pt electrodes, $j = 1.5$ mA cm^{-2}, $Q = 2.2$ F, MeCN, HBF_4, 0 °C; (d) (i) Pd/C, 1,4-cyclohexadiene, EtOH, 35 °C, (ii) Tf_2O, pyridine, 0 °C, (iii) $Pd(PPh_3)_4$, Et_3N, HCOOH, DMF, 60 °C; (e) (i) K_2CO_3, MeOH, rt, (ii) $CeCl_3 \cdot 7H_2O$, $NaBH_4$, MeOH, 0 °C, (iii) *N*,*N*-dimethylformamidedineopentyl acetal, dioxane, 80 °C.

conjugated nucleophilic substitution cyclization. Thebaine is a biosynthetic precursor of codeine and morphine, and it is also an industrial semisynthetic precursor of related drugs such as naloxone, oxycodone, or buprenorphine. This electrochemical strategy is expected to improve the current industrial synthesis process, avoiding the use of traditional oxidants and making it more environmentally friendly. Based on this strategy, the Opatz team has also achieved efficient total electrochemical synthesis of (−)-oxycodone.[188]

In 2021, Dong's group developed an asymmetric catalytic "cut-and-sew" strategy that efficiently constructed all-carbon fused-ring structures and quaternary stereocenters. Based on this strategy, they achieved the first asymmetric total synthesis of the morphine alkaloid (−)-thebainone A (**591**) (Scheme 44).[189] Initially, the key ketal-containing substrate (**595**) was prepared through a Mitsunobu coupling reaction between the phenol **594** and the alcohol **593**, which was synthesized *via* Birch reduction and ketal formation from the anisole **592**.

After optimizing the conditions for the asymmetric "cut-and-sew" reaction, the key intermediate **596** was obtained with 80% yield and 97 : 3 er. The ketone in **596** was reduced *via* $LiAlH_4$, followed by acetate protection and *in situ* ketal removal to yield

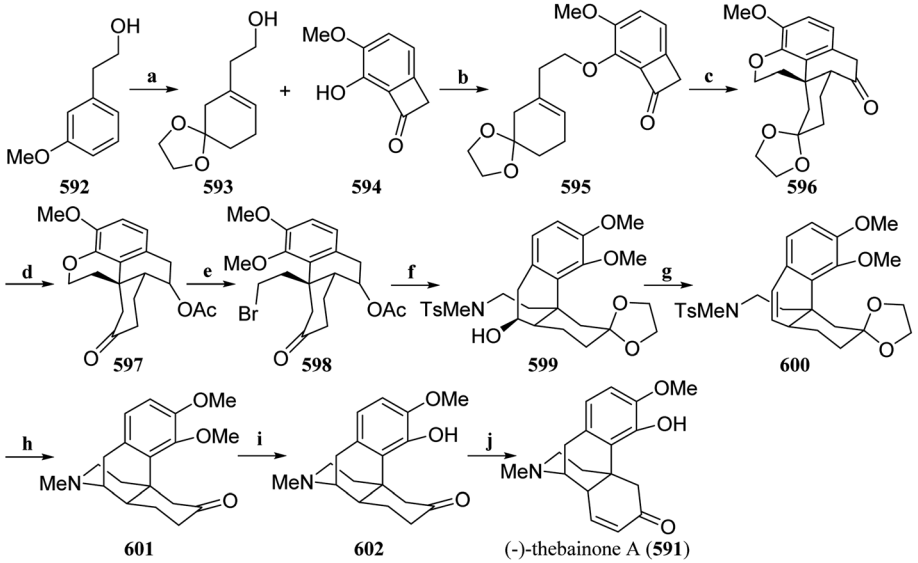

Scheme 44 Total synthesis of (−)-thebainone A (**591**) by Dong's group. Reagents and conditions: (a) (i) Li/NH_3, *t*BuOH, THF, −78 °C, (ii) PPTS, glycol, DCM, rt; (b) DEAD, PPh_3, THF, rt; (c) $[Rh(COD)_2]NTf_2$, (*R*)-DTBM-segphos, 1,2-DFB, 130 °C; (d) (i) $LiAlH_4$, THF, 0 °C, (ii) Ac_2O, pyridine, DMAP, then 2 M HCl, 0 °C; (e) (i) BBr_3, DCM, −30 °C, (ii) CH_2N_2, MeOH, Et_2O, rt; (f) $TMSOCH_2CH_2OTMS$, TMSOTf, then pyridine, then TsNHMe, Cs_2CO_3, then MeOH; (g) Martin's sulfurane, DCM, rt; (h) sodium naphthalenide, THF, −30 °C, then 2 M HCl; (i) NaSEt, DMF, 100 °C; (j) TFA, MeCN, $Pd(TFA)_2$, DMSO, 80 °C.

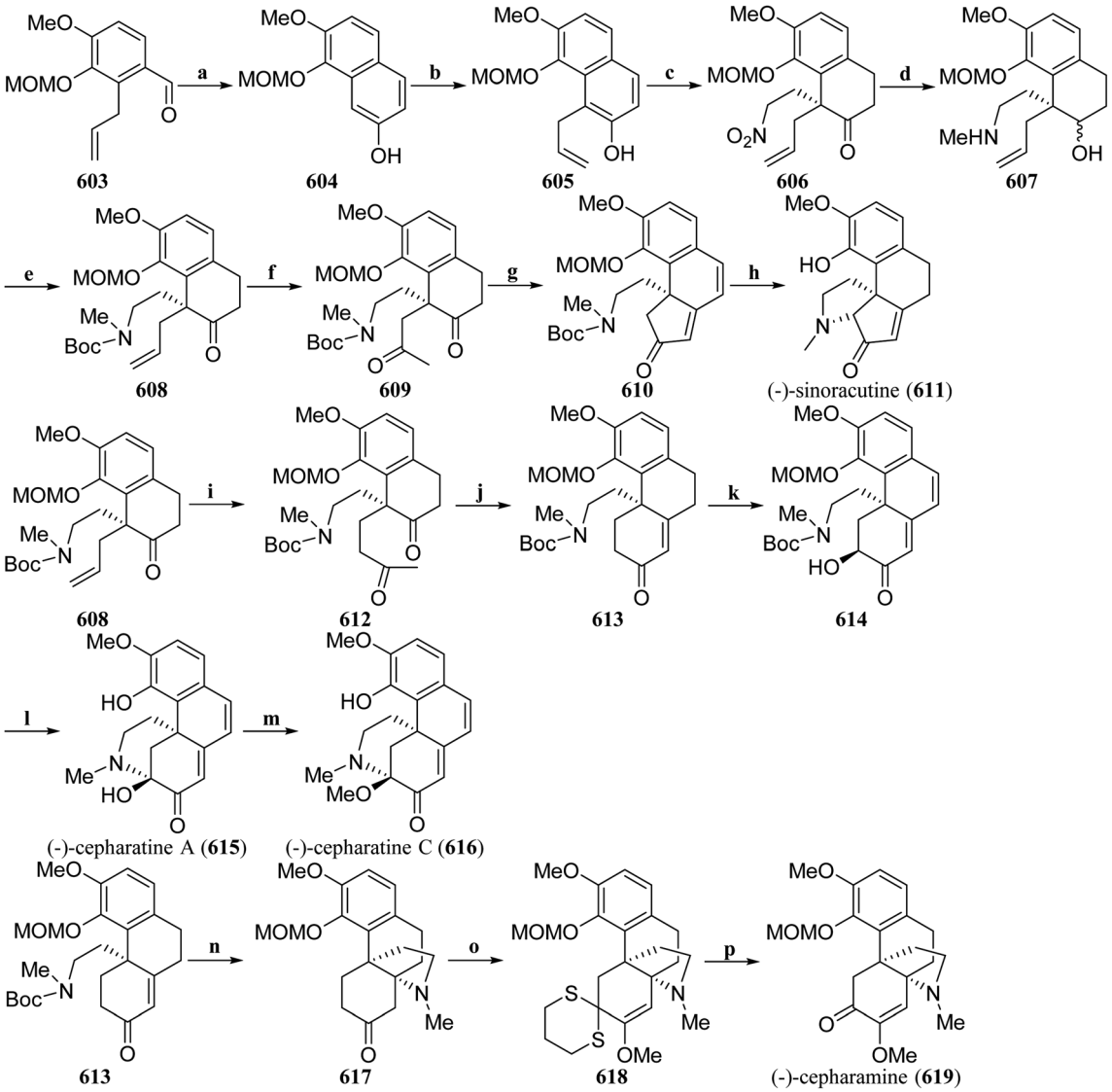

Scheme 45 Total synthesis of the three sub-classes of hasubanan alkaloids (**611**, **615**, **616** and **619**) by Zhu's group. Reagents and conditions: (a) $PdCl_2$, $CuCl_2$, O_2, DMF/H_2O, rt, then NaOH, MeOH; (b) (i) allyl bromide, K_2CO_3, acetone, reflux, (ii) 1,2-dichlorobenzene, 180 °C; (c) (i) (1*R*,2*R*)-Takemoto thiourea catalyst, nitroethylene, 3 Å MS, rt, (ii) L-selectride, THF, −78 °C; (d) (i) $LiAlH_4$, Et_2O, 0 °C-rt, (ii) $ClCO_2Me$, Na_2CO_3, THF/H_2O, rt, (iii) $LiAlH_4$, THF, reflux; (e) Boc_2O, DCM, rt, then DMP, $NaHCO_3$, 0 °C-rt; (f) $PdCl_2$, O_2, NMP/H_2O; (g) KO*t*Bu, toluene/*t*BuOH, 0 °C-rt, (ii). DDQ, DCE, 50 °C; (h) LHMDS, NBS, −78 °C, THF, then TFA, DCM, rt; (i) isopropenylboronic acid pinacol ester, Grubbs second-generation catalyst, DCM, 50 °C, then $NaBO_3 \cdot 4H_2O$, THF/H_2O, rt; (j) 0.5 M NaOMe in MeOH, reflux; (k) (i) LHMDS, MoOPH, THF, −78 °C to −20 °C, (ii) DDQ, DCE, 50 °C; (l) DMP, DCM, 0 °C-rt, then TFA; (m) H_2SO_4 (1 M in MeOH)/$CH(OMe)_3$/MeOH = 0.1/1/1, 65 °C; (n) TMSOTf, 2,6-lutidine, DCM, 0 °C-rt, then TBAF, 0 °C; (o) (i) KO*t*Bu, Et_2O/HCO_2Et, 0 °C-rt, then trimethylene dithiotosylate, AcOK, MeOH, reflux, (ii) KO*t*Bu, Me_2SO_4, DMSO, rt; (p) PIFA, TFA, MeCN/H_2O, then TFA, rt.

the ketone **597**. The C–O bond in the dihydropyran moiety of **597** was cleaved using BBr_3 and methylated to produce **598**. Afterthe ketone was protected and aminated *via* an SN_2 reaction, followed by the removal of the Ac protecting group, compound **599** was obtained. Upon elimination of the alcohol moiety using Martin's sulfurane, a formal hydroamination process occurred in **600** using sodium naphthalenide, completing the construction of the piperidine ring and revealing the ketone moiety. The more sterically hindered methyl ether in **601** was selectively cleaved under the nucleophilic conditions to give **602**. Finally, the asymmetric total synthesis of (−)-thebainone A (**591**) was achieved through the α,β-desaturation of the ketone **602** *via* the $Pd(TFA)_2$/DMSO system described by Ellman and colleagues.[190] This synthetic strategy, with its deconstructive approach, provides new insights for building more complex structures.

Zhu's group established the asymmetric catalytic enantioselective construction of tricyclic enone intermediates in 2021 and developed three different intramolecular C–N bond formation processes,[191] achieving the enantioselective total synthesis of three topologically distinct hasubanan alkaloids (Scheme 45). The aldehyde **603** underwent Wacker oxidation,

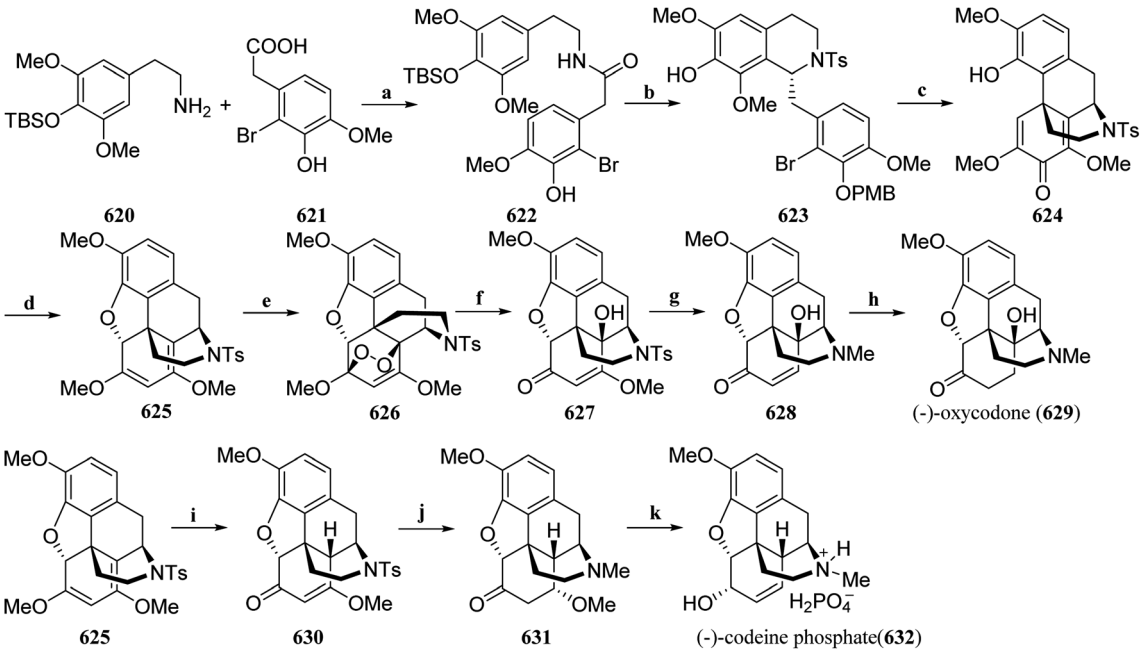

Scheme 46 Bioinspired total synthesis of (−)-oxycodone (**629**) and (−)-codeine (**632**) by Qin's group. Reagents and conditions: (a) TBTU, Et_3N, DCM, 0 °C-rt; (b) (i) K_2CO_3, PMBCl, MeCN, 40 °C, (ii) Tf_2O, 2-fluoropyridine, DCM, −30 °C, (iii) $[Ir(cod)Cl]_2$, (*R*)-BINAP, TEAI, $CHCl_3$, H_2, 0 °C, then Et_3N, TsCl, (iv) KF, HBr, MeCN/H_2O, 50 °C; (c) (i) $Pd(PPhtBu_2)_2Cl_2$, *t*BuOK, DME, 85 °C, (ii) HOAc, 90 °C; (d) (i) $NaBH_4$, MeOH/DCM, 0 °C, (ii) dimethylformamide dimethyl acetal, 1,4-dioxane, 60 °C, (e) TPP, O_2, blue LED, DCM, rt; (f) Pd/C, HCO_2H, iPrOH/H_2O, H_2, rt; (g) (i) $LiAlH_4$, DME, 40 °C, (ii) $(HCHO)_n$, MeOH, then $NaBH_4$, rt, then $PdCl_2$, H_2, MeOH, 30 °C, (iii) IBX, DMSO, rt, (iv) TsOH, THF, 60 °C; (h) Pd/C, H_2, MeOH, 30 °C; (i) (i) $NaBH_4$, MeOH/DCM, 0 °C, (ii) dimethylformamide dimethyl acetal, 1,4-dioxane, 60 °C, (iii) Pd/C, HCO_2H, iPrOH/H_2O, H_2, rt; (j) (i) $LiAlH_4$, DME, 40 °C, (ii) $(HCHO)_n$, MeOH, then $NaBH_4$, rt, then $PdCl_2$, H_2, MeOH, 30 °C, (iii) IBX, DMSO, rt; (k) (i) TsOH, THF, 50 °C, (ii) $NaBH_4$, MeOH, 0 °C.

aldol condensation, and aromatization to obtain the β-naphthol **604**. After allylation of the phenolic hydroxyl group, the α-allyl-β-naphthol **605** was obtained through Claisen rearrangement. Following You's reported reaction conditions,[192] the Takemoto's catalyst catalyzed a dearomatizative Michael addition reaction between the β-naphthol **605** and nitroethylene, resulting in an α,α-disubstituted β-naphthalenone. Reduction of the enone gave **606**. Further reduction with $LiAlH_4$ produced amino alcohol, which was then *N*-acylated under Schotten–Baumann conditions and subsequently reduced to obtain the *N*-methylamine **607**. The amino group of **607** was protected with a Boc group, followed by *in situ* oxidation of the secondary alcohol to produce the key synthetic intermediate ketone **608**. The Wacker oxidation of **608** gave the diketone intermediate **609**, which underwent intramolecular aldol condensation, and cyclopentenone was dehydrogenated to obtain a highly π-conjugated tricyclic compound **610**. After carbonyl α-bromination, the *O*-MOM and *N*-Boc protecting groups were removed and cyclized to obtain (−)-sinoracutine (**611**). Under the action of the second-generation Grubbs catalyst, **608** underwent a cross-metathesis reaction with isopropenylboronic acid pinacol ester, and diketone **612** was obtained after oxidation. The intramolecular aldol condensation reaction gave tricyclic enone **613**, which was deprotonated and hydroxylated to form an α-hydroxy ketone, and dehydrogenated to form the highly conjugated intermediate **614**. Oxidation of **614** to dione followed by removal of the *N*-Boc and *O*-MOM protecting groups and hemiaminal formation afforded (−)-cepharatine A (**615**). Methylation of the alcohol hydroxyl group produced (−)-cepharatine C (**616**).

The aza-[4.4.3]-propellane structure **617** was constructed from **613** by domino-*N*-deprotection/intramolecular aza-Michael addition reaction, and the methyl enol ether **618** was obtained by regioselective thioneation. Hydrolysis of dithioketal and removal of the *O*-MOM protecting group produced (−)-cepharamine (**619**). This strategy is expected to be widely used in the synthesis of members of this natural product family, and it can be used for the synthesis of morphine alkaloids and their derivatives by slightly adjusting the reaction route, which is important for reference.

Qin and Zhang *et al.* established a new strategy in 2022 for the efficient synthesis of opioid natural products and their pharmaceutical molecules (Scheme 46), utilizing Ir-catalyzed asymmetric hydrogenation of imine and biomimetic intramolecular dearomatization coupling as the key reactions.[193] The condensation of phenethylamine **620** and the carboxylic acid **621** produced the amide **622**, followed by PMB protection of the phenolic hydroxyl group and subsequent Bischler–Napieralski cyclization to construct the isoquinoline skeleton, resulting in **623** after asymmetric hydrogenation. Optimization of the intramolecular dearomatization coupling reaction enabled a 50-gram-scale reaction, leading to **624** after removal of the PMB protecting group. The reduction of the carbonyl group in **624** resulted in the formation of a dihydrofuran ring, generating the key pentacyclic core skeleton **625** on a 10-gram scale. The singlet

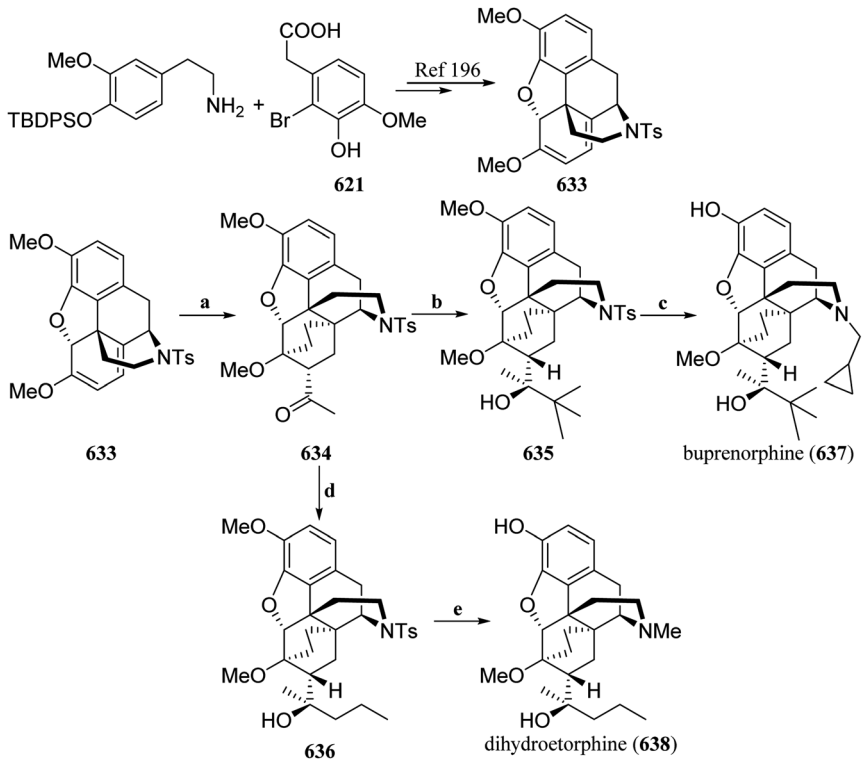

Scheme 47 Total synthesis of buprenorphine (**637**) and dihydroetorphine (**638**) by Qin's group. Reagents and conditions: (a) (i) methylvinyl ketone, PhMe, 80 °C, (ii) Pd/C, AcOH, MeOH, H_2, rt; (b) *t*-BuMgCl, PhMe, rt; (c) (i) $LiAlH_4$, THF, 0–60 °C, (ii) cyclopropanecarbaldehyde, MeOH, then $NaBH_4$, rt, (iii) EtONa, *tert*-dodecanethiol, DMSO, 150 °C; (d) *n*-PrMgCl, PhMe, 50 °C; (e) (i) $LiAlH_4$, THF, 0–60 °C, (ii). $(HCHO)_n$, MeOH, then $NaBH_4$, rt, (iii) EtONa, *tert*-dodecanethiol, DMSO, 150 °C.

oxygen produced by photocatalysis was subjected to [4 + 2] cycloaddition reaction with **625** to generate **626.** Under acidic conditions, catalytic hydrogenation cleaved the O–O bond, resulting in the tertiary hydroxyl compound **627**. The reduction of **627** removed the Ts protecting group while reducing the carbonyl group, and the *N*-methyl group was introduced *via* reductive amination. Hydrogenation of the double bond, followed by IBX oxidation and acid-catalyzed dehydration elimination, produced **628.** Catalytic hydrogenation reduced the alkene moiety in **628**, resulting in (−)-oxycodone (**629**) with an overall yield of 11%.

The key intermediate **625** underwent keto–enol tautomerization and alkene migration to form the ketone **630**, which could be converted into **631** under similar reaction conditions. Elimination of the methoxy group in **631**, followed by diastereoselective reduction of the carbonyl group, provided (−)-codeine (**632**) with an overall yield of 13%. This synthetic strategy can also be widely applied to the efficient synthesis of opioid drugs such as (−)-oxymorphone, (−)-naloxone, (−)-naltrexone, and (−)-nalbuphine, with costs comparable to those of the currently widely used semisynthetic methods from cultivated poppies, demonstrating significant application value. Importantly, the entire synthesis process requires only one column chromatography step, and most intermediates can be purified through simple work-up or recrystallization, greatly increasing the industrial application prospects of this reaction strategy.

Based on the biomimetic dearomatization arene coupling strategy, Qin's group realized the asymmetric total synthesis of buprenorphine and dihydroetorphine from the key intermediate, in 2022 (Scheme 47).[194] According to the previous research,[195] the synthesis of the intermediate **633** was realized. The Diels–Alder cycloaddition of methylvinyl ketone with the diene **633** gave the adduct, then hydrogenated the double bond to furnish **634**. The carbonyl group in **634** reacted with different Grignard reagents to obtain two important intermediates **635** and **636**. Next, the tosyl (Ts) group was removed, and the resulting secondary amine was directly subjected to reductive amination with cyclopropanecarbaldehyde and paraformaldehyde. Finally, the regioselective *O*-demethylation gave buprenorphine (**637**) and dihydroetorphine (**638**).

Based on the potential biosynthetic pathway of hasubanan alkaloids, Nagasawa *et al.* established a versatile synthetic strategy (Scheme 48).[196] The optically pure compound **640** could be obtained through several simple transformation steps from commercially available aldehydes. Through a key diastereoselective oxidative phenolic coupling reaction, the hasubanan tricyclic dienone skeletons **641** and **642** with different substituents could be constructed in one step. **641** underwent reductive debromination to obtain **643**. Under acidic conditions, **642** and **643** underwent aza-Michael reaction and silanol elimination to obtain the conjugated dienones **644** and **645**. After protected the phenolic hydroxyl groups with MOM, Davis oxidation produced the corresponding α-hydroxy ketones **646**

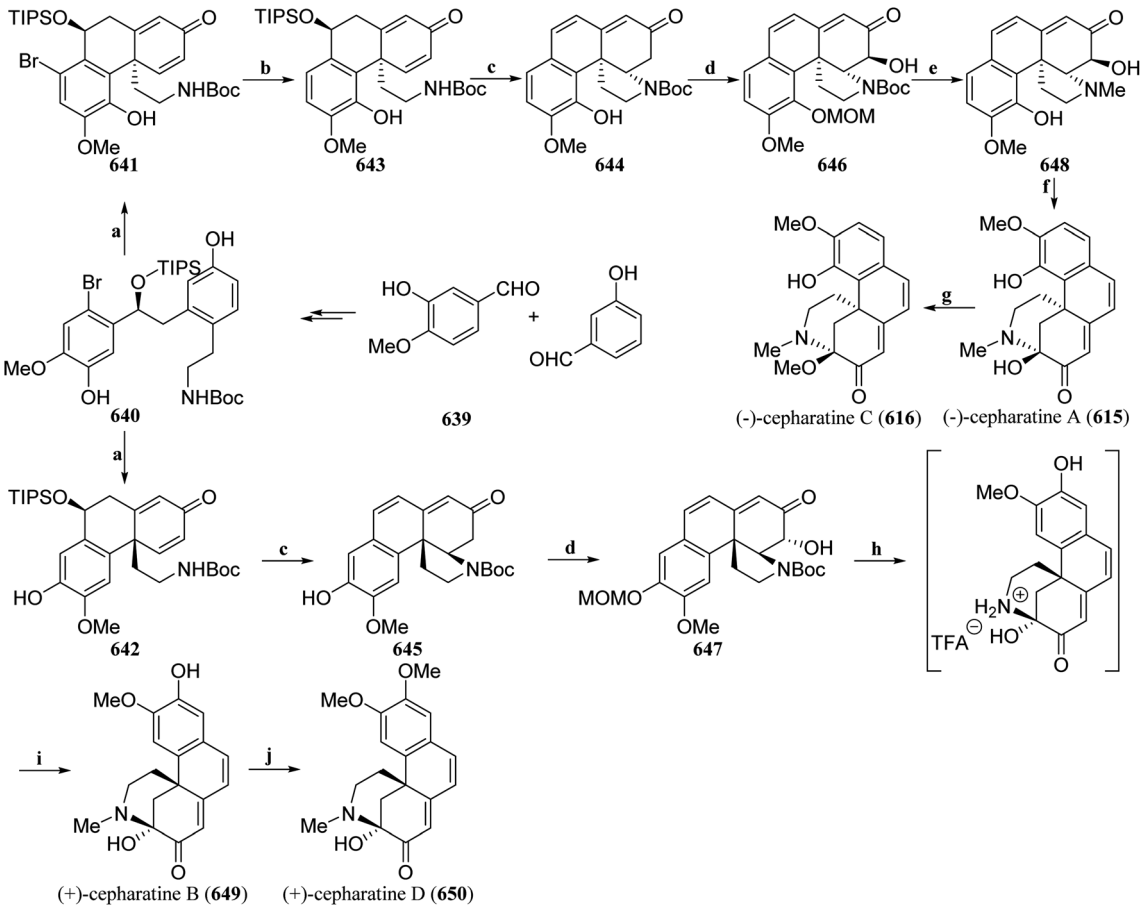

Scheme 48 Total synthesis of cepharatines A–D by Nagasawa's group. Reagents and conditions: (a) PIDA, MeOH, HFIP, 0 °C; (b) HCOONa, $Pd(PPh_3)_4$, DMF, 90 °C; (c) HCl, DCM, rt; (d) (i) MOMCl, i-Pr_2NEt, DCM, rt, (ii) Davis oxidation agent, KHMDS, THF, −78 °C; (e) (i) TFA, rt, (ii) HCHO aq., $NaBH_3CN$, MeCN, rt; (f) neat, rt; (g) $CH(OMe)_3$, H_2SO_4, MeOH, 65 °C; (h) TFA, rt; (i) HCHO aq., $NaBH_3CN$, MeCN, rt; (j) $TMSCHN_2$, PhMe/MeOH, rt.

and **647**. After the deprotection and reductive amination of **646**, a key biosynthetic intermediate **648** was obtained, which can spontaneously undergo a retro-aza-Michael reaction and hemiaminal formation at room temperature, efficiently produced (−)-cepharatine A (**615**), which could be methylated to obtain (−)-cepharatine C (**616**). The reaction precursor **647** underwent deprotection under acidic conditions, simultaneously triggering retro-aza-Michael reaction and hemiaminal formation to

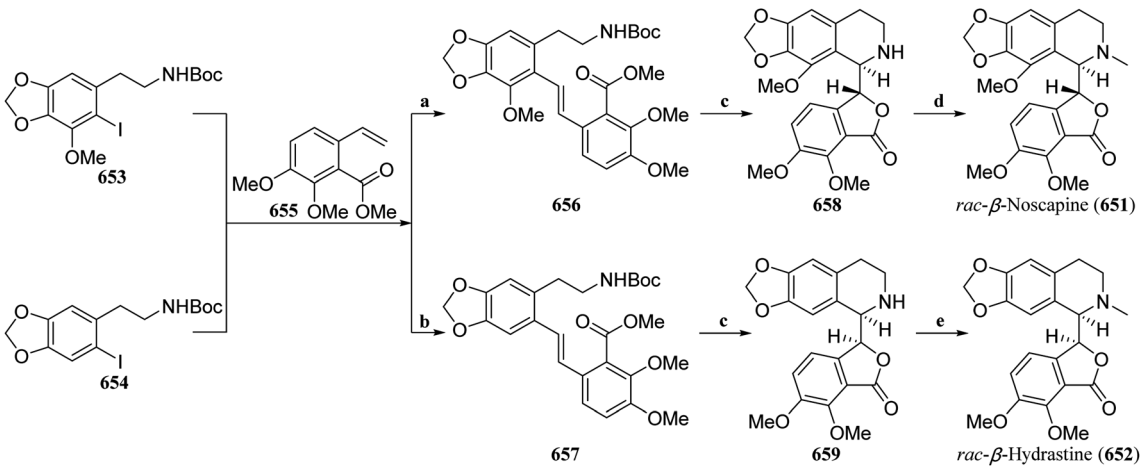

Scheme 49 Total synthesis of *rac*-β-noscapine (**651**) *rac*-β-hydrastine (**652**) by Zhao's group. Reagents and conditions: (a) $Pd_2(dba)_3$, DIPEA, DMF, 110 °C; (b) $Pd(OAc)_2$, AgOAc, HOAc, 117 °C; (c) (i) oxone, $NaHCO_3$, acetone-DCM-H_2O, 0 °C, (ii) CF_3COOH, DCM, 0 °C; (d) HCHO, HCOOH, rt; (e) (i) HCHO, HCOOH, rt, (ii) MeOK, MeOH, rt.

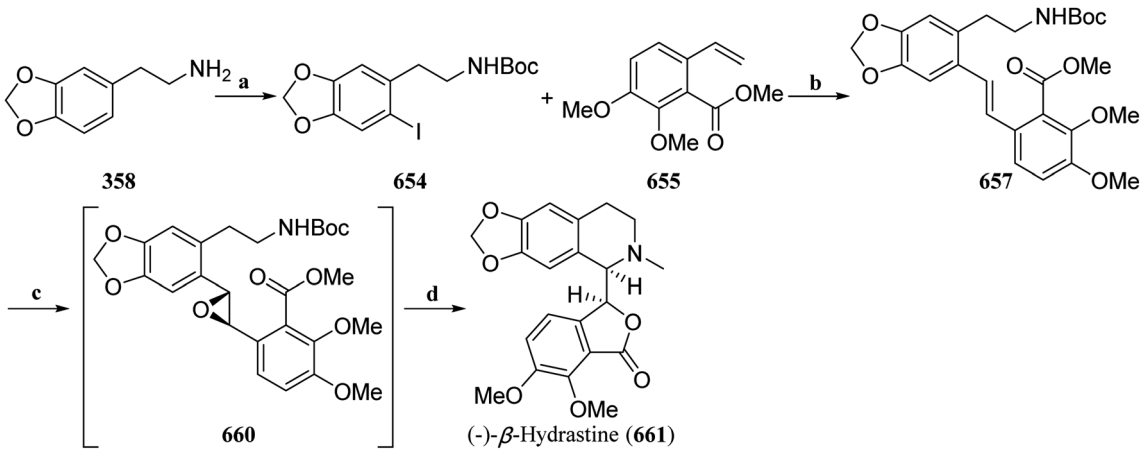

Scheme 50 Total synthesis of (−)-β-hydrastine (**661**) by Zhao's group. Reagents and conditions: (a) (i) $(Boc)_2O$, TEA, DCM, rt, (ii) CF_3COOAg, DCM, −5 °C; (b) $Pd(OAc)_2$, AgOAc, HOAc, 117 °C; (c) Shi catalyst, oxone, K_2CO_3, Bu_4NHSO_4, CH_3CN-buffer, 0 °C; (d) (i) CF_3COOH, DCM, 0 °C, (ii) HCHO, HCOOH, rt, (iii) MeOK, MeOH, rt.

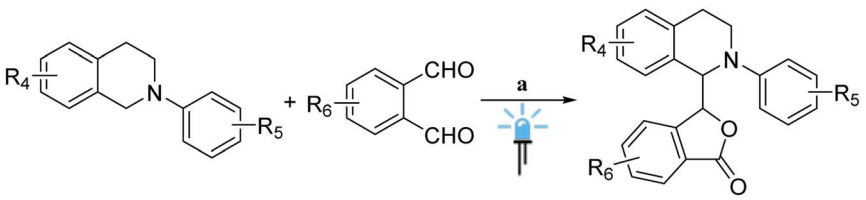

Scheme 51 Photocatalytic efficient construction of phthalide isoquinoline skeleton by Hong and Sun's group. Reagents and conditions: (a) $[Ir(dF(CF_3)ppy)_2(dt\text{-}bpy)]PF_6$, $Cu(OTf)_2$, toluene, Ar, blue LED, rt.

form an unstable hemiaminal, which was then reductively aminated *in situ* to obtain (+)-cepharatine B (**649**). Methylation then afforded (+)-cepharatine D (**650**). This synthetic strategy not only provides a new synthetic pathway but also offers potential clues for elucidating the undetermined biosynthetic pathway of cepharatines.

3.1.8 Phthalideisoquinoline alkaloids. Zhao's group developed a new one-pot acid-catalyzed epoxide ring-opening/intramolecular transesterification cascade cyclization strategy to construct the phthalide tetrahydroisoquinoline skeleton and efficiently achieved the total synthesis of (±)-β-noscapine (**651**) and (±)-β-hydrastine (**652**). Selective aryl iodination of *N*-Boc-protected phenylethylamine derivatives produced **653** and **654**, which underwent Heck coupling with the styrene derivative **655** under Pd-catalyzed to produce the (*E*)-stilbenes **656** and **657**. After epoxidation of the *trans*-alkene, the key transformation to construct the phthalide tetrahydroisoquinoline skeletons **658** and **659** was achieved under one-pot under optimal conditions. Reductive amination followed by *N*-methylation completed the total synthesis of the target compounds (Scheme 49).[197]

Furthermore, by further optimizing the asymmetric epoxidation conditions, the key chiral phthalide tetrahydroisoquinoline skeleton **660** was successfully synthesized in one-pot. After reductive amination and *N*-methylation, epimerization under alkaline conditions resulted in the first asymmetric total synthesis of (−)-β-hydrastine (**661**). This novel synthetic strategy is expected to find widespread application in the diastereo- and enantioselective total synthesis of such natural products (Scheme 50).[198]

Despite the practicality of photoredox strategies, their application in the total synthesis of natural products remains a challenge, presumably owing to the difficulty in performing stereoselective reactions with substrates laden with specific functional groups. However, the concise and efficient construction of natural product derivatives through this strategy still holds significant practical importance in areas such as drug development. For example, Hong and Sun *et al.* developed a strategy combining visible light catalysis and copper-catalyzed radical–radical cross-coupling method, which allowed for the one-step construction of the phthalide isoquinoline skeleton, enabling the efficient synthesis of a series of *N*-aryl phthalide isoquinolines containing various substituents (Scheme 51).[199]

3.1.9 Various isoquinoline alkaloids. The benzoindolizidine skeleton is present in various polycyclic isoquinoline alkaloid natural products. Based on the strategy of visible light-mediated photoredox catalysis for generating amidyl radical intermediates from *N*-alkylbenzamide, Rao and Yu *et al.* constructed a benzoindolizidine skeleton through 5-*exo*-trig cyclization and intramolecular radical addition reactions between these reactive radical intermediates and unactivated olefins,

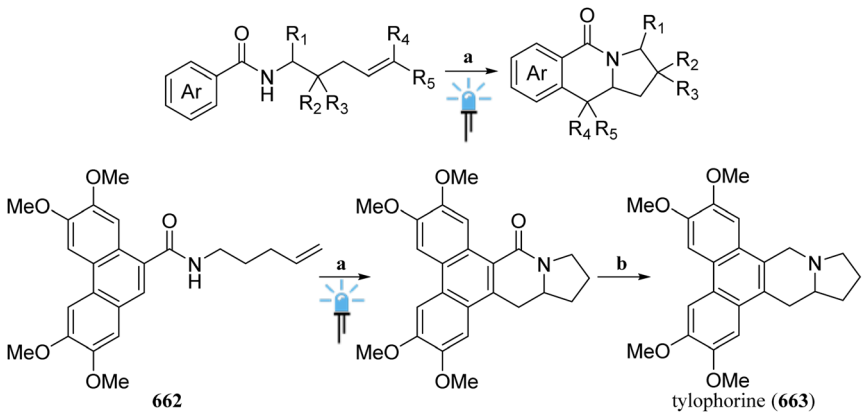

Scheme 52 Total synthesis of tylophorine (**663**) by Rao's group. Reagents and conditions: (a) $[Ir(dF(CF_3)ppy)_2(dCF_3bpy)]PF_6$, $NBu_4OP(O)(OBu)_2$, $PhSCF_3$, $PhCF_3$, blue LED, rt; (b) Red-Al, dioxane, THF, rt.

establishing a concise and efficient synthetic route (Scheme 52).[200] Furthermore, when **662** was used as the starting material, the natural product tylophorine (**663**) could be synthesized concisely.

Ohno and Inuki *et al.* efficiently constructed a 6,6-spirocyclic structure through visible light-mediated photoredox catalytic stereoselective radical cyclization reaction, using it as the key intermediate to achieve the first total synthesis of zephycarinatines C (**671**) and D (**672**) (Scheme 53).[201] According to the coupling method reported by Macherla *et al.*,[202] the carboxylic acid **664** reacted with oxazolidine **665** to obtain amide **666**. After hydrolysis of the ester group, the key reaction precursor **667** was generated. Under the reaction conditions of visible light-catalyzed carboxylic acid to generate the radical intermediate, **667** was smoothly cyclized to obtain the critical spirocyclic skeleton **668**. In addition, the reaction conditions for the continuous flow chemistry system, which can produce cyclization products with moderate yields, were screened, laying a foundation for further expanding the synthesis scale. Under acidic conditions, the oxazolidine ring of **668** was opened to obtain the corresponding alcohol, which was then oxidized and amidated to give **669**. The oxidation of **669** produced an α,β-unsaturated ketone, which underwent intramolecular 1,4-addition to obtain **670**. After selective reduction of the carbonyl group, stereoinversion introduced a methoxy group, followed by *N*-alkylation, completing the first total synthesis of zephycarinatines C (**671**) and D (**672**).

In 2020, Yang *et al.*[207] (Scheme 54) efficiently constructed a chiral unnatural amino acid synthesis unit by referencing the palladium-catalyzed arylation reaction of the alanine-derived amide developed by Yu's group.[203–205] Based on the amino acid ester (**675**), they completed the collective synthesis of a series of renieramycin-type tetrahydroisoquinolines, achieving the first asymmetric total synthesis of (−)-jorunnamycin A (**248**), (−)-fennebricin A (**686**) and (−)-renieramycin J (**685**) (Scheme 54).[206] Under the optimal conditions reported by Yu, aryl iodide compound **673** underwent an arylation reaction with alanine derivative **674**. After removing the amide directing

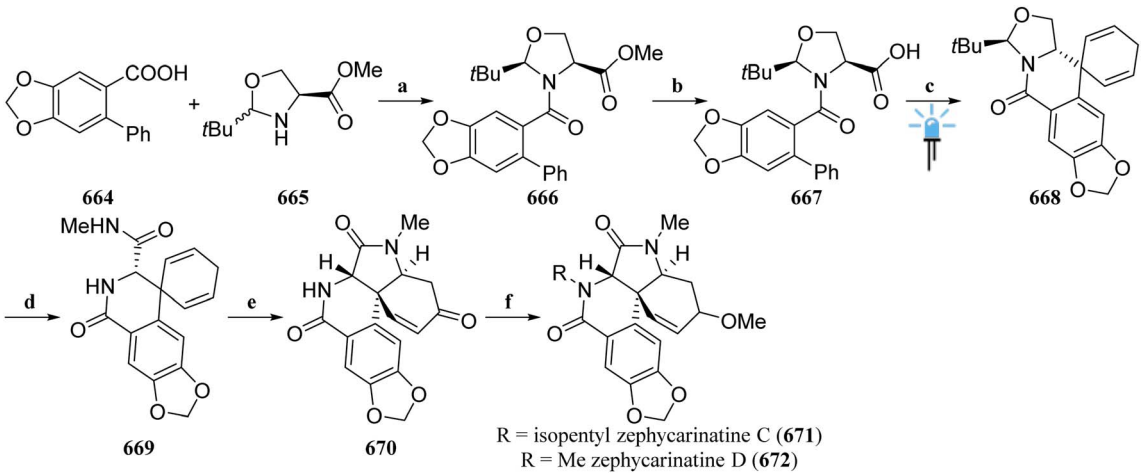

Scheme 53 Total synthesis of zephycarinatines C (**671**) and D (**672**) by Ohno's group. Reagents and conditions: (a) Et_3N, DCM, then MsCl, 0 °C-rt; (b) $LiOH \cdot H_2O$, MeOH, 40 °C; (c) $[Ir(dF(CF_3)ppy)_2(dtbpy)]PF_6$, K_2CO_3, MeCN, blue LED, batch, rt, or $[Ir(dF(CF_3)ppy)_2(dtbpy)]PF_6$, TMG, MeCN, blue LED, flow, rt; (d) (i) $TsOH \cdot H_2O$, $MeCN/H_2O$, 90 °C, (ii) AZADOL, $NaClO_2$, NaOCl, MeCN/pH 7 buffer, 0 °C-rt, (iii) $MeNH_2$, EDC, HOBt, DIPEA, DMF, 0 °C-rt; (e) NMO, TPAP, MeCN, −20–0 °C; (f) (i) $LiAlH_4$, THF, −78 °C, (ii) Ms_2O, Et_3N, DCM, −40 °C, then MeOH. rt, (iii) NaH, DMF, isopentyl bromide or MeI, 0 °C-rt.

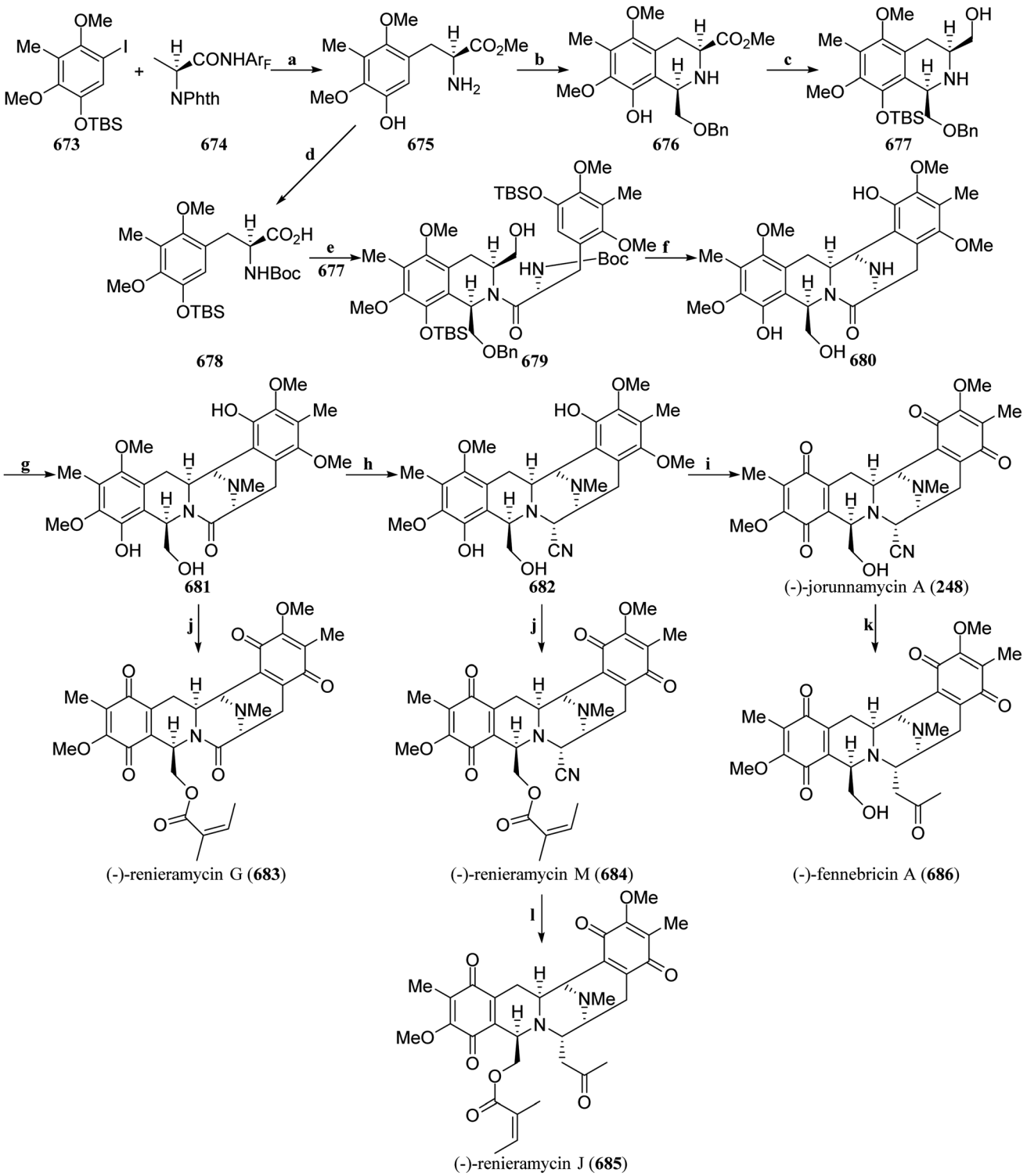

Scheme 54 Total synthesis of (−)-fennebricin A (**686**), (−)-renieramycin J (**685**), (−)-renieramycin G (**683**), (−)-renieramycin M (**684**), and (−)-jorunnamycin A (**248**) by Yang's group. Reagents and conditions: (a) (i) $Pd(TFA)_2$, Ag_2CO_3, 2-picoline, CF_3COOH, DCE, 100 °C, (ii) $BF_3{\cdot}Et_2O$, MeOH, 100 °C, (iii) ethylenediamine, DCM/MeOH, 40 °C; (b) benzoxyacetaldehyde, AcOH, 4A MS, DCM, rt; (c) (i) imidazole, TBSCl, DMF, rt, (ii) $LiAlH_4$, THF, 0 °C; (d) (i) LiOH, MeOH/H_2O, rt, (ii) imidazole, TBSCl, DMF, rt; (e) BOPCl, Et_3N, DCM, 0 °C; (f) (i) DMP, DCM, 0 °C-rt, (ii) TBAF, THF, 0 °C, (iii) TFSA, 0 °C; (g) HCHO, $NaCNBH_3$, AcOH, MeOH, rt; (h) (i) $LiAlH_4$, THF, −20–0 °C, (ii) TMSCN, $BF_3{\cdot}Et_2O$, DCM, −30 °C; (i) DDQ, acetone/H_2O, rt; (j) (i) angelic acid, Et_3N, 2,4,6-trichlorobenzoyl chloride, toluene, 90 °C, (ii) DDQ, acetone/H_2O, rt; (k) (i) imidazole, TBSCl, DMF, rt, (ii) $AgNO_3$, acetone, rt, (iii) HF·pyridine, THF, 0 °C-rt; (l) $AgNO_3$, acetone, 50 °C.

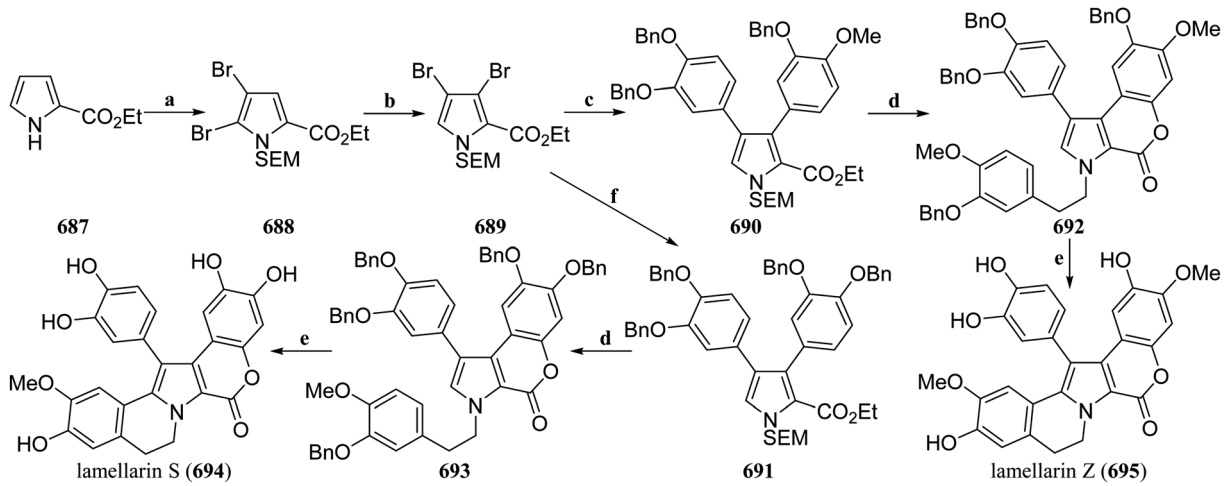

Scheme 55 Total synthesis of lamellarin S (**694**) and Z (**695**) by Okano's group. Reagents and conditions: (a) (i) Br_2, $CHCl_3$, 0 °C-rt, (ii) NaH, SEMCl, THF, 0 °C-rt; (b) (i) LDA, THF, −78 °C, (ii) H_2O, −78 °C; (c) (i) arylboronate ester, $Pd(dba)_3$, $P(4\text{-}CF_3C_6H_4)_3$, $Ba(OH)_2\cdot 8H_2O$, 1,4-dioxane/H_2O, reflux, (ii) arylboronate ester, $Pd(PPh_3)_4$, $Ba(OH)_2\cdot 8H_2O$, 1,4-dioxane/H_2O, reflux; (d) (i) KOH, 18-crown-6, EtOH, reflux, (ii) $Pd(OAc)_4$, EtOAc, reflux, (iii) TFA, DCM, rt, then evaporation, $NH_2OH\cdot HCl$, Na_2CO_3, THF/H_2O, rt, (iv) phenylethyl alcohol, PPh_3, DIAD, THF, rt; (e) (i) PIFA, $BF_3\cdot Et_2O$, DCM, −40 °C, (ii) Pd/C, H_2, EtOH/EtOAc, rt; (f) arylboronate ester, $Pd(PPh_3)_4$, $Ba(OH)_2\cdot 8H_2O$, 1,4-dioxane/H_2O, reflux.

group, TBS protecting group, and phthalimide protecting group, the key reaction precursor, amino ester **675**, was obtained. From **675**, two fragments **677** and **678** of the pentacyclic ring system of tetrahydroisoquinoline could be constructed, respectively. The Boc group protected the amino group on the **675**, and then hydrolyzed the ester, the phenolic hydroxyl group was protected by TBS to obtain **678**. The intermolecular Pictet–Spengler reaction of **675** with benzoxyacetaldehyde was used to synthesize **676**, TBS protected the phenol hydroxyl group, and reduction the ester group to obtain the alcohol **677**. Coupling of **677** and **678** produced the amide **679**. Subsequent oxidation of the primary alcohol with DMP led to a hemiaminal, and after removing the hydroxyl protecting group, an intramolecular Pictet–Spengler reaction took place, simultaneously removing the Boc group and completing the construction of the pentacyclic backbone **680**. After reductive amination, *N*-methylamine **681** was obtained. The reduction of **681** with $LiAlH_4$ gave an unstable hemiaminal intermediate, which was immediately converted to a more stable compound **682** under the conditions of TMSCN and $BF_3\cdot Et_2O$. Oxidation of **682** with DDQ produced (−)-jorunnamycin A (**248**). TBS then protected the alcohol hydroxyl group of (−)-jorunnamycin A, which underwent an intermolecular Mannich reaction. Removal of TBS protection gave (−)-fennebricin A (**686**). Acylation of **682** with angelic acid, followed by DDQ oxidation, generated (−)-renieramycin M (**684**), which underwent an intermolecular Mannich reaction leading to the formation of (−)-renieramycin J (**685**). Additionally, the acylation of **681** with angelic acid and subsequent DDQ oxidation gave (−)-renieramycin G (**683**).

Okano's group established a divergent synthetic method for symmetric/asymmetric lamellarins and their homologs in 2020 [207] based on their recent discovery that the ester group promoted halogen dance as a key reaction.[208] The nitrogen atom of ethyl pyrrole-2-carboxylate **687** was protected, followed by bromination to obtain the α,β-dibromopyrrole **688**. Treatment with LDA facilitated the smooth migration of the α-bromo group, resulting in the β,β′-dibromopyrrole **689**. Owing to the different reactivities of the bromo groups, the two bromo groups at the β positions could be converted into the same or different aryl derivatives **690** and **691** *via* the Suzuki–Miyaura coupling reaction. After ester hydrolysis, Pd-catalyzed intramolecular esterification occurred. Following deprotection, *N*-alkylation with phenylethyl alcohol was performed under Mitsunobu conditions to obtain the *N*-alkylated derivatives **692** and **693**. The hypervalent iodine PIFA promoted the formation of C–C bonds, constructing the lamellarin skeleton. Deprotection then led to the generation of Lamellarin S (**694**) and Z (**695**) (Scheme 55). This synthetic strategy could also be applied to the synthesis of other pyrrolidine alkaloids.

In 2021, Okano's group further optimized the synthetic strategy,[209] achieving a bottom-up synthesis of lamellarin alkaloids (Scheme 56). The LDA-induced migration of the α-bromo group produced the intermediate, α-pyrrolyl lithium, which could be converted into the corresponding organozinc compound. This compound could then be coupled with aryl iodide *via* Pd catalysis to obtain the fully substituted pyrrole derivative **696**, in a one-pot. After deprotection and cyclization, the tetrahydroisoquinoline skeleton **697** was constructed. Similarly, halogen-lithium exchange was carried out according to the different reactivities of the bromine groups, which could replace the β-bromide near the ester group with the boronic acid ester group to obtain the key synthetic intermediate **698**. This synthetic intermediate enables the total synthesis of the lamellarins L (**699**), J (**700**), and G (**701**) through stepwise arylation.

In 2022, Samanta *et al.* developed a cheap Ru(II)-catalyzed C–H bond arylation reaction based on quinone-type carbene migratory insertion, efficiently constructing the

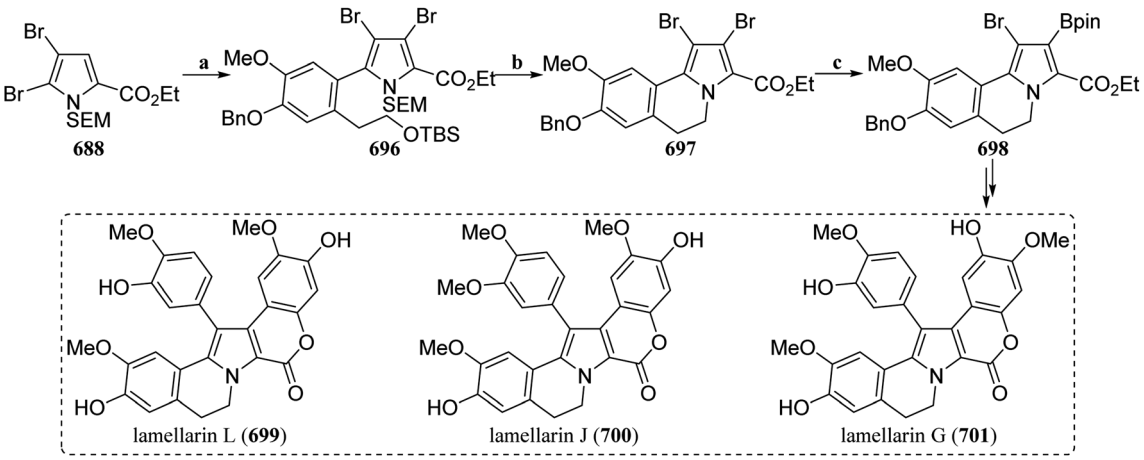

Scheme 56 Total synthesis of lamellarin L (**699**), J (**700**) and G (**701**) by Okano's group. Reagents and conditions: (a) (i) LDA, THF, −78 °C, (ii) $ZnCl_2 \cdot TMEDA$, −78 °C, (iii) $Pd(PPh_3)_4$, aryl iodide, 60 °C; (b) (i) TFA, CH_2Cl_2, rt, (ii) Na_2CO_3, THF/H_2O, rt, (iii) MsCl, Et_3N, CH_2Cl_2, 0 °C; (c) 3,5-$(CF_3)_2C_6H_3Li$, THF, −78 °C, then i-PrO-Bpin, −78 °C-rt.

indolocoumarin skeleton by combining it with a Brønstead acid-promoted cyclization reaction (Scheme 57).[210] This new method was applied to achieve the total synthesis of isolamellarins A and B. First, the tetrahydroisoquinoline **702** and allyl acetate derivatives **703**/**704** underwent Baylis–Hillman reaction to construct the tetrahydroisoquinoline-fused pyrrole skeletons **705** and **706**. After amidation of the ester groups, these compounds were converted into the key precursors **707** and **708**. Under optimal reaction conditions, the amides **707** and **708** reacted with *o*-quinonediazide to complete the total synthesis of isolamellarins A (**709**) and B (**710**).

Wang *et al.* achieved the first total synthesis of sinopyrine B (**711**)[211] using a unique formal [3 + 2] cyclization between amino-substituted malononitrile developed by their group and TMS-acetylene as the key step to construct the pyrrolo[2,1-α]isoquinoline skeleton.[212] Phenylethylamine **712** was obtained *via* the Henry reaction with nitromethane, TBS protection of hydroxyl group and reduction reaction of the inexpensive isovanillin **639**, which was cyclized with paraformaldehyde by Picket–Spengler to construct an isoquinoline backbone **713**. Through the subsequent ammonolysis of ethyl formate, formamide **714** was obtained. Under established reaction conditions, formamide **714** reacted with TMSCN to generate the key intermediate **715**, which underwent a formal [3 + 2] cyclization with TMS-acetylene to complete the construction of the pyrrolo[2,1-α]isoquinoline skeleton **716**. Finally, DIBAL-H was used to reduce the cyano group to obtain aldehyde **717**, followed by the removal of TMS and TBS groups to complete the first total synthesis of sinopyrine B (**711**) with a total yield of 7% (Scheme 58). This concise and efficient synthetic strategy provides new ideas for the synthesis of other biologically active natural products or pharmacological molecules containing the pyrrolo[2,1-α]isoquinoline skeleton.

3.1.10. Summary. Synthetic chemistry remains at the core of drug discovery and development in the pharmaceutical industry, providing a continuous and diverse source of raw

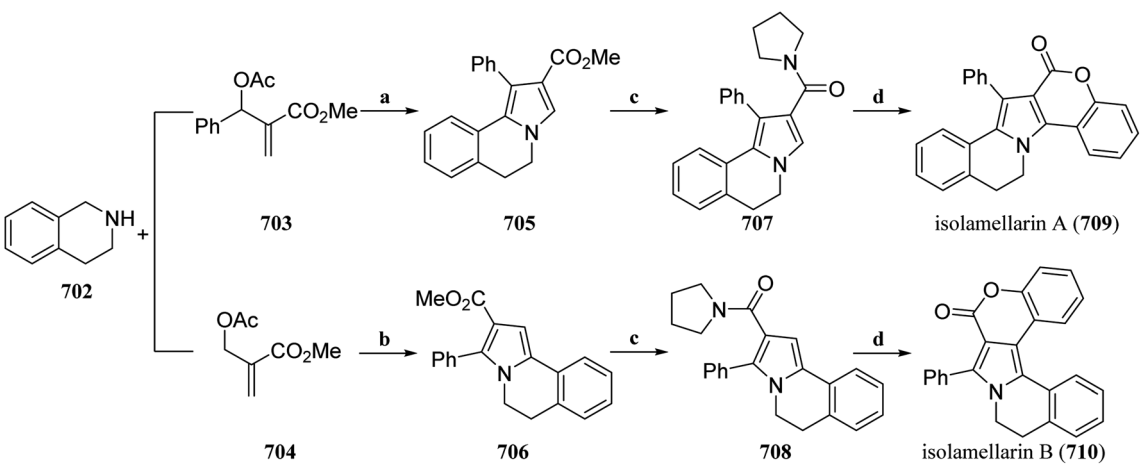

Scheme 57 Total synthesis of isolamellarin A (**709**) and isolamellarin B (**710**) by Samanta's group. Reagents and conditions: (a) (i) CuBr, TBHP, m-xylene, reflux, (ii) DDQ, m-xylene, rt; (b) (i) CuBr, TBHP, m-xylene, 140 °C, (ii) $Pd(OAc)_2$, PPh_3, bromobenzene, CS_2CO_3, rt; (c) pyrrolidine, LiHMDS, toluene, rt; (d) *o*-quinonediazide, $[Ru(p\text{-cymene})Cl_2]_2$, $AgNTf_2$, PivOH, ^{t}AMOH, 90 °C, then AcOH, 130 °C.

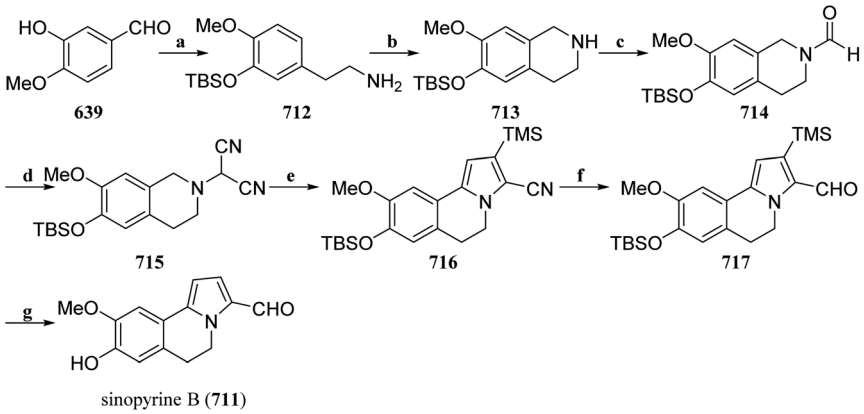

Scheme 58 Total synthesis of sinopyrine B (**711**) by Wang's group. Reagents and conditions: (a) (i)CH_3NO_2, CH_3COONH_4, AcOH, 100 °C, (ii) TBSCl, Et_3N, DCM, 0 °C, (iii) $NaBH_4$, MeOH, 0 °C, (iv) Pd/C, H_2, MeOH, rt; (b) $(HCHO)_n$, TFA, DCM, 0 °C; (c) HCOOEt, HCOOH, 60 °C; (d) TMSCN, $Cu(OTf)_2$, *n*-heptane, 80 °C; (e) DDQ, DMF, 80 °C; (f) DIBAL-H, Et_2O, 0 °C; (g) TBAF, THF, 0 °C.

materials for drug development. Research on the synthesis of isoquinoline alkaloid natural products not only lays the material foundation for in-depth studies on the biological activity of related natural products, especially with the first (asymmetric) total synthesis of natural products such as ampullosine (**254**), berbanine (**270**), berbidine (**271**), *rac*-muraricine (**72**), dactylicapnosine A (**342**), dactylicapnosine B (**343**), dactyllactone A (**405**), pallimamine (**446**), *O*,*N*-dimethylhamatine (**458**), (−)-thebainone A (**591**), and (+)-corynoloxine (**520**), but also offers diverse synthetic strategies and practical synthetic pathways for the efficient preparation of isoquinoline alkaloid natural products and their novel analogs. Related synthetic research not only expands the diversity of isoquinoline alkaloids but also aids in the discovery of new compounds with better biological activity, thus injecting new vitality into drug research and development.

Photoredox catalysis and electrochemical synthesis methods can generate highly reactive intermediates under mild and environmentally friendly reaction conditions, achieving target transformations with high selectivity and efficiency, significantly increasing substrate compatibility and expanding the scope of application. In many cases, they have become alternatives or complements to traditional organic synthesis reactions, providing more direct and unique ways of chemical bond breaking and building for organic synthesis.[112–115] Furthermore, it also offers new directions for retrosynthetic analysis of complex compounds such as natural products, making the synthesis of these compounds simpler and more efficient.[116,117] These novel synthetic strategies have not only been applied in the first total synthesis of isoquinoline alkaloid natural products such as dactyllactone A (**405**), zephycarinatines C (**671**) and D (**672**), but also optimized the synthesis strategies of isoquinoline alkaloids such as (−)-thebaine (**590**), (−)-oxycodone (**629**), Amaryllidaceae alkaloids (**581**, **582a,b**, **583a,b**), tylophorine (**663**), *rac*-norlaudanosine (**310**), *rac*-laudanosine (**311**), and *rac*-xylopinine (**312**), providing new synthetic pathways. Research on the combined application of continuous flow reaction technology,[213–216] it is expected to further expand their potential for large-scale production applications. Currently, the efficient preparation of protoberberine (PB) and 13-methylprotoberberine (13-MePB) at the gram scale has been achieved through the combination of electrochemical synthesis methods and continuous flow reaction systems (Scheme 28).[161]

As an emerging reaction technology, the continuous flow reaction allows for safer, more environmentally friendly, and efficient conversions than traditional synthesis processes, while generating less waste.[118] In recent years, continuous flow reactions have been widely used in synthesis research and in the industrial production of pharmaceuticals, pesticides, chemical products, and their intermediates,[217,218] showing great application potential.[119,120] Chen's group achieved the first fully continuous flow asymmetric synthesis method for natural tetrahydroprotoberberine alkaloids (Scheme 26).[158] Compared with traditional synthesis processes, this continuous flow reaction process is more efficient (the reaction time is reduced from 100 hours to 32.5 minutes) and more environmentally friendly (no intermediate purification is needed, reducing solvent usage and waste generation). However, it is regrettable that this process still faces certain challenges in terms of scaled-up mass production, and further in-depth research is urgently needed.

3.2. Biosynthesis of isoquinoline alkaloids

Isoquinoline alkaloids are mostly extracted and isolated from plants. Through in-depth research, many natural products with potential application value have been discovered. However, the natural content of isoquinoline alkaloids in plants is relatively low, which severely limits further in-depth research and industrial applications.[219] Although several high-value isoquinoline alkaloids, such as morphine, are still obtained through large-scale planting, many problems remain, such as needing to occupy a large amount of farmland, unstable yields caused by environmental impacts, and environmental pollution caused by complex separation and purification. Therefore, researchers are committed to overcoming this problem through chemical synthesis. Chemical synthesis is currently the most

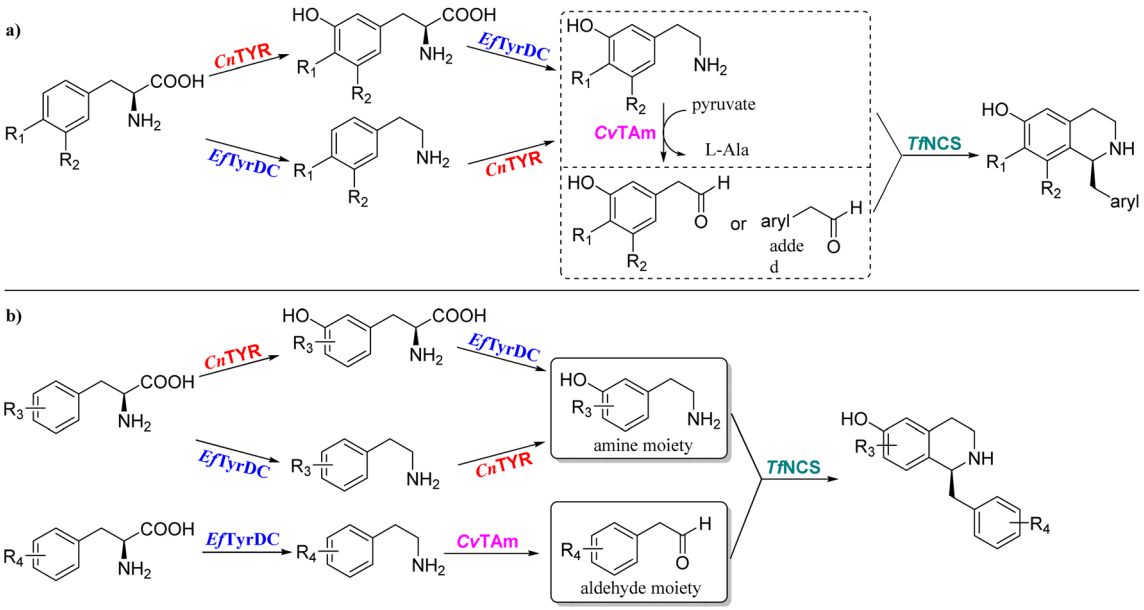

Scheme 59 (a) Benzylisoquinoline biosynthesis and (b) halo benzylisoquinoline biosynthesis by Hailes's group.

commonly used method to obtain isoquinoline alkaloids. A variety of isoquinoline alkaloid natural products and their analogs can be obtained through different synthesis strategies. These findings provide a rich material basis for the applied research on isoquinoline alkaloids. However, for structurally complex isoquinoline alkaloids, chemical synthesis still has serious limitations, such as multiple reaction steps, the influence of byproducts, and poor regio- and stereospecificity. Moreover, similar to plant extraction, chemical synthesis can also cause environmental pollution.

With the continuous development of biotechnology, biosynthetic strategies provide a new and promising option for obtaining isoquinoline alkaloids. Through biotechnology methods, such as gene sequencing, transcriptomics, and proteomics, researchers have elucidated the biosynthetic pathways of various isoquinoline alkaloids in their natural hosts. With the help of gene editing technology, DNA synthesis technology, metabolic engineering, protein engineering, and synthetic biology, the biosynthesis of isoquinoline alkaloids and their derivatives has been achieved, offering advantages such as high efficiency, strong specificity, and environmental friendliness. Currently, enzymatic biosynthesis and microbial cell factories are the most widely used biosynthetic strategies. In this section, we will introduce the latest progress in the biosynthesis of isoquinoline alkaloids according to the two commonly used biosynthetic strategies.

3.2.1 Enzymatic biosynthesis. The biosynthesis of isoquinoline alkaloids requires the participation of multiple enzymes. *In vitro* enzymatic biosynthesis allows for the editing and modification of key synthetic enzymes through biotechnology. By regulating reaction conditions such as the temperature and pH, the efficient biosynthesis of various isoquinoline alkaloids can be achieved. Additionally, a multienzyme cascade reaction system can efficiently convert simple raw materials into high-value isoquinoline alkaloids with ideal stereospecificity through various combinations of precursor synthesis enzymes, N-heterocycle synthesis enzymes, and post-modification enzymes.[220] This is difficult to achieve with chemical synthesis strategies. Although *in vitro* biocatalytic cascades draw inspiration from natural biosynthetic pathways, they offer greater flexibility in terms of reaction design. Furthermore, *in vitro* methods are not influenced by the inherent metabolic network of the natural host, reducing background reactions and making product separation and purification easier. Therefore, enzymatic biosynthesis of isoquinoline alkaloids holds tremendous production potential, especially for those with complex structures.

Hailes and Ward *et al.* successfully constructed a one-pot multienzyme cascade reaction *in vitro* by combining the tyrosinase *Cn*TYR, the tyrosine decarboxylase *Ef*TyrDC, and additional enzymes including the transaminase *Cv*TAm and the norcoclaurine synthase *Tf*NCS. Using four different tyrosine derivatives as substrates, they achieved efficient biosynthesis of two natural and six unnatural benzylisoquinolines with high stereoselectivity and a 23–66% isolated yield (Scheme 59a).[221] Moreover, this one-pot multienzyme cascade reaction could be successfully scaled up to 1 g, demonstrating the potential application value of this strategy. Subsequently, Hailes *et al.* combined *Cn*TYR, *Ef*TyrDC, *Cv*TAm, and *Tf*NCS in a parallel multienzyme cascade reaction system, achieving the biosynthesis of halogenated and dihalogenated benzylisoquinoline alkaloids with high enantiomeric purity, which was difficult to achieve through chemical synthesis (Scheme 59b).[222] In particular, after mutagenesis to produce a tyrosinase mutant, the tolerance to halogenated tyrosine was improved, increasing the range of substrates. The combination of this multienzyme cascade strategy and an enzyme mutagenesis strategy has

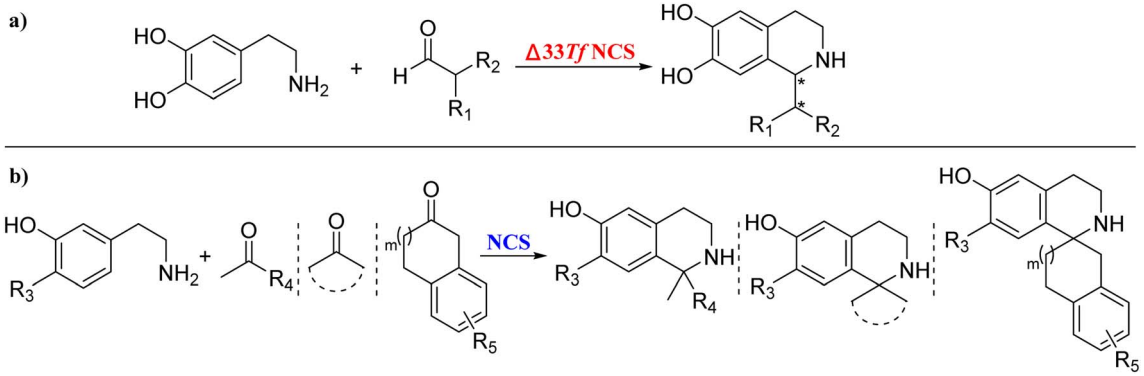

Scheme 60 Biosynthesis of dopamine derivatives with (a) aldehydes, (b) ketones by Hailes's group.

strong potential for use in the synthesis of chiral benzylisoquinoline alkaloids.

Norcoclaurine synthase (NCS) promotes the Pictet–Spengler reaction between dopamine derivatives and aryl aldehydes in plants, generating a single enantiomer of benzylisoquinoline.[223] However, previous reports have indicated that NCS has poor tolerance for α-methyl substituted aldehydes, making it difficult to obtain the target product.[224] Hailes's group showed that wild-type *T. flavum* NCS (Δ33*Tf*NCS) exhibited good tolerance to α-methyl substituted aldehydes, generating THIQ products with two defined stereocenters (Scheme 60a).[225] This transformation, which is difficult to achieve through traditional chemical synthesis, provides a new strategy for the synthesis of corydaline-like isoquinoline alkaloids. Active site mutants could further improve the diastereomeric ratio and conversion rate, demonstrating their potential in enzyme catalysis engineering. Several selected NCS variants showed tolerance to aliphatic ketones, α-substituted ketones, cyclic ketones, and diketones, achieving chemically challenging 1,1′-substituted and spiro-tetrahydroisoquinoline derivatives (Scheme 60b).[226]

In the biosynthetic pathway of plants, methyltransferase (MT) plays a role downstream of norcoclaurine synthase (NCS) to achieve methylation,[227] which is crucial for the biosynthesis and diversification of benzylisoquinolines. However, the high cost of the cofactor *S*-adenosylmethionine (SAM) limits its application in larger-scale *in vitro* biocatalytic reactions. Based on previous studies and a modular *in vitro* cofactor supply system consisting of the enzymes *Ec*MAT and *Ec*MTAN from *Escherichia coli*,[228] Hailes *et al.* established an *in vitro* one-pot multienzyme cascade reaction system. With two MT enzymes, *Rn*COMT and *Mx*SafC, which have unique characteristics, as the core, combined with enzymes such as *Cj*-6-OMT and *Tf*NCS, they achieved efficient construction of methylated THIQ alkaloid natural products and their derivatives with high enantiomeric purity (Scheme 61).[229]

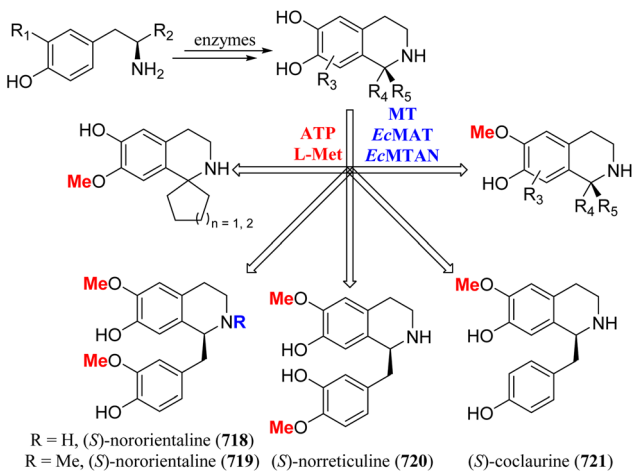

Scheme 61 Biosynthesis of methylated THIQs *in vitro via* one-pot cascades by Hailes's group.

Unlike the NCS mechanism of action, the unique catalytic mechanism of IRED does not rely on groups such as the C6-hydroxyl of the isoquinoline ring, making it tolerant to highly modified DHIQ precursors. Using the previously identified IRED as a key enzyme,[230] Qu *et al.* designed a new multienzyme cascade reaction system that achieved phenylisoquinoline derivatives that are difficult to obtain in the NCS cascade reaction system (Scheme 62).[231] First, high-yield chemically synthesized 1-phenyl and 1-benzyl-6,7-dimethoxydihydroisoquinoline precursors were constructed. These precursors were reduced by the imine reductase IR45 to obtain the corresponding (*S*)-THIQ, which was subsequently methylated by *N*-methyltransferase (CNMT). This process efficiently synthesized isoquinoline natural products and their medicinal derivatives with almost 100% yield.

3.2.2 Microbial cell factory. Compared with plants, microbial systems are genetically easier to control and cultivate. Therefore, through techniques such as cell engineering, enzyme engineering, fermentation condition optimization, and protein engineering, microbial cell factories for the production of important industrial products can be constructed.[232] This also provides a new avenue for the synthesis of isoquinoline alkaloids and their derivatives with high application value. However, the natural biosynthetic pathways or enzymes involved in the synthesis of different isoquinoline alkaloids have not been fully elucidated, posing significant challenges and difficulties in achieving their biosynthesis in heterologous hosts. With the rapid development and widespread application

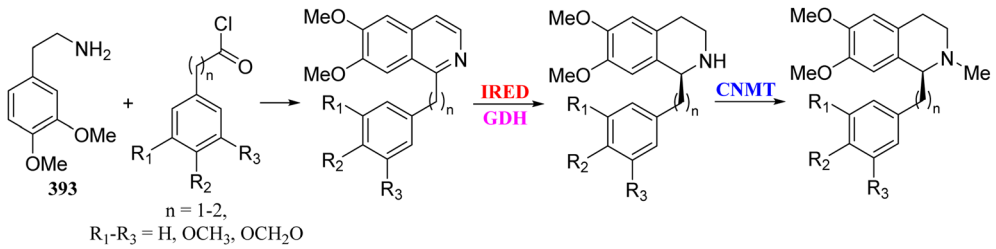

Scheme 62 Biosynthesis of THIQs *in vitro via* IRED approach by Qu's group.[232]

of multiomics technologies such as genomics, transcriptomics, proteomics, and metabolomics, the natural biosynthetic pathways or key enzymes of various isoquinoline alkaloids have gradually become clearer in recent years,[233–239] laying the foundation for studying the microbial heterologous synthesis of isoquinoline alkaloids. *Escherichia coli* and *Saccharomyces cerevisiae* are currently the most widely used heterologous microorganisms because of their short growth cycles, clear genetic backgrounds, and simple cultivation conditions.

Smolke's group analyzed the crystal structure of the essential enzyme (*S*)-scoulerine 9-*O*-methyltransferase of the berberine natural product biosynthesis pathway in *Thalictrum flavum*, and used this crystal structure information to construct a series of mutants to analyze the structure-activity relationship of *Tf*S9OMT, and found specific mutants with regioselective and substrate-selective changes. Using these engineered *Tf*S9OMT mutants, the first *de novo* yeast strains producing (*S*)- tetrahydropalmatine and (*S*)-tetrahydropalmatrubine were constructed.[240] The results of this study suggest that characterizing enzyme structures to guide protein engineering can provide specific enzymes for heterologous biosynthetic pathways, which has important potential for the targeted production of difficult-to-synthesize but high-value isoquinoline alkaloids and their derivatives.

The *in vivo* engineering biocatalytic cascade method based on the whole-cell system has proven to be a powerful tool for synthesizing more high-value products.[241] Based on the new biosynthetic method for 4-hydroxyphenylacetaldehyde,[242] Xiao *et al.* established four enzymatic cascade reactions in *Escherichia coli via* the decarboxylase BLPad or AnPad, the styrene monooxygenase StyAB, styrene oxide isomerase RostyC, and the norcoclaurine synthase Δ29*Tf*NCS. Through the cascade of four biocatalytic reactions: decarboxylation-epoxidation-isomerization-condensation, the efficient synthesis of two natural isoquinoline alkaloids and their derivatives was achieved from coumaric acid derivatives and dopamine derivatives.[243] Furthermore, it can efficiently synthesize isoquinoline alkaloids using lignocellulosic biomass as the raw material, with the target compound concentration exceeding 1 g L^{-1}.

Despite the fact that some key functional enzymes remain unidentified, a semi-biosynthetic strategy combined with mild chemical transformation conditions can help compensate for the lack of certain functional enzymes. Examples of the microbial production of artemisinin[244] and vinblastine[245] have demonstrated the effectiveness and feasibility of this semi-biosynthetic strategy, which is expected to find widespread application in industrial production in the future. Based on the yeast biosynthesis platform established in the early stage for the production of key intermediates of tetrahydropapaverine,[246,247] Smolke's group developed *N*-methylcoclaurine hydroxy-lase variants and scoulerine 9-*O*-methyltransferase variants through protein engineering, and combined with a series of genetic modifications to achieve *de novo* biosynthesis of tetrahydropapaverine. Subsequently, semi-biosynthesis of papaverine was achieved under chemical transformation conditions using hydrogen peroxide as an oxidant.[248] Based on this semi-biosynthetic strategy, Li *et al.* recently used 15 enzymes to modify the initial yeast strains to obtain an engineered yeast strain and established a complete semibiosynthetic pathway for *de novo* production of berberine through chemical transformation by heating the bioreactor.[249] Furthermore, this engineered yeast was tolerant of fluorotyrosine, enabling the biosynthesis of fluorinated benzylisoquinoline and fluorinated berberine.

Multiple platforms for the *de novo* heterologous biosynthesis of benzylisoquinoline alkaloids have been constructed based on engineered *S. cerevisiae* strains. However, developing microbial strains and biosynthetic platforms capable of producing bisbenzylisoquinoline alkaloids remains a challenge. The Smolke's group reported a breakthrough in 2021, discovering that the enzymes PbDRS-DRR and BsCYP80A1 can function in yeast, achieving epimerization of benzylisoquinoline alkaloids and facilitating the coupling of two benzylisoquinoline alkaloid monomers. Thus, they constructed an engineered yeast strain capable of producing bisbenzylisoquinoline alkaloids.[250] Through strain engineering, protein engineering, and optimization of fermentation conditions, efficient biosynthesis of guattegaumerine and berbamunine was achieved.

Escherichia coli is currently one of the most commonly used heterologous microorganisms in addition to *S. cerevisiae*. Moreover, compared to the yeast system, *E. coli* has a greater capacity to produce tetrahydroprotoberberine intermediates.[251,252] However, it is unfortunate that berberine bridge enzyme (BBE), as the rate-limiting enzyme in the tetrahydroprotoberberine (THPB) biosynthetic pathway, does not function in *E. coli*, which limits the reconstruction of the THPB biosynthetic pathway in this organism. In 2021, Liu *et al.* overcame the functional expression barrier of BBE in *E. coli* through a combination of strategies such as screening BBE from different sources, optimizing codons, protein tagging strategies, and optimizing promoters.[253] They reconstructed the biosynthetic pathways of (*S*)-scoulerine, (*S*)-tetrahydropalmatine, (*S*)-

corydalmine, and related intermediates in *E. coli*. After the culture conditions were optimized, efficient biosynthesis of these compounds was achieved in the corresponding engineered *E. coli* microbial cell factories.

3.2.3 Comparison and prospects of the biosynthesis and chemical synthesis of isoquinoline alkaloids. The advantages of faster efficiency, more reliable production cycles, and higher purity of target compounds make microbial cell factories an attractive option for synthesizing high-value isoquinoline alkaloids and their derivatives. However, achieving large-scale production still faces considerable challenges.[254] For example, assessing the performance deficiencies of strains and constructed pathways largely relies on low-throughput analytical methods, which are inefficient. Furthermore, with the development of cellular engineering, longer and more complex heterologous metabolic pathways can now be incorporated into microbial factories. However, this also increases the likelihood of crosstalk with natural cellular functions in the host cells.[255] Researchers are continuously developing new technologies to enable large-scale production in microbial cell factories as soon as possible. By modifying the metabolic pathways of organelles in eukaryotic cells, better production results can be achieved while avoiding crosstalk with cytosolic factors.[256] The further development of biosensors that can directly report the performance of target compound production pathways in living cells provides direction for the evolutionary design of microbial cell factories.[257–259] Cheminformatics computational tools have shown tremendous application value in predicting reactions, pathways, and enzymes in synthetic biology and metabolic engineering using large amounts of data. This aids in driving large-scale biological production of valuable natural chemicals, drugs, and biological products.[260]

Compared with traditional organic synthesis, biosynthesis excels in terms of regioselectivity and stereoselectivity. However, due to the specificity of enzymes, they have unique requirements for reaction substrates, which limits the range of substrates suitable for biosynthesis. Additionally, since the natural biosynthetic pathways or enzymes of many isoquinoline alkaloids have not been fully elucidated, the isoquinoline alkaloids that have been extensively studied and biosynthesized include mainly phenylisoquinoline alkaloids, benzylisoquinoline alkaloids, and berberine. Many complex or newly isolated isoquinoline alkaloids cannot be obtained through biosynthetic pathways in the short term. Organic total synthesis, on the other hand, has advantages in this regard, especially in terms of substrate compatibility and the synthesis of diverse derivatives. This makes traditional organic synthesis play a crucial role in the early research process of isoquinoline drug development or the discovery of novel isoquinoline alkaloid activities. With the development of new chemical synthesis techniques such as photocatalysis, electrocatalysis, and continuous flow chemistry, organic synthesis is expected to achieve the green and efficient synthesis of isoquinoline alkaloids and their derivatives.[261]

In recent years, the development of plant metabolic pathways, enzyme engineering, and biotechnology methods has led to a number of breakthroughs in the microbial synthesis of plant secondary metabolites. As a plant secondary metabolite with important research and medicinal value, the biosynthesis of isoquinoline alkaloids has important research significance. To date, researchers have analyzed the biosynthetic pathway of benzylisoquinoline alkaloids (BIAs) and have identified a variety of microbial BIA synthesis pathways, including the thebaine and magnoflorine pathways. On this basis, the synthesis pathways of these alkaloids in microorganisms have been reconstructed by simulating the synthesis pathway of BIA in plants, and the biosynthesis of BIA has been realized. However, owing to the complex structure of most BIAs and the lengthy metabolic pathways, the catalytic enzymes involved have wide selectivity for BIA intermediates in the main metabolic flow pathways, resulting in uncontrollable metabolic flow and a low yield of target compounds. Moreover, the structure of isoquinoline alkaloids is complex and diverse, their biosynthetic pathways are difficult to analyze, and the biosynthesis of diverse isoquinoline alkaloids in a short period of time is difficult. Chemical synthesis is highly important for the construction of diverse isoquinoline alkaloids and their derivatives and for the in-depth study of their physiological activities. Moreover, with the analysis of the biosynthesis pathway, the total synthesis strategy of isoquinoline alkaloids by modifying some enzymes instead of expensive noble metal catalysts has been widely studied. Therefore, the combination of the flexible and diverse characteristics of chemical synthesis and the potential for inexpensive and efficient biosynthesis is important for future research on isoquinoline alkaloids.

However, there is no doubt that biosynthesis, especially the establishment of microbial cell factories, has extremely attractive advantages for the green and efficient production of high-value isoquinoline alkaloids. Furthermore, advancements in technologies such as enzyme immobilization, novel screening methods, and enzyme mutagenesis are expected to gradually overcome many limitations of biocatalysis, including poor stability, low efficiency, and a narrow substrate range. This will make enzyme catalysis a more feasible and sustainable option for synthesizing small molecules.[262] As research on the natural biosynthetic pathways and key functional enzymes of isoquinoline alkaloids deepens, and with the continuous development of biotechnology, the efficiency of biosynthesis is expected to be further improved, and costs will be reduced in the future.

4. Conclusion

Owing to their various chemical structures and pharmacological activities, isoquinoline alkaloids have high probabilities of success in drug discovery and development. Continuing our previous review (covering 2014–2018), this manuscript summarizes and provides updated literature on novel isoquinoline alkaloids isolated during the period of 2019–2023, and more than 250 molecules with various pharmacological activities were isolated. A new class of phenanthridine alkaloids that includes dehydroambiguanine A (**194**) with antiproliferative activity,[97] and the wide application of isoquinoline alkaloids was highlighted. The identification of new compounds, significant biological activities or novel

mechanisms of action will undoubtedly contribute to the continual development of new drugs in the future.

However, the potential of this promising and expanding platform of active natural compounds has only been partially realized by both the academic community and the pharmaceutical industry. As we critically reviewed, although the synthesis strategies have been continuously optimized and more efficient, inexpensive and environmentally friendly synthetic routes for this class of natural products have been discovered over the past five years, achieving large-scale production of isoquinoline alkaloids still faces considerable challenges, hindering further research on these promising compounds, especially in pharmacology and clinical trials. For nearly five years, only Yamada reported a scaled-up synthesis strategy for (−)-emetine in 2023,[263] which is capable of synthesizing the target compound at a scale of 237.1 grams. Additionally, Qin's team established a new strategy for opioid natural products and their drug molecules in 2022 (Scheme 46),[193] which can perform reactions at a maximum scale of 50 grams. The entire synthesis process requires only a one column chromatography step, and most of the intermediates can be purified through simple processing or recrystallization. This strategy is expected to achieve scaled-up production of more than 100 grams through further optimization.

Moreover, although many isoquinoline alkaloids have been discovered from plants in recent decades, only a few compounds with promising biological activity have been identified, which severely limits further drug development. Currently, marine bacteria produce a plethora of compounds with unusual chemical structures and represent a new natural resource for finding alkaloids with valuable biological functions.[108] Table S1† shows that an increasing number of promising isoquinoline alkaloids have been isolated and identified from marine bacteria. For example, Zhang *et al.*[108] reported that a promising lead, turbinmicin, from a sea squirt microbiome component, *Micromonospora* sp., exhibits a broad safety index, better *in vitro* potency by targeting Sec14 and mouse model efficacy against multidrug-resistant fungal pathogens, which could help combat devastating global fungal pathogens such as *C. auris*.

In summary, continued attention and long-term research on the isolation and identification of naturally occurring isoquinoline alkaloids will lead to targeted pharmacological modeling, and developing new strategies for the total synthesis of isoquinolines will provide important support for synthetic modifications, resulting in new and better drugs based on the original effects of these alkaloids.

5. Data availability

The data supporting this article have been included as part of the ESI.†

6. Conflicts of interest

All authors declare that they have no competing interests.

7. Acknowledgements

This work was supported financially by the National Key Research and Development Program of China (2023YFD1800803, 2023YFD1801304), the National Natural Science Foundation of China (32373055, 32302924), the Outstanding Youth Fund of Gansu Province (23JRRA563), the Innovation Project of the Chinese Academy of Agricultural Sciences (No. CAAS-ASTIP-2015-LIHPS), and China Agriculture Research System (CARS-37).

8. References

1 K. Bhadra and G. S. Kumar, *Med. Res. Rev.*, 2011, **31**, 821–862.
2 I. I. Koleva, T. A. van Beek, A. E. M. F. Soffers, B. Dusemund and I. M. C. M. Rietjens, *Mol. Nutr. Food Res.*, 2012, **56**, 30–52.
3 D. K. Liscombe, B. P. MacLeod, N. Loukanina, O. I. Nandi and P. J. Facchini, *Phytochemistry*, 2005, **66**, 1374–1393.
4 D. Santoro, G. Bellinghieri and V. Savica, *J. Nephrol.*, 2011, **24**, S133–S136.
5 J. T. Zhu, L. X. Song, S. N. Shen, W. X. Fu, Y. Y. Zhu and L. Liu, *Molecules*, 2023, **28**, 7789.
6 X.-F. Shang, C.-J. Yang, S. L. MorrisNatschke, J.-C. Li, X.-D. Yin, Y.-Q. Liu, X. Guo, J.-W. Peng, M. Goto, J.-Y. Zhang and K.-H. Lee, *Med. Res. Rev.*, 2020, **40**, 2212–2289.
7 C. Weber and T. Opatz, *The Alkaloids: Chemistry and Biology*, 2019, vol. 81, pp. 1–114.
8 N. Tajuddeen and G. Bringmann, *Nat. Prod. Rep.*, 2021, **38**, 2154–2186.
9 E. Plazas, M. C. M. Avila, D. R. Munoz and L. E. S. Cuca, *Pharmacol. Res.*, 2022, **177**, 106126.
10 L. Xu, Y. Li, Y. Dai and J. Peng, *Pharmacol. Res.*, 2018, **130**, 451–465.
11 M. Iranshahy, R. J. Quinn and M. Iranshahi, *RSC Adv.*, 2014, **4**, 15900–15913.
12 D. J. Newman and G. M. Cragg, *J. Nat. Prod.*, 2016, **79**, 629–661.
13 C. Freestone and R. Eccles, *J. Pharm. Pharmacol.*, 1997, **49**, 1045–1049.
14 M. E. Pyne and V. J. J. Martin, *Curr. Opin. Green Sustainable Chem.*, 2022, **33**, 100561.
15 M. Xu, L. Liu, C. Qi, B. Deng and X. Cai, *Planta Med.*, 2008, **74**, 1423–1429.
16 M. Heinrich and H. L. Teoh, *J. Ethnopharmacol.*, 2004, **92**, 147–162.
17 H. A. Blair, *Drugs*, 2018, **78**, 1847–1853.
18 S. Dhillon, *Drugs*, 2019, **79**, 563–572.
19 A. H. Gaur, J. S. McCarthy, J. C. Panetta, R. H. Dallas, J. Woodford, L. Tang, A. M. Smith, T. B. Stewart, K. C. Branum, B. B. Freeman III, N. D. Patel, E. John, S. Chalon, S. Ost, R. N. Heine, J. L. Richardson, R. Christensen, P. M. Flynn, Y. Van Gessel, B. Mitasev, J. J. Moehrle, F. Gusovsky, L. Bebrevska and R. K. Guy, *Lancet Infect. Dis.*, 2020, **20**, 964–975.

20 Y.-L. Wang, C.-Y. Wu and S.-W. Zhai, *Nat. Prod. Res.*, 2023, **37**, 1867–1871.
21 J. Zhang, C. Zhang, F.-C. Xu, Quesheng, Q.-Y. Zhang, P.-F. Tu and H. Liang, *Phytochemistry*, 2019, **159**, 199–207.
22 D. Luo, N. Lyu, L.-M. Liao, Q. Gao, Y.-K. Li, J. Li, X. Liu, X.-M. Li, G.-Y. Yang, Y.-Q. Ye, Q.-F. Hu and M. Dong, *China J. Chin. Mater. Med.*, 2020, **45**, 2568–2570.
23 H. Xia, Y. Liu, G. Xia, Y. Liu, S. Lin and L. Guo, *Front. Immunol.*, 2021, **12**, 685556.
24 J.-J. Xue, J.-Y. Li, B.-J. Li, Y.-T. Jin, C.-H. Wang, C.-M. Xue, H.-M. Zhang, Z.-L. Li, D.-H. Li and H.-M. Hua, *China J. Chin. Mater. Med.*, 2022, **47**, 2676–2680.
25 J. Liu, Q. Lin, Q.-M. Zhou, C.-W. Meng, L. Xiong, X. Wang, L.-L. Miao, L. Guo and C. Peng, *China J. Chin. Mater. Med.*, 2022, **47**, 3265–3269.
26 Y. Han, T. Hou, Z.-H. Zhang, Y.-D. Wang, J.-X. Cheng, H. Zhou, J.-X. Wang, J.-T. Feng, Y.-F. Liu, Z.-M. Guo and X.-M. Liang, *Fitoterapia*, 2022, **159**, 105175.
27 H. Fukumi, H. Kurihara, T. Hata, C. Tamura, H. Mishima, A. Kubo and T. Arai, *Tetrahedron Lett.*, 1977, **18**, 3825–3828.
28 A. Kubo, Y. Kitahara, S. Nakahara, R. Iwata and R. Numata, *Chem. Pharm. Bull.*, 1988, **36**, 4355–4363.
29 Y. Tian, W. Gui, P. B. Smith, I. Koo, L. A. Murray, M. T. Cantorna, G. H. Perdew and A. D. Patterson, *J. Agric. Food Chem.*, 2019, **67**, 9286–9294.
30 D. Copmans, S. Kildgaard, S. A. Rasmussen, M. Slezak, N. Dirkx, M. Partoens, C. V. Esguerra, A. D. Crawford, T. O. Larsen and P. A. M. de Witte, *Mar. Drugs*, 2019, **17**, 607.
31 Y. N. Kim, Y. K. Ji, N.-H. Kim, N. Van Tu, J.-R. Rho and E. J. Jeong, *Mar. Drugs*, 2021, **19**, 90.
32 C. Nord, J. J. Levenfors, J. Bjerketorp, C. Sahlberg, B. Guss, B. Oberg and A. Broberg, *Molecules*, 2019, **24**, 4616.
33 M. Shaaban, K. A. Shaaban, G. Kelter, H. H. Fiebig and H. Laatsch, *Mar. Drugs*, 2021, **19**, 715.
34 C.-M. Liu, F.-H. Yao, X.-H. Lu, X.-X. Zhang, L.-X. Luo, X. Liang and S.-H. Qi, *Mar. Drugs*, 2022, **20**, 78.
35 R. S. Conceicao, I. M. A. Reis, A. P. M. Cerqueira, C. J. Perez, M. C. dos Santos Junior, A. Branco, D. R. Ifa and M. B. Botura, *Phytochem. Anal.*, 2020, **31**, 711–721.
36 J. M. Lima, G. M. Leme, E. V. Costa and Q. B. Cass, *J. Chromatogr. B: Anal. Technol. Biomed. Life Sci.*, 2021, **1164**, 122493.
37 X.-H. Duan, X.-W. Zhang, P. He, M. Qin, L. Pei, J.-C. Zhao and C.-H. Li, *J. Chin. Med. Mater.*, 2021, **44**, 76–78.
38 T. El-Elimat, M. B. Alhawarri, J. Rivera-Chavez, J. E. Burdette, A. Czarnecki, M. Al-Gharaibeh, A. H. Al Sharie, A. Alhusban, F. Q. Alali and N. H. Oberlies, *Fitoterapia*, 2020, **146**, 104706.
39 Y. Si, X. Li, T. Guo, W. Wei, J. Zhang, A. Jia, Y. Wang, A. Zhao, J. Chang and S. Feng, *Fitoterapia*, 2021, **154**, 105021.
40 T. Doncheva, N. Kostova, V. Valcheva, R. Toshkovska, V. Vutov and S. Philipov, *Nat. Prod. Res.*, 2020, **34**, 668–674.
41 H. Wen, X. Yuan, C. Li, J. Li and H. Yue, *Nat. Prod. Res.*, 2024, **38**, 1392–1397.
42 K. Du, Y. Liu, K. Zong, Y. Wang, J. Li and D. Meng, *Phytochemistry*, 2022, **200**, 113240.
43 T. Luo, Z. Li, X.-M. Deng, K. Jiang, D. Liu, H.-H. Zhang, T. Shi, L.-Y. Liu, H.-X. Wen, Q.-E. Li and Z. Wang, *Bioorg. Med. Chem.*, 2022, **60**, 116705.
44 L.-Y. Wang, B.-L. Qiu, H. Xia, G. Xia, B.-B. Xiao, J.-F. Zhang, W.-C. Zhong and S. Lin, *J. Nat. Prod.*, 2020, **83**, 489–496.
45 J. Zhang, C. Zhang, F. C. Xu, Quesheng, Q. Y. Zhang, P. F. Tu and H. Liang, *Phytochemistry*, 2019, **159**, 199–207.
46 A. O. Whaley, A. K. Whaley, V. Toporkova, E. Fock, N. Rukoyatkina, S. N. Smirnov, G. B. Satimov, B. A. Abduraxmanov and S. Gambaryan, *Fitoterapia*, 2023, **171**, 105697.
47 Z.-T. Peng, H.-X. Huo, L.-H. Chao, Y.-L. Song, D.-F. Liu, Z.-W. Wang, Y. Zhang, Y.-F. Zhao, P.-F. Tu, J. Zheng and J. Li, *Phytochemistry*, 2023, **209**, 113637.
48 N. Sun and Y. Han, *J. Asian Nat. Prod. Res.*, 2021, **23**, 1–8.
49 J.-J. Xue, C.-Y. Jiang, D.-L. Zou, B.-J. Li, J.-C. Lu, D.-H. Li, B. Lin, Z.-L. Li and H.-M. Hua, *Org. Lett.*, 2020, **22**, 7439–7442.
50 E. V. Costa, L. d. N. Soares, J. d. S. Chaar, V. R. Silva, L. d. S. Santos, H. H. F. Koolen, F. M. A. d. Silva, J. F. Tavares, G. Zengin, M. B. P. Soares and D. P. Bezerra, *Molecules*, 2021, **26**, 3714.
51 H.-L. Wei, Y.-P. Zhao, J.-X. Wang, Y. Han, H. Li, H. Zhou, T. Hou, C.-J. Wang, Y.-M. Yao, X.-L. Zhang, Y.-F. Liu and X.-M. Liang, *Bioorg. Chem.*, 2022, **127**, 106027.
52 H.-L. Wei, Y. Han, H. Zhou, T. Hou, Y.-M. Yao, C.-M. Wen, C.-R. Wang, J.-X. Wang, A.-J. Shen, X.-L. Zhang, H. Li and Y.-F. Liu, *Phytochemistry*, 2022, **194**, 113015.
53 A. Hostalkova, J. Marikova, L. Opletal, J. Korabecny, D. Hulcova, J. Kunes, L. Novakova, D. I. Perez, D. Jun, T. Kucera, V. Andrisano, T. Siatka and L. Cahlikova, *J. Nat. Prod.*, 2019, **82**, 239–248.
54 Y.-C. Chen, Y.-Y. Liu, L. Chen, D.-M. Tang, Y. Zhao and X.-D. Luo, *J. Agric. Food Chem.*, 2023, **71**, 16090–16101.
55 H.-L. Zeng, Y.-X. Cai, S.-S. Xu, S.-F. Wu, Y.-L. Li, X.-L. Chen, L.-Y. Kong and J.-G. Luo, *Fitoterapia*, 2023, **165**, 105404.
56 K. Jiang, X. Liu, Y.-M. Liu, L.-N. Wang, Y.-T. Xiao and F.-C. Wu, *J. Nat. Prod.*, 2023, **86**, 2162–2170.
57 S. Ali, M. Alamzeb, M. U. Rashid and W. N. Setzer, *J. Nat. Prod.*, 2020, **83**, 1383–1393.
58 J. Xiao, J.-Y. Song, B. Lin, W. Li, Y.-Q. Yang, J.-Y. Liu, Y. Hou, G. Chen and N. Li, *J. Nat. Prod.*, 2020, **83**, 864–872.
59 P.-T. Sun, Y.-G. Cao, G.-M. Xue, M. Li, C.-L. Zhang, F. Zhao, Z.-Y. Cao, D. Wang, K. R. Gustafson, X.-K. Zheng, W.-S. Feng and H. Chen, *Org. Lett.*, 2022, **24**, 1476–1480.
60 Z. Cao, S. Zhu, Z. Xue, F. Zhang, L. Zhang, Y. Zhang, Y. Guo, G. Zhan, X. Zhang and Z. Guo, *Phytochemistry*, 2022, **202**, 113321.
61 Y.-M. Wang, W.-Z. Ming, H. Liang, Y.-J. Wang, Y.-H. Zhang and D.-L. Meng, *Bioorg. Chem.*, 2020, **95**, 103489.
62 H. Guinaudeau, M. Leboeuf and A. Cave, *J. Nat. Prod.*, 1979, **42**, 325–360.
63 H. Guinaudeau, M. Shamma, B. Tantisewie and K. Pharadai, *J. Nat. Prod.*, 1982, **45**, 355–357.
64 C.-F. Ding, Z. Dai, H.-F. Yu, X.-D. Zhao and X.-D. Luo, *Chin. J. Nat. Med.*, 2019, **17**, 698–706.

65 L. Xu, W. Yang, J. Hu, C.-M. Han and P.-F. Li, *J. Asian Nat. Prod. Res.*, 2020, **22**, 618–625.
66 T. A. Majrashi, F. Zulfiqar, A. G. Chittiboyina, Z. Ali and I. A. Khan, *Nat. Prod. Res.*, 2019, **33**, 2823–2829.
67 J. Qin, S.-Y. Zhang, Y.-B. Zhang, L.-F. Chen, N.-H. Chen, Z.-N. Wu, D. Luo, G.-C. Wang and Y.-L. Li, *Nat. Prod. Res.*, 2021, **35**, 3254–3260.
68 B. Wang, Y.-J. Zhao, Y.-L. Zhao, Y.-P. Liu, X.-N. Li, H. Zhang and X.-D. Luo, *Org. Lett.*, 2020, **22**, 257–260.
69 H. Ma, X. Jin, F. Wang, J. Jiang, L. Cheng, S. Hu, G. Zhang and H. Xu, *Nat. Prod. Res.*, 2023, **9**, 1–7.
70 S.-A. Wuken, X. Yin, J. Mi, S.-G. Jiao, H.-X.-G. Zhang, X.-C. Zhou, P.-F. Tu, X.-Y. Chai and C.-S. Liu, *Chin. J. Exp. Tradit. Med. Formulae*, 2019, **25**, 172–175.
71 Y. Han, T. Hou, Z.-H. Zhang, Y.-H. Zhu, J.-X. Cheng, H. Zhou, J.-X. Wang, J.-T. Feng, Y.-F. Liu, Z.-M. Guo and X.-M. Liang, *Phytochemistry*, 2022, **199**, 113209.
72 J.-G. Lu, Y. Wang, M.-R. Yang, C.-Y. Wang, J. Meng, J. Liu, Z. Yang, K. Wu, L.-P. Bai, G.-Y. Zhu and Z.-H. Jiang, *Arch. Pharmacal Res.*, 2022, **45**, 631–643.
73 L.-M. Dai, R.-Z. Huang, J. Zhu, Z.-S. Song, Z.-G. Hong, F. Qin and H. Wang, *J. Mol. Struct.*, 2023, **1293**, 136240.
74 B. K. Lombe, D. Feineis and G. Bringmann, *Nat. Prod. Rep.*, 2019, **36**, 1513–1545.
75 S. Singh, N. Pathak, E. Fatima and A. S. Negi, *Eur. J. Med. Chem.*, 2021, **226**, 113839.
76 P. Patel, *Phytomed. Plus*, 2021, **1**, 100070.
77 J. Dickerhoff, N. Brundridge, S. A. McLuckey and D. Yang, *J. Med. Chem.*, 2021, **64**, 16205–16212.
78 S.-H. Yan, L.-M. Hu, X.-H. Hao, J. Liu, X.-Y. Tan, Z.-R. Geng, J. Ma and Z.-L. Wang, *iScience*, 2022, **25**, 104773.
79 K. Wang, C. Gu, G. Yu, J. Lin, Z. Wang, Q. Lu, Y. Xu, D. Zhao, X. Jiang, W. Mai, S. Liu and H. Yang, *Liver Res.*, 2022, **6**, 167–174.
80 F. Xu, M. Liu, Y. Liao, Y. Zhou, P. Zhang, Y. Zeng and Z. Liu, *Phytomed*, 2022, **104**, 154314.
81 K.-B. Wang, Y. Liu, J. Li, C. Xiao, Y. Wang, W. Gu, Y. Li, Y.-Z. Xia, T. Yan, M.-H. Yang and L.-Y. Kong, *Nat. Commun.*, 2022, **13**, 6016.
82 M. A. Leyva-Peralta, R. E. Robles-Zepeda, R. S. Razo-Hernandez, L. P. A. Berber, K. O. Lara, E. Ruiz-Bustos and J. C. Galvez-Ruiz, *Anti-Cancer Agents Med. Chem.*, 2019, **19**, 1820–1834.
83 S. Gaba, A. Saini, G. Singh and V. Monga, *Bioorg. Med. Chem.*, 2021, **38**, 116143.
84 C. Fu, G. Guan and H. Wang, *Curr. Pharm. Des.*, 2018, **24**, 2760–2764.
85 F. Bray, J. Ferlay, I. Soerjomataram, R. L. Siegel, L. A. Torre and A. Jemal, *Ca-Cancer J. Clin.*, 2018, **68**, 394–424.
86 Q. Su, M. Fan, J. Wang, A. Ullah, M. A. Ghauri, B. Dai, Y. Zhan, D. Zhang and Y. Zhang, *Cell Death Dis.*, 2019, **10**, 939.
87 Q. Su, J. Wang, F. Liu and Y. Zhang, *Toxicol. In Vitro*, 2020, **66**, 104840.
88 J. Wang, Q. Su, Q. Wu, K. Chen, A. Ullah, M. A. Ghauri and Y. Zhang, *Arch. Pharmacal Res.*, 2021, **44**, 1025–1036.
89 D. T. Tshitenge, T. Bruhn, D. Feineis, D. Schmidt, V. Mudogo, M. Kaiser, R. Brun, F. Wuerthner, S. Awale and G. Bringmann, *J. Nat. Prod.*, 2019, **82**, 3150–3164.
90 S. Fayez, D. Feineis, L. A. Assi, E.-J. Seo, T. Efferth and G. Bringmann, *RSC Adv.*, 2019, **9**, 15738–15748.
91 S. Fayez, T. Bruhn, D. Feineis, L. A. Assi, S. Awale and G. Bringmann, *J. Nat. Prod.*, 2020, **83**, 1139–1151.
92 N. Tajuddeen, S. Fayez, P. P. Kushwaha, D. Feineis, L. Ake Assi, S. Kumar and G. Bringmann, *Nat. Prod. Res.*, 2023, 1–5, DOI: **10.1080/14786419.2023.2194648**.
93 J.-P. Mufusama, D. Feineis, V. Mudogo, M. Kaiser, R. Brun and G. Bringmann, *RSC Adv.*, 2019, **9**, 12034–12046.
94 D. T. Tshitenge, T. Bruhn, D. Feineis, V. Mudogo, M. Kaiser, R. Brun and G. Bringmann, *Sci. Rep.*, 2019, **9**, 9812.
95 B. K. Lombe, D. Feineis, V. Mudogo, M. Kaiser and G. Bringmann, *J. Nat. Prod.*, 2021, **84**, 1335–1344.
96 S. Fayez, J. Li, D. Feineis, L. A. Assi, M. Kaiser, R. Brun, M. A. Anany, H. Wajant and G. Bringmann, *J. Nat. Prod.*, 2019, **82**, 3033–3046.
97 Z. Liu, Z. Mi, P. Wang, S. Chang, N. Han and J. Yin, *Nat. Prod. Res.*, 2020, **34**, 3305–3312.
98 D. Katoch, D. Kumar, Y. S. Padwad, B. Singh and U. Sharma, *Nat. Prod. Res.*, 2020, **34**, 233–240.
99 D. B. MacLean, *The Alkaloids: Chem Pharmacol.*, 1985, vol. 24, pp. 253–286.
100 C.-L. Zhang, Q.-L. Huang, J. Chen, W.-J. Zhang, H.-X. Jin, H.-B. Wang, C. B. Naman and Z.-Y. Cao, *J. Nat. Prod.*, 2019, **82**, 2713–2720.
101 C.-L. Zhang, Q.-L. Huang, Q. Zhu, J. Chen, F. Zhang and Z.-Y. Cao, *Fitoterapia*, 2020, **144**, 104494.
102 S. Ka, M. Masi, N. Merindol, R. Di Lecce, M. B. Plourde, M. Seck, M. Gorecki, G. Pescitelli, I. Desgagne-Penix and A. Evidente, *Phytochemistry*, 2020, **175**, 112390.
103 Y.-L. Liu, Y. Wang, X.-R. He, L.-S. Gan, F. Xu, Y.-J. Xu, X.-N. Wang, T. Shen and Z.-W. Zhou, *Fitoterapia*, 2022, **156**, 105086.
104 M.-S. Zhang, Y. Deng, S.-B. Fu, D.-L. Guo and S.-J. Xiao, *Molecules*, 2018, **23**, 1539.
105 J. Bracegirdle, L. P. Robertson, P. A. Hume, M. J. Page, A. V. Sharrock, D. F. Ackerley, A. R. Carroll and R. A. Keyzers, *J. Nat. Prod.*, 2019, **82**, 2000–2008.
106 G. A. U. Ecoy, S. Chamni, K. Suwanborirux, P. Chanvorachote and C. Chaotham, *J. Nat. Prod.*, 2019, **82**, 1861–1873.
107 D. W. Prebble, D. C. Holland, L. P. Robertson, V. M. Avery and A. R. Carroll, *Org. Lett.*, 2020, **22**, 9574–9578.
108 F. Zhang, M. Zhao, D. R. Braun, S. S. Ericksen, J. S. Piotrowski, J. Nelson, J. Peng, G. E. Ananiev, S. Chanana, K. Barns, J. Fossen, H. Sanchez, M. G. Chevrette, I. A. Guzei, C. Zhao, L. Guo, W. Tang, C. R. Currie, S. R. Rajski, A. Audhya, D. R. Andes and T. S. Bugni, *Science*, 2020, **370**, 974–978.
109 M. Chrzanowska, A. Grajewska and M. D. Rozwadowska, *Chem. Rev.*, 2016, **116**, 12369–12465.
110 R. Singh, S. Kumar, M. T. Patil, C. M. Sun and D. B. Salunke, *Adv. Synth. Catal.*, 2020, **362**, 4027–4077.

111 N. Tajuddeen, D. Feineis, H. Ihmels and G. Bringmann, *Acc. Chem. Res.*, 2022, **55**, 2370–2383.
112 X.-Y. Yu, J.-R. Chen and W.-J. Xiao, *Chem. Rev.*, 2021, **121**, 506–561.
113 K. P. S. Cheung, S. Sarkar and V. Gevorgyan, *Chem. Rev.*, 2022, **122**, 1543–1625.
114 A. Y. Chan, I. B. Perry, N. B. Bissonnette, B. F. Buksh, G. A. Edwards, L. I. Frye, O. L. Garry, M. N. Lavagnino, B. X. Li, Y. Liang, E. Mao, A. Millet, J. V. Oakley, N. L. Reed, H. A. Sakai, C. P. Seath and D. W. C. MacMillan, *Chem. Rev.*, 2022, **122**, 1485–1542.
115 L. Capaldo, D. Ravelli and M. Fagnoni, *Chem. Rev.*, 2022, **122**, 1875–1924.
116 S. P. Pitre and L. E. Overman, *Chem. Rev.*, 2022, **122**, 1717–1751.
117 C. Zhu, N. W. J. Ang, T. H. Meyer, Y. Qiu and L. Ackermann, *ACS Cent. Sci.*, 2021, **7**, 415–431.
118 M. B. Plutschack, B. Pieber, K. Gilmore and P. H. Seeberger, *Chem. Rev.*, 2017, **117**, 11796–11893.
119 H. Kim, K.-I. Min, K. Inoue, D. J. Im, D.-P. Kim and J.-i. Yoshida, *Science*, 2016, **352**, 691–694.
120 C. Liu, J. Xie, W. Wu, M. Wang, W. Chen, S. B. Idres, J. Rong, L.-W. Deng, S. A. Khan and J. Wu, *Nat. Chem.*, 2021, **13**, 451–457.
121 D. F. Vargas, E. L. Larghi and T. S. Kaufman, *Nat. Prod. Rep.*, 2019, **36**, 354–401.
122 D. F. Vargas, E. L. Larghi and T. S. Kaufman, *RSC Adv.*, 2019, **9**, 33096–33106.
123 D. F. Vargas, E. L. Larghi and T. S. Kaufman, *Eur. J. Org Chem.*, 2018, 5605–5614.
124 S. Fonzo, D. F. Vargas and T. S. Kaufman, *Synthesis*, 2019, **51**, 3908–3914.
125 R. Schuetz, S. Schmidt and F. Bracher, *Tetrahedron*, 2020, **76**, 131150.
126 A. Ansari, A. B. Gorde and R. Ramapanicker, *Tetrahedron*, 2021, **88**, 132121.
127 A. K. Haidar, N. D. Kjeldsen, N. S. Troelsen, V. Previtali, K. P. Lundquist, T. O. Larsen and M. H. Clausen, *Molecules*, 2022, **27**, 521.
128 T. Choshi, T. Kumemura, H. Fujioka, Y. Hieda and S. Hibino, *Heterocycles*, 2012, **84**, 587–595.
129 R. Schuetz, M. Mueller, S. Gerndt, K. Bartel and F. Bracher, *Arch. Pharm.*, 2020, **353**, e2000106.
130 M. Keller, K. Sauvageot-Witzku, F. Geisslinger, N. Urban, M. Schaefer, K. Bartel and F. Bracher, *Beilstein J. Org. Chem.*, 2021, **17**, 2716–2725.
131 M. J. Scharf and B. List, *J. Am. Chem. Soc.*, 2022, **144**, 15451–15456.
132 A. Lipp, M. Selt, D. Ferenc, D. Schollmeyer, S. R. Waldvogel and T. Opatz, *Org. Lett.*, 2019, **21**, 1828–1831.
133 S. Elavarasan, J. Preety, R. Abinaya, T. Saravanan, K. K. Balasubramanian, N. Venkatramaiah and B. Baskar, *Chem.–Asian J.*, 2022, **17**, e202200878.
134 W. Liu, B. Hong, J. Wang and X. Lei, *Acc. Chem. Res.*, 2020, **53**, 2569–2586.
135 Y.-J. Wu, J.-H. Chen, M.-Y. Teng, X. Li, T.-Y. Jiang, F.-R. Huang, Q.-J. Yao and B.-F. Shi, *J. Am. Chem. Soc.*, 2023, **145**, 24499–24505.
136 W. Xu, Z. Huang, X. Ji and J.-P. Lumb, *ACS Catal.*, 2019, **9**, 3800–3810.
137 Z. Huang, X. Ji and J.-P. Lumb, *Org. Lett.*, 2019, **21**, 9194–9197.
138 M. Lafrance, N. Blaquière and K. Fagnou, *Chem. Commun.*, 2004, 2874–2875.
139 R. Schuetz, M. Meixner, I. Antes and F. Bracher, *Org. Biomol. Chem.*, 2020, **18**, 3047–3068.
140 Y. Zhao, Y. Li, B. Wang, J. Zhao, L. Li, X.-D. Luo and H. Zhang, *J. Org. Chem.*, 2020, **85**, 13772–13778.
141 P. Pieper, E. McHugh, M. Amaral, A. G. Tempone and E. A. Anderson, *Tetrahedron*, 2020, **76**, 130814.
142 G. P. Perecim, V. M. Deflon, G. R. Martins, L. M. C. Pinto, G. A. Casagrande, D. Oliveira-Silva and C. Raminelli, *Tetrahedron*, 2020, **76**, 131461.
143 J. Lv, Z.-H. Li, A.-J. Deng and H.-L. Qin, *Org. Biomol. Chem.*, 2022, **20**, 658–666.
144 H. Hamamoto, Y. Shiozaki, H. Nambu, K. Hata, H. Tohma and Y. Kita, *Chem.–Eur. J.*, 2004, **10**, 4977–4982.
145 B. B. J. Tra, A. Abolle, V. Coeffard and F.-X. Felpin, *Eur. J. Org Chem.*, 2022, **2022**, e202200301.
146 H. Takikawa, A. Nishii, T. Sakai and K. Suzuki, *Chem. Soc. Rev.*, 2018, **47**, 8030–8056.
147 T. R. Cipriano da Silva, R. B. Oliveira, A. L. M. Nicastro, R. P. Ureshino and C. Raminelli, *ChemistrySelect*, 2023, **8**, e202302821.
148 H.-G. Cheng, S. Chen, R. Chen and Q. Zhou, *Angew. Chem., Int. Ed.*, 2019, **58**, 5832–5844.
149 M. Bai, S. Jia, J. Zhang, H.-G. Cheng, H. Cong, S. Liu, Z. Huang, Y. Huang, X. Chen and Q. Zhou, *Angew. Chem., Int. Ed.*, 2022, **61**, e202205245.
150 S. Jia, M. Bai, S. Zhou, R. Sheng, H.-G. Cheng and Q. Zhou, *Sci. China: Chem.*, 2023, **66**, 3136–3140.
151 S. Nishimoto, H. Nakahashi and M. Toyota, *Tetrahedron Lett.*, 2020, **61**, 152599.
152 R. Chen, S. Jia, Y. Man, H.-G. Cheng and Q. Zhou, *Synthesis*, 2024, **56**, 1695–1701.
153 G. He, B. List and M. Christmann, *Angew. Chem., Int. Ed.*, 2021, **60**, 13591–13596.
154 D. Stubba, G. Lahm, M. Geffe, J. W. Runyon, A. J. Arduengo III and T. Opatz, *Angew. Chem., Int. Ed.*, 2015, **54**, 14187–14189.
155 J. Yu, Z. Zhang, S. Zhou, W. Zhang and R. Tong, *Org. Chem. Front.*, 2018, **5**, 242–246.
156 S. Uenishi, R. Kakigi, K. Hideshima, A. Miyawaki, J. Matsuoka, T. Ogata, K. Tomioka and Y. Yamamoto, *Tetrahedron*, 2021, **90**, 132165.
157 W. Li, M. Jiang, W. Chen, Y. Chen, Z. Yang, P. Tang and F. Chen, *J. Org. Chem.*, 2021, **86**, 8143–8153.
158 W. Li, M. Jiang, M. Liu, X. Ling, Y. Xia, L. Wan and F. Chen, *Chem.–Eur. J.*, 2022, **28**, e202200700.
159 R. Boda and G. D. Cuny, *Tetrahedron*, 2022, **129**, 133146.

160 A. Cervi, P. Aillard, N. Hazeri, L. Petit, C. L. L. Chai, A. C. Willis and M. G. Banwell, *J. Org. Chem.*, 2013, **78**, 9876–9882.
161 W. Li, S. Huang, M. Jiang, Y. Chen, Z. Yang, P. Tang and F. Chen, *ChemCatChem*, 2023, **15**, e202201553.
162 E. D. Slack, R. Seupel, D. H. Aue, G. Bringmann and B. H. Lipshutz, *Chem.–Eur. J.*, 2019, **25**, 14237–14245.
163 Y.-I. Jo, C.-Y. Lee and C.-H. Cheon, *Org. Lett.*, 2020, **22**, 4653–4658.
164 Y.-I. Jo, C.-Y. Lee and C.-H. Cheon, *J. Org. Chem.*, 2020, **85**, 12770–12776.
165 D. Berthold and W. van Otterlo, *Chem.–Eur. J.*, 2023, **29**, e202302070.
166 B. M. Trost, C.-I. J. Hung and Z. Jiao, *J. Am. Chem. Soc.*, 2019, **141**, 16085–16092.
167 B. M. Trost, C.-I. Hung, T. Saget and E. Gnanamani, *Nat. Catal.*, 2018, **1**, 523–530.
168 B. M. Trost, C.-I. J. Hung and E. Gnanamani, *ACS Catal.*, 2019, **9**, 1549–1557.
169 I. Ninomiya, O. Yamamoto and T. Naito, *J. Chem. Soc., Perkin Trans. 1*, 1980, 212–216.
170 L. S. Hutchings-Goetz, C. Yang, J. W. B. Fyfe and T. N. Snaddon, *Angew. Chem., Int. Ed.*, 2020, **59**, 17556–17564.
171 C. M. Pearson, J. W. B. Fyfe and T. N. Snaddon, *Angew. Chem., Int. Ed.*, 2019, **58**, 10521–10527.
172 A. D. C. Parenty, K. M. Guthrie, Y. F. Song, L. V. Smith, E. Burkholder and L. Cronin, *Chem. Commun.*, 2006, **11**, 1194–1196.
173 P. J. Murphy, J. Tibble-Howlings, R. M. Kowalczyk and K. Stevens, *Tetrahedron Lett.*, 2020, **61**, 151785.
174 B. Sheng, C. Zeng, J. Chen, W.-C. Ye, W. Tang, P. Lan and M. G. Banwell, *Eur. J. Org Chem.*, 2022, **2022**, e202101511.
175 N. Aravindan and M. Jeganmohan, *J. Org. Chem.*, 2021, **86**, 14826–14843.
176 N. Aravindan, V. Vinayagam and M. Jeganmohan, *Org. Lett.*, 2022, **24**, 5260–5265.
177 N. Aravindan and M. Jeganmohan, *Org. Lett.*, 2023, **25**, 3853–3858.
178 J. Fu, B. Li, X. Wang, H. Wang, M. Deng, H. Yang, B. Lin, M. Cheng, L. Yang and Y. Liu, *Org. Lett.*, 2022, **24**, 8310–8315.
179 Z. Jin and G. Yao, *Nat. Prod. Rep.*, 2019, **36**, 1462–1488.
180 M. B. Uphade and K. R. Prasad, *Tetrahedron*, 2020, **76**, 131661.
181 R.-S. Tang, L.-Y. Chen, C.-H. Lai and T.-H. Chuang, *Org. Lett.*, 2020, **22**, 9337–9341.
182 Y. Pang, H. Xiao, W. Ou, X. Zhang, X. Wang and S. Huang, *Tetrahedron Lett.*, 2020, **61**, 151733.
183 C. J. J. Hall, I. S. Marriott, K. E. Christensen, A. J. Day, W. R. F. Goundry and T. J. Donohoe, *Chem. Commun.*, 2022, **58**, 4966–4968.
184 Y. Menjo, A. Hamajima, N. Sasaki and Y. Hamada, *Org. Lett.*, 2011, **13**, 5744–5747.
185 T.-Y. Zhang, L.-Y. Zhang, X. Liang, K. Wei and Y.-R. Yang, *Org. Lett.*, 2022, **24**, 2905–2909.
186 D. Pollok, L. M. Grossmann, T. Behrendt, T. Opatz and S. R. Waldvogel, *Chem.–Eur. J.*, 2022, **28**, e202201523.
187 A. Lipp, D. Ferenc, C. Guetz, M. Geffe, N. Vierengel, D. Schollmeyer, H. J. Schaefer, S. R. Waldvogel and T. Opatz, *Angew. Chem., Int. Ed.*, 2018, **57**, 11055–11059.
188 A. Lipp, M. Selt, D. Ferenc, D. Schollmeyer, S. R. Waldvogel and T. Opatz, *Org. Lett.*, 2019, **21**, 1828–1831.
189 S.-H. Hou, A. Y. Prichina and G. Dong, *Angew. Chem., Int. Ed.*, 2021, **60**, 13057–13064.
190 D. Sun, B. Pedersen and J. A. Ellman, *Chem. Sci.*, 2019, **10**, 535–541.
191 G. Li, Q. Wang and J. Zhu, *Nat. Commun.*, 2021, **12**, 36.
192 S.-G. Wang, X.-J. Liu, Q.-C. Zhao, C. Zheng, S.-B. Wang and S.-L. You, *Angew. Chem., Int. Ed.*, 2015, **54**, 14929–14932.
193 X. Zhou, W. Li, R. Zhou, X. Wu, Y. Huang, W. Hou, C. Li, Y. Zhang, W. Nie, Y. Wang, H. Song, X.-Y. Liu, Z. Zheng, F. Xie, S. Li, W. Zhong and Y. Qin, *CCS Chem.*, 2021, **3**, 1376–1383.
194 Y. Tang, Y. Zhang, J. Zhao, F. Xue, H. He, F. Xue, X.-Y. Liu and Y. Qin, *Tetrahedron Lett.*, 2022, **104**, 154027.
195 H. He, F. Xue, Z. Hu, P. Li, Q. Xiao, M. Zhang, F. Xue, D. Zhang, H. Song, X.-Y. Liu, Z. Zheng, S. Li, W. Zhong and Y. Qin, *Org. Chem. Front.*, 2022, **9**, 2322–2327.
196 M. Odagi, T. Matoba and K. Nagasawa, *J. Org. Chem.*, 2022, **87**, 1065–1073.
197 J. Li, Y. Liu, X. Song, T. Wu, J. Meng, Y. Zheng, Q. Qin, D. Zhao and M. Cheng, *Org. Lett.*, 2019, **21**, 7149–7153.
198 J. Li, T. Wu, X. Song, Y. Zheng, J. Meng, Q. Qin, Y. Liu, D. Zhao and M. Cheng, *RSC Adv.*, 2020, **10**, 18953–18958.
199 M. Zhang, M. Zhao, Y. Wang, L. Chen, B. Liu, X. You, W. Sun, L. Hong and G. Li, *J. Org. Chem.*, 2023, **88**, 1720–1729.
200 C. Zhang, Y. Wang, Y. Song, H. Gao, Y. Sun, X. Sun, Y. Yang, M. He, Z. Yang, L. Zhan, Z.-X. Yu and Y. Rao, *CCS Chem.*, 2019, **1**, 352–364.
201 H. Takeuchi, S. Inuki, K. Nakagawa, T. Kawabe, A. Ichimura, S. Oishi and H. Ohno, *Angew. Chem., Int. Ed.*, 2020, **59**, 21210–21215.
202 T. Ling, V. R. Macherla, R. R. Manam, K. A. McArthur and B. C. M. Potts, *Org. Lett.*, 2007, **9**, 2289–2292.
203 J. He, S. Li, Y. Deng, H. Fu, B. N. Laforteza, J. E. Spangler, A. Homs and J.-Q. Yu, *Science*, 2014, **343**, 1216–1220.
204 G. Chen, T. Shigenari, P. Jain, Z. Zhang, Z. Jin, J. He, S. Li, C. Mapelli, M. M. Miller, M. A. Poss, P. M. Scola, K.-S. Yeung and J.-Q. Yu, *J. Am. Chem. Soc.*, 2015, **137**, 3338–3351.
205 G. Chen, Z. Zhuang, G.-C. Li, T. G. Saint-Denis, Y. Hsiao, C. L. Joe and J.-Q. Yu, *Angew. Chem., Int. Ed.*, 2017, **56**, 1506–1509.
206 Y. Zheng, X.-D. Li, P.-Z. Sheng, H.-D. Yang, K. Wei and Y.-R. Yang, *Org. Lett.*, 2020, **22**, 4489–4493.
207 D. Morikawa, K. Morii, Y. Yasuda, A. Mori and K. Okano, *J. Org. Chem.*, 2020, **85**, 8603–8617.
208 Y. Hayashi, K. Okano and A. Mori, *Org. Lett.*, 2018, **20**, 958–961.
209 K. Morii, Y. Yasuda, D. Morikawa, A. Mori and K. Okano, *J. Org. Chem.*, 2021, **86**, 13388–13401.
210 S. Sarkar and R. Samanta, *Org. Lett.*, 2022, **24**, 4536–4541.

211 J. Li, L. M. Jiang, F. Cheng, Y.-J. Zhou, D.-S. Duan, D.-Y. Zhu, K. Zhang, Z. Xiong and S.-H. Wang, *Tetrahedron Lett.*, 2022, **106**.
212 X.-Q. Mou, Z.-L. Xu, L. Xu, S.-H. Wang, B.-H. Zhang, D. Zhang, J. Wang, W.-T. Liu and W. Bao, *Org. Lett.*, 2016, **18**, 4032–4035.
213 M. A. Bajada, J. Sanjose-Orduna, G. Di Liberto, S. Tosoni, G. Pacchioni, T. Noel and G. Vile, *Chem. Soc. Rev.*, 2022, **51**, 3898–3925.
214 T. Noel, Y. Cao and G. Laudadio, *Acc. Chem. Res.*, 2019, **52**, 2858–2869.
215 L. Buglioni, F. Raymenants, A. Slattery, S. D. A. Zondag and T. Noel, *Chem. Rev.*, 2022, **122**, 2752–2906.
216 M. Elsherbini and T. Wirth, *Acc. Chem. Res.*, 2019, **52**, 3287–3296.
217 A. C. Brewer, P. C. Hoffman, J. R. Martinelli, M. E. Kobierski, N. Mullane and D. Robbins, *Org. Process Res. Dev.*, 2019, **23**, 1484–1498.
218 K. P. Cole, J. M. Groh, M. D. Johnson, C. L. Burcham, B. M. Campbell, W. D. Diseroad, M. R. Heller, J. R. Howell, N. J. Kallman, T. M. Koenig, S. A. May, R. D. Miller, D. Mitchell, D. P. Myers, S. S. Myers, J. L. Phillips, C. S. Polster, T. D. White, J. Cashman, D. Hurley, R. Moylan, P. Sheehan, R. D. Spencer, K. Desmond, P. Desmond and O. Gowran, *Science*, 2017, **356**, 1144–1150.
219 F. Ghirga, A. Bonamore, L. Calisti, I. D'Acquarica, M. Mori, B. Botta, A. Boffi and A. Macone, *Int. J. Mol. Sci.*, 2017, **18**, 2464.
220 B. Gao, B. Yang, X. Feng and C. Li, *Nat. Prod. Rep.*, 2022, **39**, 139–162.
221 Y. Wang, N. Tappertzhofen, D. Mendez-Sanchez, M. Bawn, B. Lyu, J. M. Ward and H. C. Hailes, *Angew. Chem., Int. Ed.*, 2019, **58**, 10120–10125.
222 Y. Wang, F. Subrizi, E. M. Carter, T. D. Sheppard, J. M. Ward and H. C. Hailes, *Nat. Commun.*, 2022, **13**, 5436.
223 R. Roddan, J. M. Ward, N. H. Keep and H. C. Hailes, *Curr. Opin. Chem. Biol.*, 2020, **55**, 69–76.
224 B. R. Lichman, M. C. Gershater, E. D. Lamming, T. Pesnot, A. Sula, N. H. Keep, H. C. Hailes and J. M. Ward, *FEBS J.*, 2015, **282**, 1137–1151.
225 R. Roddan, G. Gygli, A. Sula, D. Mendez-Sanchez, J. Pleiss, J. M. Ward, N. H. Keep and H. C. Hailes, *ACS Catal.*, 2019, **9**, 9640–9649.
226 J. Zhao, D. Mendez-Sanchez, R. Roddan, J. M. Ward and H. C. Hailes, *ACS Catal.*, 2021, **11**, 131–138.
227 T. Gurkok, E. Ozhuner, I. Parmaksiz, S. Ozcan, M. Turktas, A. Ipek, I. Demirtas, S. Okay and T. Unver, *Front. Plant Sci.*, 2016, **7**, 98.
228 J. Siegrist, S. Aschwanden, S. Mordhorst, L. Thoeny-Meyer, M. Richter and J. N. Andexer, *ChemBioChem*, 2015, **16**, 2576–2579.
229 F. Subrizi, Y. Wang, B. Thair, D. Mendez-Sanchez, R. Roddan, M. Cardenas-Fernandez, J. Siegrist, M. Richter, J. N. Andexer, J. M. Ward and H. C. Hailes, *Angew. Chem., Int. Ed.*, 2021, **60**, 18673–18679.
230 J. Zhu, H. Tan, L. Yang, Z. Dai, L. Zhu, H. Ma, Z. Deng, Z. Tian and X. Qu, *ACS Catal.*, 2017, **7**, 7003–7007.
231 L. Yang, J. Zhu, C. Sun, Z. Deng and X. Qu, *Chem. Sci.*, 2020, **11**, 364–371.
232 A. L. Meadows, K. M. Hawkins, Y. Tsegaye, E. Antipov, Y. Kim, L. Raetz, R. H. Dahl, A. Tai, T. Mahatdejkul-Meadows, L. Xu, L. Zhao, M. S. Dasika, A. Murarka, J. Lenihan, D. Eng, J. S. Leng, C.-L. Liu, J. W. Wenger, H. Jiang, L. Chao, P. Westfall, J. Lai, S. Ganesan, P. Jackson, R. Mans, D. Platt, C. D. Reeves, P. R. Saija, G. Wichmann, V. F. Holmes, K. Benjamin, P. W. Hill, T. S. Gardner and A. E. Tsong, *Nature*, 2016, **537**, 694–697.
233 H. Shuai, M. Myronovskyi, B. Rosenkraenzer, C. Paulus, S. Nadmid, M. Stierhof, D. Kolling and A. Luzhetskyy, *ACS Chem. Biol.*, 2022, **17**, 598–608.
234 N. S. Roy, I.-Y. Choi, T. Um, M. J. Jeon, B.-Y. Kim, Y.-D. Kim, J.-K. Yu, S. Kim and N.-S. Kim, *Plants*, 2021, **10**, 1314.
235 I. Desgagne-Penix, *Phytochem. Rev.*, 2021, **20**, 409–431.
236 C. Guo, Y. Chen, D. Wu, Y. Du, M. Wang, C. Liu, J. Chu and X. Yao, *Int. J. Mol. Sci.*, 2022, **23**, 10898.
237 Y. Yang, P. Hu, X. Zhou, P. Wu, X. Si, B. Lu, Y. Zhu and Y. Xia, *Fitoterapia*, 2020, **140**, 104412.
238 L. M. T. Chacon, H. Leiva, I. C. Z. Vahos, D. C. Restrepo and E. Osorio, *Biocatal. Agric. Biotechnol.*, 2023, **50**, 102670.
239 X. Liu, J. Bu, Y. Ma, Y. Chen, Q. Li, X. Jiao, Z. Hu, G. Cui, J. Tang, J. Guo and L. Huang, *Plant Physiol. Biochem.*, 2021, **168**, 507–515.
240 T. R. Valentic, J. T. Payne and C. D. Smolke, *ACS Catal.*, 2020, **10**, 4497–4509.
241 S. Wu, R. Snajdrova, J. C. Moore, K. Baldenius and U. T. Bornscheuer, *Angew. Chem., Int. Ed.*, 2021, **60**, 88–119.
242 M. Zhao, X. Hong, Abdullah, R. Yao and Y. Xiao, *Green Chem.*, 2021, **23**, 838–847.
243 M. Zhao, Z. Qin, A. Abdullah and Y. Xiao, *Green Chem.*, 2022, **24**, 3225–3234.
244 D. K. Ro, E. M. Paradise, M. Ouellet, K. J. Fisher, K. L. Newman, J. M. Ndungu, K. A. Ho, R. A. Eachus, T. S. Ham, J. Kirby, M. C. Y. Chang, S. T. Withers, Y. Shiba, R. Sarpong and J. D. Keasling, *Nature*, 2006, **440**, 940–943.
245 J. Zhang, L. G. Hansen, O. Gudich, K. Viehrig, L. M. M. Lassen, L. Schruebbers, K. B. Adhikari, P. Rubaszka, E. Carrasquer-Alvarez, L. Chen, V. D'Ambrosio, B. Lehka, A. K. Haidar, S. Nallapareddy, K. Giannakou, M. Laloux, D. Arsovska, M. A. K. Jorgensen, L. J. G. Chan, M. Kristensen, H. B. Christensen, S. Sudarsan, E. A. Stander, E. Baidoo, C. J. Petzold, T. Wulff, S. E. O'Connor, V. Courdavault, M. K. Jensen and J. D. Keasling, *Nature*, 2022, **609**, 341–347.
246 S. Galanie, K. Thodey, I. J. Trenchard, M. F. Interrante and C. D. Smolke, *Science*, 2015, **349**, 1095–1100.
247 I. J. Trenchard, M. S. Siddiqui, K. Thodey and C. D. Smolke, *Metab. Eng.*, 2015, **31**, 74–83.
248 O. K. Jamil, A. Cravens, J. T. Payne, C. Y. Kim and C. D. Smolke, *Proc. Natl. Acad. Sci. U. S. A.*, 2022, **119**, e2205848119.
249 J. Han and S. Li, *Commun. Chem.*, 2023, **6**, 27.

250 J. T. Payne, T. R. Valentic and C. D. Smolke, *Proc. Natl. Acad. Sci. U. S. A.*, 2021, **118**, e2112520118.
251 W. C. DeLoache, Z. N. Russ, L. Narcross, A. M. Gonzales, V. J. J. Martin and J. E. Dueber, *Nat. Chem. Biol.*, 2015, **11**, 465–471.
252 A. Nakagawa, E. Matsumura, T. Koyanagi, T. Katayama, N. Kawano, K. Yoshimatsu, K. Yamamoto, H. Kumagai, F. Sato and H. Minami, *Nat. Commun.*, 2016, **7**, 10390.
253 W. Zhao, M. Liu, C. Shen, K. Liu, H. Liu, C. Ou, W. Dai, X. Liu and J. Liu, *Green Chem.*, 2021, **23**, 5944–5955.
254 C. E. Hodgman and M. C. Jewett, *Metab. Eng.*, 2012, **14**, 261–269.
255 S. K. Hammer and J. L. Avalos, *Nat. Chem. Biol.*, 2017, **13**, 823–832.
256 P. S. Grewal, J. A. Samson, J. J. Baker, B. Choi and J. E. Dueber, *Nat. Chem. Biol.*, 2021, **17**, 96–103.
257 S. d'Oelsnitz, W. Kim, N. T. Burkholder, K. Javanmardi, R. Thyer, Y. Zhang, H. S. Alper and A. D. Ellington, *Nat. Chem. Biol.*, 2022, **18**, 981–989.
258 M. M. Mitchler, J. M. Garcia, N. E. Montero and G. J. Williams, *Curr. Opin. Biotechnol.*, 2021, **69**, 172–181.
259 G. S. Hossain, M. Saini, R. Miyake, H. Ling and M. W. Chang, *Trends Biotechnol.*, 2020, **38**, 797–810.
260 J. Hafner, J. Payne, H. MohammadiPeyhani, V. Hatzimanikatis and C. Smolke, *Nat. Commun.*, 2021, **12**, 1760.
261 K. Lovato, P. S. Fier and K. M. Maloney, *Nat. Rev. Chem.*, 2021, **5**, 546–563.
262 R. A. Sheldon and J. M. Woodley, *Chem. Rev.*, 2018, **118**, 801–838.
263 M. Yamada, K. Azuma, I. Takizawa, Y. Ejima, M. Yamano, K. Satoh, T. Doi, H. Ueda and H. Tokuyama, *Org. Process Res. Dev.*, 2023, **27**, 343–357.